DIPLOMARBEIT

# Bjerknes Forces: A layer potential approach

zur Erlangung des akademischen Grades

**Diplom-Ingenieur**

im Rahmen des Studiums

**Technische Mathematik**

eingereicht von

**Jakob Hüpfl**
Matrikelnummer: 01227569
Alsegger Straße 33/2/7, 1180 Wien

unter der Betreuung von
**Univ.Prof. Jens Markus Melenk**
am Institut für Analysis und Scientific Computing der TU Wien

und Co-Betreuung von
**Prof. Habib Ammari**
am Seminar for Applied Mathematics der ETH Zürich

Wien, am _____

Unterschrift Verfasser

Unterschrift Betreuer

Die approbierte gedruckte Originalversion dieser Diplomarbeit ist an der TU Wien Bibliothek verfügbar
The approved original version of this thesis is available in print at TU Wien Bibliothek.
TU Bibliothek Your knowledge hub WIEN

Die approbierte gedruckte Originalversion dieser Diplomarbeit ist an der TU Wien Bibliothek verfügbar
The approved original version of this thesis is available in print at TU Wien Bibliothek.

# Abstract

The movements of one and two interacting bubbles inside a weak acoustic incident pressure field have been extensively studied in the past. The results have focused on bubble systems with limited or no interaction, which greatly simplified the problem. It has been shown that considering low order couplings between the bubbles produce sign reversal effects of the forces. This can produce multi bubble systems with stable separation distances, which cannot be explained by a model with no coupling.
This thesis covers theoretical derivations of the movement of two fully interacting bubbles inside an acoustic incident pressure field. A novel approach under the assumption of an inviscous fluid is introduced. The total forces are approximated in a new way and the governing equations are linearised, allowing the use of layer potential techniques. We further calculate the asymptotic forces on one and two bubbles and show that the results are consistent with past literature. Common approaches with only low order interactions produce growing errors for smaller bubble separations due to higher order coupling terms getting more significant. In contrast, our approach considers all coupling terms in the linearised model and should more accurately approximate bubbles with strong interactions. Partial results are verified by numerical computations and simulations of two bubble systems are made. Multiple sign reversal effects are observed which show the complex behaviour of the forces. Further applications and analysis of this approach could be a fruitful path of understanding the Bjerknes forces near resonance frequencies and for bubbles in close proximity with each other.

Die approbierte gedruckte Originalversion dieser Diplomarbeit ist an der TU Wien Bibliothek verfügbar
The approved original version of this thesis is available in print at TU Wien Bibliothek.
TU Bibliothek Your knowledge hub WIEN

Die approbierte gedruckte Originalversion dieser Diplomarbeit ist an der TU Wien Bibliothek verfügbar
The approved original version of this thesis is available in print at TU Wien Bibliothek.

# Kurzfassung

Die Bewegung von ein und zwei interagierenden Blasen in einem schwachen akustischen Feld sind in der Vergangenheit genau untersucht worden. Die Resultate haben sich auf Systeme mit wenig oder keiner Interaktion beschränkt, was die Analyse deutlich vereinfacht hat. Unter Beachtung von Kopplungstermen niedriger Ordnung ist gezeigt worden, dass eine Vorzeichenumkehr der Kraft auftritt. Dadurch sind Mehr-Blasensysteme mit stabilen Abständen möglich, welche nicht durch ungekoppelte Modelle erklärt werden können.

Diese Arbeit enthält theoretische Ableitungen von Bewegungen von zwei Blasen mit Interaktion in einem einfallenden akustischen Druckfeld. Ein neuer Ansatz unter der Annahme von Flüssigkeiten ohne Viskosität wird eingeführt. Die Gesamtkraft wird auf eine neue Weise approximiert und die bestimmenden Gleichungen werden linearisiert, welche die Verwendung von potentialtheoretischen Techniken erlaubt. Weiters werden die asymptotischen Kräfte für ein und zwei Blasensysteme berechnet und Resultate, konsistent mit der Literatur, werden abgeleitet. Bestehende Ansätze mit Interaktion niedriger Ordnung erzeugen zunehmend Fehler für kleinere Blasenabstände, da die Kopplungsterme höherer Ordnung an Signifikanz gewinnen. Im Gegensatz dazu betrachtet unser Ansatz alle Interaktionsterme höherer Ordnung im linearisierten Model und sollte Blasen mit starker Interaktion besser beschreiben. Teilergebnisse werden durch numerische Berechnungen verifiziert und Simulationen von Zwei-Blasensysteme werden analysiert. Mehrere Vorzeichenumkehreffekte sind sichtbar, welche das komplexe Verhalten der Kräfte verdeutlichen. Weitere Anwendung und Analyse dieses Ansatzes könnte das Verständnis der Bjerknes Kräfte nahe der Resonanzfrequenzen und für Blasen mit kleinem Trennungsabstand erweitern.

Die approbierte gedruckte Originalversion dieser Diplomarbeit ist an der TU Wien Bibliothek verfügbar
The approved original version of this thesis is available in print at TU Wien Bibliothek.
TU Bibliothek Your knowledge hub WIEN

Die approbierte gedruckte Originalversion dieser Diplomarbeit ist an der TU Wien Bibliothek verfügbar
The approved original version of this thesis is available in print at TU Wien Bibliothek.

# Acknowledgements

I would like to express my deepest gratitude to Prof. Jens Markus Melenk for his support that made this thesis possible. Further I would like to thank Prof. Habib Ammari for his co-supervision of my thesis at ETH Zürich. Bryn Davies and Erik Orvehed Hiltunen also deserve special mention for their help and valuable discussions. I would also like to thank Björn Bahr in helping proofreading this thesis.
More thanks go out to my parents who supported me and my lifelong interest in science morally and financially. Last but not least I want to thank my girlfriend for her invaluable support.

Die approbierte gedruckte Originalversion dieser Diplomarbeit ist an der TU Wien Bibliothek verfügbar
The approved original version of this thesis is available in print at TU Wien Bibliothek.
TU Bibliothek Your knowledge hub WIEN

Die approbierte gedruckte Originalversion dieser Diplomarbeit ist an der TU Wien Bibliothek verfügbar
The approved original version of this thesis is available in print at TU Wien Bibliothek.

# Contents


**1. Introduction** **3**

**2. Historical considerations** **5**
2.1. The kinetic bubble . . . . . 5
2.1.1. Added mass . . . . . 5
2.1.2. Kinematic Buoyancy approximation . . . . . 8
2.2. Pulsating bubble . . . . . 9
2.3. Bjerknes forces . . . . . 11
2.3.1. Primary Bjerknes Force . . . . . 13
2.3.2. Secondary Bjerknes Force . . . . . 14

**3. Mathematical model** **15**
3.1. Physical considerations . . . . . 15
3.1.1. Lagrange representation . . . . . 15
3.1.2. Conservation of mass . . . . . 16
3.1.3. Newtons law . . . . . 16
3.1.4. Equation of state . . . . . 17
3.1.5. Surface connections . . . . . 18
3.2. The linearized solution . . . . . 18
3.2.1. Surface connections . . . . . 19
3.2.2. Boundary conditions . . . . . 20
3.2.3. Problem formulation . . . . . 20
3.3. Force integral approximation . . . . . 21
3.4. Bjerknes Forces . . . . . 23

**4. Mathematical background** **25**
4.1. Layer potentials . . . . . 25
4.2. Spherical inclusions . . . . . 30
4.2.1. Spherical harmonics . . . . . 30
4.2.2. Layer potentials on a sphere . . . . . 31

**5. Strongly interacting systems** **35**
5.1. Bubble oscillation . . . . . 35
5.1.1. Inverting the system . . . . . 35
5.1.2. Strong interaction . . . . . 39
5.2. Resonant oscillation . . . . . 41
5.3. Scattered solution . . . . . 44
5.4. Single spherical bubble systems . . . . . 47
5.4.1. Operator relations . . . . . 47



Die approbierte gedruckte Originalversion dieser Diplomarbeit ist an der TU Wien Bibliothek verfügbar
The approved original version of this thesis is available in print at TU Wien Bibliothek.
TU Bibliothek Your knowledge hub WIEN

5.4.2. Internal pressure gradient . . . . . 49
5.4.3. Primary Bjerknes force . . . . . 52

**6. Weakly interacting system** **55**
6.1. Scaling distance decomposition . . . . . 55
6.1.1. Far field expansion . . . . . 56
6.1.2. Separated and interaction parts . . . . . 58
6.1.3. Resonance frequency and resonance coefficient . . . . . 60
6.2. Far field interaction between spheres . . . . . 64
6.3. Secondary Bjerknes force . . . . . 66

**7. Multiple strongly interacting bubbles** **69**
7.1. Surface pressure and displacement . . . . . 72
7.2. Coupling spherical bubbles . . . . . 74
7.3. Eigenfunction of two spheres . . . . . 79
7.3.1. Eigenfunction in bispherical coordinates . . . . . 80
7.3.2. Connecting bispherical to spherical coordinates . . . . . 82
7.4. Capacity matrix . . . . . 85
7.5. Asymptotic case . . . . . 88
7.5.1. Close to touching . . . . . 88
7.5.2. Far field . . . . . 89
7.6. Numerical illustration . . . . . 93
7.6.1. Similar sized bubbles . . . . . 95
7.6.2. Differently sized bubbles . . . . . 97

**8. Summary, limitations and outlook** **99**

**Bibliography** **101**

**Appendices** **103**
A. Reynolds transport theorem . . . . . 103
B. Coupling spherical bubbles . . . . . 104
C. Far field . . . . . 106
D. Empirical study . . . . . 110
D.1. Additional simulations . . . . . 110
D.2. Error . . . . . 110

Die approbierte gedruckte Originalversion dieser Diplomarbeit ist an der TU Wien Bibliothek verfügbar
The approved original version of this thesis is available in print at TU Wien Bibliothek.
TU Bibliothek Your knowledge hub WIEN

# Nomenclature

$\tilde{\mathcal{A}}_D$ Modified $\mathcal{A}_D^0$ operator. Section 5.1.1

$\mathcal{A}_D/\boldsymbol{F}$ Operator and vector valued function of the system for the potentials. $\mathcal{A}_D(\omega,\delta)\boldsymbol{\phi} = \boldsymbol{F}$ Section 5.1.1

$\mathcal{A}_D^{m,n}$ Terms of the decomposition of $\mathcal{A}_D$. Section 5.1.2

$\beta_i/\beta_{i,j}$ Phase shift for incident wave $\beta_i \coloneqq \boldsymbol{k}\cdot\boldsymbol{z}_i$ and waves travelling between bubble clusters $\beta_{i,j} \coloneqq k_l d_{i,j}$. Section 6.1

$\kappa_l/\kappa_b$ Bulk modulus of the liquid/bubble. Section 3.2

$\boldsymbol{C}/\tilde{\boldsymbol{C}}$ Capacity and normalized Capacity matrix; $\boldsymbol{C}_{i,j} \coloneqq -\langle \chi_{\partial D_i}, \varphi_j\rangle_{L^2(\partial D)}$; $\tilde{\boldsymbol{C}}_{i,j} \coloneqq |D_i|^{-1}\boldsymbol{C}_{i,j}$. Section 4.1

$\triangle\boldsymbol{x}$ Distance to the corresponding bubble cluster center $\triangle\boldsymbol{x} \coloneqq x - \boldsymbol{z}_i$ for $\boldsymbol{x}\in D_i$. Section 6.1

$\delta$ Contrast; $\delta \coloneqq \frac{\rho_b}{\rho_l}$. Section 3.2

$\rho_l/\rho_b$ Density of the liquid/bubble. Section 3.2

$\boldsymbol{F}^{\mathrm{b}}_{1/2}$ Primary/Secondary Bjerknes force. Section 3.4

$\boldsymbol{F}^{b,e}_{1/2}$ Classical approximation of the effective primary/secondary Bjerknes force. Section 2.3

$\chi_D$ Indicator function of $D$. $\chi_D|_D = 1$ and $\chi_D|_{D^c} = 0$.

$k_l/k_b$ Wave vector in the liquid/bubble. Section 3.2

$\lambda_i/\boldsymbol{v}_i$ Eigenvalue and eigenvector of $\boldsymbol{D}^{-1}\boldsymbol{C}$. $\boldsymbol{V}$ is the matrix with the eigenvectors $\boldsymbol{v}_i$ as columns. Section 5.2

$\omega$ Frequency of the incident wave. Section 3.2

$\omega_i$ Resonant frequency corresponding to eigenvalue $\lambda_i$. Section 5.2

$\omega_{M,i}$ First order in $\delta$ of resonant frequency corresponding to eigenvalue $\lambda_i$. Section 5.2

p Pressure field of the linearised problem. Section 3.2.3

$\mathrm{p}_{\mathrm{in}}$ Incident pressure field. Section 3.2.3



Die approbierte gedruckte Originalversion dieser Diplomarbeit ist an der TU Wien Bibliothek verfügbar
The approved original version of this thesis is available in print at TU Wien Bibliothek.
TU Bibliothek Your knowledge hub WIEN

$\zeta_i$ Resonant potential $\zeta_i \coloneqq \sum_i \boldsymbol{V}_{i,j}\varphi_j$. Section 5.3

$S_D^{\boldsymbol{k}}/K_D^{\boldsymbol{k}}$ Single layer potential and Neumann Poincaré operator. Section 4.1

$\boldsymbol{u}$ Displacement field of the linearised problem. Section 3.2.3

$\widehat{\boldsymbol{v}}$ For a vector field $\widehat{\boldsymbol{v}}$ is the field $\boldsymbol{v}$ in the Lagrange picture. For a vector it is the corresponding vector with unit length.

$\varphi_i$ $\varphi_i \coloneqq (S_D^0)^{-1}[\chi_{\partial D_i}]$. Section 4.1

$\boldsymbol{\phi}$ Potential of solution with decomposition $\boldsymbol{\phi} = \boldsymbol{\varphi} + \tilde{\boldsymbol{\phi}}$ and $\tilde{\boldsymbol{\phi}} \perp \boldsymbol{\varphi}_i$ for all $i$. Section 5.1.1

$c_l/c_b$ Speed of sound in the liquid/bubble, $c \coloneqq \sqrt{\frac{\kappa}{\rho}}$. Section 3.2

$Y_l^m/\tilde{Y}_l^m$ Normalized and non-normalized spherical harmonics. Section 4.2

$D$ Bubble domains $D = \cup_i D_i$. Section 4.0

$d$ Distance between bubbles.

$M/M_e$ Mass/effective mass of a bubble. Section 2.1.1

$P_l^m$ Associated Legendre Polynomials. Section 4.2

$r_i/\boldsymbol{z}_i$ Radius/Centre of spherical inclusion $D_i = B_{r_i}(\boldsymbol{z}_i)$.

Die approbierte gedruckte Originalversion dieser Diplomarbeit ist an der TU Wien Bibliothek verfügbar
The approved original version of this thesis is available in print at TU Wien Bibliothek.
TU Bibliothek Your knowledge hub WIEN

# 1. Introduction

Bubbles are made up of at least two phases and can thus produce very complex problems. There is a long history on the study of their interactions with other objects and among themselves. Two pioneers of this field were C.A. Bjerknes and his son Vilhelm Bjerknes who were the first to describe the forces on air bubbles inside a liquid [1] due to an incident pressure field. In honor of their contributions the mean translatory forces are named after them. They are mostly looked at in a linear regime, although nonlinear effects can also be relevant if the forcing amplitude gets large. We will focus on the former case and refer to a report by Werner Lauterborn and Thomas Kurz [2] for general results.
The interactions between the pressure field and bubbles are most easily measured by placing them inside a weak standing wave [3, 4]. Depending on their size and the forcing frequency they get pushed towards the pressure node or antinode. It was established that the source of this translatory force is due to the oscillations of the bubble and its interaction with the incident pressure field. Furthermore, for well separated bubbles the main parameter that decides the direction of the Bjerknes force has been found to be the phase shifts between the interface movement and an incident field. It was observed that the direction of the forces has a sudden change near the Minnaert frequency of a bubble. Minnaert [5] first noticed that bubble oscillations can be modeled by a driven harmonic oscillator with associated resonance frequency. Most interestingly, the model predicts a singularity in the coefficient of the scattered wave and thus a sudden sign reversal of the force. The derivation was later refined with dampening factors, which are made up of viscosity, thermal and radiative terms [6]. This results in a "softening" of the singularity and in a continuous change of phase.
Two contributions to the forces have commonly been stated. The primary Bjerknes force is the result of the interaction between the forcing pressure field and the bubbles interface movement. In contrast to that is the secondary Bjerknes force which acts between two bubbles and results in mutual attraction or repulsion depending if their oscillations are in or out of phase. Crum compared in his paper [3] the theoretical predictions with experimental data and derived a simple formula for this interactive force for well separated bubbles.
It turns out that the secondary Bjerknes force has a very complicated dependency on the distance and thus has not been analyzed exhaustively. Generally, three main cases were identified. The simplest cases are two bubbles repelling or attracting each other over all distances. They appear for forcing frequencies far away from the Minnaert frequency and are well understood. The most interesting situation occurs when two bubbles attract each other over large distances, while at the same time they repel each other at closer ranges. In that case the bubbles jitter at a distance from each other and make up a stable pair.
In this thesis we will cover a new model for the forces on the bubbles and present an approach using layer potential techniques for solving the system. Our model considers



Die approbierte gedruckte Originalversion dieser Diplomarbeit ist an der TU Wien Bibliothek verfügbar
The approved original version of this thesis is available in print at TU Wien Bibliothek.
TU Bibliothek Your knowledge hub WIEN

full interactions between the bubbles and is in comparison to conventional approaches not limited by the approximation of uniform bubble expansion. Due to uniformity being increasingly violated for closer separation distances this suggests that our model could prove to be more accurate for systems of bubbles in close proximity to each other. Simulations in the last chapter done for two bubble systems show complex interactions, like a bubble pair getting accelerated in the same direction by the secondary Bjerknes force, that have to the knowledge of the author not been described so far. This could indicate new movement patterns if the error due to linearisation does not get too large. This thesis will look at two types of interactions. Firstly, we will look at general strongly interacting systems. They contain full interaction terms between the bubbles and produce complex resonance frequencies. We are going to look in detail into the single and two bubble case. Second, we will look at weakly interacting systems, which are made up of bubbles, where the separation distance scales indirectly proportional with the driving frequency. This greatly simplifies the systems and allows us to use the solution of isolated bubbles to calculate the Bjerknes force. We will now give a short outline of the chapters.

In chapter *two* we are going to take a closer look at some derivations that have been used to arrive at the classical formulas for the Bjerknes forces. This will give us an idea of the approach that is often taken and provide us with reference formulas for later comparisons. In chapter *three* we will find a mathematical model using the Lagrange representation of fluid dynamics formulas and apply linearisation under the assumption of weak forcing amplitudes. Finally, a formula for the approximated forces on a bubble will be derived. Chapter *four* will cover an introduction in layer potential techniques. For later use we will also look at statements about spherical harmonics and layer potentials on spheres. Readers familiar with these techniques can skip this chapter. Chapter *five* will begin with some general observations about strongly interacting systems and descriptions of the resonance frequency and scattered solution. We will then derive the primary Bjerknes force for single spherical bubble systems. Chapter *six* introduces the weakly interacting system and shows how one can use isolated systems to calculate the resonance frequencies and scattered solutions of the full system. We will then calculate the secondary Bjerknes force for weakly interacting spherical bubbles. This chapter is independent of chapter seven and can thus be skipped if one is only interested in the strongly interacting case. In Chapter *seven* the strongly interacting case of two spherical bubbles is covered. We are going to derive the resonance potentials in spherical harmonics and find a formula of the secondary Bjerknes force. This formula will match up asymptotically with the classical approximation for well separated bubbles. Additionally, we will take a look at some simulations using our formulas in the spherical harmonics basis and discuss the observations. Finally, chapter *eight* will summarize the results and talk about limitations and possible steps forward.

Die approbierte gedruckte Originalversion dieser Diplomarbeit ist an der TU Wien Bibliothek verfügbar
The approved original version of this thesis is available in print at TU Wien Bibliothek.
TU Bibliothek Your knowledge hub WIEN

# 2. Historical considerations

In this chapter we will take a look at some historical derivations of the primary and secondary Bjerknes forces. The classical experiment to see the primary Bjerknes force is made up of a system with a standing incident wave $\mathrm{p_{in}}(\boldsymbol{x}, t) = \tilde{\mathrm{p}}_{\mathrm{in}} \sin(\omega t) \cos(\boldsymbol{k} \cdot \boldsymbol{x} + \beta)$. Depending on the size of the bubbles and the forcing frequency $\omega$ the bubbles will get pushed towards the pressure nodes $\cos(\boldsymbol{k} \cdot \boldsymbol{x} + \beta) = 0$ or anti-nodes $\sin(\boldsymbol{k} \cdot \boldsymbol{x} + \beta) = 0$. The secondary Bjerknes force on the other hand is most easily calculated in a system of well separated bubbles. There we can consider them separately and only include the first order interactions afterwards. To achieve this we will first calculate how a bubble oscillates inside of a primary pressure field and then look at the secondary pressure field that gets radiated outward from said bubble. Finally, we can combine these two results and arrive at an approximation of the secondary Bjerknes force.
For easier considerations we will assume that the liquid has no viscosity, has zero curl and that the bubble is not rotating. In the kinetic bubble section we will look at how the movement of a rigid sphere inside of a liquid can be approximated. In the pulsating bubble section we will derive the movement of the bubble walls and the secondary pressure field. Finally in the Bjerknes forces section we will derive the primary and secondary Bjerknes forces.

## 2.1. The kinetic bubble

In this section we assume that a rigid sphere with radius $r$ moves along the $z$ axis of the system with velocity $v_z(t)$. We neglect the viscosity and compressibility of the liquid and assume that the homogeneous liquid has a curl free velocity field. This reduces the forces on the bubble to only 2 contributions. The first one appears due to the undisturbed flow, which we will approximate with Buoyancy considerations and the second one is a virtual or added mass term [7, p. 100]. We will now use the conservation of energy for a simpler description. The energy is made up of the kinetic energy of the sphere and the liquid and some potential energy, namely

$$E_{kin,l} + E_{kin,b} + E_{pot} = E = const. \tag{2.1.1}$$

We thus have due to $\partial_t E_{kin,b} = \partial_t \left( \frac{M v_z^2}{2} \right) = v_z M \partial_t v_z$ for $M := |B_r| \rho_b$ that

$$\partial_t E_{kin,l} + v_z M \partial_t v_z = -\partial_t E_{pot}. \tag{2.1.2}$$

### 2.1.1. Added mass

This section is going to reproduce the arguments of [7, p. 91]. We will now start by establishing the kinetic energy of the liquid.



Die approbierte gedruckte Originalversion dieser Diplomarbeit ist an der TU Wien Bibliothek verfügbar
The approved original version of this thesis is available in print at TU Wien Bibliothek.
TU Bibliothek Your knowledge hub WIEN

For that we first make the assumption $\mathrm{rot}(\boldsymbol{v}) = 0$ for the velocity field $\boldsymbol{v}$ of the liquid. We have thus a potential $\phi$ with

$$\boldsymbol{v} = \nabla\phi. \tag{2.1.3}$$

The incompressibility of the liquid now gives us

$$\Delta\phi = 0. \tag{2.1.4}$$

Furthermore we approximate the bubble as a rigid sphere which pushes the liquid in normal direction to the surface. We thus have the boundary condition

$$\frac{\mathrm{d}\phi}{\mathrm{d}\boldsymbol{n}}(r,\theta,\phi) = v_z\cos(\theta). \tag{2.1.5}$$

Furthermore we assume that the impact of the bubble movement declines over the distance, more specifically for large $\boldsymbol{x}$ we have

$$\frac{\mathrm{d}\phi}{\mathrm{d}|\boldsymbol{x}|}(\boldsymbol{x}) = \mathcal{O}(|\boldsymbol{x}|^{-2}). \tag{2.1.6}$$

A basis of the general solutions in spherical coordinates are the well known solid harmonics, they can be derived by separation of variables of the laplace equation. We arrive at the general solution

$$\phi(\boldsymbol{x}) = \sum_{l}\sum_{m=-l}^{l} a_{l,m}\frac{1}{|\boldsymbol{x}|^{l+1}}Y_l^m(\hat{\boldsymbol{x}}) + b_{l,m}|\boldsymbol{x}|^l Y_l^m(\hat{\boldsymbol{x}}) \tag{2.1.7}$$

with the spherical harmonics $Y_l^m$. For the definition of $Y_l^m$ see section 4.2.1. Under the asymptotic condition the second terms disappears and we get

$$\phi(\boldsymbol{x}) = \sum_{l}\frac{1}{|\boldsymbol{x}|^{l+1}}\sum_{m=-l}^{l} a_{l,m}Y_l^m(\hat{\boldsymbol{x}}). \tag{2.1.8}$$

The solution to the boundary conditions is now

$$\phi = -\frac{r^3}{2|\boldsymbol{x}|^2}v_z\cos(\theta). \tag{2.1.9}$$

Figure 2.1 (a) shows the velocity field of such a sphere moving through the liquid. The red arrows represent the normal component of the sphere's velocity on the boundary and the blue arrows the velocity of the liquid.
Next we will look at the kinetic energy of the liquid. We note that due to $\phi$ being harmonic and equation 2.1.9 we get

$$\begin{aligned} E_{kin,l} &= \frac{\rho_l}{2}\int_{\mathbb{R}^3/B_r}\boldsymbol{v}^2\,\mathrm{d}\boldsymbol{x} = \frac{\rho_l}{2}\int_{R^3/B_r}\nabla\cdot(\phi\nabla\phi)\,\mathrm{d}\boldsymbol{x} \\ &= -\frac{\rho_l}{2}\int_{\partial B_r}\phi\frac{\mathrm{d}\phi}{\mathrm{d}\boldsymbol{n}}\,\mathrm{d}\sigma = \frac{\pi r^3 v_z^2\rho_l}{3}. \end{aligned} \tag{2.1.10}$$

Die approbierte gedruckte Originalversion dieser Diplomarbeit ist an der TU Wien Bibliothek verfügbar
The approved original version of this thesis is available in print at TU Wien Bibliothek.
TU Bibliothek Your knowledge hub WIEN

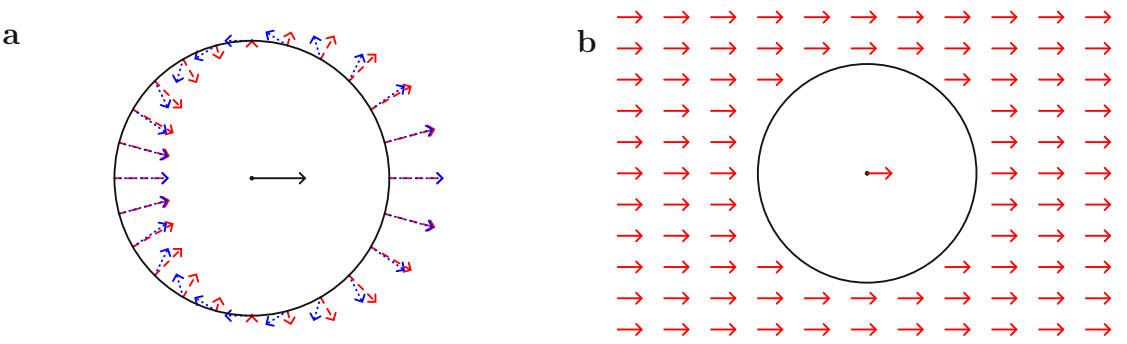


Figure 2.1.: (a) Sketch of a bubble moving inside an incompressible liquid. The blue arrows represent the velocity of the liquid, while the red arrows represent the radial components of the velocity. (b) Sketch of a bubble getting accelerated along with the liquid. The red arrows represent the acceleration field of the liquid and the bubble.

We further see that

$$\partial_t E_{kin,l} = \frac{2\pi r^3 \rho_l v_z \partial_t v_z}{3}. \tag{2.1.11}$$

Plugging this into the energy equation 2.1.2 and dividing by $v_z$ we arrive at

$$|B_r|\rho_b \partial_t v_z + \frac{2\pi r^3 \rho_l \partial_t v_z}{3} = |B_r| \left(\rho_b + \frac{\rho_l}{2}\right) \partial_t v_z = -\frac{\partial_t E_{pot}}{v_z}. \tag{2.1.12}$$

This equation tells us that we can consider the impact of the movement of the liquid on the bubble as an added inertial mass of the bubble. The total effective mass is thus

$$M_e \coloneqq |D| \left(\rho_b + \frac{\rho_l}{2}\right). \tag{2.1.13}$$

We restate 2.1.12 now to

$$\boxed{M_e \partial_t v_z = -\frac{\partial_t E_{pot}}{v_z} =: F^e} \tag{2.1.14}$$

with the effective force $\boldsymbol{F}^e$. For our calculations in the later chapters we will look at the total force that acts directly on the gas inside the bubble, which has mass $M = |B_r|\rho_b$. We can see that the forces with effective mass $\boldsymbol{F}^e$ and the forces with normal mass $\boldsymbol{F}$ are related by

$$\frac{\boldsymbol{F}^e}{M_e} = \frac{\mathrm{d}\boldsymbol{v}}{\mathrm{d}t} = \frac{\boldsymbol{F}}{M} \tag{2.1.15}$$

for $\boldsymbol{v}$ being the velocity of the bubble. We thus get

$$\boldsymbol{F} = \boldsymbol{F}^e \frac{M}{M_e} = \boldsymbol{F}^e \frac{2\delta}{1+2\delta} = 2\delta \boldsymbol{F}^e + \mathcal{O}(\delta^2). \tag{2.1.16}$$

with the contrast $\delta \coloneqq \frac{\rho_b}{\rho_l} < \frac{1}{2}$.

Die approbierte gedruckte Originalversion dieser Diplomarbeit ist an der TU Wien Bibliothek verfügbar
The approved original version of this thesis is available in print at TU Wien Bibliothek.
TU Bibliothek Your knowledge hub WIEN

### 2.1.2. Kinematic Buoyancy approximation

In the books by Vilhelm Bjerknes [1], where he wrote down the work done by him and his father Carl Anton Bjerknes, he introduced a force acting on objects inside a liquid flow. A translation of his explanation reads as follows.

> A body moving at the same rate as a translatory accelerated liquid experiences a buoyancy with the same direction as the acceleration and with a magnitude of the acceleration times the mass of the displaced liquid.

This can be easily seen by considering a reference frame in which the liquid and bubbles are stationary and experience a force in the opposite direction of the acceleration instead of moving. In this transformed system we get a conventional Buoyancy force, which is proportional to the displaced mass of the liquid. See figure 2.1 (b) for a sketch of such a field.
Bjerknes now assumes two generalizations in order to apply this principle to real systems.

- First, he assumes that this law still holds if the liquid does not strictly follow a linear movement, but instead a weakly curved path.
- Second, the bubble does not need to follow the movement of the liquid exactly. This would result in an additional inertia, which gets neglected. He then observed that the incident flow can be taken instead of the real flow to calculate the force.

Using these generalizations and Eulers equation we arrive at

$$\boldsymbol{F}^e \approx \int_{D(t)} \rho_l \dot{\boldsymbol{v}}_{in}\, \mathrm{d}\boldsymbol{x} = -\int_{D(t)} \nabla \mathrm{p}_{\mathrm{in}}\, \mathrm{d}\boldsymbol{x}, \tag{2.1.17}$$

where $\mathrm{p}_{\mathrm{in}}$ is the incident pressure field in the liquid without the inclusion.
We can arrive at the same result using the energy equation if we assume that the pressure field is approximately the incident field and that $\mathrm{p}_{\mathrm{in}}(\boldsymbol{z})$ is constant in time. We can then write for the potential energy

$$E_{pot} \approx -\int_{\mathbb{R}^3\setminus\overline{D(t)}} \mathrm{p}_{\mathrm{in}}(\boldsymbol{z})\, \mathrm{d}\boldsymbol{z} = -\int_{\mathbb{R}^3} \mathrm{p}_{\mathrm{in}}(\boldsymbol{z})\, \mathrm{d}\boldsymbol{z} + \int_{D(t)} \mathrm{p}_{\mathrm{in}}(\boldsymbol{z})\, \mathrm{d}\boldsymbol{z}. \tag{2.1.18}$$

We now get for the displacement vector $\boldsymbol{u}(t)$ of the sphere

$$\begin{aligned} \frac{\mathrm{d}}{\mathrm{d}t} E_{pot} \approx & \frac{\mathrm{d}}{\mathrm{d}t} \int_{D(t)} \mathrm{p}_{\mathrm{in}}(\boldsymbol{z})\, \mathrm{d}\boldsymbol{z} = \frac{\mathrm{d}}{\mathrm{d}t} \int_{D} \mathrm{p}_{\mathrm{in}}(\boldsymbol{x}+\boldsymbol{u}(t))\, \mathrm{d}\boldsymbol{x} \\ = & \boldsymbol{v} \cdot \int_{D} \nabla \mathrm{p}_{\mathrm{in}}(\boldsymbol{x}+\boldsymbol{u}(t))\, \mathrm{d}\boldsymbol{x} = \boldsymbol{v} \cdot \int_{D(t)} \nabla \mathrm{p}_{\mathrm{in}}\, \mathrm{d}\boldsymbol{z}. \end{aligned} \tag{2.1.19}$$

This provides us with the approximation for the velocity $\boldsymbol{v}$ of the bubble (which can also be found in [8])

$$\boxed{M_e \partial_t \boldsymbol{v} \approx -\int_{D(t)} \nabla \mathrm{p}_{\mathrm{in}}\, \mathrm{d}\boldsymbol{x}.} \tag{2.1.20}$$

Die approbierte gedruckte Originalversion dieser Diplomarbeit ist an der TU Wien Bibliothek verfügbar
The approved original version of this thesis is available in print at TU Wien Bibliothek.
TU Bibliothek Your knowledge hub WIEN

## 2.2. Pulsating bubble

We will now look at the case of a bubble, that is uniformly expanding and contracting and has no translatory motion. Minnaert first noticed that the air water system can be modeled by a harmonic oscillator. We are going to follow the guide of [9] to see this. We will assume a background pressure of $\mathrm{p}_0$ and that near the bubble a uniform incident pressure field $\mathrm{p}_{\mathrm{in}}(t)$ is the source of the movement. Further the bubble has the radius $r_0 + u(t)$ which is changing in time. The velocity field $\boldsymbol{v}$ again follows $\operatorname{rot} \boldsymbol{v} = 0$ and thus we have the potential $\phi$ with

$$\boldsymbol{v} = \nabla \phi \tag{2.2.1}$$

and

$$\Delta \phi = 0. \tag{2.2.2}$$

Additionally, we have in spherical coordinates $(r, \theta, \varphi)$ that

$$\frac{\mathrm{d}\phi}{\mathrm{d}\boldsymbol{n}} = \partial_t u \tag{2.2.3}$$

at $r = r_0 + u(t)$. Using the asymptotic boundary condition 2.1.6 this leads to

$$\phi(r, \theta, \varphi) = -\partial_t u \frac{(r_0 + u)^2}{r}. \tag{2.2.4}$$

The kinetic energy of the liquid can now be calculated

$$\begin{aligned} E_{kin,l} &= \frac{\rho_l}{2} \int_{\mathbb{R}^3 / D(t)} \boldsymbol{v}^2 \,\mathrm{d}\sigma = 2\pi\rho_l \int_{r_0+u(t)}^{\infty} r^2 \left( \partial_t u(t) \frac{(r_0 + u(t))^2}{r^2} \right)^2 \mathrm{d}r \\ &= 2\pi\rho_l (\partial_t u(t))^2 (r_0 + u(t))^4 \int_{r_0+u(t)}^{\infty} r^{-2} \,\mathrm{d}r \\ &= 2\pi\rho_l (\partial_t u(t))^2 (r_0 + u(t))^3 \end{aligned} \tag{2.2.5}$$

Next, we will look at the bubble interior. We assume that a reversible adiabatic process takes place, namely for the pressure inside the bubble $P(t)$ we have

$$P(t)|D(t)|^\gamma = const. \tag{2.2.6}$$

Thus, the excess pressure $\mathrm{p} \coloneqq P - \mathrm{p}_0$ compared to the bubble in equilibrium with $u = 0$ on the inside only depends on the radius of the bubble. For $D(u) = \frac{4\pi(r_0+u)^3}{3}$ this turns the last equation to

$$\mathrm{p}(u) = P - p_0 = \mathrm{p}_0 \left( \frac{|D|^\gamma}{|D(u)|^\gamma} - 1 \right) = \mathrm{p}_0 \left( \left( 1 + \frac{u}{r_0} \right)^{-3\gamma} - 1 \right). \tag{2.2.7}$$

Die approbierte gedruckte Originalversion dieser Diplomarbeit ist an der TU Wien Bibliothek verfügbar
The approved original version of this thesis is available in print at TU Wien Bibliothek.
TU Bibliothek Your knowledge hub WIEN

Next we will calculate the potential energy contribution due to the pressure inside the bubble. We have

$$\begin{aligned} E_{pot,b} &= -\int_{D(t)} \mathrm{p}(t)\,\mathrm{d}\boldsymbol{x} = -\int_0^{u(t)} 4\pi(r_0+u)^2\mathrm{p}(u)\,\mathrm{d}u \\ &= -4\pi\int_0^{u(t)} (r_0+u)^2\mathrm{p}_0\left((r_0+u)^{-3\gamma}r_0^{3\gamma}-1\right)\mathrm{d}u \\ &= -4\pi\int_{r_0}^{u(t)+r_0} u^2\mathrm{p}_0\left(u^{-3\gamma}r_0^{3\gamma}-1\right)\mathrm{d}u \\ &= -4\pi\mathrm{p}_0\left(\frac{r_0^{3\gamma}}{3-3\gamma}((u(t)+r_0)^{3-3\gamma}-r_0^{3-3\gamma})-\frac{1}{3}((u(t)+r_0)^3-r_0^3)\right). \end{aligned} \tag{2.2.8}$$

Finally we get the potential energy due to the extra external pressure

$$E_{pot,e} = \int_{D(t)} \mathrm{p}_{\mathrm{in}}(t)\,\mathrm{d}\boldsymbol{x} = \frac{4\pi(r_0+u(t))^3}{3}\mathrm{p}_{\mathrm{in}}(t). \tag{2.2.9}$$

After neglecting the kinetic energy of the gas inside the bubble we have the Lagrangian

$$L \coloneqq E_{kin,l} - E_{pot,b} - E_{pot,e}. \tag{2.2.10}$$

Before proceeding we note that

$$\frac{\partial E_{pot,b}}{\partial u} = 4\pi\mathrm{p}_0(u(t)+r_0)^2\left(1-\left(\frac{u(t)}{r_0}+1\right)^{-3\gamma}\right). \tag{2.2.11}$$

This results in the Euler Lagrange equation

$$\begin{aligned} \frac{\mathrm{d}}{\mathrm{d}t}\frac{\partial L}{\partial(\partial_t u)} - \frac{\partial L}{\partial u} =& 6\pi(r_0+u(t))^2\rho_l(\partial_t u(t))^2 + 4\pi(r_0+u(t))^3\rho_l(\partial_t^2 u(t)) \\ &+ 4\pi(r_0+u(t))^2\left(\mathrm{p}_{\mathrm{in}}(t)+p_0\left(1-\left(\frac{u(t)}{r_0}+1\right)^{-3\gamma}\right)\right) \\ =& 0. \end{aligned} \tag{2.2.12}$$

We can rewrite this to

$$\begin{aligned} M(u)(\partial_t^2 u(t)) + \frac{\partial_u M(u)}{2}(\partial_t u(t))^2 \\ = -4\pi(r_0+u(t))^2\left(\mathrm{p}_{\mathrm{in}}(t)+p_0\left(1-\left(\frac{u(t)}{r_0}+1\right)^{-3\gamma}\right)\right) \end{aligned} \tag{2.2.13}$$

for $M(u) \coloneqq 4\pi(r_0+u(t))^3\rho_l$. This is the *Rayleigh-Plesset equation*. If we linearise it for small $\boldsymbol{u}$ then we get the equation of a driven harmonic oscillator

$$\partial_t^2 u(t) + \omega_M^2 u(t) = -\frac{\mathrm{p}_{\mathrm{in}}(t)}{\rho_l r_0} \tag{2.2.14}$$

Die approbierte gedruckte Originalversion dieser Diplomarbeit ist an der TU Wien Bibliothek verfügbar
The approved original version of this thesis is available in print at TU Wien Bibliothek.
TU Bibliothek Your knowledge hub WIEN

with the frequency

$$\omega_M := \sqrt{\frac{3\gamma \mathrm{p}_0}{\rho_l r_0^2}}. \tag{2.2.15}$$

For $\mathrm{p}_{\mathrm{in}}(t) = \tilde{\mathrm{p}}_{\mathrm{in}} \sin(\omega t)$ this gives us the solution

$$u(t) = \frac{\tilde{\mathrm{p}}_{\mathrm{in}} \sin(\omega t + \alpha)}{\rho_l r_0 (\omega^2 - \omega_M^2)}. \tag{2.2.16}$$

In our derivation we arrived at an undampened harmonic oscillator and have thus $\alpha = 0$. If we had done a more careful approach we would have gotten dampening terms for radiation loss, viscosity and surface tension [6]. One can prove that

$$\alpha = \arctan\left(\left(2\frac{\mu}{\rho_l r_0^2} + 2\frac{\mu_{th}}{\rho_l r_0^2} + \frac{\omega^2 r_0}{2c_l}\right)\frac{2\omega}{\omega^2 - \omega_0^2}\right), \tag{2.2.17}$$

where the sum is made up of three terms, which are due to viscous, thermal and acoustic effects respectively.
The oscillations are the source of a secondary pressure field. We have (due to the Euler equation) for a liquid particle with trajectory $\boldsymbol{r}(t)$ that

$$\begin{aligned}
\nabla \mathrm{p} =& -\rho_l \partial_t(\boldsymbol{v}(\boldsymbol{r}, t)) = -\rho_l \left(\partial_t \boldsymbol{v} + \sum_i \partial_i \boldsymbol{v} \partial_t \boldsymbol{r}_i\right) \\
=& -\rho_l \left(\frac{\partial_t(\partial_t u (r_0 + u)^2)}{r^2} - 2\frac{\partial_t u (r_0 + u)^2}{r^3} \widehat{\boldsymbol{e}}_r \cdot \boldsymbol{v}\right) \widehat{\boldsymbol{e}}_r \\
=& -\rho_l \left(\frac{\partial_t^2 u (r_0 + u)^2 + 2(\partial_t u)^2 (r_0 + u)}{r^2} + 2(\partial_t u)^2 \frac{(r_0 + u)^4}{r^5}\right) \widehat{\boldsymbol{e}}_r,
\end{aligned} \tag{2.2.18}$$

where we used equation 2.2.4, $\partial_t r = \boldsymbol{v}$ and $\widehat{\boldsymbol{e}}_r$ is the unit vector in radial direction. We now neglect all higher order terms in $u$ and use equation 2.2.16 to get

$$\nabla \mathrm{p} \doteq -\rho_l \frac{(\partial_t^2 u) r_0^2}{r^2} \widehat{\boldsymbol{e}}_r = \frac{\tilde{\mathrm{p}}_{\mathrm{in}} r_0 \omega^2}{r^2 (\omega^2 - \omega_M^2)} \sin(\omega t + \alpha) \widehat{\boldsymbol{e}}_r, \tag{2.2.19}$$

We can see a sketch of the field in figure 2.2 (a). Overall we arrive at

$$\mathrm{p} - \mathrm{p}_{\mathrm{in}} - \mathrm{p}_0 \doteq -\frac{\tilde{\mathrm{p}}_{\mathrm{in}} r_0 \omega^2}{r(\omega^2 - \omega_M^2)} \sin(\omega t + \alpha). \tag{2.2.20}$$

## 2.3. Bjerknes forces

The force on the bubble is a result of the changing volume of the bubble interacting with the changing pressure field near the bubble. The inclusion experiences a force that pushes it back and forth depending on the point in time during the oscillation. Over a period this will result in an overall translatory movement of the bubble.

Die approbierte gedruckte Originalversion dieser Diplomarbeit ist an der TU Wien Bibliothek verfügbar
The approved original version of this thesis is available in print at TU Wien Bibliothek.
TU Bibliothek Your knowledge hub WIEN

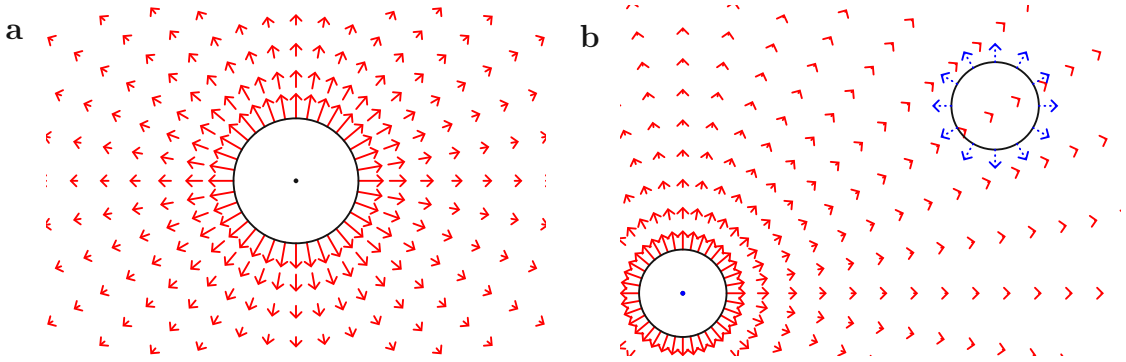


Figure 2.2.: (a) Sketch of a pulsating bubble. The red arrows represent the velocity field. (b) Sketch of the approach for calculating the secondary Bjerknes force. We neglect the interactions between the bubbles and use the field created by the oscillations of the first bubble to calculate the forces on the second bubble.

Before calculating this force we will first note that for rigid bubbles and a weak monochromatic incident wave $\mathrm{p}_{\mathrm{in}}(\boldsymbol{x},t) = \sin(\omega t + \alpha)\mathrm{p}_{\mathrm{in}}(\boldsymbol{x})$ no mean translatory force occurs. To see this we set $T \coloneqq \frac{2\pi}{\omega}$ and have

$$\begin{aligned} \frac{1}{T}\int_0^T \boldsymbol{F}^e(t)\,\mathrm{d}t &= -\frac{1}{T}\int_0^T \int_D \nabla \mathrm{p}_{\mathrm{in}}(\boldsymbol{x},t)\,\mathrm{d}\boldsymbol{x}\,\mathrm{d}t \\ &= -\frac{1}{T}\int_0^T \sin(\omega t+\alpha)\,\mathrm{d}t \int_D \nabla \mathrm{p}_{\mathrm{in}}(\boldsymbol{x})\,\mathrm{d}\boldsymbol{x} = 0. \end{aligned} \tag{2.3.1}$$

In contrast to this we will now look at bubbles with changing volume. For a weak incident pressure field with low frequency the bubble approximately still expands uniformly, as in the last section. Due to the slow change of the pressure gradient, we assume that the previous derivations still hold. We now define

**Definition 2.3.1.** *The primary Bjerknes force $\boldsymbol{F}_1$, for an incident pressure field of frequency $\omega$, is the mean force that a bubble experiences over a period.*

We get by using the kinematic buoyancy approximation the effective Bjerknes force

$$\boldsymbol{F}_1^{b,e} \coloneqq -\frac{1}{T}\int_0^T \int_{D(t)} \nabla \mathrm{p}_{\mathrm{in}}(\boldsymbol{x},t)\,\mathrm{d}\boldsymbol{x}\,\mathrm{d}t, \tag{2.3.2}$$

where $T$ is the period length of the incident pressure field.
If we have a system with more than 1 bubble then we also get a secondary force.

**Definition 2.3.2.** *The secondary Bjerknes force $\boldsymbol{F}_{2,i}$, for an incident pressure field of frequency $\omega$, on bubble $i$ is the additional force due to the interactions with the other bubbles compared to the single bubble system containing only bubble $i$.*

For the secondary Bjerknes force we will consider low order coupling between the bubbles. Namely we calculate the scattered pressure field by only considering a single bubble

Die approbierte gedruckte Originalversion dieser Diplomarbeit ist an der TU Wien Bibliothek verfügbar
The approved original version of this thesis is available in print at TU Wien Bibliothek.
TU Bibliothek Your knowledge hub WIEN

system. Then we add this to the incident pressure gradient on the other bubble, while calculating the pulsations directly with the incident pressure field. We can see a sketch of this approach in figure 2.2 (b). The first bubble creates a secondary pressure field, the gradient of this field is depicted as red arrows. The second bubble oscillates due to the incident field, depicted by the blue arrows.
If $\mathrm{p}_i$ is the solution to the problem with bubble $i$ removed then we get

$$\begin{aligned} \boldsymbol{F}_{2,i}^{b,e} &:= -\frac{1}{T}\int_0^T \int_{D_i(t)} \nabla \mathrm{p}_i(\boldsymbol{x},t)\,\mathrm{d}\boldsymbol{x}\,\mathrm{d}t - \boldsymbol{F}_{1,i}^{b,e} \\ &\approx -\frac{1}{T}\int_0^T \int_{\tilde{D}_i(t)} \nabla(\mathrm{p}_i - \mathrm{p}_{\mathrm{in}})(\boldsymbol{x},t)\,\mathrm{d}\boldsymbol{x}\,\mathrm{d}t, \end{aligned} \tag{2.3.3}$$

where $\boldsymbol{F}_{1,i}^{b,e}$ is the first Bjerknes force of a system with only bubble $i$ and $\tilde{D}_i(t)$ is the oscillating volume of bubble $i$ in this system. In total we can thus calculate the mean acceleration on the bubble

$$\boxed{M_e\langle \partial_t \boldsymbol{v}\rangle \approx \langle \boldsymbol{F}^{b,e}\rangle.} \tag{2.3.4}$$

### 2.3.1. Primary Bjerknes Force

We will now look at a one bubble systems. We assume small $\boldsymbol{k}$ and a weak standing incident wave $\mathrm{p}_{\mathrm{in}}(\boldsymbol{x},t) = \tilde{\mathrm{p}}_{\mathrm{in}}\sin(\omega t)\cos(\boldsymbol{k}\cdot\boldsymbol{x}+\beta)$. In the lowest order of $\boldsymbol{k}$ we see that $\nabla \mathrm{p}_{\mathrm{in}}$ is constant in space and get the approximation

$$\boldsymbol{F}_1^{b,e} \approx -\frac{1}{T}\int_0^T |D(t)|\nabla \mathrm{p}_{\mathrm{in}}(t)\,\mathrm{d}t. \tag{2.3.5}$$

For easier calculations we place the bubble at the center of the coordinate system. $|D(t)|$ can now be calculated by fixing the position of the inclusion and allowing it to only uniformly contract and expand like we did in section 2.2. This gives us for a bubble with radius $r_1$ that

$$\begin{aligned} \boldsymbol{F}_1^{b,e} \approx& \frac{1}{T}\int_0^T \frac{4\pi}{3}\left(r_1 + \frac{\tilde{\mathrm{p}}_{\mathrm{in}}\cos(\beta)\sin(\omega t+\alpha)}{\rho_l r_1(\omega^2-\omega_M^2)}\right)^3 \tilde{\mathrm{p}}_{\mathrm{in}}\boldsymbol{k}\sin(\beta)\sin(\omega t)\,\mathrm{d}t \\ \doteq& \frac{1}{T}\int_0^T \frac{4\pi}{3} r_1^3 \tilde{\mathrm{p}}_{\mathrm{in}}\boldsymbol{k}\sin(\omega t)\,\mathrm{d}t \\ &+ \frac{1}{T}\int_0^T 4\pi r_1^2 \frac{\tilde{\mathrm{p}}_{\mathrm{in}}\cos(\beta)\sin(\omega t+\alpha)}{\rho_l r_1(\omega^2-\omega_M^2)}\tilde{\mathrm{p}}_{\mathrm{in}}\boldsymbol{k}\sin(\beta)\sin(\omega t)\,\mathrm{d}t \\ =& \pi r_1 \frac{\tilde{\mathrm{p}}_{\mathrm{in}}^2\cos(\alpha)\sin(2\beta)}{\rho_l(\omega^2-\omega_M^2)}\boldsymbol{k}. \end{aligned} \tag{2.3.6}$$

Note that we neglected the higher order parts in $\tilde{\mathrm{p}}_{\mathrm{in}}$. This gives us

$$\boxed{\boldsymbol{F}_1^{b,e} \approx \pi r_1 \frac{\tilde{\mathrm{p}}_{\mathrm{in}}^2\cos(\alpha)\sin(2\beta)}{\rho_l(\omega^2-\omega_M^2)}\boldsymbol{k}.} \tag{2.3.7}$$

Die approbierte gedruckte Originalversion dieser Diplomarbeit ist an der TU Wien Bibliothek verfügbar
The approved original version of this thesis is available in print at TU Wien Bibliothek.
TU Bibliothek Your knowledge hub WIEN

### 2.3.2. Secondary Bjerknes Force

For a two bubble system with the same assumptions as in the 1 bubble case we get

$$\boldsymbol{F}_2^{b,e} \approx -\frac{1}{T}\int_0^T |\tilde{D}_1(t)|\nabla(\mathrm{p}_1 - \mathrm{p}_{\mathrm{in}})(t)\,\mathrm{d}t. \tag{2.3.8}$$

Here $p_1$ is the scattered pressure field if we remove bubble 1 and $\tilde{D}_1(t)$ the oscillating volume of bubble 1 in a system with the other bubbles removed. We assume that the distance between the bubbles is $d$ and $\mathrm{p}_{\mathrm{in}}(\boldsymbol{z}_i, t) \doteq \tilde{\mathrm{p}}_{\mathrm{in}}\cos(\beta_i)\sin(\omega t)$ in the lowest order of $\boldsymbol{k}$ at the location $\boldsymbol{z}_i$ of bubble $i$. $\widehat{\boldsymbol{d}}$ is the unit vector in the direction from the centres of bubble 1 to bubble 2. For the gradient we will use equation 2.2.19 for the second bubble and equation 2.2 for $\tilde{D}_1(t)$. We thus get similarly to the case of the primary Bjerknes force that

$$\begin{aligned}
\boldsymbol{F}_2^{b,e} \approx& -\frac{1}{T}\int_0^T \frac{4\pi}{3}\left(r_1 + \frac{\tilde{\mathrm{p}}_{\mathrm{in}}\cos(\beta_1)\sin(\omega t + \alpha_1)}{\rho_l r_1(\omega^2 - \omega_{M,1}^2)}\right)^3 \\
&\frac{\tilde{\mathrm{p}}_{\mathrm{in}}\cos(\beta_2) r_2\omega^2}{d^2(\omega^2 - \omega_{M,2}^2)}\sin(\omega t + \alpha_2)(-\widehat{\boldsymbol{d}})\,\mathrm{d}t \\
\doteq& \frac{1}{T}\int_0^T 4\pi r_1^2 \frac{\tilde{\mathrm{p}}_{\mathrm{in}}\cos(\beta_1)\sin(\omega t + \alpha_1)}{\rho_l r_1(\omega^2 - \omega_{M,1}^2)}\frac{\tilde{\mathrm{p}}_{\mathrm{in}}\cos(\beta_2) r_2\omega^2}{d^2(\omega^2 - \omega_{M,2}^2)}\sin(\omega t + \alpha_2)\widehat{\boldsymbol{d}}\,\mathrm{d}t \\
=& 2\pi r_1 r_2 \tilde{\mathrm{p}}_{\mathrm{in}}^2 \frac{\cos(\beta_1)\cos(\beta_2)\cos(\alpha_1 - \alpha_2)\omega^2}{d^2\rho_l(\omega^2 - \omega_{M,1}^2)(\omega^2 - \omega_{M,2}^2)}\widehat{\boldsymbol{d}}.
\end{aligned} \tag{2.3.9}$$

This gives us

$$\boxed{\boldsymbol{F}_2^{b,e} \approx 2\pi r_1 r_2 \tilde{\mathrm{p}}_{\mathrm{in}}^2 \frac{\cos(\beta_1)\cos(\beta_2)\cos(\alpha_1 - \alpha_2)\omega^2}{d^2\rho_l(\omega^2 - \omega_{M,1}^2)(\omega^2 - \omega_{M,2}^2)}\widehat{\boldsymbol{d}}.} \tag{2.3.10}$$

We can thus see that we get a repulsive force if the frequency is between the resonance frequencies and an attractive force for the other cases. Note that the $\beta_i$ are due to spatial positioning of the bubbles, while the $\alpha_i$ correspond to the phase shifts of the bubble oscillations due to dampening.

Die approbierte gedruckte Originalversion dieser Diplomarbeit ist an der TU Wien Bibliothek verfügbar
The approved original version of this thesis is available in print at TU Wien Bibliothek.
TU Bibliothek Your knowledge hub WIEN

# 3. Mathematical model

In this chapter we will informally motivate a linear model and an expression for the Bjerknes force for weak incident pressure fields. In the section Physical considerations we introduce the Lagrange representation and derive the governing equations for the displacement and pressure field using conservation of mass and momentum. After that we will linearise the equations, set the boundary conditions and connect the bubble interior to the liquid. Finally the last two sections cover our approximations of the forces on the bubble by an integral that only depends on surface terms. This will be convenient for our layer potential approach.

## 3.1. Physical considerations

The system is made up of a liquid with gas inclusions, namely connected $D_i(t)$, which are not touching and have smooth surfaces. We further set $D := \cup_i D_i$. Our goal is now to model the forces on the bubbles created by an incident pressure field.

### 3.1.1. Lagrange representation

We will work with the Lagrange representation, where we look at the evolution of mass parcels in space and time. A reference system will be used which is made up of the static inclusions $D_i$ that correspond to a system which does not evolve in time and transform it onto the evolving system. The function $\hat{z} : \mathbb{R}^3/(\partial D) \times (-T, T) \to \mathbb{R}^d$ maps the reference frame to the time slices for the liquid and the gas. We are further going to assume that the bubbles do not combine or split up. Thus we require that $\hat{\boldsymbol{z}}(\cdot, t)$ has a bijective continuous continuation from $\overline{D_i}$ to $\overline{D_i}(t)$ and from $\mathbb{R}^3/D_i$ to $\mathbb{R}^3/D_i(t)$. We can see in figure 3.1 a representation of the mapping. We further assume that

$$\hat{\boldsymbol{z}} \in C^2(\mathbb{R}^d \backslash \partial D \times (-T, T)), \tag{3.1.1}$$

and the derivatives of $\hat{z}$ have a continuous continuation on $\partial D$ from both sides separately and smooth $\partial D_i(t)$. We will also assume that the reference frame can be identified with the system at time 0 by $\hat{\boldsymbol{z}}(\boldsymbol{x}, 0) = \boldsymbol{x}$. We thus get for the displacement field $\hat{\boldsymbol{u}}$ and the transformation matrix $\hat{\boldsymbol{T}}$ that

$$\hat{\boldsymbol{u}}(\boldsymbol{x}, t) := \hat{\boldsymbol{z}}(\boldsymbol{x}, t) - \hat{\boldsymbol{z}}(\boldsymbol{x}, 0) = \hat{\boldsymbol{z}}(\boldsymbol{x}, t) - \boldsymbol{x}, \qquad \hat{\boldsymbol{T}}_{i,j} := \partial_i \hat{\boldsymbol{z}}_j = \delta_{i,j} + \partial_i \hat{\boldsymbol{u}}_j. \tag{3.1.2}$$

In figure 3.2 (a) we can see a sketch of the displacement field. For weak incident fields we get that $\det \hat{\boldsymbol{T}} > 0$, which provides us with the matrix inverse of $\hat{\boldsymbol{T}}$ and local invertability of the first derivatives of $\hat{\boldsymbol{z}}(\cdot, t)$. For this section we will notify a vector in the Lagrange representation (reference system) with $\boldsymbol{x}$, while $\boldsymbol{z}$ represents a vector in the Eulerian



Die approbierte gedruckte Originalversion dieser Diplomarbeit ist an der TU Wien Bibliothek verfügbar
The approved original version of this thesis is available in print at TU Wien Bibliothek.
TU Bibliothek Your knowledge hub WIEN

**a**

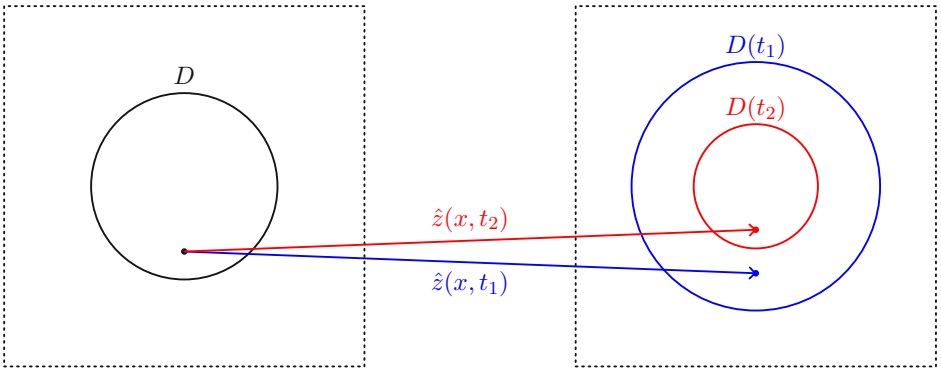


Figure 3.1.: (a) Sketch of reference frame and the mapping into the evolving system.

representation (at a time slice). For a function $f$ in the Eulerian system we define a corresponding function $\hat{f}$ in the reference system,

$$\hat{f}(\boldsymbol{x}, t) \coloneqq f(\hat{z}(\boldsymbol{x}, t), t). \tag{3.1.3}$$

In order to derive the differential equation we will look at the laws governing parcels of the fluids. Figure 3.2 (a) shows an example on how parcles can change for an expanding bubble.

### 3.1.2. Conservation of mass

We assume the conservation of mass $M$ for a parcel $V$

$$\frac{\mathrm{d}M}{\mathrm{d}t}(t) = 0. \tag{3.1.4}$$

We will now use Reynolds transport theorem A.1. We have for the density $\rho$ of the parcel $V(t)$ at $\boldsymbol{z}$ and time $t$ that

$$\frac{\mathrm{d}M}{\mathrm{d}t}(V, t) = \frac{\mathrm{d}}{\mathrm{d}t}\int_{V(t)} \rho(\boldsymbol{z}, t)\,\mathrm{d}z = \int_V \left(\frac{\mathrm{d}}{\mathrm{d}t}\hat{\rho} + \hat{\rho}(\hat{\boldsymbol{T}}^{-1}\nabla_{\boldsymbol{x}}) \cdot \frac{\mathrm{d}\hat{\boldsymbol{z}}}{\mathrm{d}t}\right) \det(\hat{\boldsymbol{T}})(\boldsymbol{x}, t)\,\mathrm{d}x. \tag{3.1.5}$$

Due to $\det \hat{\boldsymbol{T}} > 0$, $V$ being arbitrary and $\partial_t \hat{\boldsymbol{z}} = \partial_t \hat{\boldsymbol{u}}$ this results in

$$\frac{\mathrm{d}}{\mathrm{d}t}\hat{\rho} + \hat{\rho}(\hat{\boldsymbol{T}}^{-1}\nabla) \cdot \frac{\mathrm{d}\hat{\boldsymbol{u}}}{\mathrm{d}t} = 0. \tag{3.1.6}$$

This is the continuity equation in the reference frame.

### 3.1.3. Newtons law

We now assume that we can neglect the Lamé terms and thus have no shear stress. We also assume that only the pressure gradient is a significant force contribution. By Newtons second law we have for a parcel $V$

$$\partial_t \int_{V(t)} \rho(\boldsymbol{z}, t)(\partial_t \hat{\boldsymbol{z}})(\boldsymbol{x}(\boldsymbol{z}, t), t)\,\mathrm{d}\boldsymbol{z} = -\int_{V(t)} \nabla_{\boldsymbol{z}} \mathrm{p}(\boldsymbol{z}, t)\,\mathrm{d}\boldsymbol{z}. \tag{3.1.7}$$

Die approbierte gedruckte Originalversion dieser Diplomarbeit ist an der TU Wien Bibliothek verfügbar
The approved original version of this thesis is available in print at TU Wien Bibliothek.
TU Bibliothek Your knowledge hub WIEN

Using Reynolds transport theorem A.1 and the continuity equation 3.1.6 we get

$$\int_V \hat{\rho}(\boldsymbol{x},t)\frac{\mathrm{d}^2\hat{\boldsymbol{z}}}{\mathrm{d}t^2}(\boldsymbol{x},t)\det(\hat{\boldsymbol{T}})\,\mathrm{d}\boldsymbol{x} = -\int_V (\hat{\boldsymbol{T}}^{-1}\nabla_{\boldsymbol{x}})\hat{\mathrm{p}}(\boldsymbol{x},t)\det(\hat{\boldsymbol{T}})\,\mathrm{d}\boldsymbol{x} \tag{3.1.8}$$

Due to $V$ being arbitrary and $\partial_t\hat{\boldsymbol{z}} = \partial_t\hat{\boldsymbol{u}}$ this gives us in the reference frame

$$\boxed{\left(\hat{\rho}\frac{\mathrm{d}^2\hat{\boldsymbol{u}}}{\mathrm{d}t^2}\right)(\boldsymbol{x},t) = -\left((\hat{\boldsymbol{T}}^{-1}\nabla)\hat{\mathrm{p}}\right)(\boldsymbol{x},t).} \tag{3.1.9}$$

This equation can also be directly derived by taking the Euler equation and transforming it into the reference frame.

### 3.1.4. Equation of state

We now make the assumption that the pressure only depends on the density of the fluid. This is especially true for an adiabatic process as we will see later on. We have the equations of state

$$\hat{\mathrm{p}} = f_l(\hat{\rho}), \qquad \hat{\mathrm{p}} = f_b(\hat{\rho}) \tag{3.1.10}$$

inside the liquid and bubble respectively. For $\hat{\mathrm{p}} = f(\hat{\rho})$ we get

$$\frac{\mathrm{d}\hat{\mathrm{p}}}{\mathrm{d}t}(\boldsymbol{x},t) = \frac{\mathrm{d}f(\hat{\rho}(\boldsymbol{x},t))}{\mathrm{d}t} = \frac{\mathrm{d}f}{\mathrm{d}\hat{\rho}}(\hat{\rho}(\boldsymbol{x},t))\frac{\mathrm{d}\hat{\rho}}{\mathrm{d}t}(\boldsymbol{x},t) \tag{3.1.11}$$

and we can thus define the bulk modulus

$$\hat{\kappa}_{l/b}(\boldsymbol{x},t) \coloneqq \hat{\rho}(\boldsymbol{x},t)\frac{\mathrm{d}f_{l/b}}{\mathrm{d}\hat{\rho}}(\hat{\rho}(\boldsymbol{x},t)). \tag{3.1.12}$$

Next we rewrite equation 3.1.6 to

$$\boxed{\frac{\mathrm{d}}{\mathrm{d}t}\hat{\mathrm{p}} + \hat{\kappa}(\hat{\boldsymbol{T}}^{-1}\nabla)\cdot\frac{\mathrm{d}\hat{\boldsymbol{u}}}{\mathrm{d}t} = 0,} \tag{3.1.13}$$

where $\hat{\kappa}$ is defined piecewise by the corresponding equations of state inside and outside the bubble. Finally by combining equation (3.1.9) and (3.1.13) we arrive at

$$\frac{\mathrm{d}}{\mathrm{d}t}\frac{1}{\hat{\kappa}}\frac{\mathrm{d}\hat{\mathrm{p}}}{\mathrm{d}t} - (\hat{\boldsymbol{T}}^{-1}\nabla)\cdot\frac{1}{\hat{\rho}}(\hat{\boldsymbol{T}}^{-1}\nabla)\hat{\mathrm{p}} - \left(\hat{\boldsymbol{T}}^{-1}\left(\frac{\mathrm{d}}{\mathrm{d}t}\hat{\boldsymbol{T}}\right)\hat{\boldsymbol{T}}^{-1}\nabla\right)\cdot\frac{\mathrm{d}\hat{\boldsymbol{u}}}{\mathrm{d}t} = 0. \tag{3.1.14}$$

One thing to note is that historically the bubble is assumed to be an ideal gas with the deformation as an adiabatic process. This approximation holds in the low frequency domain and was often used to derive the bubble wall oscillations. A parcel $V$ undergoing a reversible adiabatic process follows $\mathrm{p}(t)V^{\gamma}(t) = \text{const}$. This gives us the equation of state

$$\hat{\mathrm{p}}(\boldsymbol{x},t)\hat{\rho}^{-\gamma}(\boldsymbol{x},t) = \mathrm{p}(\hat{\boldsymbol{z}}(\boldsymbol{x},t),t)\rho^{-\gamma}(\hat{\boldsymbol{z}}(\boldsymbol{x},t),t) = \mathrm{p}_0\rho_b^{-\gamma}, \tag{3.1.15}$$

where $\mathrm{p}_0$ is the pressure and $\rho_b$ the density inside the static bubble. For the density this would mean that

$$\hat{\rho} = \rho_b\left(\frac{\hat{\mathrm{p}}}{\mathrm{p}_0}\right)^{\frac{1}{\gamma}}. \tag{3.1.16}$$

Die approbierte gedruckte Originalversion dieser Diplomarbeit ist an der TU Wien Bibliothek verfügbar
The approved original version of this thesis is available in print at TU Wien Bibliothek.
TU Bibliothek Your knowledge hub WIEN

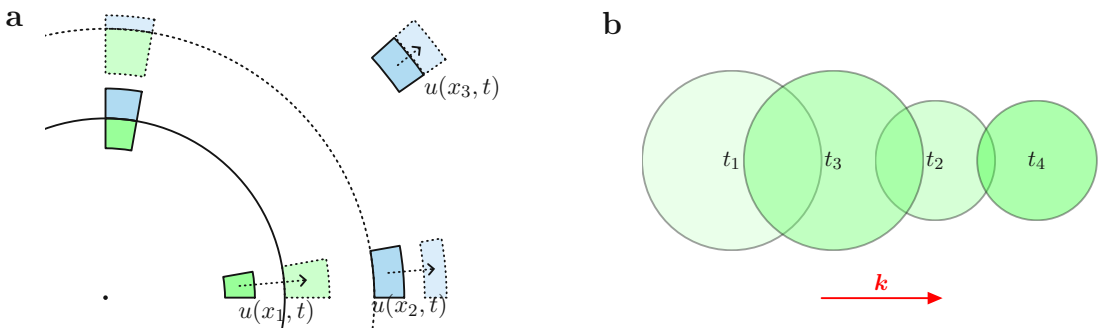


Figure 3.2.: (a) Sketch of displacement of volume elements due to bubble expansion using the breathing approximation. The solid lines correspond to the system at $t = 0$. (b) Sketch of movement of bubble due to Bjerknes force. The mean translatory movement of the bubble is described by the Bjerknes force.

Further the bulk modulus inside of the bubble is then

$$\hat{\kappa} = \gamma \hat{\mathrm{p}}(\boldsymbol{z}, t) = \kappa_b \frac{\hat{\mathrm{p}}(\boldsymbol{z}, t)}{\mathrm{p}_0}. \tag{3.1.17}$$

We note that for our work we only need the assumption of conservation of mass and an equation of state where $\hat{\mathrm{p}}$ only depends on $\hat{\rho}$.

### 3.1.5. Surface connections

We have so far not looked at the connection between problems inside and outside the bubble. For that we need additional assumptions. First we are going to assume that the liquid and the gas do not mix up. This lead us to the *no penetration condition*, namely

$$\boldsymbol{v} \cdot \boldsymbol{n}|_+ = \boldsymbol{v} \cdot \boldsymbol{n}|_- \tag{3.1.18}$$

on $\partial D(t)$. Secondly we note that we neglect surface tension terms and assume that the pressure is continuous

$$\mathrm{p}|_+ = \mathrm{p}|_- \tag{3.1.19}$$

on $\partial D(t)$.

## 3.2. The linearized solution

If the nonlinear effects are small then we find an approximation by linearizing the pde. We look at the static solution

$$\begin{aligned} \mathrm{p}_0 &\coloneqq \text{const}, \\ \boldsymbol{u}_0 &\coloneqq 0 \end{aligned} \tag{3.2.1}$$

and with $\chi_D$ being the indicator function of $D$ we have

$$\begin{aligned} \kappa_0 &\coloneqq \chi_D(\boldsymbol{x})\kappa_b + \chi_{\mathbb{R}^d \setminus \overline{D}}(\boldsymbol{x})\kappa_l, \\ \rho_0 &\coloneqq \chi_D(\boldsymbol{x})\rho_b + \chi_{\mathbb{R}^d \setminus \overline{D}}(\boldsymbol{x})\rho_l. \end{aligned} \tag{3.2.2}$$

Die approbierte gedruckte Originalversion dieser Diplomarbeit ist an der TU Wien Bibliothek verfügbar
The approved original version of this thesis is available in print at TU Wien Bibliothek.
TU Bibliothek Your knowledge hub WIEN

Note that $\kappa_b, \kappa_l$ represents the bulk modulus for the static bubble on the inside and outside respectively. Similarly $\rho_b, \rho_l$ is the density of the bubble and liquid for that system. Finally we have the speed of sound

$$c_l \coloneqq \sqrt{\frac{\kappa_l}{\rho_l}}, \qquad c_b \coloneqq \sqrt{\frac{\kappa_b}{\rho_b}}. \tag{3.2.3}$$

We now look at solutions of 3.1.14 close to the static solution, namely

$$\hat{\mathrm{p}} = \mathrm{p}_0 + \epsilon\tilde{\mathrm{p}}, \qquad \hat{\boldsymbol{u}} = \boldsymbol{u}_0 + \epsilon\tilde{\boldsymbol{u}}, \qquad \hat{\rho} = \rho_0 + \epsilon\tilde{\rho}, \qquad \hat{\kappa} = \kappa_0 + \epsilon\tilde{\kappa}. \tag{3.2.4}$$

Note that knowledge of the equations of state would allow us to find relations between the terms. Recall for example the reversible adiabatic process, which allows us to deduce terms for $\tilde{\rho}, \tilde{\kappa}$ inside the bubble depending only on $\hat{\mathrm{p}}$, see for example equations 3.1.17 and 3.1.16. Before linearising the differential equation note that we have $\hat{\boldsymbol{z}}(\boldsymbol{x}, t) = \boldsymbol{x} + \mathcal{O}(\epsilon)$ and thus $\hat{\boldsymbol{T}} = \mathbb{1} + \epsilon\tilde{\boldsymbol{T}}$. We will assume that $\epsilon \ll 1$ and only look at the lowest order in the resulting differential equation. Equations 3.1.9 and 3.1.13 turn to

$$\begin{aligned} \rho_0 \frac{\mathrm{d}^2\tilde{\boldsymbol{u}}}{\mathrm{d}t^2} + \nabla\tilde{\mathrm{p}} &= \mathcal{O}(\epsilon), \\ \kappa_0 \nabla \cdot \frac{\mathrm{d}\tilde{\boldsymbol{u}}}{\mathrm{d}t} + \frac{\mathrm{d}\tilde{\mathrm{p}}}{\mathrm{d}t} &= \mathcal{O}(\epsilon). \end{aligned} \tag{3.2.5}$$

Combining the equations gives us

$$\boxed{\frac{\mathrm{d}}{\mathrm{d}t}\frac{1}{\kappa_0}\frac{\mathrm{d}\tilde{\mathrm{p}}}{\mathrm{d}t} - \nabla \cdot \frac{1}{\rho_0}\nabla\tilde{\mathrm{p}} = \mathcal{O}(\epsilon).} \tag{3.2.6}$$

We will denote the linearised solution of this differential equation by p with linearised displacement field $\boldsymbol{u}$.

### 3.2.1. Surface connections

For the surface connection terms we note that slippage can take place in our model. This means that the outermost gas layer can move in relation to the innermost liquid layer. The no penetration condition reads for all $\boldsymbol{z} \in \partial D(t)$ in the reference frame

$$(\partial_t\hat{\boldsymbol{u}}|_+ \cdot \boldsymbol{n})(\boldsymbol{x}|_+(\boldsymbol{z}, t), t) = (\partial_t\hat{\boldsymbol{u}}|_- \cdot \boldsymbol{n})(\boldsymbol{x}|_-(\boldsymbol{z}, t), t), \tag{3.2.7}$$

where the subscript $\pm$ notifies the functions on the outside and inside of the bubble. Due to the assumption of $\hat{z} \in C^2$ and $\partial D(t)$ smooth we have $(\partial_t\hat{\boldsymbol{u}}|_\pm \cdot \boldsymbol{n}) \in C^1$ on the surface. With this and $|\boldsymbol{x}|_\pm(\boldsymbol{z}, t) - \boldsymbol{x}|_\pm(\boldsymbol{z}, 0)| = \mathcal{O}(\epsilon)$ we get

$$(\partial_t\hat{\boldsymbol{u}}|_\pm \cdot \boldsymbol{n})(\boldsymbol{x}|_\pm(\boldsymbol{z}, t), t) = (\partial_t\hat{\boldsymbol{u}}|_\pm \cdot \boldsymbol{n})(\boldsymbol{x}|_\pm(\boldsymbol{z}, 0), t) + \mathcal{O}(\epsilon^2). \tag{3.2.8}$$

We set $\boldsymbol{x}|_+(\boldsymbol{z}, 0) = \boldsymbol{x}|_-(\boldsymbol{z}, 0)$ and thus get

$$(\partial_t\hat{\boldsymbol{u}}|_+ \cdot \boldsymbol{n})(\boldsymbol{x}, t) = (\partial_t\hat{\boldsymbol{u}}|_- \cdot \boldsymbol{n})(\boldsymbol{x}, t) + \mathcal{O}(\epsilon^2). \tag{3.2.9}$$

Die approbierte gedruckte Originalversion dieser Diplomarbeit ist an der TU Wien Bibliothek verfügbar
The approved original version of this thesis is available in print at TU Wien Bibliothek.
TU Bibliothek Your knowledge hub WIEN

The same calculations work for $\hat{\mathrm{p}}$. Thus a natural choices for surface conditions of the linearized equation is

$$\begin{aligned} p|_+ &= p|_-, \\ \partial_t \boldsymbol{u}|_+ \cdot \boldsymbol{n} &= \partial_t \boldsymbol{u}|_- \cdot \boldsymbol{n} \end{aligned} \tag{3.2.10}$$

on $\partial D$.

### 3.2.2. Boundary conditions

For our purposes we are going to work with an incident pressure wave $\mathrm{p}_{\mathrm{in}}$ and analyse the response of the system. We will look at a plane incident waves $\mathrm{p}_{\mathrm{in}}(\boldsymbol{x}, t) = \tilde{\mathrm{p}}_{\mathrm{in}} e^{\mathrm{i}(\boldsymbol{k}\cdot\boldsymbol{x}+\omega t)}$ of a single frequency. Fourier transforming the pde 3.2.6 provides us with

$$\boxed{\frac{\omega^2}{\kappa_0}\mathrm{p}(\boldsymbol{x},\omega) + \nabla \cdot \frac{1}{\rho_0}\nabla \mathrm{p}(\boldsymbol{x},\omega) = 0.} \tag{3.2.11}$$

We now define the wave vectors in $k_l := \omega/c_l$ and $k_b := \omega/c_b$ inside the liquid and bubble respectively. It is now natural to take the Sommerfeld Radiation Condition in order to select the outgoing solutions for the scattered field.

**Definition 3.2.1.** *For the Helmholtz equation in 3 dimensions the Sommerfeld Radiation Condition (S.R.C.) for $p$ with incident field $p_{in}$ is*

$$\lim_{|\boldsymbol{x}|\to\infty} |\boldsymbol{x}| \left( \frac{\mathrm{d}}{\mathrm{d}|\boldsymbol{x}|} - \mathrm{i}k_l \right) (p - p_{in}) = 0 \tag{3.2.12}$$

*for $k_l := \omega/c_l$.*

To show the significance of the S.R.C. we note that it gets fulfilled by outgoing plane waves and violated by incoming ones. Going forward we are only going to look at incident waves with real $\omega$ and will assume that we have no resonance oscillations of the system. This fixes our solution to the frequency of the incident wave also called the forcing frequency.

### 3.2.3. Problem formulation

We will combine the results of the last sections for the formulation of the problem. We have an incident wave $\mathrm{p}_{\mathrm{in}}$, which is solution to $k_l^2 \mathrm{p}_{\mathrm{in}} + \Delta \mathrm{p}_{\mathrm{in}} = 0$. We now get that p is solution to our model if and only if $p$ has no resonance oscillations and

$$\boxed{\begin{array}{ll} k_l^2 \mathrm{p} + \Delta \mathrm{p} = 0 & \text{in } \mathbb{R}^3/\overline{D}, \\ k_b^2 \mathrm{p} + \Delta \mathrm{p} = 0 & \text{in } D, \\ \mathrm{p}|_- - \mathrm{p}|_+ = \mathrm{p}_{\mathrm{in}} & \text{on } \partial D, \\ \frac{\mathrm{dp}}{\mathrm{d}\boldsymbol{n}}|_- - \delta \frac{\mathrm{dp}}{\mathrm{d}\boldsymbol{n}}|_+ = \delta \frac{\mathrm{dp_{in}}}{\mathrm{d}\boldsymbol{n}} & \text{on } \partial D, \\ \lim_{|\boldsymbol{x}|\to\infty} |\boldsymbol{x}| \left( \frac{\mathrm{d}}{\mathrm{d}|\boldsymbol{x}|} - \mathrm{i}k_l \right) (\mathrm{p} - \mathrm{p}_{\mathrm{in}}) = 0 & \text{(S.R.C.)} \end{array}} \tag{3.2.13}$$

Die approbierte gedruckte Originalversion dieser Diplomarbeit ist an der TU Wien Bibliothek verfügbar
The approved original version of this thesis is available in print at TU Wien Bibliothek.
TU Bibliothek Your knowledge hub WIEN

for the contrast $\delta := \rho_l^{-1}\rho_b$, $c_{l/b} := \sqrt{\rho_{l/b}^{-1}\kappa_{l/b}}$, $\boldsymbol{k}_{l/b} = c_{l/b}^{-1}\omega$. We note that $\delta \sim 10^{-3}$ for a water air mixture. This will be the starting point later on for our expansion in $\omega$ and $\delta$. We also get for the displacement field

$$\boxed{\begin{array}{ll} \boldsymbol{u} = (\omega^2\rho_l)^{-1}\nabla \mathrm{p} & \text{for } \boldsymbol{x} \in \mathbb{R}^3/\overline{D}, \\ \boldsymbol{u} = (\omega^2\rho_b)^{-1}\nabla \mathrm{p} & \text{for } \boldsymbol{x} \in D. \end{array}} \tag{3.2.14}$$

## 3.3. Force integral approximation

In this section we will derive an approximation of the force on the bubbles. In the same way as we did for the linearisation of the pde we will look at solutions close to the static solution. The first relevant term is going to be of order $\epsilon^2$. Then we will approximate this force using the solution of the linearised problem and find a representation using surface integrals, which are more convenient to evaluate in our layer potential approach.
First we start by considering the non linear momentum equation 3.1.9 and define the force that acts on a bubble.

**Definition 3.3.1.** *The total force on the bubble for a solution close to the static solution* $\hat{p} = p_0 + \epsilon\tilde{p}$ *and* $\hat{\boldsymbol{u}} = \boldsymbol{u}_0 + \epsilon\tilde{u}$ *is*

$$\boldsymbol{F}(\tilde{p}, \tilde{\boldsymbol{u}}, t) := -\int_D \left((\hat{\boldsymbol{T}}^{-1}\nabla)\hat{p}\right) \det(\hat{\boldsymbol{T}})\, \mathrm{d}\boldsymbol{x}. \tag{3.3.1}$$

The next lemma expands the force in $\epsilon$ for later use.

**Lemma 3.3.2.** *The force on the inclusion close to the static solution can be written as*

$$\boldsymbol{F}(\tilde{p}, \tilde{\boldsymbol{u}}) = -\int_D \sum_{m=0}^{\infty} \epsilon^{m+1} \left(-\tilde{\boldsymbol{T}}\right)^m \nabla\tilde{p} \left(1 + \epsilon\nabla\cdot\tilde{\boldsymbol{u}} + \frac{\epsilon^2}{2}((\nabla\cdot\tilde{\boldsymbol{u}})^2 - \operatorname{Tr}\tilde{\boldsymbol{T}}^2) + \epsilon^3 \det(\tilde{\boldsymbol{T}})\right) \mathrm{d}\boldsymbol{x} \tag{3.3.2}$$

*where* $\tilde{\boldsymbol{T}}_{i,j} := \partial_i\tilde{\boldsymbol{u}}_j$.

*Proof.* We note the Jacobi identity

$$\partial_\epsilon \det(\hat{\boldsymbol{T}}) = \det(\hat{\boldsymbol{T}}) \operatorname{Tr}(\hat{\boldsymbol{T}}^{-1}\partial_\epsilon\hat{\boldsymbol{T}}). \tag{3.3.3}$$

Further this tells us for $\hat{\boldsymbol{T}} = \mathbb{1} + \epsilon\tilde{\boldsymbol{T}}$ that

$$\partial_\epsilon^2 \det(\hat{\boldsymbol{T}}) = \det(\hat{\boldsymbol{T}}) \left((\operatorname{Tr}(\hat{\boldsymbol{T}}^{-1}\partial_\epsilon\hat{\boldsymbol{T}}))^2 - \operatorname{Tr}(\hat{\boldsymbol{T}}^{-1}\partial_\epsilon\hat{\boldsymbol{T}}\hat{\boldsymbol{T}}^{-1}\partial_\epsilon\hat{\boldsymbol{T}})\right). \tag{3.3.4}$$

Finally using the Neuman series for the inverse of $\hat{\boldsymbol{T}} = \mathbb{1} + \epsilon\tilde{\boldsymbol{T}}$ provides the result. □

Before the next lemma we are going to approximate this force by replacing the pressure and displacement fields with the linearised solutions. We can then use the defining differential equations to find a surface integral representation of the force.
Next we see that

Die approbierte gedruckte Originalversion dieser Diplomarbeit ist an der TU Wien Bibliothek verfügbar
The approved original version of this thesis is available in print at TU Wien Bibliothek.
TU Bibliothek Your knowledge hub WIEN

**Lemma 3.3.3.** *We get for a solution inside the inclusion $p \in H^2(D)$ of 3.2.13 with $p|_{\partial D} \in H^1(\partial D)$ defined from the inside that*

$$\boldsymbol{F}_2(p, \boldsymbol{u}, t) = \frac{1}{\rho_b \omega^2} \int_{\partial D} (\nabla_T p)^2 \boldsymbol{n} - (\nabla p|_- \cdot \boldsymbol{n}) \nabla_T p \, \mathrm{d}\sigma \tag{3.3.5}$$

*where $\nabla p|_-$ is defined by continuous continuation from inside the bubble, $\boldsymbol{F}_2(p, \boldsymbol{u}, t)$ defined in lemma 3.3.2 and $\nabla_T$ is the tangential derivative.*

*Proof.* We note that

$$\boldsymbol{u} = \frac{1}{\rho_b \omega^2} \nabla \mathrm{p} \tag{3.3.6}$$

and

$$\Delta \mathrm{p} \partial_i \mathrm{p} = \nabla \cdot (\nabla \mathrm{p} \partial_i \mathrm{p}) - \nabla \mathrm{p} \cdot \nabla \partial_i \mathrm{p}. \tag{3.3.7}$$

This results in

$$\begin{aligned} ((\boldsymbol{T} - \nabla \cdot \boldsymbol{u}) \nabla \mathrm{p})_i &= \frac{1}{\rho_b \omega^2} \left(2(\partial_i \nabla \mathrm{p}) \cdot \nabla \mathrm{p} - \nabla \cdot (\nabla \mathrm{p} \partial_i \mathrm{p})\right) \\ &= \frac{1}{\rho_b \omega^2} \left(\partial_i (\nabla \mathrm{p})^2 - \nabla \cdot (\nabla \mathrm{p} \partial_i \mathrm{p})\right). \end{aligned} \tag{3.3.8}$$

Using the divergence theorem and noting that

$$(\nabla \mathrm{p})^2 \boldsymbol{n} - (\boldsymbol{n} \cdot \nabla \mathrm{p}) \nabla \mathrm{p} = (\nabla_T \mathrm{p})^2 \boldsymbol{n} - (\nabla \mathrm{p}|_- \cdot \boldsymbol{n}) \nabla_T \mathrm{p} \tag{3.3.9}$$

provides the result. □

Like in historical approaches we are going to consider the mean force over a period.

**Definition 3.3.4.** *The mean force over one period $T := \frac{2\pi}{\omega}$ for an incident wave with frequency $\omega$ is*

$$\langle \boldsymbol{F} \rangle := \frac{1}{T} \int_0^T \boldsymbol{F}(t) \, \mathrm{d}t. \tag{3.3.10}$$

For the same reason as we saw that the force for a static bubble disappears over a period, we will now see the same thing happening for the first order of the force.

**Lemma 3.3.5.** *The mean Force on the inclusion over one period of an incident field with frequency $\omega$ results in*

$$\langle \boldsymbol{F} \rangle = \langle \boldsymbol{F}_2 \rangle + \mathcal{O}(\epsilon^3). \tag{3.3.11}$$

*Proof.* The linearised solution p is also of the same frequency and thus

$$\langle \boldsymbol{F}_1 \rangle = 0. \tag{3.3.12}$$

□

Die approbierte gedruckte Originalversion dieser Diplomarbeit ist an der TU Wien Bibliothek verfügbar
The approved original version of this thesis is available in print at TU Wien Bibliothek.
TU Bibliothek Your knowledge hub WIEN

## 3.4. Bjerknes Forces

In this section we will define the primary and secondary Bjerknes force in light of the last section. The *primary Bjerknes force* is the mean force felt by a single bubble in a pressure field,

$$\boldsymbol{F}(\hat{\mathrm{p}}, \hat{u}) \coloneqq -\frac{1}{T}\int_0^T \int_D \left((\hat{\boldsymbol{T}}^{-1}\nabla)\hat{\mathrm{p}}\right) \det(\hat{\boldsymbol{T}})\,\mathrm{d}\boldsymbol{x}\,\mathrm{d}t, \tag{3.4.1}$$

where $T$ is the period length of the incident pressure field. Using lemma 3.3.3 we arrive at the approximation

$$\boldsymbol{F}_1^{\mathrm{b}}(\mathrm{p}) \coloneqq \frac{1}{\rho_b\omega^2}\frac{1}{T}\int_0^T \int_{\partial D} (\nabla_T \mathrm{p})^2 \boldsymbol{n} - (\nabla \mathrm{p}|_- \cdot \boldsymbol{n})\,\nabla_T \mathrm{p}\,\mathrm{d}\sigma\,\mathrm{d}t. \tag{3.4.2}$$

For simpler notation we omitted the $\epsilon^2$ term. We will later see that the forces contain the term $\tilde{\mathrm{p}}_{\mathrm{in}}^2$ and we note that in the physical system the incident field is proportional to $\epsilon$. This justifies not including $\epsilon^2$ as we can move the factor into $\tilde{\mathrm{p}}_{\mathrm{in}}$. The presence of bubbles creates secondary pressure fields. The secondary Bjerknes force is the difference between the force of the multi bubble system compared to the 1 bubble system where we remove the other bubbles.
We define the approximation of the *secondary Bjerknes force* on bubble $i$ by

$$\boldsymbol{F}_{2,i}^{\mathrm{b}}(\mathrm{p}) \coloneqq \frac{1}{\rho_b\omega^2}\frac{1}{T}\int_0^T \int_{\partial D_i} (\nabla_T \mathrm{p})^2 \boldsymbol{n} - (\nabla \mathrm{p}|_- \cdot \boldsymbol{n})\,\nabla_T \mathrm{p}\,\mathrm{d}\sigma\,\mathrm{d}t - \boldsymbol{F}_{1,i}^{\mathrm{b}}(\mathrm{p}), \tag{3.4.3}$$

where $\boldsymbol{F}_{1,i}^{\mathrm{b}}$ is the first Bjerknes force for the system with only bubble $i$.

Die approbierte gedruckte Originalversion dieser Diplomarbeit ist an der TU Wien Bibliothek verfügbar
The approved original version of this thesis is available in print at TU Wien Bibliothek.
TU Bibliothek Your knowledge hub WIEN

Die approbierte gedruckte Originalversion dieser Diplomarbeit ist an der TU Wien Bibliothek verfügbar
The approved original version of this thesis is available in print at TU Wien Bibliothek.

# 4. Mathematical background

In this chapter we are going to set some basic definitions and theorems that we will need for later analysis. In the first section we will look at the layer potentials and some basic properties. Then we will describe how the layer potentials behave for spherical bubbles and state some properties of spherical harmonics. Readers familiar with these topics may skip this chapter. We start out by defining the domain of the bubbles.

**Definition 4.0.1.** *We have for the bubbles*

$$D := \bigcup_{i=0}^{M} D_i, \tag{4.0.1}$$

*where $D_i, D_j$ for $i \neq j$ are disjoint sets in $\mathbb{R}^3$ and each $D_i$ is a bounded and simply connected domain with $\partial D \in C^{1,s}$ for $s \in (0,1)$.*

## 4.1. Layer potentials

Now we will look at the single layer and the Neumann-Poincaré operator, which we will later use to find the solution. This section orients itself on [10]. We start out by characterizing the fundamental solution of the Helmholtz equation for outgoing solutions. This will motivate the choice for the single layer potential.

**Lemma 4.1.1.** *The outgoing fundamental solution of the Helmholtz equation $(\Delta+\boldsymbol{k}^2)p = f$ is*

$$G^{\boldsymbol{k}}(\boldsymbol{x}) := -\frac{1}{4\pi|\boldsymbol{x}|}e^{\mathrm{i}\boldsymbol{k}|\boldsymbol{x}|}. \tag{4.1.1}$$

*Proof.* We start with the Helmholtz equation

$$(\Delta + k^2)G^{\boldsymbol{k}}(\boldsymbol{x}) = -\delta(\boldsymbol{x}). \tag{4.1.2}$$

For $\boldsymbol{x} \in \mathbb{R}^3/B_\epsilon$ and due to rotational symmetry we get in spherical coordinates

$$\frac{1}{r}\partial_r^2(rG^{\boldsymbol{k}}(r)) + k^2G^{\boldsymbol{k}}(r) = 0. \tag{4.1.3}$$

This gets solved by

$$G^{\boldsymbol{k}}(r) = A_\pm\frac{e^{\pm\mathrm{i}kr}}{r}. \tag{4.1.4}$$

For $\phi \in C_c^\infty$ we now have

$$-\int_{\partial B_\epsilon}\frac{\mathrm{d}}{\mathrm{d}\boldsymbol{n}}G^{\boldsymbol{k}}(r)\phi\,\mathrm{d}\sigma = -\int_{\partial B_\epsilon}\phi\,\mathrm{d}\sigma(\partial_rG^{\boldsymbol{k}})(\epsilon) \to \phi(0)\lim_{\epsilon\to0}(-4\pi\epsilon^2(\partial_rG^{\boldsymbol{k}})(\epsilon)). \tag{4.1.5}$$



Die approbierte gedruckte Originalversion dieser Diplomarbeit ist an der TU Wien Bibliothek verfügbar
The approved original version of this thesis is available in print at TU Wien Bibliothek.
TU Bibliothek Your knowledge hub WIEN

We note that

$$\lim_{\epsilon\to 0}(-4\pi\epsilon^2(\partial_r G^{\boldsymbol{k}})(\epsilon)) = -4\pi A_\pm \lim_{\epsilon\to 0}\epsilon^2\frac{e^{\pm \mathrm{i}\boldsymbol{k}\epsilon}}{\epsilon}\left(\pm\mathrm{i}\boldsymbol{k}-\frac{1}{\epsilon}\right) = 4\pi A_\pm = -1 \tag{4.1.6}$$

we get $A_\pm = -\frac{1}{4\pi}$. Using the S.R.C. we choose the outgoing solution. □

We are now ready to define the single layer potential. The definition tells us that we can view the layer potential as the solution of the Helmholtz equation due to sources on the surfaces of the bubbles.

**Definition 4.1.2.** *The single layer potential $S_D^k : L^2(\partial D) \to H^1_{loc}(\mathbb{R}^3)$ is defined by*

$$S_D^k[\Phi](\boldsymbol{x}) \coloneqq \int_{\partial D} G^{\boldsymbol{k}}(\boldsymbol{x}-\boldsymbol{y})\Phi(\boldsymbol{y})\,\mathrm{d}\sigma(\boldsymbol{y}). \tag{4.1.7}$$

*Furthermore we define the Neumann-Poincaré operator $K_D^{k,*} : L^2(\partial D) \to L^2(\partial D)$ by*

$$K_D^{k,*}[\Phi](\boldsymbol{x}) \coloneqq \int_{\partial D} \frac{\mathrm{d}}{\mathrm{d}\boldsymbol{n}_{\boldsymbol{x}}} G^{\boldsymbol{k}}(\boldsymbol{x}-\boldsymbol{y})\Phi(\boldsymbol{y})\,\mathrm{d}\sigma(\boldsymbol{y}), \tag{4.1.8}$$

*where $\boldsymbol{n}_{\boldsymbol{x}}$ is the outward normal derivative at $\boldsymbol{x}$.*

For more details on layer potential operators see [10, p. 68-75].
Note that the single layer potential follows the Sommerfeld Radiation Condition and is a solution to the Helmholtz equation. The next theorem shows us that (for non resonance frequencies) we even have a unique solution to our model 3.2.13 and that we can represent the solution using layer potentials.

**Theorem 4.1.3.** *Suppose that $k_b^2$ is not a Dirichlet eigenvalue of $-\Delta$ on $D$. If $p$ is a solution of 3.2.13 then we get*

$$p(\boldsymbol{x}) = \begin{cases} S_D^{k_l}[\psi](\boldsymbol{x}) + p_{in}(\boldsymbol{x}) & \boldsymbol{x}\in\mathbb{R}^d/\overline{D}, \\ S_D^{k_b}[\phi](\boldsymbol{x}) & \boldsymbol{x}\in D \end{cases} \tag{4.1.9}$$

*for some $(\phi,\psi)\in L^2(\partial D)\times L^2(\partial D)$ under the conditions*

$$\begin{cases} S_D^{k_b}[\phi](\boldsymbol{x}) - S_D^{k_l}[\psi](\boldsymbol{x}) = p_{in}(\boldsymbol{x}) & \boldsymbol{x}\in\partial D, \\ \left(-\frac{1}{2}+K_D^{k_b,*}\right)[\phi](\boldsymbol{x}) - \delta\left(\frac{1}{2}+K_D^{k_l,*}\right)[\psi](\boldsymbol{x}) = \delta\frac{\mathrm{d}p_{in}}{\mathrm{d}\boldsymbol{n}}(\boldsymbol{x}) & \boldsymbol{x}\in\partial D. \end{cases} \tag{4.1.10}$$

*Proof.* For the proof see [10, p. 73-75]. □

In order to approximate the Layer potential operators we are next going to define an asymptotic expansion of them. We will see that we can split up the layer potentials into an operator of a Laplace problem with a perturbation. This approach has been commonly used before see for example [11].

Die approbierte gedruckte Originalversion dieser Diplomarbeit ist an der TU Wien Bibliothek verfügbar
The approved original version of this thesis is available in print at TU Wien Bibliothek.
TU Bibliothek Your knowledge hub WIEN

**Definition 4.1.4.** *We define for $n \in \mathbb{N}$, the continuous linear operators $S_D^n : L^2(\partial D) \to H^1_{loc}(\mathbb{R}^3)$ and $K_D^n : L^2(\partial D) \to L^2(\partial D)$ with*

$$\begin{aligned} S_D^n[\Phi](\boldsymbol{x}) &:= -\frac{\mathrm{i}^n}{4\pi n!}\int_{\partial D} |\boldsymbol{x}-\boldsymbol{y}|^{n-1}\Phi(\boldsymbol{y})\,\mathrm{d}\sigma, \\ K_D^n[\Phi](\boldsymbol{x}) &:= -\frac{\mathrm{i}^n(n-1)}{4\pi n!}\int_{\partial D} (\boldsymbol{x}-\boldsymbol{y})\cdot\boldsymbol{n}_{\boldsymbol{x}}|\boldsymbol{x}-\boldsymbol{y}|^{n-3}\Phi(\boldsymbol{y})\,\mathrm{d}\sigma. \end{aligned} \tag{4.1.11}$$

*We note that $K_D^0$ is defined as the Cauchy principal value integral and corresponds to the Neumann-Poincare operator of the Laplace equation.*

For the well-definedness of $S_D^0$ and $K_D^0$ note that they are just $S_D^k$ and $K_D^{k,*}$ for $k = 0$, alternatively see [12].
We will now prove the well-definedness for $n > 0$. We have for a compact set $K \subset \mathbb{R}^3$ that

$$\begin{aligned} \|\nabla S_D^n[\Phi]\|^2_{L^2(K)} &= \int_K \left(\frac{(n-1)}{4\pi n!}\int_{\partial D}(\boldsymbol{x}-\boldsymbol{y})|\boldsymbol{x}-\boldsymbol{y}|^{n-3}\Phi(\boldsymbol{y})\,\mathrm{d}\sigma(\boldsymbol{y})\right)^2 \mathrm{d}\boldsymbol{x} \\ &\le \left(\frac{(n-1)}{4\pi n!}\right)^2 |\partial D|\int_K\int_{\partial D}\left(|\boldsymbol{x}-\boldsymbol{y}|^{n-2}\Phi(\boldsymbol{y})\right)^2 \mathrm{d}\sigma(\boldsymbol{y})\,\mathrm{d}\boldsymbol{x}, \end{aligned} \tag{4.1.12}$$

where we used the Jensen inequality. Similarly we see that

$$\begin{aligned} \|S_D^n[\Phi]\|^2_{L^2(K)} &= \int_K \left(\frac{1}{4\pi n!}\int_{\partial D}|\boldsymbol{x}-\boldsymbol{y}|^{n-1}\Phi(\boldsymbol{y})\,\mathrm{d}\sigma(\boldsymbol{y})\right)^2 \mathrm{d}\boldsymbol{x} \\ &\le \left(\frac{1}{4\pi n!}\right)^2 |\partial D|\int_K\int_{\partial D}\left(|\boldsymbol{x}-\boldsymbol{y}|^{n-1}\Phi(\boldsymbol{y})\right)^2 \mathrm{d}\sigma(\boldsymbol{y})\,\mathrm{d}\boldsymbol{x}. \end{aligned} \tag{4.1.13}$$

For $K$ having non zero measure, $C_1(K) := \sup_{\boldsymbol{x}\in\partial D,\boldsymbol{y}\in K}|\boldsymbol{x}-\boldsymbol{y}|$ we get

$$\|S_D^n\|_{\mathcal{L}(L^2(\partial D),H^1(K))} \le \frac{\sqrt{|K||\partial D|}}{4\pi n!}\sqrt{C_1(K)^{2n-2}+C_1(K)^{2n-4}(n-1)^2} \tag{4.1.14}$$

and thus $S_D^n$ is continuous. We can prove the statement for $K_D^n$ in a similar way.
We will now further simplify the inequalities to proof the next lemma. By introducing a parameter $k < \min(C_1(K), 1)$ we see that

$$k^n\,\|S_D^n\|_{\mathcal{L}(L^2(\partial D),H^1(K))} \le C_0\sqrt{|K||\partial D|}\frac{(C_1(K)k)^{n-1}}{(n-1)!} \tag{4.1.15}$$

Note that we get after replacing the volume integral in the above proof by the boundary integral of $\partial D$ that

$$k^n\,\|S_D^n\|_{\mathcal{L}(L^2(\partial D),H^1(\partial D))} \le C_0\frac{(C_1k)^{n-1}}{(n-1)!}, \tag{4.1.16}$$

where $H^1(\partial D)$ denotes the space of functions with $L^2(\partial D)$ tangential derivatives. $S_D^n$ can thus be viewed as an continuous operator between $L^2(\partial D)$ and $H^1(\partial D)$. Finally due to $\frac{\mathrm{d}}{\mathrm{d}\boldsymbol{n}}S_D^n = K_D^n$ we get

$$k^n\,\|K_D^n\|_{\mathcal{L}(L^2(\partial D))} \le C_0k\frac{(C_1k)^{n-2}}{(n-2)!}. \tag{4.1.17}$$

These inequalities provide us now with the following lemma.

Die approbierte gedruckte Originalversion dieser Diplomarbeit ist an der TU Wien Bibliothek verfügbar
The approved original version of this thesis is available in print at TU Wien Bibliothek.
TU Bibliothek Your knowledge hub WIEN

**Lemma 4.1.5.** *For small $k$ we get that*

$$S_D^k - S_D^0 = \sum_{n=1}^{\infty} k^n S_D^n, \qquad K_D^{k,*} - K_D^0 = \sum_{n=1}^{\infty} k^n K_D^n \tag{4.1.18}$$

*on $\mathcal{L}(L^2(\partial D), H^1(\partial D))$ and $\mathcal{L}(L^2(\partial D), L^2(\partial D))$ respectively.*

*Proof.* We see that

$$\left\| K_D^k - \sum_{n=0}^{N} k^{2n} K_D^n \right\|_{\mathcal{L}(L^2(\partial D))} \leq C_0 k \sum_{n=N+1}^{\infty} \frac{(C_1 k)^{n-2}}{(n-2)!} \xrightarrow{N\to\infty} 0 \tag{4.1.19}$$

The convergence for $S_D^k$ can be proven in the same way by taking lemma 4.1.6 and the considerations before this lemma. □

This shows us that for small $k$ the lowest order dominates and the rest can be handled as a perturbation. We can write $S_D^k - S_D^0 = \mathcal{O}(k)$ in the operator norm. If we restrict $S_D^0$ to the surface of the inclusions then we have the following nice properties.

**Lemma 4.1.6.** *$S_D^0 : L^2(\partial D) \to H^1(\partial D)$ is bijective with bounded inverse. Further $S_D^0 : L^2(\partial D) \to L^2(\partial D)$ is self-adjoint.*

*Proof.* For the first part see [12, p. 38]. Self-adjointness follows directly from the definition. □

We will now state an important property of $S_D^0$.

**Lemma 4.1.7.** *We have on $\partial D$ the following jump relations*

$$\frac{\mathrm{d}}{\mathrm{d}\boldsymbol{n}}(S_D^0[\phi])\Big|_{\pm} = \left(\pm\frac{1}{2} + K_D^0\right)[\phi]. \tag{4.1.20}$$

*Proof.* See [12]. □

The kernel of $\left(-\frac{1}{2} + K_D^0\right)$ will in our derivations play a special role and allow us to find the resonance frequencies later on. We will now characterize it.

**Lemma 4.1.8.** *For the inclusions $D_i$ the kernel of $\left(-\frac{1}{2} + K_D^0\right)$ has the basis functions*

$$\varphi_i \coloneqq (S_D^0)^{-1}[\chi_{\partial D_i}] \tag{4.1.21}$$

*for the indicator function $\chi_{\partial D_i}$ on $\partial D_i$.*

*Proof.* If $\phi \in \ker\left(-\frac{1}{2} + K_D^0\right)$ then we have due to the jump condition that

$$0 = \left(-\frac{1}{2} + K_D^0\right)[\phi] = \frac{\mathrm{d}}{\mathrm{d}\boldsymbol{n}} S_D^0[\phi]|_-. \tag{4.1.22}$$

$S_D^0[\phi]$ is harmonic inside the inclusions and fulfills the homogeneous Neumann boundary condition. It is well known that the solutions are unique up to a constant. Due to the 0 function being a solution inside the inclusions, we arrive at the statement. □

Die approbierte gedruckte Originalversion dieser Diplomarbeit ist an der TU Wien Bibliothek verfügbar
The approved original version of this thesis is available in print at TU Wien Bibliothek.
TU Bibliothek Your knowledge hub WIEN

The capacitance matrix contains important geometry information of our problem. We will use the normalized capacity matrix later on to find approximations of the resonance frequencies.

**Definition 4.1.9** (Capacitance matrix)**.** *For inclusions $D_i$ the capacitance matrix is defined by*

$$\boldsymbol{C}_{i,j} \coloneqq \left\langle -S_D^0[\varphi_i], \varphi_j \right\rangle_{L^2(\partial D)} = -\int_{\partial D_i} \varphi_j \, \mathrm{d}\sigma. \tag{4.1.23}$$

*The normalized capacitance matrix is defined by*

$$\tilde{\boldsymbol{C}}_{i,j} \coloneqq \frac{\boldsymbol{C}_{i,j}}{|D_i|}. \tag{4.1.24}$$

The next lemma will be used to prove some integral relations afterwards.

**Lemma 4.1.10.** *The Plemelj's symmetrization principle identity holds*

$$S_D^0 K_D^0 = K_D^{0,*} S_D^0. \tag{4.1.25}$$

*Proof.* For the proof see [10, p. 25] and note that the definition of $K_D^0$ and $K_D^{0,*}$ are exactly opposite in the reference. □

We will next expand on a lemma found in [13].

**Lemma 4.1.11.** *For all $\xi \in L^2(\partial D)$ we have*

1. $\int_{\partial D} S_D^0[\phi] \left(-\frac{1}{2} + K_D^0\right)[\eta] \, \mathrm{d}\sigma = 0$ *for all* $\eta \in L^2(\partial D)$ *iff* $\phi \in \ker\left(-\frac{1}{2} + K_D^0\right)$,
2. $\int_{\partial D_j} \left(-\frac{1}{2} + K_D^0\right)[\xi] \, \mathrm{d}\sigma = 0$,
3. $\int_{\partial D_j} \left(\frac{1}{2} + K_D^0\right)[\xi] \, \mathrm{d}\sigma = \int_{\partial D_j} \xi \, \mathrm{d}\sigma$,
4. $\int_{\partial D_j} K_D^n[\xi] \, \mathrm{d}\sigma = -\int_{D_j} S_D^{n-2}[\xi] \, \mathrm{d}\sigma$ *for* $n > 1$,
5. $\int_{\partial D_j} K_D^3[\xi] \, \mathrm{d}\sigma = \frac{\mathrm{i}|D_j|}{4\pi} \int_{\partial D} \xi \, \mathrm{d}\sigma$.

*Proof.* We use the Plemelj's symmetrization principle identity to get

$$\begin{aligned} \int_{\partial D} S_D^0[\phi] \left(-\frac{1}{2} + K_D^0\right)[\xi] \, \mathrm{d}\sigma &= \int_{\partial D} \left(-\frac{1}{2} + K_D^{0,*}\right) S_D^0[\phi] \xi \, \mathrm{d}\sigma \\ &= \int_{\partial D} S_D^0 \left(-\frac{1}{2} + K_D^0\right)[\phi] \xi \, \mathrm{d}\sigma. \end{aligned} \tag{4.1.26}$$

The bijectivity of $S_D^0$ now proves the first statement. The second statement follows from the first statement and lemma 4.1.8. The third statement follows from the second one.

Die approbierte gedruckte Originalversion dieser Diplomarbeit ist an der TU Wien Bibliothek verfügbar
The approved original version of this thesis is available in print at TU Wien Bibliothek.
TU Bibliothek Your knowledge hub WIEN

For the fourth statement we see that for $n > 1$

$$\begin{aligned}\int_{\partial D_j} K_D^n[\xi]\,\mathrm{d}\sigma &= \int_{\partial D_j} \frac{\mathrm{d}}{\mathrm{d}\boldsymbol{n}} S_D^n[\xi]\,\mathrm{d}\sigma = \int_{D_j} \Delta S_D^n[\xi]\,\mathrm{d}\sigma \\ &= -\frac{\mathrm{i}^n}{4\pi n!}\int_{D_j}\int_{\partial D} \Delta_x |\boldsymbol{x}-\boldsymbol{y}|^{n-1}\Phi(\boldsymbol{y})\,\mathrm{d}\sigma(\boldsymbol{y})\,\mathrm{d}\sigma(\boldsymbol{x}) \\ &= -\frac{\mathrm{i}^n}{4\pi n!}\int_{D_j}\int_{\partial D} n(n-1)|\boldsymbol{x}-\boldsymbol{y}|^{n-3}\Phi(\boldsymbol{y})\,\mathrm{d}\sigma(\boldsymbol{y})\,\mathrm{d}\sigma(\boldsymbol{x}) \\ &= -\int_{D_j} S_D^{n-2}[\Phi]\,\mathrm{d}\sigma(\boldsymbol{x})\end{aligned} \tag{4.1.27}$$

Finally for the fifth statement we look at

$$\begin{aligned}\int_{\partial D_j} K_D^n[\xi]\,\mathrm{d}\sigma &= -\frac{\mathrm{i}^n(n-1)}{4\pi n!}\int_{\partial D_j}\int_{\partial D} (\boldsymbol{x}-\boldsymbol{y})\cdot\boldsymbol{n}_{\boldsymbol{x}}|\boldsymbol{x}-\boldsymbol{y}|^{n-3}\Phi(\boldsymbol{y})\,\mathrm{d}\sigma(\boldsymbol{y})\,\mathrm{d}\sigma(\boldsymbol{x}) \\ &= -\frac{\mathrm{i}^n(n-1)}{4\pi n!}\int_{\partial D}\int_{D_j} \nabla\cdot((\boldsymbol{x}-\boldsymbol{y})|\boldsymbol{x}-\boldsymbol{y}|^{n-3})\,\mathrm{d}\sigma(\boldsymbol{x})\Phi(\boldsymbol{y})\,\mathrm{d}\sigma(\boldsymbol{y}).\end{aligned} \tag{4.1.28}$$

The proof is concluded by noting that

$$\int_{D_j} \nabla\cdot(\boldsymbol{x}-\boldsymbol{y})\,\mathrm{d}\sigma(\boldsymbol{x}) = 3|D_j|. \tag{4.1.29}$$

□

## 4.2. Spherical inclusions

In this thesis we will do some final calculations for spherical inclusions. Note that although we have a reference sphere that does not mean that our forces are only accurate for spherical expansions. Due to the connection between the pressure gradient and the displacement field we can get arbitrary deformations of the bubble during the oscillations. In this section we will look at properties of spherical harmonics and the layer potentials for a spherical inclusion.

### 4.2.1. Spherical harmonics

The Legendre Polynomials are defined for $|t| \leq 1$ by the following generating function

$$\frac{1}{\sqrt{1+t^2-2tx}} = \sum_l P_l(x)t^n. \tag{4.2.1}$$

The associated Legendre polynomials $P_l^m$ are now defined by

$$P_l^m(x) \coloneqq (-1)^m(1-x^2)^{m/2}\frac{\mathrm{d}^m}{\mathrm{d}x^m}P_l(x). \tag{4.2.2}$$

Taking the derivative in t of the generating relation immediately gives us the following lemma.

Die approbierte gedruckte Originalversion dieser Diplomarbeit ist an der TU Wien Bibliothek verfügbar
The approved original version of this thesis is available in print at TU Wien Bibliothek.
TU Bibliothek Your knowledge hub WIEN

**Lemma 4.2.1.** *A well known recurrence relation for associated Legendre Polynomials is*

$$(l-m+1)P_{l+1}^m(x) = (2l+1)xP_l^m(x) - (l+m)P_{l-1}^m(x). \tag{4.2.3}$$

We can now define the non-normalized spherical harmonics

$$\tilde{Y}_l^m(\theta,\phi) \coloneqq P_l^m(\cos(\theta))e^{\mathrm{i}m\phi} \tag{4.2.4}$$

and the (normalized) spherical harmonics

$$Y_l^m(\theta,\phi) \coloneqq \sqrt{\frac{2l+1}{4\pi}\frac{(l-m)!}{(l+m)!}}P_l^m(\cos(\theta))e^{\mathrm{i}m\phi}. \tag{4.2.5}$$

Note that the spherical harmonics make up a complete orthonormal system on the unit sphere. We will denote $Y_l^m(\hat{\boldsymbol{z}}) \coloneqq Y_l^m(\theta,\phi)$ for a unit vector $\hat{\boldsymbol{z}}$ with spherical coordinates $\theta,\phi$. The next theorem is the well known addition theorem for spherical harmonics

**Theorem 4.2.2.** *We have*

$$P_l(\widehat{\boldsymbol{x}}\cdot\widehat{\boldsymbol{y}}) = \frac{4\pi}{2l+1}\sum_{m=-l}^{l} Y_l^{m,*}(\widehat{\boldsymbol{x}})Y_l^m(\widehat{\boldsymbol{y}}). \tag{4.2.6}$$

Finally we will state a shift lemma for spherical harmonics

**Lemma 4.2.3.** *We can shift spherical harmonics by*

$$\frac{1}{|\boldsymbol{x}-\boldsymbol{y}|^{l+1}}\tilde{Y}_l^m(\widehat{\boldsymbol{x}-\boldsymbol{y}}) = \sum_{l'=0}^{\infty}\sum_{m'=-l'}^{l'}\frac{(l+l'-m-m')!}{(l-m)!(l'+m')!}|\boldsymbol{y}|^{l'}(\tilde{Y}_{l'}^{m'})^*(\hat{\boldsymbol{y}})\frac{1}{|\boldsymbol{x}|^{l+l'+1}}\tilde{Y}_{l+l'}^{m+m'}(\hat{\boldsymbol{x}}) \tag{4.2.7}$$

*and*

$$|\boldsymbol{x}-\boldsymbol{y}|^l\tilde{Y}_l^m(\widehat{\boldsymbol{x}-\boldsymbol{y}}) = \sum_{l'=0}^{l}\sum_{m'=-l'}^{l'}\frac{(-1)^{l'+m'}(l+m)!|\boldsymbol{y}|^{l'}|\boldsymbol{x}|^{l-l'}}{(l'+m')!(l-l'+m-m')!}(\tilde{Y}_{l'}^{m'})^*(\hat{\boldsymbol{y}})\tilde{Y}_{l-l'}^{m+m'}(\hat{\boldsymbol{x}}). \tag{4.2.8}$$

*Proof.* For a proof see [14]. □

### 4.2.2. Layer potentials on a sphere

The layer potentials on a sphere take on an especially easy form. We will first state a relation between the Single Layer Potential and Neumann-Poincaré operator.

**Lemma 4.2.4.** *For a spherical inclusion $D = B_{r_1}(\boldsymbol{z}_1)$ we have*

$$K_D^n[\phi](\boldsymbol{x}) = \frac{n-1}{2r_1}S_D^n[\phi](\boldsymbol{x}) \tag{4.2.9}$$

*and more specifically*

$$K_D^0[\phi](\boldsymbol{x}) = -\frac{1}{2r_1}S_D^0[\phi](\boldsymbol{x}) \tag{4.2.10}$$

*for $\boldsymbol{x}\in\partial D$.*

Die approbierte gedruckte Originalversion dieser Diplomarbeit ist an der TU Wien Bibliothek verfügbar
The approved original version of this thesis is available in print at TU Wien Bibliothek.
TU Bibliothek Your knowledge hub WIEN

*Proof.* For $\boldsymbol{x}, \boldsymbol{y} \in \partial B_{r_1}(\boldsymbol{z}_1)$ and $\boldsymbol{x} \neq \boldsymbol{y}$ we have

$$\frac{(\boldsymbol{x}-\boldsymbol{y})\cdot \boldsymbol{n}_x}{|\boldsymbol{x}-\boldsymbol{y}|^2} = \frac{1}{2r_1}. \tag{4.2.11}$$

This can be seen by using spherical coordinates with $\boldsymbol{x}$ in $z$ direction. Then $(\boldsymbol{x}-\boldsymbol{y})\cdot\boldsymbol{n}_x = r_1(1-\cos(\theta))$ and $|\boldsymbol{x}-\boldsymbol{y}|^2 = 2r_1^2(1-\cos(\theta))$. Inserting this in the definition provides the statement. □

We will prove a spherical harmonic expansion that allows us to find an easy representation of $S_D^0$ on the sphere.

**Lemma 4.2.5.** *We have on a sphere $\boldsymbol{x}, \boldsymbol{y} \in \partial B_{r_1}(\boldsymbol{z}_1)$ that*

$$\frac{1}{|\boldsymbol{x}-\boldsymbol{y}|} = \frac{1}{r_1}\sum_l \frac{4\pi}{2l+1}\sum_{m=-l}^{l} Y_l^{m,*}(\widehat{\boldsymbol{x}})Y_l^m(\widehat{\boldsymbol{y}}). \tag{4.2.12}$$

*Proof.* Without loss of generality we assume $\boldsymbol{z}_1 = \boldsymbol{0}$ and get

$$|\boldsymbol{x}-\boldsymbol{y}| = \sqrt{\boldsymbol{x}^2+\boldsymbol{y}^2-2\boldsymbol{x}\cdot\boldsymbol{y}} = r_1\sqrt{2-2\widehat{\boldsymbol{x}}\cdot\widehat{\boldsymbol{y}}}. \tag{4.2.13}$$

Using the generating function of the Legendre polynomials, namely

$$\frac{1}{\sqrt{1+t^2-2tz}} = \sum_l P_l(z)t^n \tag{4.2.14}$$

for $t=1$ and $z = \widehat{\boldsymbol{x}}\cdot\widehat{\boldsymbol{y}}$ we arrive at

$$\frac{1}{|\boldsymbol{x}-\boldsymbol{y}|} = \frac{1}{r_1}\sum_l P_l(\widehat{\boldsymbol{x}}\cdot\widehat{\boldsymbol{y}}). \tag{4.2.15}$$

Finally using the addition theorem 4.2.2 we arrive at the statement. □

This lemma provides us immediately with the relation for the Single Layer Potential.

**Corollary 4.2.6.** *We have*

$$\begin{aligned} S^0_{B_{r_1}}[Y_l^m] &= -\frac{r_1}{2l+1}Y_l^m, \\ \left(\frac{1}{2}-K^0_{B_{r_1}}\right)[Y_l^m] &= \frac{l+1}{2l+1}Y_l^m, \\ \left(-\frac{1}{2}-K^0_{B_{r_1}}\right)[Y_l^m] &= -\frac{l}{2l+1}Y_l^m. \end{aligned} \tag{4.2.16}$$

*Proof.* Inserting lemma 4.2.5 into the definition and using the orthonormality property of the spherical harmonics provides the result. □

This representation will now allow us to prove that the kernel of $\left(-\frac{1}{2}+K_D^0\right)$ for a single sphere is made up of the constant functions.

Die approbierte gedruckte Originalversion dieser Diplomarbeit ist an der TU Wien Bibliothek verfügbar
The approved original version of this thesis is available in print at TU Wien Bibliothek.
TU Bibliothek Your knowledge hub WIEN

**Corollary 4.2.7.** *For a spherical inclusion $D = B_{r_1}(\boldsymbol{z}_1)$ we have*

$$K_D^0[1] = \frac{1}{2} \tag{4.2.17}$$

*and*

$$\varphi_1 = (S_D^0)^{-1}(\chi_{\partial D}) = -\frac{1}{r_1}. \tag{4.2.18}$$

*Proof.* We have due to lemma 4.2.4 and lemma 4.2.6

$$K_D^0[1] = -\frac{1}{2r_1} S_D^0[1] = -\frac{1}{2r_1}(-r_1) = \frac{1}{2}. \tag{4.2.19}$$

□

Finally we will derive how the layer potential operators act on $\varphi_1$.

**Lemma 4.2.8.** *We have on a sphere $D = \partial B_{r_1}(\boldsymbol{z}_1)$ that*

$$S_D^n[\varphi_1] = \frac{\mathrm{i}^n}{(n+1)!} 2^n r_1^n \tag{4.2.20}$$

*and*

$$K_D^n[\varphi_1] = \frac{\mathrm{i}^n (n-1)}{(n+1)!} 2^{n-1} r_1^{n-1}. \tag{4.2.21}$$

*Proof.* Without loss of generality we assume $\boldsymbol{z}_1 = \mathbf{0}$ and have

$$|\boldsymbol{x} - \boldsymbol{y}| = \sqrt{\boldsymbol{x}^2 + \boldsymbol{y}^2 - 2\boldsymbol{x} \cdot \boldsymbol{y}}. \tag{4.2.22}$$

This results in

$$\begin{aligned} S_D^n[\varphi_1] =& \frac{-\mathrm{i}^n}{4\pi n!} \int_{\partial B_{r_1}} |\boldsymbol{x} - \boldsymbol{y}|^{n-1} \varphi_1 \, \mathrm{d}\theta \\ =& \frac{-\mathrm{i}^n \varphi_1 r_1^2}{2n!} \int_0^\pi 2^{\frac{n-1}{2}\frac{n-1}{2}} (r_1^2 - r_1^2 \cos(\theta))^{\frac{n-1}{2}} \sin(\theta) \, \mathrm{d}\sigma \\ =& \frac{-\mathrm{i}^n \varphi_1 r_1^{n+1}}{n!} 2^{\frac{n-3}{2}} \int_0^2 u^{\frac{n-1}{2}} \, \mathrm{d}u \\ =& \frac{\mathrm{i}^n r_1^n}{(n+1)!} 2^n. \end{aligned} \tag{4.2.23}$$

Using lemma 4.2.4 we arrive at the second statement. □

Die approbierte gedruckte Originalversion dieser Diplomarbeit ist an der TU Wien Bibliothek verfügbar
The approved original version of this thesis is available in print at TU Wien Bibliothek.
TU Bibliothek Your knowledge hub WIEN

Die approbierte gedruckte Originalversion dieser Diplomarbeit ist an der TU Wien Bibliothek verfügbar
The approved original version of this thesis is available in print at TU Wien Bibliothek.

# 5. Strongly interacting systems

In this chapter we will look at multi bubble systems and analyse them using layer potential techniques. In the first section we rewrite the equations for the potentials, invert the system and simplify it by only consider the lowest asymptotic orders. For this we will expand upon the approach by Ammari et al. [15]. In section 2 and 3 we will derive a formula for the Minnaert frequency and a solution to our problem 3.2.13. Finally we will look at the 1 bubble case and derive the primary Bjerknes force.

## 5.1. Bubble oscillation

We saw in the last chapter in theorem 4.1.3 that the solution to our model can be formulated using the single layer potential. We have for an incident $\mathrm{p}_{\mathrm{in}}$ (which is solution to the free Helmholtz equation in the liquid with frequency $\omega$) that

$$\mathrm{p}(\boldsymbol{x}) = \begin{cases} S_D^{k_l}[\psi](\boldsymbol{x}) + \mathrm{p}_{\mathrm{in}}(\boldsymbol{x}) & \boldsymbol{x} \in \mathbb{R}^d / \overline{D}, \\ S_D^{k_b}[\phi](\boldsymbol{x}) & \boldsymbol{x} \in D \end{cases} \tag{5.1.1}$$

with the conditions

$$\begin{cases} S_D^{k_b}[\phi](\boldsymbol{x}) - S_D^{k_l}[\psi](\boldsymbol{x}) = \mathrm{p}_{\mathrm{in}}(\boldsymbol{x}) & \boldsymbol{x} \in \partial D, \\ \left(-\frac{1}{2} + K_D^{k_b,*}\right)[\phi](\boldsymbol{x}) - \delta\left(\frac{1}{2} + K_D^{k_l,*}\right)[\psi](\boldsymbol{x}) = \delta \frac{\mathrm{d}\mathrm{p}_{\mathrm{in}}}{\mathrm{d}\boldsymbol{n}}(\boldsymbol{x}) & \boldsymbol{x} \in \partial D, \end{cases} \tag{5.1.2}$$

$k_l := \omega/c_l$, $k_b := \omega/c_b$ and $\delta := \rho_b/\rho_l$. We note that in our application both $\delta$ and $\omega$ are assumed to be very small values. We therefore are going to take the approach of expanding the operators in said parameters. In order to find the potential functions $\phi, \psi$ we need to invert the system of the boundary equations.

### 5.1.1. Inverting the system

In this subsection we will reformulate the equations in terms of an operator, then we expand it asymptotically and see that it can be viewed as a perturbation of an operator of a Laplace problem. We then make the latter invertible by some slight changes and use the Neumann series to invert the operator equation.
For simpler notation we define the Hilbert spaces

$$\mathcal{H} := L^2(\partial D) \times L^2(\partial D), \qquad \mathcal{H}_1 := H^1(\partial D) \times L^2(\partial D). \tag{5.1.3}$$

and the operator

$$\mathcal{A}_D(\omega, \delta) := \begin{pmatrix} S_D^{k_b} & -S_D^{k_l} \\ \left(-\frac{1}{2} + K_D^{k_b,*}\right) & \delta\left(\frac{1}{2} + K_D^{k_l,*}\right) \end{pmatrix} \tag{5.1.4}$$



Die approbierte gedruckte Originalversion dieser Diplomarbeit ist an der TU Wien Bibliothek verfügbar
The approved original version of this thesis is available in print at TU Wien Bibliothek.
TU Bibliothek Your knowledge hub WIEN

with $\mathcal{A}_D(\omega,\delta):\mathcal{H}\to\mathcal{H}_1$. We further set

$$\boldsymbol{\phi} \coloneqq \begin{pmatrix}\phi\\ \psi\end{pmatrix}, \qquad \boldsymbol{F} \coloneqq \begin{pmatrix}\mathrm{p_{in}}\\ \delta\frac{\mathrm{dp_{in}}}{\mathrm{d}\boldsymbol{n}}\end{pmatrix}. \tag{5.1.5}$$

We can rewrite equations 5.1.2 to

$$\boxed{\mathcal{A}_D(\omega,\delta)\boldsymbol{\phi}=\boldsymbol{F}.} \tag{5.1.6}$$

Our problem thus reduces to inverting the operator $\mathcal{A}_D$. We are working in the low frequency $\omega$ and low contrast $\delta$ domain and thus $\mathcal{A}_D$ can be considered as the $\mathcal{A}_D(0,0)$ operator with a small error. This sort of approach is common in perturbation theory. Due to $S_D^0$ being symmetric we can denote

$$\mathcal{A}_D^0 \coloneqq \mathcal{A}_D(0,0)=\begin{pmatrix}S_D^0 & -S_D^0\\ (-\frac{1}{2}+K_D^0) & 0\end{pmatrix}, \quad \mathcal{A}_D^{0,*} \coloneqq \mathcal{A}_D(0,0)^*=\begin{pmatrix}S_D^0 & (-\frac{1}{2}+K_D^{0,*})\\ -S_D^0 & 0\end{pmatrix}. \tag{5.1.7}$$

An easy way to solve perturbed systems is by using the Neumann series for the inversion of the operator. Sadly, here this is not possible, because $\mathcal{A}_D^0$ is not invertible. To fix this we are going to extend this operator in the next lemmas. We will first look at its kernel which is the problematic part of the domain.

**Lemma 5.1.1.** *We have*

$$\ker\mathcal{A}_D^0=\operatorname*{span}_i\{\boldsymbol{\varphi}_i\}, \qquad \boldsymbol{\varphi}_i\coloneqq\begin{pmatrix}\varphi_i\\ \varphi_i\end{pmatrix} \tag{5.1.8}$$

*for* $\varphi_i \coloneqq \left(S_D^0\right)^{-1}[\chi_{\partial D_i}]$ *and* $D_i$ *being the connected parts of* $D$*. Further we get*

$$\ker\mathcal{A}_D^{0,*}=\operatorname*{span}_i\left\{\begin{pmatrix}0\\ S_D^0[\varphi_i]\end{pmatrix}\right\}. \tag{5.1.9}$$

*Proof.* We remind ourselves of lemma 4.1.8, namely

$$\ker\left(-\frac{1}{2}+K_D\right)=\operatorname*{span}_i\{\varphi_i\}. \tag{5.1.10}$$

The first statement follows now due to $S_D^0$ being invertible. Next for $\boldsymbol{u}\in\ker\mathcal{A}_D^{0,*}$ we see that the structure of $\mathcal{A}_D^{0,*}$ and the invertability of $S_D^0$ fixes the upper entry to 0. We further get for arbitrary $\boldsymbol{\phi}\in\mathcal{H}$ that

$$0=\left\langle\mathcal{A}_D^{0,*}\boldsymbol{u},\boldsymbol{\phi}\right\rangle_{\mathcal{H}}=\left\langle\left(-\frac{1}{2}+K_D^{0,*}\right)[\boldsymbol{u}_2],\boldsymbol{\phi}_1\right\rangle_{L^2}=\left\langle\boldsymbol{u}_2,\left(-\frac{1}{2}+K_D^0\right)[\boldsymbol{\phi}_1]\right\rangle_{L^2}. \tag{5.1.11}$$

Due to lemma 4.1.11 1 this results in $(S_D^0)^{-1}[\boldsymbol{u}_2]\in\ker\left(-\frac{1}{2}+K_D^0\right)$ and thus the statement. ∎

We will now modify $\mathcal{A}_D^0$ to make it invertible.

Die approbierte gedruckte Originalversion dieser Diplomarbeit ist an der TU Wien Bibliothek verfügbar
The approved original version of this thesis is available in print at TU Wien Bibliothek.
TU Bibliothek Your knowledge hub WIEN

**Definition 5.1.2.** *We define an operator from* $\ker \mathcal{A}_D^0$ *to* $\mathcal{H}_1$

$$P_0\left[\sum_i c_i \boldsymbol{\varphi_i}\right] \coloneqq \sum_i c_i \begin{pmatrix} 0 \\ \frac{\chi_{\partial D_i}}{\sqrt{|\partial D_i|}} \end{pmatrix}, \tag{5.1.12}$$

*We now define a modified* $\mathcal{A}_D^0$ *operator, namely*

$$\tilde{\mathcal{A}}_D[\boldsymbol{\phi}] \coloneqq \mathcal{A}_D^0[\boldsymbol{\phi}] + P_0[P_{\ker}\boldsymbol{\phi}], \tag{5.1.13}$$

*for* $P_{\ker}$ *being the orthogonal projection onto the kernel of* $\mathcal{A}_D^0$.

The next lemma shows that the operator really has the properties that we want and can thus be used in the inversion of the system if we can control the difference to $\mathcal{A}_D^0$.

**Lemma 5.1.3.** $\tilde{\mathcal{A}}_D$ *is a bijective bounded linear operator from* $\mathcal{H}$ *to* $\mathcal{H}_1$*, with* $\tilde{\mathcal{A}}_D[\boldsymbol{\varphi}_i] = \begin{pmatrix} 0 \\ \frac{\chi_{\partial D_i}}{\sqrt{|\partial D_i|}} \end{pmatrix}$. *Further* $\tilde{\mathcal{A}}_D^*$ *is a bijective bounded linear operator from* $\mathcal{H}_1$ *to* $\mathcal{H}$.

*Proof.* Linearity and boundedness follows from the same properties of $P_0$ and $\mathcal{A}_D^0$. For injectivity note that $\operatorname{Im}\mathcal{A}_D^0 \perp \ker \mathcal{A}_D^{0,*}$ and thus $\operatorname{Im}\mathcal{A}_D^0 \perp \operatorname{Im} P_0$. If we now assume that $\tilde{\mathcal{A}}_D[\boldsymbol{\phi}] = \mathbf{0}$ then $\mathcal{A}_D^0[\boldsymbol{\phi}] = \mathbf{0}$, which results in $\phi_1 = \phi_2 = \sum_i c_i\varphi_i$. Further we have $P_0[P_{\ker}\boldsymbol{\phi}] = \mathbf{0}$ and $\langle \boldsymbol{\varphi_i}, \boldsymbol{\phi}\rangle_{\mathcal{H}}$ for all $i$. In total this gives us $\boldsymbol{\phi} = \mathbf{0}$.
Next we will prove surjectivity. Due to the bijectivity of $S_D^0$ we only need to consider the second coordinate of $\mathcal{H}_1$. We note that $-\frac{1}{2} + K_D^0$ is invertible on $L_0^2(\partial D)$ [10, p. 23], which gives us surjectivity by construction. We get

$$\tilde{\mathcal{A}}_D[\boldsymbol{\varphi}_i] = P_0[\boldsymbol{\varphi}_i] = \begin{pmatrix} 0 \\ \frac{\chi_{\partial D_i}}{\sqrt{|\partial D_i|}} \end{pmatrix}. \tag{5.1.14}$$

The bijectivity of $\tilde{\mathcal{A}}_D^*$ now follows directly from the bijectivity of $\tilde{\mathcal{A}}_D$ due to $\mathcal{H}_1$ and $\mathcal{H}$ being Banach spaces. □

For easier notation we are going to split up the potential into the kernel of $\tilde{\mathcal{A}}_D$ and an orthogonal part.

**Definition 5.1.4.** *We split up the solution into*

$$\boldsymbol{\phi} = \boldsymbol{\varphi} + \tilde{\boldsymbol{\phi}}, \tag{5.1.15}$$

*with*

$$\boldsymbol{\varphi} \coloneqq \sum_i \boldsymbol{c_i}\boldsymbol{\varphi}_i \tag{5.1.16}$$

*and* $\tilde{\boldsymbol{\phi}} \perp \boldsymbol{\varphi}_i$ *for all* $i$.

We can now invert $\mathcal{A}_D$. The following theorem will set the defining equations for the coefficients $\boldsymbol{c}$ from Definition 5.1.4. It further finds relations for $\boldsymbol{\phi}$ that we regularly use later on.

Die approbierte gedruckte Originalversion dieser Diplomarbeit ist an der TU Wien Bibliothek verfügbar
The approved original version of this thesis is available in print at TU Wien Bibliothek.
TU Bibliothek Your knowledge hub WIEN

**Theorem 5.1.5.** *For* $\mathcal{B}_D \coloneqq \mathcal{A}_D - \mathcal{A}_D^0$, $\left\|\tilde{\mathcal{A}}_D^{-1}\mathcal{B}_D\right\| < 1$ *and* $\boldsymbol{c}, \boldsymbol{\phi}, \boldsymbol{\varphi}$ *defined in definition 5.1.4 we get*

$$\boldsymbol{\phi} = \mathrm{I}_D[\tilde{\mathcal{A}}_D^{-1}\boldsymbol{F} + \boldsymbol{\varphi}] \tag{5.1.17}$$

*with*

$$\mathrm{I}_D[\xi] \coloneqq \left(\sum_{n=0}(-\tilde{\mathcal{A}}_D^{-1}\mathcal{B}_D)^n\right)\xi. \tag{5.1.18}$$

*Furthermore we have for the Matrix* $\boldsymbol{A}$ *with* $(\boldsymbol{Ac})_i \coloneqq \boldsymbol{T}_i[\sum_j \boldsymbol{c}_j\varphi_j]$ *and vector* $\boldsymbol{R}[\boldsymbol{F}]$ *with* $\boldsymbol{R}_i[\boldsymbol{F}] \coloneqq \int_{\partial D_i}\boldsymbol{F}_2\,\mathrm{d}\sigma - \boldsymbol{T}_i[\tilde{\mathcal{A}}_D^{-1}\boldsymbol{F}]$ *for*

$$\boldsymbol{T}_i[\boldsymbol{\xi}] \coloneqq \int_{\partial D_i}(\mathcal{B}_D\,\mathrm{I}_D\,\boldsymbol{\xi})_2\,\mathrm{d}\sigma. \tag{5.1.19}$$

*that*

$$\boldsymbol{Ac} = \boldsymbol{R}[\boldsymbol{F}]. \tag{5.1.20}$$

*Proof.* We have

$$\mathcal{A}_D\boldsymbol{\phi} = \boldsymbol{F}. \tag{5.1.21}$$

Using definition 5.1.2 we get that $\mathcal{A}_D = \tilde{\mathcal{A}}_D - P_0P_{\ker} + \mathcal{B}_D$, $P_{\ker}\boldsymbol{\phi} = \boldsymbol{\varphi}$ and taking the inverse $(\tilde{\mathcal{A}}_D + \mathcal{B}_D)^{-1}$ results in

$$\boldsymbol{\phi} - (\tilde{\mathcal{A}}_D + \mathcal{B}_D)^{-1}P_0\boldsymbol{\varphi} = (\tilde{\mathcal{A}}_D + \mathcal{B}_D)^{-1}\boldsymbol{F}. \tag{5.1.22}$$

We have $P_0\boldsymbol{\varphi} = \tilde{\mathcal{A}}_D\boldsymbol{\varphi}$ and due to $\left\|\tilde{\mathcal{A}}_D^{-1}\mathcal{B}_D\right\| < 1$ we arrive at the first result by taking the Neumann series. Taking the scalar product of the first statement with $\boldsymbol{\varphi}_i$ gives us

$$\left\langle\boldsymbol{\varphi}_i, \tilde{\mathcal{A}}_D^{-1}\mathcal{B}_D\left(\sum_{n=0}(-\tilde{\mathcal{A}}_D^{-1}\mathcal{B}_D)^n\right)\boldsymbol{\varphi}\right\rangle_{\mathcal{H}} = \left\langle\boldsymbol{\varphi}_i, \tilde{\mathcal{A}}_D^{-1}\left(\sum_{n=0}(-\mathcal{B}_D\tilde{\mathcal{A}}_D^{-1})^n\right)\boldsymbol{F}\right\rangle_{\mathcal{H}}. \tag{5.1.23}$$

This turns to

$$\left\langle\tilde{\mathcal{A}}_D^{-1,*}\boldsymbol{\varphi}_i, \mathcal{B}_D\left(\sum_{n=0}(-\tilde{\mathcal{A}}_D^{-1}\mathcal{B}_D)^n\right)\boldsymbol{\varphi}\right\rangle_{\mathcal{H}_1} = \left\langle\tilde{\mathcal{A}}_D^{-1,*}\boldsymbol{\varphi}_i, \left(\sum_{n=0}(-\mathcal{B}_D\tilde{\mathcal{A}}_D^{-1})^n\right)\boldsymbol{F}\right\rangle_{\mathcal{H}_1}. \tag{5.1.24}$$

Next we note that due to $\langle\chi_{\partial D_i}, (-\frac{1}{2} + K_D^0)\xi\rangle_{L^2(\partial D)} = 0$ we get for $\boldsymbol{\xi} \in (\ker\mathcal{A}_D^0)^\perp$ that

$$\begin{aligned}\left\langle\tilde{\mathcal{A}}_D^*\begin{pmatrix}0\\ \frac{\chi_{\partial D_i}}{\sqrt{|\partial D_i|}}\end{pmatrix}, \boldsymbol{\xi}\right\rangle_{L^2(\partial D)} &= \left\langle\frac{\chi_{\partial D_i}}{\sqrt{|\partial D_i|}}, (\tilde{\mathcal{A}}_D\boldsymbol{\xi})_2\right\rangle_{L^2(\partial D)}\\ &= \left\langle\frac{\chi_{\partial D_i}}{\sqrt{|\partial D_i|}}, (P_0P_{\ker}\boldsymbol{\xi})_2\right\rangle_{L^2(\partial D)}\\ &= 0.\end{aligned} \tag{5.1.25}$$

We have thus

$$\tilde{\mathcal{A}}_D^*[\ker\mathcal{A}_D^{0,*}] = (\ker\mathcal{A}_D^0)^{\perp\perp} = \ker\mathcal{A}_D^0. \tag{5.1.26}$$

Die approbierte gedruckte Originalversion dieser Diplomarbeit ist an der TU Wien Bibliothek verfügbar
The approved original version of this thesis is available in print at TU Wien Bibliothek.
TU Bibliothek Your knowledge hub WIEN

This together with the bijectivity of $\tilde{\mathcal{A}}_D^*$ results in $\tilde{\mathcal{A}}_D^{-1,*}[\ker \mathcal{A}_D^0] = \ker \mathcal{A}_D^{0,*}$. After applying this to equation 5.1.24 we arrive at

$$\left\langle \chi_{D_i}, \left( \mathcal{B}_D \left( \sum_{n=0} (-\tilde{\mathcal{A}}_D^{-1} \mathcal{B}_D)^n \right) \boldsymbol{\varphi} \right)_2 \right\rangle_{L^2(\partial D)} = \left\langle \chi_{D_i}, \left( \left( \sum_{n=0} (-\mathcal{B}_D \tilde{\mathcal{A}}_D^{-1})^n \right) \boldsymbol{F} \right)_2 \right\rangle_{L^2(\partial D)} \tag{5.1.27}$$

for all $i$ and thus the second statement. □

Finally we will state some general relations that will be used for later calculations.

**Lemma 5.1.6.** *We have*

$$\tilde{\mathcal{A}}_D^{-1} \begin{pmatrix} 0 \\ \chi_{\partial D_i} \end{pmatrix} = \sqrt{|\partial D_i|} \varphi_i \begin{pmatrix} 1 \\ 1 \end{pmatrix}, \qquad \tilde{\mathcal{A}}_D^{-1} \begin{pmatrix} \chi_{\partial D_i} \\ 0 \end{pmatrix} = \frac{1}{2} \varphi_i \begin{pmatrix} 1 \\ -1 \end{pmatrix}. \tag{5.1.28}$$

*Proof.* For $\tilde{\mathcal{A}}_D \begin{pmatrix} \phi \\ \psi \end{pmatrix} = \begin{pmatrix} 0 \\ \chi_{\partial D_i} \end{pmatrix}$ we note that $\begin{pmatrix} 0 \\ \chi_{\partial D_i} \end{pmatrix} \in \ker \mathcal{A}_D^*$ and thus $\phi = \psi = \sqrt{|\partial D|} \varphi_i$.
For $\tilde{\mathcal{A}}_D \begin{pmatrix} \phi \\ \psi \end{pmatrix} = \begin{pmatrix} \chi_{\partial D_i} \\ 0 \end{pmatrix}$ we get

$$\phi - \psi = (S_D^0)^{-1}[\chi_{\partial D_i}] = \varphi_i. \tag{5.1.29}$$

The second entry tells us that $\phi = \sum_i c_i \varphi_i$ and $\langle \phi, \varphi_j \rangle_{L^2(\partial D)} + \langle \phi, \varphi_j \rangle_{L^2(\partial D)} = 0$ for all $j$. Thus $\phi = -\psi = \frac{1}{2} \varphi_i$. □

### 5.1.2. Strong interaction

We will now take a closer look at the interaction parts of $\mathcal{A}_D$ for small perturbations. Using the expansion terms for $S_D^{\boldsymbol{k}}, K_D^{\boldsymbol{k}}$ that we stated in definition 4.1.4 we expand $\mathcal{A}_D$.

**Definition 5.1.7.** *We have*

$$\mathcal{A}_D = \sum_{m=0}^{\infty} \omega^m \sum_{n=0,1} \delta^n \mathcal{A}_D^{m,n} \tag{5.1.30}$$

*with* $\mathcal{A}_D^{0,0} := \mathcal{A}_D^0$ *and for* $m > 0$

$$\mathcal{A}_D^{m,0} := \begin{pmatrix} \frac{1}{c_b^m} S_D^m & -\frac{1}{c_l^m} S_D^m \\ \frac{1}{c_b^m} K_D^m & 0 \end{pmatrix}, \qquad \mathcal{A}_D^{m,1} := \begin{pmatrix} 0 & 0 \\ 0 & -\frac{1}{c_b^m} K_D^m \end{pmatrix}, \tag{5.1.31}$$

$$\mathcal{A}_D^{0,1} := \begin{pmatrix} 0 & 0 \\ 0 & -\left(\frac{1}{2} + K_D^0\right) \end{pmatrix}. \tag{5.1.32}$$

We will especially note that the following operators have zero entries in the second row

$$\mathcal{A}_D^{1,0} := \begin{pmatrix} \frac{1}{c_b} S_D^1 & -\frac{1}{c_l} S_D^1 \\ 0 & 0 \end{pmatrix}, \qquad \mathcal{A}_D^{1,1} := \begin{pmatrix} 0 & 0 \\ 0 & 0 \end{pmatrix} \tag{5.1.33}$$

The next lemma gives us an easier representation for the matrix of lemma 5.1.5. We will use this to find the resonance frequency and the scattering coefficients later on.

Die approbierte gedruckte Originalversion dieser Diplomarbeit ist an der TU Wien Bibliothek verfügbar
The approved original version of this thesis is available in print at TU Wien Bibliothek.
TU Bibliothek Your knowledge hub WIEN

**Lemma 5.1.8.** *The matrix $\boldsymbol{A}$ of theorem 5.1.5 can be up to order $\mathcal{O}(\omega^4 + \delta\omega^2)$ written as*

$$\boldsymbol{A}_4(\omega,\delta) \coloneqq -k_b^2\boldsymbol{D} + \delta\boldsymbol{C} + \frac{i}{8\pi}\delta\,(k_b - k_l)\,\boldsymbol{C}\mathbf{1}_M\boldsymbol{C} - \frac{\mathrm{i}}{8\pi}k_b^2(k_b + k_l)\boldsymbol{D}\mathbf{1}_M\boldsymbol{C}, \tag{5.1.34}$$

*where $\mathbf{1}_M$ is a matrix of ones with dimensions $M$ by $M$, $\boldsymbol{D} \coloneqq \mathrm{Diag}(|D_1|,\dots,|D_M|)$ and $\boldsymbol{C}$ the capacity matrix.*

*Proof.* Due to $(\mathcal{A}_D^{1,0}\boldsymbol{c})_2 = (\mathcal{A}_D^{1,1}\boldsymbol{c})_2 = 0$ we get

$$\begin{aligned}\boldsymbol{A}_{i,j} = \int_{\partial D_i} \left(\left(\omega^2\mathcal{A}_D^{2,0} + \omega^3\mathcal{A}_D^{3,0} + \delta\mathcal{A}_D^{0,1} - \omega^3\mathcal{A}_D^{2,0}\tilde{\mathcal{A}}_D^{-1}\mathcal{A}_D^{1,0} - \omega\delta\mathcal{A}_D^{0,1}\tilde{\mathcal{A}}_D^{-1}\mathcal{A}_D^{1,0}\right)[\boldsymbol{\varphi_j}]\right)_2 \mathrm{d}\sigma \\ + \mathcal{O}(\omega^4 + \delta\omega^2).\end{aligned} \tag{5.1.35}$$

Next we note that

$$\mathcal{A}_D^{1,0}[\boldsymbol{\varphi}_j] = \begin{pmatrix} (\frac{1}{c_b} - \frac{1}{c_l})S_D^1[\varphi_j] \\ 0 \end{pmatrix} \tag{5.1.36}$$

and by lemma 5.1.6 we get

$$\tilde{\mathcal{A}}_D^{-1}\begin{pmatrix} c\chi_{\partial D_j} \\ 0 \end{pmatrix} = \begin{pmatrix} \frac{c}{2}\varphi_j \\ -\frac{c}{2}\varphi_j \end{pmatrix}. \tag{5.1.37}$$

Due to $S_D^1$ being constant and lemma 4.1.11 this results in

$$\begin{aligned}\int_{\partial D_i} \mathcal{A}_D^{0,1}\tilde{\mathcal{A}}_D^{-1}\mathcal{A}_D^{1,0}[\boldsymbol{\varphi}_j]\,\mathrm{d}\sigma &= \int_{\partial D_i} \frac{1}{2}\left(\frac{1}{2} + K_D^0\right)\left(\frac{1}{c_b} - \frac{1}{c_l}\right)S_D^1[\varphi_j]\sum_k \varphi_k\,\mathrm{d}\sigma \\ &= \frac{-i}{8\pi}\left(\frac{1}{c_b} - \frac{1}{c_l}\right)\left(\int_{\partial D}\varphi_j\,\mathrm{d}\sigma\right)\int_{\partial D_i}\sum_k \varphi_k\,\mathrm{d}\sigma \\ &= \frac{-i}{8\pi}\left(\frac{1}{c_b} - \frac{1}{c_l}\right)\left(\sum_k C_{k,j}\right)\left(\sum_k C_{i,k}\right) \\ &= \frac{-i}{8\pi}\left(\frac{1}{c_b} - \frac{1}{c_l}\right)(\boldsymbol{C}\mathbf{1}_M\boldsymbol{C})_{i,j}.\end{aligned} \tag{5.1.38}$$

Further by again using lemma 4.1.11 we have

$$\begin{aligned}\int_{\partial D_i} \mathcal{A}_D^{2,0}\tilde{\mathcal{A}}_D^{-1}\mathcal{A}_D^{1,0}[\boldsymbol{\varphi}_j]\,\mathrm{d}\sigma &= \frac{1}{2c_b^2}\left(\frac{1}{c_b} - \frac{1}{c_l}\right)\int_{\partial D_i} S_D^1[\varphi_j]\sum_k K_D^2[\varphi_k]\,\mathrm{d}\sigma \\ &= \frac{i}{8\pi c_b^2}\left(\frac{1}{c_b} - \frac{1}{c_l}\right)\left(\int_{\partial D}\varphi_j\,\mathrm{d}\sigma\right)\int_{D_i}\sum_k S_D^0[\varphi_k]\,\mathrm{d}\sigma \\ &= \frac{-i}{8\pi c_b^2}\left(\frac{1}{c_b} - \frac{1}{c_l}\right)\left(\sum_k C_{k,j}\right)|D_i| \\ &= \frac{-i}{8\pi c_b^2}\left(\frac{1}{c_b} - \frac{1}{c_l}\right)(\boldsymbol{D}\mathbf{1}_M\boldsymbol{C})_{i,j},\end{aligned} \tag{5.1.39}$$

Die approbierte gedruckte Originalversion dieser Diplomarbeit ist an der TU Wien Bibliothek verfügbar
The approved original version of this thesis is available in print at TU Wien Bibliothek.
TU Bibliothek Your knowledge hub WIEN

and

$$\begin{aligned}
\int_{\partial D_i} \mathcal{A}_D^{2,0}[\boldsymbol{\varphi}_j]\,\mathrm{d}\sigma &= \frac{1}{c_b^2}\int_{\partial D_i} K_D^2[\varphi_j]\,\mathrm{d}\sigma = -\frac{1}{c_b^2}\int_{D_i} S_D^0[\varphi_j] = -\frac{1}{c_b^2}\boldsymbol{D}_{i,j},\\
\int_{\partial D_i} \frac{1}{c_b^3}\mathcal{A}_D^{3,0}[\boldsymbol{\varphi}_j]\,\mathrm{d}\sigma &= \frac{1}{c_b^3}\int_{\partial D_i} K_D^3[\varphi_j]\,\mathrm{d}\sigma = \frac{1}{c_b^3}\frac{\mathrm{i}|D_i|}{4\pi}\int_{\partial D}\varphi_j\,\mathrm{d}\sigma\\
&= -\frac{1}{c_b^3}\frac{\mathrm{i}|D_i|}{4\pi}\sum_k \boldsymbol{C}_{k,j} = \frac{-\mathrm{i}}{4\pi}\frac{1}{c_b^3}(\boldsymbol{D}\mathbf{1}\boldsymbol{C})_{i,j}\\
\int_{\partial D_i} \mathcal{A}_D^{0,1}[\boldsymbol{\varphi}_j]\,\mathrm{d}\sigma &= -\int_{\partial D_i}\left(\frac{1}{2}+K_D^0\right)\varphi_j\,\mathrm{d}\sigma = \boldsymbol{C}_{i,j}.
\end{aligned} \tag{5.1.40}$$

Finally we get

$$\begin{aligned}
\int_{\partial D_i}\left(\frac{1}{2}+K_D^0\right)(S_D^0)^{-1}S_D^1[\varphi_j]\,\mathrm{d}\sigma &= \frac{-i}{4\pi}\left(\int_{\partial D}\varphi_j\,\mathrm{d}\sigma\right)\int_{\partial D_i}(S_D^0)^{-1}[1]\,\mathrm{d}\sigma\\
&= \frac{-i}{4\pi}\left(\sum_k C_{k,j}\right)\left(\sum_k C_{i,k}\right) = \frac{-i}{4\pi}(\boldsymbol{C}\mathbf{1}\boldsymbol{C})_{i,j}.
\end{aligned} \tag{5.1.41}$$

Putting all equations together provides the result. □

## 5.2. Resonant oscillation

In this section we are going to look at resonant oscillations, which are the oscillations that can occur even if there is no incident pressure field. They are only possible for special frequencies called the resonance frequencies. For our purposes we will only look at the frequencies with positive real part.

**Definition 5.2.1.** *For $\delta$ a complex value $\omega_i(\delta)$ with positive real part is a resonance frequency of the inclusions iff the kernel of $\mathcal{A}_D(\omega_i(\delta),\delta)$ is non trivial.*

The resonances can be viewed as the characteristic values of the operator-valued analytic function $\mathcal{A}_D(\cdot,\delta)$. We will now note the following result of the Ghoberg Sigal theory.

**Lemma 5.2.2.** *There exists a $\delta_0$ so that for all $|\delta|<\delta_0$ the characteristic values $\omega_i(\delta)$, to the operator valued analytic function $\mathcal{A}_D(\omega,\delta)$, have $\omega_i(0)=0$ and are smooth in $\delta$.*

*Proof.* For a proof see [16]. □

We can now expand the resonance frequencies for small $\delta$.

**Lemma 5.2.3.** *For each resonance frequency $\omega_i$ we have a normalized eigenvector $\boldsymbol{v}_i$ with eigenvalue $\lambda_i$ of the normalized capacity matrix $\boldsymbol{D}^{-1}\boldsymbol{C}$ for $\boldsymbol{D} \coloneqq \mathrm{Diag}(|D_1|,\dots,|D_M|)$ so that we get*

$$\omega_i = \omega_{M,i} + \mathrm{i}\tau_i + \mathcal{O}(\delta^{3/2}), \tag{5.2.1}$$

Die approbierte gedruckte Originalversion dieser Diplomarbeit ist an der TU Wien Bibliothek verfügbar
The approved original version of this thesis is available in print at TU Wien Bibliothek.
TU Bibliothek Your knowledge hub WIEN

*with the frequency*

$$\omega_{M,i} \coloneqq \sqrt{\delta\lambda_i c_b^2} \tag{5.2.2}$$

*and*

$$\tau_i \coloneqq -\frac{1}{8\pi}\frac{c_b^2}{c_l}\delta\lambda_i^2\frac{\boldsymbol{v}_i^H \boldsymbol{D}\mathbf{1}_M\boldsymbol{D}\boldsymbol{v}_i}{\boldsymbol{v}_i^H\boldsymbol{D}\boldsymbol{v}_i}, \tag{5.2.3}$$

*where $\mathbf{1}_M$ is a matrix of ones with dimensions $M$ by $M$.*

*Proof.* Due to lemma 5.1.8 we have

$$\left(-k_b^2\boldsymbol{D} + \delta\boldsymbol{C} + \frac{i}{8\pi}\delta\left(k_b - k_l\right)\boldsymbol{C}\mathbf{1}_M\boldsymbol{C} - \frac{\mathrm{i}}{8\pi}k_b^2(k_b + k_l)\boldsymbol{D}\mathbf{1}_M\boldsymbol{C}\right)\boldsymbol{c} = \mathcal{O}((\omega^2+\delta)^2|\boldsymbol{c}|). \tag{5.2.4}$$

Up to order $\mathcal{O}((\omega^3 + \delta\omega + \delta^2)|\boldsymbol{c}|)$ this gives us

$$\left(-k_b^2\boldsymbol{D} + \delta\boldsymbol{C} + \mathcal{O}(\omega^3 + \delta\omega + \delta^2)\right)\boldsymbol{c} = 0. \tag{5.2.5}$$

Thus we have

$$\boldsymbol{c} = \boldsymbol{v} + \tilde{\boldsymbol{c}}, \tag{5.2.6}$$

where $\boldsymbol{v}$ is an eigenvector of $\boldsymbol{D}^{-1}\boldsymbol{C}$ with eigenvalue $\lambda$, the vector $\tilde{\boldsymbol{c}} = \mathcal{O}((\delta+\omega)|\boldsymbol{c}|)$ and

$$\omega^2 = \omega_M^2 + \mathcal{O}\left(\delta^{\frac{3}{2}}\right) \tag{5.2.7}$$

for $\omega_M \coloneqq \sqrt{\delta\lambda c_b^2}$. Using lemma 5.1.8 up to full order we get

$$\left(-k_b^2\boldsymbol{D} + \delta\boldsymbol{C} + \frac{i}{8\pi}\delta\left(k_b - k_l\right)\boldsymbol{C}\mathbf{1}_M\boldsymbol{C} - \frac{\mathrm{i}}{8\pi}k_b^2(k_b + k_l)\boldsymbol{D}\mathbf{1}_M\boldsymbol{C}\right)\boldsymbol{c} = \mathcal{O}(\delta^2|\boldsymbol{c}|). \tag{5.2.8}$$

This turns to

$$\begin{aligned}\mathcal{O}(\delta^2|\boldsymbol{c}|) = &\left(-k_b^2\boldsymbol{D} + \delta\boldsymbol{C}\right)\tilde{\boldsymbol{c}} \\ &+ \left(-k_b^2\boldsymbol{D} + \delta\boldsymbol{C} + \frac{i}{8\pi}\delta\left(k_b - k_l\right)\boldsymbol{C}\mathbf{1}_M\boldsymbol{C} - \frac{\mathrm{i}}{8\pi}k_b^2(k_b + k_l)\boldsymbol{D}\mathbf{1}_M\boldsymbol{C}\right)\boldsymbol{v}.\end{aligned} \tag{5.2.9}$$

Next we note that $\boldsymbol{C}$ is symmetric because of the self adjointness of $S_D^0$. With this and the symmetry of $\boldsymbol{D}$ we can follow symmetry for $\left(-k_b^2\boldsymbol{D} + \delta\boldsymbol{C}\right)$. We thus have $\boldsymbol{v}^H\left(-k_b^2\boldsymbol{D} + \delta\boldsymbol{C}\right) = \mathcal{O}((\delta+\omega)|\boldsymbol{c}|)$. With this we get

$$\boldsymbol{v}^H\left(-k_b^2\boldsymbol{D} + \delta\boldsymbol{C} + \frac{i}{8\pi}\delta\left(k_b - k_l\right)\boldsymbol{C}\mathbf{1}_M\boldsymbol{C} - \frac{\mathrm{i}}{8\pi}k_b^2(k_b + k_l)\boldsymbol{D}\mathbf{1}_M\boldsymbol{C}\right)\boldsymbol{v} = \mathcal{O}(\delta^2|\boldsymbol{c}|^2). \tag{5.2.10}$$

Die approbierte gedruckte Originalversion dieser Diplomarbeit ist an der TU Wien Bibliothek verfügbar
The approved original version of this thesis is available in print at TU Wien Bibliothek.
TU Bibliothek Your knowledge hub WIEN

Due to $\boldsymbol{v}$ being a normalized eigenvector we have $|\boldsymbol{c}| = \mathcal{O}(1)$ and

$$\begin{aligned}
\omega^2 =& c_b^2 \boldsymbol{v}^H \frac{\delta \boldsymbol{C} + \frac{i}{8\pi}\delta\left(k_b - k_l\right)\boldsymbol{C}\mathbf{1}_M\boldsymbol{C} - \frac{\mathrm{i}}{8\pi}k_b^2(k_b + k_l)\boldsymbol{D}\mathbf{1}_M\boldsymbol{C}}{\boldsymbol{v}^H\boldsymbol{D}\boldsymbol{v}}\boldsymbol{v} + \mathcal{O}(\delta^2) \\
=& c_b^2 \boldsymbol{v}^H \frac{\lambda\delta\boldsymbol{D} + \frac{i}{8\pi}\delta\omega_M\left(c_b^{-1} - c_l^{-1}\right)\boldsymbol{C}\mathbf{1}_M\boldsymbol{C} - \frac{\mathrm{i}}{8\pi}\lambda^{-1}\omega_M^3 c_b^{-2}(c_b^{-1} + c_l^{-1})\boldsymbol{C}\mathbf{1}_M\boldsymbol{C}}{\boldsymbol{v}^H\boldsymbol{D}\boldsymbol{v}}\boldsymbol{v} + \mathcal{O}(\delta^2) \\
=& c_b^2 \boldsymbol{v}^H \frac{\lambda\delta\boldsymbol{D} + \frac{i}{8\pi}\delta\omega_M\left(\left(c_b^{-1} - c_l^{-1}\right) - \left(c_b^{-1} + c_l^{-1}\right)\right)\boldsymbol{C}\mathbf{1}_M\boldsymbol{C}}{\boldsymbol{v}^H\boldsymbol{D}\boldsymbol{v}}\boldsymbol{v} + \mathcal{O}(\delta^2) \\
=& \omega_M^2 - \frac{i}{4\pi}\frac{c_b^2}{c_l}\delta\omega_M\frac{\boldsymbol{v}^H\boldsymbol{C}\mathbf{1}_M\boldsymbol{C}\boldsymbol{v}}{\boldsymbol{v}^H\boldsymbol{D}\boldsymbol{v}} + \mathcal{O}(\delta^2).
\end{aligned} \tag{5.2.11}$$

Using the Ansatz $\omega = \omega_M + \mathrm{i}\tau + \mathcal{O}(\omega^3 + \delta\omega)$, with $\tau \propto \delta$ we see that

$$2\tau\omega_M = -\frac{1}{4\pi}\frac{c_b^2}{c_l}\lambda^2\delta\omega_M\frac{\boldsymbol{v}^H\boldsymbol{C}\mathbf{1}_M\boldsymbol{C}\boldsymbol{v}}{\boldsymbol{v}^H\boldsymbol{D}\boldsymbol{v}} + \mathcal{O}(\delta^2). \tag{5.2.12}$$

Finally we arrive at

$$\tau \coloneqq -\frac{1}{8\pi}\frac{c_b^2}{c_l}\delta\frac{\boldsymbol{v}^H\boldsymbol{C}\mathbf{1}_M\boldsymbol{C}\boldsymbol{v}}{\boldsymbol{v}^H\boldsymbol{D}\boldsymbol{v}}. \tag{5.2.13}$$

□

For a single spherical bubble this simplifies to a simple equation.

**Corollary 5.2.4.** *For a single spherical inclusion the resonance frequency $\omega_1$ is*

$$\omega_1 = \sqrt{\frac{3\delta c_b^2}{r_1^2}} - i\delta\frac{3}{2}\frac{c_b^2}{c_l r_1} + \mathcal{O}(\delta^{3/2}). \tag{5.2.14}$$

*Proof.* With $\boldsymbol{V} = 1$,

$$\boldsymbol{D} = \frac{4\pi r_1^3}{3}, \qquad \boldsymbol{C} = 4\pi r_1 \tag{5.2.15}$$

and lemma 5.2.3 we arrive at the statement. □

**Remark 5.2.5.** *We will now verify that this result is consistent with past results by considering a reversible adiabatic process and especially use equation 3.1.17. We then get*

$$\omega_{M,1} = \sqrt{\frac{3\delta c_b^2}{r_1^2}} = \sqrt{\frac{3c_b^2\rho_b}{r_1^2\rho_l}} = \sqrt{\frac{3\kappa_b}{r_1^2\rho_l}} = \sqrt{\frac{3\gamma p_0}{r_1^2\rho_l}}. \tag{5.2.16}$$

*The right side is exactly the historic Minnaert frequency that we saw in 2.2.15 in the lowest order. We also have for frequencies close to the resonance frequency $\omega - \omega_1 = \mathcal{O}(\delta)$ that*

$$\tau_1 = -\frac{r_1}{2c_l}\omega_{M,1}^2 = -\frac{r_1}{2c_l}\omega^2 + \mathcal{O}(\delta^{3/2}). \tag{5.2.17}$$

*Which corresponds to the acoustic dampening term in equation 2.2.17. Note that the different sign appears due to the resonance frequency and thus the complex term appearing in the denominator of the solution.*

Die approbierte gedruckte Originalversion dieser Diplomarbeit ist an der TU Wien Bibliothek verfügbar
The approved original version of this thesis is available in print at TU Wien Bibliothek.
TU Bibliothek Your knowledge hub WIEN

## 5.3. Scattered solution

In this section we will consider the impact of an incident plane wave

$$\mathrm{p}_{\mathrm{in}} = \tilde{\mathrm{p}}_{\mathrm{in}} e^{\mathrm{i}\boldsymbol{k}\cdot\boldsymbol{x}} \tag{5.3.1}$$

and derive the scattered solution. Note that all terms share the time dependence $e^{\mathrm{i}\omega t}$ and therefore we do not need to consider it for now. We will first prove an auxiliary lemma which will help us in the main proof of lemma 5.3.4. The main idea is to work in the basis of eigenvectors of $\tilde{\boldsymbol{C}}$ in order to diagonalize the relations for the coefficients of the functions.

**Lemma 5.3.1.** *$\boldsymbol{A}$ defined in theorem 5.1.5 in the basis of the normalized eigenvectors $\boldsymbol{V}$ of $\boldsymbol{D}^{-1}\boldsymbol{C}$ turns, up to order $\mathcal{O}(\sum_i(\omega_i-\omega)(\omega_i+\omega)^2)$, to*

$$\tilde{\boldsymbol{A}}_4 \coloneqq -\frac{1}{c_b^2}\boldsymbol{D}\boldsymbol{V}(\boldsymbol{\omega}^2-\boldsymbol{\Omega}^2) \tag{5.3.2}$$

*where $\boldsymbol{\Omega} \coloneqq \mathrm{Diag}(\omega_1,\dots,\omega_M)$ contains resonance frequencies corresponding to the eigenvectors $\boldsymbol{v}_i$, $\boldsymbol{\omega}$ is the identity matrix times $\omega$, $\boldsymbol{D} = \mathrm{Diag}(|D_1|,\dots,|D_M|)$ and $\boldsymbol{V} = \mathcal{O}(1)$. Further $\boldsymbol{R}$ defined in theorem 5.1.5 turns up to order $\omega^3+\omega\delta$ to*

$$\boldsymbol{R}_3 \coloneqq \frac{\tilde{p}_{in}}{2c_b^2}\boldsymbol{D}\boldsymbol{V}\left(\boldsymbol{\omega}^2+\boldsymbol{\Omega}_M^2\right)\boldsymbol{V}^{-1}\mathbf{1}_{M,1} \tag{5.3.3}$$

*for $\boldsymbol{\Omega}_M \coloneqq \mathrm{Diag}(\omega_{M,1},\dots,\omega_{M,M})$ being the matrix of $\omega_{M,i}$.*

*Proof.* For $\omega=\omega_i$ with corresponding $\boldsymbol{c}_i$ so that

$$\boldsymbol{A}(\omega_i,\delta)\boldsymbol{c}_i = 0 \tag{5.3.4}$$

we get

$$\begin{aligned}\mathcal{O}((\omega^2+\delta)^2) =& (\boldsymbol{A}_4(\omega,\delta)-\boldsymbol{A}_4(\omega_i,\delta))\boldsymbol{c}_i\\ =& -c_b^{-2}\boldsymbol{D}\boldsymbol{c}_i(\omega^2-\omega_i^2)+\mathcal{O}((\omega-\omega_i)(\omega+\omega_i)^2|\boldsymbol{c}_i|).\end{aligned} \tag{5.3.5}$$

We note that $\boldsymbol{c}_i = \boldsymbol{v}_i+\mathcal{O}(\omega_i)$, where $\boldsymbol{v}_i$ is a normalized eigenvalue of $\tilde{\boldsymbol{C}}$ and thus get

$$-c_b^{-2}\boldsymbol{D}\boldsymbol{v}_i(\omega^2-\omega_i^2) = \mathcal{O}((\omega-\omega_i)(\omega+\omega_i)^2). \tag{5.3.6}$$

This provides the first statement. We get that

$$\begin{aligned}&\int_{\partial D_i}\left(-\omega^2\mathcal{A}_D^{2,0}\tilde{\mathcal{A}}_D^{-1}\boldsymbol{F}-\delta\mathcal{A}_D^{0,1}\tilde{\mathcal{A}}_D^{-1}\boldsymbol{F}\right)_2\mathrm{d}\sigma\\ &=\frac{\tilde{\mathrm{p}}_{\mathrm{in}}}{2}\sum_j\int_{\partial D_i}-k_b^2K_D^2[\varphi_j]-\delta\left(\frac{1}{2}+K_D^0\right)[\varphi_j]\,\mathrm{d}\sigma+\mathcal{O}(\omega^3+\omega\delta)\\ &=\frac{\tilde{\mathrm{p}}_{\mathrm{in}}}{2}\left(k_b^2|D_i|+\delta\sum_j C_{i,j}\right)+\mathcal{O}(\omega^3+\omega\delta)=\left(\frac{\tilde{\mathrm{p}}_{\mathrm{in}}}{2}\left(k_b^2\boldsymbol{D}+\delta\boldsymbol{C}\right)\mathbf{1}_{M,1}\right)_i+\mathcal{O}(\omega^3+\omega\delta)\\ &=\left(\frac{\tilde{\mathrm{p}}_{\mathrm{in}}}{2c_b^2}\boldsymbol{D}\boldsymbol{V}\left(\boldsymbol{\omega}^2+\boldsymbol{\Omega}_M^2\right)\boldsymbol{V}^{-1}\mathbf{1}_{M,1}\right)_i+\mathcal{O}(\omega^3+\omega\delta).\end{aligned} \tag{5.3.7}$$

□

Die approbierte gedruckte Originalversion dieser Diplomarbeit ist an der TU Wien Bibliothek verfügbar
The approved original version of this thesis is available in print at TU Wien Bibliothek.
TU Bibliothek Your knowledge hub WIEN

Next we introduce a scaling relation between $\omega$ and $\delta$.

**Definition 5.3.2.** *We have the scaling relation*

$$\omega - \omega_{M,i} \sim \delta^{\mu_i} \tag{5.3.8}$$

*for all $i$ with $\frac{1}{2} \leq \mu_i \leq 1$, $\mu_- := \min_i \mu_i$, $\mu_+ := \max_i \mu_i$ and $\mu := 2 + 2(\mu_- - 2\mu_+)$.*

This relation signifies that the forcing frequency stays close or at least does not in a relative sense move away from the resonance frequencies of the system. We proof the following auxiliary lemma for later use.

**Lemma 5.3.3.** *For the scaling relation 5.3.2 and $\boldsymbol{c}$ defined in 5.1.4 we get*

$$\boldsymbol{c}_j + \frac{\tilde{p}_{in}}{2} = (\boldsymbol{V}\boldsymbol{d}\boldsymbol{V}^{-1}\mathbf{1}_{M,1})_j + \mathcal{O}(\omega^{\mu}) \tag{5.3.9}$$

*and*

$$\boldsymbol{c}_j - \frac{\tilde{p}_{in}}{2} = \omega^2(\boldsymbol{V}\boldsymbol{\Omega}_M^{-2}\boldsymbol{d}\boldsymbol{V}^{-1}\mathbf{1}_{M,1})_j + \mathcal{O}(\omega^{\mu}) \tag{5.3.10}$$

*for $\boldsymbol{d} = \mathrm{Diag}(d_1, \ldots, d_M)$ and*

$$d_i := \tilde{p}_{in}\omega_{M,i}^2 \frac{-(\omega^2 - \omega_{M,i}^2) + 2\mathrm{i}\tau_i\omega_{M,i}}{(\omega^2 - \omega_{M,i}^2)^2 + 4\tau_i^2\omega_{M,i}^2} = \frac{-\tilde{p}_{in}\omega_{M,i}^2 e^{\mathrm{i}\alpha_i}}{\sqrt{(\omega^2 - \omega_{M,i}^2)^2 + \left(4\tau_i^2\omega_{M,i}^2\right)}} \tag{5.3.11}$$

*with*

$$\alpha_i := \begin{cases} \arctan\left(-\frac{2\tau_i\omega_{M,i}}{\omega^2 - \omega_{M,i}^2}\right) + \pi, & \omega < \omega_{M,i}, \\ \arctan\left(-\frac{2\tau_i\omega_{M,i}}{\omega^2 - \omega_{M,i}^2}\right), & \omega > \omega_{M,i}. \end{cases} \tag{5.3.12}$$

*Proof.* We denote by $\boldsymbol{\Omega}_M, \mathrm{i}\boldsymbol{\tau}$ the diagonal matrices containing the two lowest orders of the resonance frequency. Lemma 5.3.1 gives us

$$\boldsymbol{A}\boldsymbol{V} + \mathcal{O}(\omega^{2+2\mu_-}) = \tilde{\boldsymbol{A}}_4 := -\frac{1}{c_b^2}\boldsymbol{D}\boldsymbol{V}(\boldsymbol{\omega}^2 - (\boldsymbol{\Omega}_M^2 + \mathrm{i}2\boldsymbol{\Omega}_M\boldsymbol{\tau})). \tag{5.3.13}$$

and

$$\boldsymbol{R} + \mathcal{O}(\omega^3) = \boldsymbol{R}_3 := \frac{\tilde{\mathrm{p}}_{\mathrm{in}}}{2c_b^2}\boldsymbol{D}\boldsymbol{V}(\boldsymbol{\omega}^2 + \boldsymbol{\Omega}_M^2)\boldsymbol{V}^{-1}\mathbf{1}_{M,1}. \tag{5.3.14}$$

We note that $\boldsymbol{A}\boldsymbol{c} = \boldsymbol{R} + \mathcal{O}(\omega^3)$ and by using the Neumann series thus get

$$\begin{aligned}(\boldsymbol{V}^{-1}\boldsymbol{c})_i =& (\tilde{\boldsymbol{A}}_4^{-1}\boldsymbol{R}_3)_i + \mathcal{O}(\omega^{2+2(\mu_- - 2\mu_+)}) \\ =& \left(\left(\left(c_b^{-2}\boldsymbol{D}\boldsymbol{V}\right)^{-1}\tilde{\boldsymbol{A}}_4\right)^{-1}\left(c_b^{-2}\boldsymbol{D}\boldsymbol{V}\right)^{-1}\boldsymbol{R}\right)_i + \mathcal{O}(\omega^{2+2(\mu_- - 2\mu_+)}).\end{aligned} \tag{5.3.15}$$

Next we note that

$$\left(\left(c_b^{-2}\boldsymbol{D}\boldsymbol{V}\right)^{-1}\tilde{\boldsymbol{A}}_4\right)^H\left(\left(c_b^{-2}\boldsymbol{D}\boldsymbol{V}\right)^{-1}\tilde{\boldsymbol{A}}_4\right) = (\boldsymbol{\omega}^2 - \boldsymbol{\Omega}_M^2)^2 + 4\boldsymbol{\tau}^2\boldsymbol{\Omega}_M^2. \tag{5.3.16}$$

Die approbierte gedruckte Originalversion dieser Diplomarbeit ist an der TU Wien Bibliothek verfügbar
The approved original version of this thesis is available in print at TU Wien Bibliothek.
TU Bibliothek Your knowledge hub WIEN

On the same line we have

$$\left(\left(c_b^{-2}\boldsymbol{DV}\right)^{-1}\tilde{\boldsymbol{A}}_4\right)^H\left(c_b^{-2}\boldsymbol{DV}\right)^{-1}\boldsymbol{R}_3 = -\frac{\tilde{\mathrm{p}}_{\mathrm{in}}}{2}\left(\boldsymbol{\omega}^4-\boldsymbol{\Omega}_M^4-4\mathrm{i}\boldsymbol{\tau}\boldsymbol{\omega}^2\boldsymbol{\Omega}_M\right)\boldsymbol{V}^{-1}\mathbf{1}_{M,1} + \mathcal{O}(\omega^{4+2\mu_-}). \tag{5.3.17}$$

Finally we can use these two results to arrive at

$$\begin{aligned}\tilde{\boldsymbol{A}}_4^{-1}\boldsymbol{R}_3 &= \left(\left(\left(c_b^{-2}\boldsymbol{DV}\right)^{-1}\tilde{\boldsymbol{A}}_4\right)^H\left(\left(c_b^{-2}\boldsymbol{DV}\right)^{-1}\tilde{\boldsymbol{A}}_4\right)\right)^{-1}\left(\left(c_b^{-2}\boldsymbol{DV}\right)^{-1}\tilde{\boldsymbol{A}}_4\right)^H\left(c_b^{-2}\boldsymbol{DV}\right)^{-1}\boldsymbol{R}_3\\ &= -\frac{\tilde{\mathrm{p}}_{\mathrm{in}}}{2}((\boldsymbol{\omega}^2-\boldsymbol{\Omega}_M^2)^2+4\boldsymbol{\tau}^2\boldsymbol{\Omega}_M^2)^{-1}\left(\boldsymbol{\omega}^4-\boldsymbol{\Omega}_M^4-4\mathrm{i}\boldsymbol{\tau}\boldsymbol{\omega}^2\boldsymbol{\Omega}_M\right)\boldsymbol{V}^{-1}\mathbf{1}_{M,1}\\ &\quad+\mathcal{O}(\omega^{2+2(\mu_--2\mu_+)})\end{aligned} \tag{5.3.18}$$

Next we note that we can replace $\omega$ by $\omega_{M,i}$ in the highest order. Due to this we have

$$\begin{aligned}c_j+\frac{\tilde{\mathrm{p}}_{\mathrm{in}}}{2} &= \sum_i \boldsymbol{V}_{j,i}\frac{\tilde{\mathrm{p}}_{\mathrm{in}}}{2}\left(1-\frac{\omega^4-\omega_{M,i}^4+4\mathrm{i}\tau_i\omega_{M,i}\omega_{M,i}^2}{(\omega^2-\omega_{M,i}^2)^2+4\tau_i^2\omega_{M,i}^2}\right)(\boldsymbol{V}^{-1}\mathbf{1}_{M,1})_i+\mathcal{O}(\omega^{2+2(\mu_--2\mu_+)})\\ &= -\sum_i \boldsymbol{V}_{j,i}\tilde{\mathrm{p}}_{\mathrm{in}}\omega_{M,i}^2\left(\frac{-\omega_{M,i}^2+\omega^2+2\mathrm{i}\tau_i\omega_{M,i}}{(\omega^2-\omega_{M,i}^2)^2+4\tau_i^2\omega_{M,i}^2}\right)(\boldsymbol{V}^{-1}\mathbf{1}_{M,1})_i+\mathcal{O}(\omega^{2+2(\mu_--2\mu_+)}).\end{aligned} \tag{5.3.19}$$

The formula for $c_j-\frac{\tilde{\mathrm{p}}_{\mathrm{in}}}{2}$ can be seen in the same way. □

Finally we can find the approximations for the coefficients of the resonance potential in the basis of eigenvectors.

**Lemma 5.3.4.** *Under the scaling assumption 5.3.2 we get for the solutions $\phi,\psi$ to 5.1.6 that*

$$\phi = \sum_i \zeta_i d_i(\boldsymbol{V}^{-1}\mathbf{1}_{M,1})_i+\mathcal{O}(\omega^{\mu}) \tag{5.3.20}$$

*and*

$$\psi = \sum_i \zeta_i\frac{\omega^2}{\omega_{M,i}^2}d_i(\boldsymbol{V}^{-1}\mathbf{1}_{M,1})_i+\mathcal{O}(\omega^{\mu}). \tag{5.3.21}$$

*for the resonance potentials $\zeta_i \coloneqq \sum_j \boldsymbol{V}_{j,i}\varphi_j$ and $d_i$ defined in lemma 5.3.3.*

*Proof.* We note that due to theorem 5.1.5 we get

$$\begin{aligned}\tilde{\boldsymbol{\phi}} &= \left(\tilde{\mathcal{A}}_D^{-1}\boldsymbol{F}\right)+\mathcal{O}(\omega^{2-2\mu_+}) = \frac{\tilde{\mathrm{p}}_{\mathrm{in}}}{2}\sum_i\varphi_i\begin{pmatrix}1\\-1\end{pmatrix}+\mathcal{O}(\omega^{2-2\mu_+})\\ &= \frac{\tilde{\mathrm{p}}_{\mathrm{in}}}{2}\sum_i\zeta_i(\boldsymbol{V}^{-1}\mathbf{1}_{M,1})_i\begin{pmatrix}1\\-1\end{pmatrix}+\mathcal{O}(\omega^{2-2\mu_+}).\end{aligned} \tag{5.3.22}$$

This results in the potentials $\phi=\sum_i\frac{\tilde{\mathrm{p}}_{\mathrm{in}}}{2}\varphi_i+\varphi$ and $\psi=-\sum_i\frac{\tilde{\mathrm{p}}_{\mathrm{in}}}{2}\varphi_i+\varphi$. Using lemma 5.3.3 we get the result. □

Die approbierte gedruckte Originalversion dieser Diplomarbeit ist an der TU Wien Bibliothek verfügbar
The approved original version of this thesis is available in print at TU Wien Bibliothek.
TU Bibliothek Your knowledge hub WIEN

The single bubble case again simplifies a lot.

**Corollary 5.3.5.** *Under the scaling assumption 5.3.2 we get for a single inclusion*

$$d_1 = \frac{-\tilde{p}_{in}\omega_M^2 e^{\mathrm{i}\alpha}}{\sqrt{(\omega^2-\omega_M^2)^2 + \left(\frac{C}{4\pi}k_l\omega_M^2\right)^2}} \tag{5.3.23}$$

*with*

$$\alpha := \begin{cases} \arctan\left(\frac{\frac{C}{4\pi}\omega_M^2 k_l}{\omega^2-\omega_M^2}\right) + \pi, & \omega < \omega_M \\ \arctan\left(\frac{\frac{C}{4\pi}\omega_M^2 k_l}{\omega^2-\omega_M^2}\right), & \omega > \omega_M \end{cases} \tag{5.3.24}$$

*for $\mu = \frac{1}{2}$ we get the more simple form*

$$d_1 = \frac{-\tilde{p}_{in}\omega_M^2}{\omega^2-\omega_M^2} + \mathcal{O}(\omega^{2-2\mu}). \tag{5.3.25}$$

*Proof.* We note that $\boldsymbol{V} = 1$ and

$$\tau = -\frac{C\omega_M^2}{8\pi c_l}. \tag{5.3.26}$$

Inserting this in lemma 5.3.4 provides the statement. □

Note that we can exchange $\omega$ with $\omega_M$ in the imaginary term due to the difference being of higher order. As we already noted in remark 5.2.5 this provides the well known phase shift term for a bubble with no viscosity and thermal effects [17].

## 5.4. Single spherical bubble systems

In this section we will derive the pressure field and its gradient on the bubble surface for a single spherical bubble. Afterwards we will use these relations to find a formula for the primary Bjerknes force and compare the result to historical derivations.

### 5.4.1. Operator relations

This subsection contains basics calculations for $\tilde{\mathcal{A}}_D^{-1}$ and $\mathcal{A}_D^{i,j}$ for a single bubble and can be skipped for readers not interested in the details. We will first state some results for the operator $\tilde{\mathcal{A}}_D^{-1}$.

**Lemma 5.4.1.** *We have for $D = B_{r_1}$ and $l > 0$ that*

$$\tilde{\mathcal{A}}_D^{-1}\begin{pmatrix}0\\Y_l^m\end{pmatrix} = -\frac{2l+1}{l}Y_l^m\begin{pmatrix}1\\1\end{pmatrix}, \qquad \tilde{\mathcal{A}}_D^{-1}\begin{pmatrix}Y_l^m\\0\end{pmatrix} = \frac{2l+1}{r_1}Y_l^m\begin{pmatrix}0\\1\end{pmatrix}. \tag{5.4.1}$$

*We further have*

$$\tilde{\mathcal{A}}_D^{-1}\begin{pmatrix}0\\Y_0^0\end{pmatrix} = -\sqrt{4\pi}Y_0^0\begin{pmatrix}1\\1\end{pmatrix}, \qquad \tilde{\mathcal{A}}_D^{-1}\begin{pmatrix}Y_0^0\\0\end{pmatrix} = -\frac{1}{2r_1}Y_0^0\begin{pmatrix}1\\-1\end{pmatrix}. \tag{5.4.2}$$

Die approbierte gedruckte Originalversion dieser Diplomarbeit ist an der TU Wien Bibliothek verfügbar
The approved original version of this thesis is available in print at TU Wien Bibliothek.
TU Bibliothek Your knowledge hub WIEN

*Proof.* For $\tilde{\mathcal{A}}_D \begin{pmatrix} \phi \\ \psi \end{pmatrix} = \begin{pmatrix} 0 \\ Y_l^m \end{pmatrix}$ we note that due to the first entry being 0 and the bijectivity of $S_D^0$ we get $\phi = \psi$. Further using lemma 4.2.4 we see that

$$\left(-\frac{1}{2} + K_D^0\right)[\phi] = -\frac{1}{2}\left(1 + \frac{1}{r_1} S_D^0\right)[\phi] = Y_l^m. \tag{5.4.3}$$

Using the Ansatz $\phi = cY_l^m$ and lemma 4.2.6 we arrive at

$$-\frac{1}{2}\left(1 - \frac{1}{2l+1}\right) cY_l^m = Y_l^m. \tag{5.4.4}$$

This gives us $\phi = -\frac{2l+1}{l} Y_l^m$. We note that $\langle Y_l^m, Y_0^0 \rangle_{L^2(\partial D)} = 0$ and $P_0 P_{\ker} \begin{pmatrix} Y_l^m \\ Y_l^m \end{pmatrix} = \mathbf{0}$. This concludes the proof of the first statement.
For the second statement we set $\tilde{\mathcal{A}}_D \begin{pmatrix} \phi \\ \psi \end{pmatrix} = \begin{pmatrix} Y_l^m \\ 0 \end{pmatrix}$. We get

$$\left(-\frac{1}{2} + K_D^0\right)[\phi] = 0 \tag{5.4.5}$$

and thus $\phi = cY_0^0$. We now have

$$S_D^0[cY_0^0 - \psi] = Y_l^m \tag{5.4.6}$$

and due to lemma 4.2.6 arrive at $\psi = \frac{2l+1}{r_1} Y_l^m + cY_0^0$. With $\langle \phi, Y_0^0 \rangle_{L^2(\partial D)} + \langle \psi, Y_0^0 \rangle_{L^2(\partial D)} = 0$ this results in $c = 0$.
The last 2 statements follow directly from lemma 5.1.6.

□

We now rewrite this for the first orders of a plane wave.

**Corollary 5.4.2.** *We have*

$$\tilde{\mathcal{A}}_D^{-1} \begin{pmatrix} \boldsymbol{n}\cdot\boldsymbol{k} \\ 0 \end{pmatrix} = \begin{pmatrix} 0 \\ \frac{3}{r_1} \boldsymbol{n}\cdot\boldsymbol{k} \end{pmatrix}, \qquad \tilde{\mathcal{A}}_D^{-1} \begin{pmatrix} (\boldsymbol{n}\cdot\boldsymbol{k})^2 \\ 0 \end{pmatrix} = \begin{pmatrix} -\frac{1}{6r_1}\boldsymbol{k}^2 \\ \frac{5}{r_1}(\boldsymbol{n}\cdot\boldsymbol{k})^2 - \frac{3}{2r_1}\boldsymbol{k}^2 \end{pmatrix} \tag{5.4.7}$$

*and*

$$\tilde{\mathcal{A}}_D^{-1} \begin{pmatrix} 0 \\ \boldsymbol{n}\cdot\boldsymbol{k} \end{pmatrix} = -3 \begin{pmatrix} \boldsymbol{n}\cdot\boldsymbol{k} \\ \boldsymbol{n}\cdot\boldsymbol{k} \end{pmatrix}, \qquad \tilde{\mathcal{A}}_D^{-1} \begin{pmatrix} 0 \\ (\boldsymbol{n}\cdot\boldsymbol{k})^2 \end{pmatrix} = \left(-\frac{5}{2}(\boldsymbol{n}\cdot\boldsymbol{k})^2 + \boldsymbol{k}^2 \frac{\frac{5}{2} - \sqrt{4\pi}}{3}\right) \begin{pmatrix} 1 \\ 1 \end{pmatrix}. \tag{5.4.8}$$

*Proof.* Follows directly from lemma 5.4.1. We choose the coordinate system with $z$ entry in $\boldsymbol{k}$ direction. We thus have

$$\boldsymbol{k}\cdot\boldsymbol{n} = |\boldsymbol{k}| \sqrt{\frac{4\pi}{3}} Y_1^0 \tag{5.4.9}$$

and

$$(\boldsymbol{k}\cdot\boldsymbol{n})^2 = \boldsymbol{k}^2 \frac{1}{3}\left(\sqrt{\frac{16\pi}{5}} Y_2^0 + \sqrt{4\pi} Y_0^0\right). \tag{5.4.10}$$

Die approbierte gedruckte Originalversion dieser Diplomarbeit ist an der TU Wien Bibliothek verfügbar
The approved original version of this thesis is available in print at TU Wien Bibliothek.
TU Bibliothek Your knowledge hub WIEN

We thus have

$$\tilde{\mathcal{A}}_D^{-1}\begin{pmatrix}\boldsymbol{k}^2\frac{1}{3}\left(\sqrt{\frac{16\pi}{5}}Y_2^0+\sqrt{4\pi}Y_0^0\right)\\0\end{pmatrix}=\boldsymbol{k}^2\frac{1}{3}\left(\sqrt{\frac{16\pi}{5}}\frac{5}{r_1}Y_2^0\begin{pmatrix}0\\1\end{pmatrix}-\sqrt{4\pi}\frac{1}{2r_1}Y_0^0\begin{pmatrix}1\\-1\end{pmatrix}\right)$$
$$=\begin{pmatrix}-\frac{1}{6r_1}\boldsymbol{k}^2\\\frac{5}{r_1}(\boldsymbol{k}\cdot\boldsymbol{n})^2-\frac{3}{2r_1}\boldsymbol{k}^2\end{pmatrix}. \tag{5.4.11}$$

Furthermore we get

$$\tilde{\mathcal{A}}_D^{-1}\begin{pmatrix}0\\\boldsymbol{k}^2\frac{1}{3}\left(\sqrt{\frac{16\pi}{5}}Y_2^0+\sqrt{4\pi}Y_0^0\right)\end{pmatrix}=\boldsymbol{k}^2\frac{1}{3}\left(-\sqrt{\frac{16\pi}{5}}\frac{5}{2}Y_2^0-\sqrt{4\pi}\sqrt{4\pi}Y_0^0\right)\begin{pmatrix}1\\1\end{pmatrix}$$
$$=\left(-\frac{5}{2}(\boldsymbol{k}\cdot\boldsymbol{n})^2-\boldsymbol{k}^2\frac{\sqrt{4\pi}-\frac{5}{2}}{3}\right)\begin{pmatrix}1\\1\end{pmatrix}. \tag{5.4.12}$$

□

The last lemma covers some terms that will appear in our derivations.

**Lemma 5.4.3.** *We have for a constant $\tilde{c}$ that*

$$\mathcal{A}_D^{0,1}\tilde{\mathcal{A}}_D^{-1}\begin{pmatrix}\mathrm{i}\boldsymbol{k}\cdot\boldsymbol{n}r_1\\0\end{pmatrix}=\begin{pmatrix}0\\-2\mathrm{i}\boldsymbol{k}\cdot\boldsymbol{n}\end{pmatrix},\qquad\mathcal{A}_D^{0,1}\tilde{\mathcal{A}}_D^{-1}\begin{pmatrix}(\boldsymbol{k}\cdot\boldsymbol{n}r_1)^2\\0\end{pmatrix}=\begin{pmatrix}0\\-3r_1(\boldsymbol{n}\cdot\boldsymbol{k})^2+\tilde{c}\end{pmatrix}. \tag{5.4.13}$$

*Proof.* We see that

$$\mathcal{A}_D^{0,1}\tilde{\mathcal{A}}_D^{-1}\begin{pmatrix}\mathrm{i}\boldsymbol{k}\cdot\boldsymbol{n}r_1\\0\end{pmatrix}=\mathcal{A}_D^{0,1}\begin{pmatrix}0\\3\mathrm{i}\boldsymbol{k}\cdot\boldsymbol{n}\end{pmatrix}=\begin{pmatrix}0\\-(\frac{1}{2}+K_D^0)[3\mathrm{i}\boldsymbol{k}\cdot\boldsymbol{n}]\end{pmatrix}=\begin{pmatrix}0\\-2\mathrm{i}\boldsymbol{k}\cdot\boldsymbol{n}\end{pmatrix}. \tag{5.4.14}$$

Further we get

$$\mathcal{A}_D^{0,1}\tilde{\mathcal{A}}_D^{-1}\begin{pmatrix}(\boldsymbol{k}\cdot\boldsymbol{n})^2\\0\end{pmatrix}=\mathcal{A}_D^{0,1}\begin{pmatrix}c_1\\\frac{5}{r_1}(\boldsymbol{n}\cdot\boldsymbol{k})^2+c_2\end{pmatrix}=\begin{pmatrix}0\\-(\frac{1}{2}+K_D^0)[\frac{5}{r_1}(\boldsymbol{n}\cdot\boldsymbol{k})^2+c_2]\end{pmatrix}$$
$$=\begin{pmatrix}0\\-\frac{1}{2}(1+\frac{1}{5})\frac{5}{r_1}(\boldsymbol{n}\cdot\boldsymbol{k})^2+\tilde{c}\end{pmatrix}=\begin{pmatrix}0\\-\frac{3}{r_1}(\boldsymbol{n}\cdot\boldsymbol{k})^2+\tilde{c}\end{pmatrix}. \tag{5.4.15}$$

□

### 5.4.2. Internal pressure gradient

Using the calculations of the last subsection we can now prove formulas for the pressure and its gradient on the surface. We are going to prove the following theorem in this subsection.

Die approbierte gedruckte Originalversion dieser Diplomarbeit ist an der TU Wien Bibliothek verfügbar
The approved original version of this thesis is available in print at TU Wien Bibliothek.
TU Bibliothek Your knowledge hub WIEN

**Theorem 5.4.4.** *For a single bubble and a standing wave $p_{in} = \tilde{p}_{in}\cos(\boldsymbol{k}\cdot\boldsymbol{z}+\gamma)$ we get for some constant $\tilde{\boldsymbol{c}}$ that*

$$p = \tilde{\boldsymbol{c}} - 3\tilde{p}_{in}\delta\sin(\gamma)\boldsymbol{k}\cdot\boldsymbol{n}r_1 - \delta\tilde{p}_{in}\frac{5}{4}r_1^2\cos(\gamma)(\boldsymbol{k}\cdot\boldsymbol{n})^2 + \mathcal{O}(\omega^5) \tag{5.4.16}$$

*and for another constant $\tilde{\boldsymbol{c}}$ that*

$$\nabla p|_- = \tilde{\boldsymbol{c}}\boldsymbol{n} - 3\delta\tilde{p}_{in}\sin(\gamma)\boldsymbol{k} - \delta\tilde{p}_{in}\frac{5}{2}r_1(\boldsymbol{k}\cdot\boldsymbol{n})\boldsymbol{k}\cos(\gamma) + \mathcal{O}(\omega^5) \tag{5.4.17}$$

*on $\partial D$. We further have in lower orders*

$$\nabla p|_- = -d_1 k_b^2\frac{r_1}{3}\cos(\gamma)\boldsymbol{n} + \mathcal{O}(\omega^{4-2\mu}), \tag{5.4.18}$$

*where $d_1$ is defined in 5.3.5 and the scaling relation 5.3.2.*

We can see that due to $\boldsymbol{u}|_- = \frac{1}{\rho_b\omega^2}\nabla \mathrm{p}\Big|_-$ that the term of order $\omega\delta$ corresponds to a translatory motion and the term of order $\delta\omega^2$ correspond to a deformation of the bubble, thus in order $\delta\omega^2$ the bubble does not in general follow the breathing approximation anymore (i.e. getting uniformly stretched/contracted), especially if it is at an antinode of a standing wave. We can see an exaggerated sketch of this in 5.1.
We will now show a few statements in order to proof theorem 5.4.4. We start out by defining vector spaces that allow us to more easily denote the next statements.

**Definition 5.4.5.** *We define*

$$\tilde{H}_s \coloneqq \operatorname{span}\{Y_j^0, j = 0,\dots,s\} \tag{5.4.19}$$

*and*

$$H_D^{s,t} \coloneqq \tilde{H}_s \times \tilde{H}_t. \tag{5.4.20}$$

The following corollary summarizes which parts of $\phi$ have to be looked at.

**Corollary 5.4.6.** *We have for all $i,j$ that*

$$\begin{aligned} &\tilde{\mathcal{A}}_D^{-1}(H_D^{0,j}) \subseteq H_D^{j,j}, && \tilde{\mathcal{A}}_D^{-1}(H_D^{i,0}) \subseteq H_D^{0,i}, \\ &\mathcal{A}_D^{i,j}(H_D^{0,0}) \subseteq H_D^{0,0}, && \mathcal{A}_D^{2,0}(H_D^{0,1}) \subseteq H_D^{1,0}, \\ &\mathcal{A}_D^{1,0}(H_D^{i,j}) \subseteq H_D^{0,0}. \end{aligned} \tag{5.4.21}$$

*Proof.* The first 2 statements follow directly from lemma 5.4.1.
Statement 3 holds due to symmetry and lemma 4.2.4. Statement 4 follows from 7.2.2. The last one follows directly from the definition. □

We will now look at the potentials of the system.

Die approbierte gedruckte Originalversion dieser Diplomarbeit ist an der TU Wien Bibliothek verfügbar
The approved original version of this thesis is available in print at TU Wien Bibliothek.
TU Bibliothek Your knowledge hub WIEN

**Lemma 5.4.7.** *We define* $\mathrm{I}_{D,5}$ *as the operator that contains all terms below order* $\omega^5, \omega^3\delta$ *of* $\mathrm{I}_d$ *defined in lemma 5.1.5. We have*

$$\mathrm{I}_{D,5}[\boldsymbol{\varphi}_i] \in H_D^{0,0}. \tag{5.4.22}$$

*We further have with the scaling relation 5.3.2 that*

$$(\mathrm{I}_5[\tilde{\mathcal{A}}_D^{-1}\boldsymbol{F}])_1 = -\delta\tilde{p}_{in}9\mathrm{i}\boldsymbol{k}\cdot\boldsymbol{n} + \delta\tilde{p}_{in}\left(\frac{5}{2}\right)^2 r_1(\boldsymbol{k}\cdot\boldsymbol{n})^2 + \tilde{c}\varphi_1 + \mathcal{O}(\omega^5) \tag{5.4.23}$$

*Proof.* Corollary 5.4.6 immediately proves the first statement. With the corollary we also see that only $\mathcal{A}_D^{0,1}$ provides a non constant second entry in $\boldsymbol{\phi}$ up to order $\omega^5$. We get due to lemma 5.4.3 for a constant $\tilde{c}$ that

$$\begin{aligned}(\mathrm{I}_5[\tilde{\mathcal{A}}_D^{-1}\boldsymbol{F}])_1 =& \tilde{\mathcal{A}}_D^{-1}\begin{pmatrix}0\\ \delta\tilde{\mathrm{p}}_{\mathrm{in}}(\mathrm{i}\boldsymbol{k}\cdot\boldsymbol{n} - r_1(\boldsymbol{k}\cdot\boldsymbol{n})^2)\end{pmatrix}\\ &- \delta\tilde{\mathcal{A}}_D^{-1}\mathcal{A}_D^{0,1}\tilde{\mathcal{A}}_D^{-1}\begin{pmatrix}\tilde{\mathrm{p}}_{\mathrm{in}}r_1(\mathrm{i}\boldsymbol{k}\cdot\boldsymbol{n} - r_1(\boldsymbol{k}\cdot\boldsymbol{n})^2\frac{1}{2})\\ 0\end{pmatrix} + \tilde{c}\varphi_1\\ =&\tilde{\mathcal{A}}_D^{-1}\begin{pmatrix}0\\ 3\delta\tilde{\mathrm{p}}_{\mathrm{in}}\mathrm{i}\boldsymbol{k}\cdot\boldsymbol{n}\end{pmatrix} - \tilde{\mathcal{A}}_D^{-1}\begin{pmatrix}0\\ \delta\tilde{\mathrm{p}}_{\mathrm{in}}\frac{5}{2}r_1(\boldsymbol{k}\cdot\boldsymbol{n})^2\end{pmatrix} + \tilde{c}\varphi_1.\end{aligned} \tag{5.4.24}$$

Using lemma 5.4.1 we arrive at the statement. □

With this statement about the potentials we will proceed by looking at the normal derivative of the pressure.

**Lemma 5.4.8.** *For a single spherical inclusion, an incident field* $p_{in} = \tilde{p}_{in}e^{\mathrm{i}(\boldsymbol{k}\cdot\boldsymbol{z})}$ *and the scaling relation 5.3.2 we get*

$$\frac{\mathrm{d}p}{\mathrm{d}\boldsymbol{n}}\Big|_- = \tilde{\boldsymbol{c}} + 3\tilde{p}_{in}\delta\mathrm{i}\boldsymbol{k}\cdot\boldsymbol{n} - \delta\tilde{p}_{in}\frac{5}{2}r_1(\boldsymbol{k}\cdot\boldsymbol{n})^2 + \mathcal{O}(\omega^5) \tag{5.4.25}$$

*on* $\partial D$*. We further have in the lower order*

$$\frac{\mathrm{d}p}{\mathrm{d}\boldsymbol{n}}\Big|_- = -d_1k_b^2\frac{r_1}{3} + \mathcal{O}(\omega^{4-2\mu}). \tag{5.4.26}$$

*Proof.* We have

$$\begin{aligned}\frac{\mathrm{dp}}{\mathrm{d}\boldsymbol{n}}\Big|_- =&\boldsymbol{c}\frac{\mathrm{d}}{\mathrm{d}\boldsymbol{n}}S_D^{k_b}[\varphi_1] + \left(-\frac{1}{2} + K_D^0\right)\left[-\delta\tilde{\mathrm{p}}_{\mathrm{in}}9\mathrm{i}\boldsymbol{k}\cdot\boldsymbol{n} + \delta\tilde{\mathrm{p}}_{\mathrm{in}}\left(\frac{5}{2}\right)^2 r_1(\boldsymbol{k}\cdot\boldsymbol{n})^2\right] + \mathcal{O}(\omega^5)\\ =&\boldsymbol{c}\frac{\mathrm{d}}{\mathrm{d}\boldsymbol{n}}S_D^{k_b}[\varphi_1] + \delta\tilde{\mathrm{p}}_{\mathrm{in}}3\mathrm{i}\boldsymbol{k}\cdot\boldsymbol{n} - \delta\tilde{\mathrm{p}}_{\mathrm{in}}\frac{5}{2}r_1(\boldsymbol{k}\cdot\boldsymbol{n})^2 + \mathcal{O}(\omega^5).\end{aligned} \tag{5.4.27}$$

Note that $\frac{\mathrm{d}}{\mathrm{d}\boldsymbol{n}}S_D^{k_l}[\varphi_1]$ is constant due to symmetry/$\varphi_i$ being constant. Next we see, using lemma 4.2.8, that

$$\left(-\frac{1}{2} + K_D^{k_b}\right)[\varphi_1] = k_b^2K_D^2[\varphi_1] + k_b^3K_D^3[\varphi_1] + \mathcal{O}(\omega^{5-2\mu}) = -k_b^2\frac{r_1}{3} - k_b^3\frac{\mathrm{i}r_1^2}{3} + \mathcal{O}(\omega^{5-2\mu}). \tag{5.4.28}$$

□

Die approbierte gedruckte Originalversion dieser Diplomarbeit ist an der TU Wien Bibliothek verfügbar
The approved original version of this thesis is available in print at TU Wien Bibliothek.
TU Bibliothek Your knowledge hub WIEN

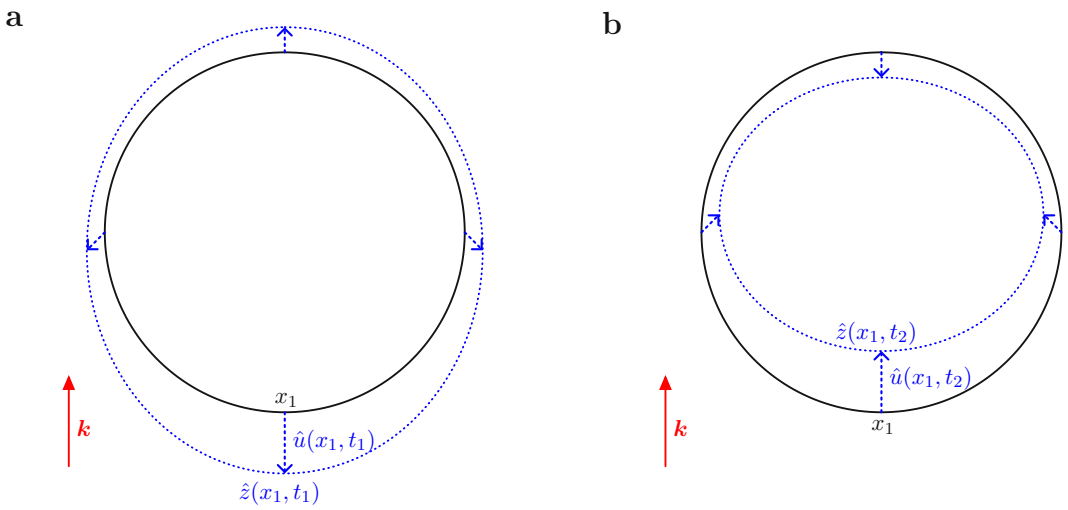


Figure 5.1.: Sketch of the deformation of a bubble at different times during a period. For this sketch we consider deformations up to order $\delta\omega^3$.

In the same way we can derive the pressure on the surface.

**Lemma 5.4.9.** *For a single spherical inclusion, an incident field* $p_{in} = \tilde{p}_{in} e^{\mathrm{i}(\boldsymbol{k}\cdot\boldsymbol{z})}$ *and the scaling relation 5.3.2 we get for a constant* $\tilde{\boldsymbol{c}}$ *that*

$$p = \tilde{\boldsymbol{c}} + 3\tilde{p}_{in}\delta\mathrm{i}\boldsymbol{k}\cdot\boldsymbol{n}r_1 - \delta\tilde{p}_{in}\frac{5}{4}r_1^2(\boldsymbol{k}\cdot\boldsymbol{n})^2 + \mathcal{O}(\omega^5) \tag{5.4.29}$$

*on* $\partial D$ *and*

$$\nabla_T p = 3\tilde{p}_{in}\delta\mathrm{i}(\boldsymbol{k} - (\boldsymbol{k}\cdot\boldsymbol{n})\boldsymbol{n}) - \delta\tilde{p}_{in}\frac{5}{2}r_1(\boldsymbol{k}\cdot\boldsymbol{n})(\boldsymbol{k} - (\boldsymbol{k}\cdot\boldsymbol{n})\boldsymbol{n}) + \mathcal{O}(\omega^5). \tag{5.4.30}$$

*Proof.* We have

$$\begin{aligned} \mathrm{p} =& S_D^{k_b}[\phi] = \boldsymbol{c}S_D^{k_b}[\varphi_1] + S_D^0\left[-\delta\tilde{\mathrm{p}}_{\mathrm{in}}9\mathrm{i}\boldsymbol{k}\cdot\boldsymbol{n} + \delta\tilde{\mathrm{p}}_{\mathrm{in}}\left(\frac{5}{2}\right)^2 r_1(\boldsymbol{k}\cdot\boldsymbol{n})^2\right] + \mathcal{O}(\omega^5) \\ =& \tilde{\boldsymbol{c}} + 3\tilde{\mathrm{p}}_{\mathrm{in}}\delta\mathrm{i}\boldsymbol{k}\cdot\boldsymbol{n}r_1 - \delta\tilde{\mathrm{p}}_{\mathrm{in}}\frac{5}{4}r_1^2(\boldsymbol{k}\cdot\boldsymbol{n})^2 + \mathcal{O}(\omega^5). \end{aligned} \tag{5.4.31}$$

□

Now in order to finish the proof of theorem 5.4.4 we add up the contributions for the standing wave $\mathrm{p}_{\mathrm{in}} = \frac{1}{2}(\tilde{\mathrm{p}}_{\mathrm{in}}e^{i\gamma}e^{i\boldsymbol{k}\cdot\boldsymbol{x}} + \tilde{\mathrm{p}}_{\mathrm{in}}e^{-i\gamma}e^{-i\boldsymbol{k}\cdot\boldsymbol{x}})$. We are now equipped to calculate the primary Bjerknes force.

### 5.4.3. Primary Bjerknes force

The following theorem shows that the first Bjerknes force is consistent with the results in literature [17]. We can see with this formula that for the case $\omega > \omega_M$ our bubble

Die approbierte gedruckte Originalversion dieser Diplomarbeit ist an der TU Wien Bibliothek verfügbar
The approved original version of this thesis is available in print at TU Wien Bibliothek.
TU Bibliothek Your knowledge hub WIEN

experiences a force toward the nearest pressure node ($\cos(\beta) = 0$). While for $\omega < \omega_M$ it is towards the closest pressure antinode ($\cos(\beta) = 1$). We can see a sketch of this in figure 5.2. Note that in the literature the force gets applied to the Minnaert bubble with added mass. This means that our force has an additional factor $2\delta$, see section 2.1.1.

**Theorem 5.4.10.** *We assume a standing incident field $p_{in} = \tilde{p}_{in}\cos(\boldsymbol{k}\cdot\boldsymbol{x}+\beta)$ and the scaling relation 5.3.2. Then the first Bjerknes force for a spherical bubble turns to*

$$\boldsymbol{F}_1^b = 2\delta\tilde{p}_{in}^2\frac{\pi r_1}{\rho_l}\frac{\cos(\alpha_1)\sin(2\beta)}{\sqrt{(\omega^2-\omega_M^2)^2+\left(r_1 k_l\omega_M^2\right)^2}}\boldsymbol{k}+\mathcal{O}(\rho_l^{-1}\omega^{3-2\mu}). \tag{5.4.32}$$

*Proof.* We remind ourselves of lemma 3.3.3,

$$\boldsymbol{F}_1^{\mathrm{b}} = \frac{1}{\rho_b\omega^2}\frac{1}{T}\int_0^T\int_{\partial D}(\nabla_T \mathrm{p}|_-)^2\boldsymbol{n}-(\nabla \mathrm{p}|_-\cdot\boldsymbol{n})\,\nabla_T \mathrm{p}|_-\,\mathrm{d}\sigma\,\mathrm{d}t. \tag{5.4.33}$$

We see that

$$\nabla_T \mathrm{p} = -3\tilde{\mathrm{p}}_{\mathrm{in}}\delta\sin(\beta)(\boldsymbol{k}-(\boldsymbol{k}\cdot\boldsymbol{n})\boldsymbol{n})\sin(\omega t)-\delta\tilde{\mathrm{p}}_{\mathrm{in}}\frac{5}{2}r_1(\boldsymbol{k}\cdot\boldsymbol{n})(\boldsymbol{k}-(\boldsymbol{k}\cdot\boldsymbol{n})\boldsymbol{n})\cos(\beta)+\mathcal{O}(\omega^5). \tag{5.4.34}$$

We thus see that due to theorem 5.4.4 we get

$$\begin{aligned}
(\nabla_T \mathrm{p}_1|_-)^2\boldsymbol{n}&-(\nabla \mathrm{p}_1|_-\cdot\boldsymbol{n})\,\nabla_T \mathrm{p}_1|_- = \\
&=\frac{\tilde{\mathrm{p}}_{\mathrm{in}}\omega_M^2\sin(\omega t+\alpha_1)}{\sqrt{(\omega^2-\omega_M^2)^2+\left(\frac{C}{4\pi}k_l\omega_M^2\right)^2}}k_b^2\frac{r_1}{3}\cos(\beta)3\tilde{\mathrm{p}}_{\mathrm{in}}\delta\sin(\beta)(\boldsymbol{k}-(\boldsymbol{k}\cdot\boldsymbol{n})\boldsymbol{n})\sin(\omega t)\\
&\quad+\tilde{c}_1\boldsymbol{k}^2\boldsymbol{n}+\tilde{c}_2(\boldsymbol{k}\cdot\boldsymbol{n})^2\boldsymbol{n}+\tilde{c}_3(\boldsymbol{k}\cdot\boldsymbol{n})\boldsymbol{k}+\mathcal{O}(\omega^7+\omega^{8-2\mu})\\
&=\frac{\tilde{\mathrm{p}}_{\mathrm{in}}\omega_M^2\sin(\omega t+\alpha_1)}{\sqrt{(\omega^2-\omega_M^2)^2+\left(\frac{C}{4\pi}k_l\omega_M^2\right)^2}}\sin(\omega t)k_b^2\frac{r_1}{2}\tilde{\mathrm{p}}_{\mathrm{in}}\delta\sin(2\beta)(\boldsymbol{k}-(\boldsymbol{k}\cdot\boldsymbol{n})\boldsymbol{n})\\
&\quad+\tilde{c}_1\boldsymbol{k}^2\boldsymbol{n}+\tilde{c}_2(\boldsymbol{k}\cdot\boldsymbol{n})^2\boldsymbol{n}+\tilde{c}_3(\boldsymbol{k}\cdot\boldsymbol{n})\boldsymbol{k}+\mathcal{O}(\omega^{8-2\mu}).
\end{aligned} \tag{5.4.35}$$

We further have

$$\int_{\partial D}\boldsymbol{k}-(\boldsymbol{k}\cdot\boldsymbol{n})\boldsymbol{n}\,\mathrm{d}\sigma = \boldsymbol{k}|\partial D|-\boldsymbol{k}\frac{1}{r_1}|D| = \frac{8}{3}\pi r_1^2\boldsymbol{k} \tag{5.4.36}$$

and the following integrals disappear

$$\int_{\partial D}\boldsymbol{k}^2\boldsymbol{n}\,\mathrm{d}\sigma = \int_{\partial D}(\boldsymbol{k}\cdot\boldsymbol{n})^2\boldsymbol{n}\,\mathrm{d}\sigma = \int_{\partial D}(\boldsymbol{k}\cdot\boldsymbol{n})\boldsymbol{k}\,\mathrm{d}\sigma = 0. \tag{5.4.37}$$

Further we see that

$$\frac{1}{T}\int_0^T\sin(\omega t+\alpha_1)\sin(\omega t)\,\mathrm{d}t = \frac{\cos(\alpha_1)}{2}. \tag{5.4.38}$$

Die approbierte gedruckte Originalversion dieser Diplomarbeit ist an der TU Wien Bibliothek verfügbar
The approved original version of this thesis is available in print at TU Wien Bibliothek.
TU Bibliothek Your knowledge hub WIEN

**a**

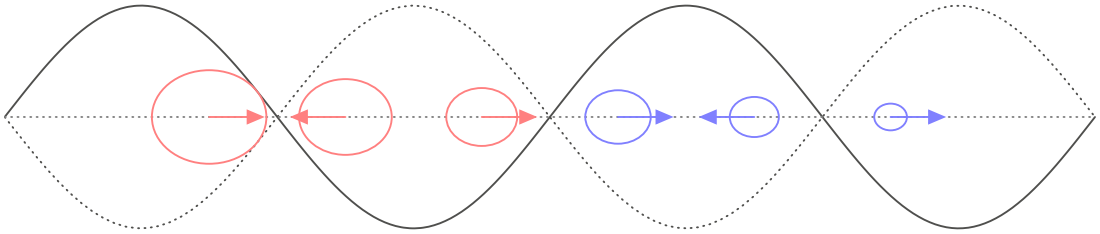

Figure 5.2.: Sketch of the directions of the primary Bjerknes forces for different configurations of a bubble in a standing wave of fixed forcing frequencies $\omega$. The red/blue circles represent bubbles with a resonance frequency smaller/larger than this frequency. They get pushed toward the nodes/anti-nodes respectively. Note that the length of the arrows are arbitrary and that we do not consider the secondary Bjerknes forces here.

This results in

$$\begin{aligned}
\boldsymbol{F}_1^{\mathrm{b}} =& \frac{1}{\rho_b \omega^2} \frac{\cos(\alpha_1)}{2} \frac{\tilde{\mathrm{p}}_{\mathrm{in}} \omega_M^2}{\sqrt{(\omega^2 - \omega_M^2)^2 + \left(\frac{C}{4\pi} k_l \omega_M^2\right)^2}} k_b^2 \frac{4\pi r_1^3}{3} \tilde{\mathrm{p}}_{\mathrm{in}} \delta \sin(2\beta) \boldsymbol{k} + \mathcal{O}(\rho_b^{-1} \omega^{5-2\mu}) \\
=& \tilde{\mathrm{p}}_{\mathrm{in}}^2 \frac{k_b^2}{\rho_l \omega^2} \frac{2\pi r_1^3}{3} \frac{\omega_M^2}{\sqrt{(\omega^2 - \omega_M^2)^2 + \left(r_1 k_l \omega_M^2\right)^2}} \cos(\alpha_1) \sin(2\beta) \boldsymbol{k} + \mathcal{O}(\rho_l^{-1} \omega^{3-2\mu}) \\
=& 2\delta \tilde{\mathrm{p}}_{\mathrm{in}}^2 \frac{\pi r_1}{\rho_l} \frac{\cos(\alpha_1) \sin(2\beta)}{\sqrt{(\omega^2 - \omega_M^2)^2 + \left(r_1 k_l \omega_M^2\right)^2}} \boldsymbol{k} + \mathcal{O}(\rho_l^{-1} \omega^{3-2\mu})
\end{aligned} \tag{5.4.39}$$

□

Die approbierte gedruckte Originalversion dieser Diplomarbeit ist an der TU Wien Bibliothek verfügbar
The approved original version of this thesis is available in print at TU Wien Bibliothek.
TU Bibliothek Your knowledge hub WIEN

# 6. Weakly interacting system

In this chapter we will define weakly interacting systems, which are made up of clusters of strongly interacting bubbles with scaling distances to the other clusters. We will the derive an appropriate scaling and separate the system into isolated and interacting parts. Finally we will apply this to separated spherical bubbles and calculate the secondary Bjerknes force for them.

## 6.1. Scaling distance decomposition

We will start out by the description of weakly interacting systems. The main idea of this approach is to fix the phase shift that a wave experiences travelling between bubble clusters. This naturally results in a scaling of the distance due to changing $\omega$. The system is made up of weakly interacting inclusion clusters $D_i$ with centres $\boldsymbol{z}_{i,0}$ for $i = 1, \dots, M$, which can be split into connected inclusions $D_{i,j}$ for $j = 1, \dots, M_i$. We can see a sketch of the setup in figure 6.1. Next we define the scaled cluster centres

$$\boldsymbol{z}_i(d) \coloneqq d\boldsymbol{z}_{i,0} \tag{6.1.1}$$

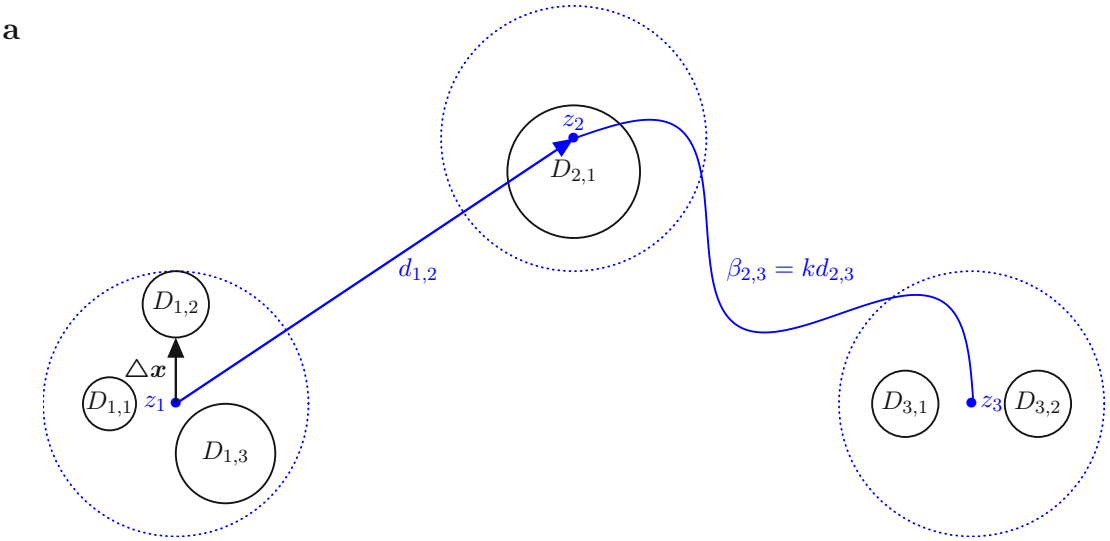


Figure 6.1.: Sketch of a far field system. The distance between the dotted areas scales and is indirect proportional to the frequency. This results in a constant phase shift for a wave propagating between inclusion clusters. We see that $M_1 = 3, M_2 = 1, M_3 = 2$ and $M = 3$.



Die approbierte gedruckte Originalversion dieser Diplomarbeit ist an der TU Wien Bibliothek verfügbar
The approved original version of this thesis is available in print at TU Wien Bibliothek.
TU Bibliothek Your knowledge hub WIEN

for the scaling factor d. The inclusion clusters will be shifted away from each other from $\boldsymbol{z}_{i,0}$ to $\boldsymbol{z}_i(d)$, namely $D_i(d) = D_i + \boldsymbol{z}_i(d-1)$. For simpler notation we write $\triangle\boldsymbol{x} \coloneqq x - \boldsymbol{z}_i$ for $\boldsymbol{x} \in \partial D_i$, $\boldsymbol{d}_{i,j} \coloneqq \boldsymbol{z}_j - \boldsymbol{z}_i$, $d_{i,j} \coloneqq |\boldsymbol{d}_{i,j}| = d|\boldsymbol{z}_{i,0} - \boldsymbol{z}_{j,0}|$ and $\widehat{\boldsymbol{d}}_{i,j}$ the unit vector in direction $\boldsymbol{d}_{i,j}$. Next we define the phase shifts that an incident plane wave and a wave travelling between the clusters experience, namely

$$\beta_i \coloneqq \boldsymbol{k} \cdot \boldsymbol{z}_i, \qquad \beta_{i,j} \coloneqq k_l d_{i,j}. \tag{6.1.2}$$

We will further assume that the distance parameter $d$ scales indirect proportional to the frequency $\omega$, more specifically we have constant $\beta_i$ and $\beta_{i,j}$. This also guarantees $r_i \ll d$ for $\omega \ll 1$, which will simplify the geometrical structure "felt" by the other bubble clusters. We define the incident plane wave for a wave vector $\boldsymbol{k}$ as

$$\mathrm{p}_{\mathrm{in}}(\boldsymbol{x}) \coloneqq \tilde{\mathrm{p}}_{\mathrm{in}} e^{\mathrm{i}\boldsymbol{k}\cdot\boldsymbol{x}}. \tag{6.1.3}$$

It is noteworthy that the problem $\boldsymbol{x} \in D_i(d)$ with

$$k_b^2 \mathrm{p}(\boldsymbol{x}) + \Delta \mathrm{p}(\boldsymbol{x}) = 0 \tag{6.1.4}$$

can be rewritten to $\boldsymbol{x} \in d^{-1}(D_i - \boldsymbol{z}_{i,0}) + \boldsymbol{z}_{i,0}$ with

$$(\tilde{k_b}^2 \tilde{\mathrm{p}} + \Delta\tilde{\mathrm{p}})(\boldsymbol{x}) = 0 \tag{6.1.5}$$

for $\tilde{k_b}^2 \coloneqq k_b^2 d^2 = \text{const}$ and $\tilde{\mathrm{p}}(\boldsymbol{x}) \coloneqq \mathrm{p}(\boldsymbol{x}d)$. Similar statements hold for the liquid part and the boundary conditions. This shows that we can rescale the size of the inclusions and move them closer together instead of increasing the distance and decreasing the frequency.

### 6.1.1. Far field expansion

Due to the distances between the clusters scaling indirect proportional to the frequency we need to find a new decomposition of $\mathcal{A}_D$ for the parts coupling between different bubble clusters. For coupling inside the same cluster we can use the expansion of strongly interacting systems. We will first look at $S_{D_i}^{k_l}$ and find a new expansion

$$S_{D_i}^{k_l}[\phi](\boldsymbol{x}) = \sum_n k_l^n \widetilde{S}_{D_i,D_j}^{\beta_{i,j},n}[\phi](\triangle\boldsymbol{x}) \tag{6.1.6}$$

for $\boldsymbol{x} \in \partial D_j$ with $j \neq i$. Note that the expansion operators $\widetilde{S}_{D_i,D_j}^{\beta_{i,j},n}$ only depend on $\triangle\boldsymbol{x}$ and thus do not scale with distance. In general this can be achieved by using the generating function of the Legendre polynomials and the recurrence relation (lemma 4.2.1). We then get for $|\boldsymbol{x}| > |\boldsymbol{y}|$ that

$$|\boldsymbol{x} - \boldsymbol{y}| = \frac{1}{|\boldsymbol{x}|} \sum_l \left(\frac{|\boldsymbol{y}|}{|\boldsymbol{x}|}\right)^l (\boldsymbol{x}^2 + \boldsymbol{y}^2) P_l(\widehat{\boldsymbol{x}} \cdot \widehat{\boldsymbol{y}}). \tag{6.1.7}$$

Die approbierte gedruckte Originalversion dieser Diplomarbeit ist an der TU Wien Bibliothek verfügbar
The approved original version of this thesis is available in print at TU Wien Bibliothek.
TU Bibliothek Your knowledge hub WIEN

This gives us for large $d$, $\boldsymbol{x} \in \partial D_i$, $\boldsymbol{y} \in \partial D_j$ and $\widehat{\boldsymbol{v}}$ the unit vector in direction $\triangle \boldsymbol{x} - \triangle \boldsymbol{y}$ that

$$\begin{aligned} |\boldsymbol{x}-\boldsymbol{y}| =& d\left|\widehat{\boldsymbol{d}}_{i,j} + (\triangle \boldsymbol{x} - \triangle \boldsymbol{y})\frac{1}{d}\right| \\ =& d\sum_l \frac{|\triangle \boldsymbol{x} - \triangle \boldsymbol{y}|^l}{d^l}(1+|\triangle \boldsymbol{x} - \triangle \boldsymbol{y}|^2)P_l\left(\widehat{\boldsymbol{v}}\cdot\widehat{\boldsymbol{d}}_{i,j}\right). \end{aligned} \tag{6.1.8}$$

We can now insert this in the definition of the layer potentials 4.1.2, use the relation between $d$ and $\omega$ and derive the expansion in $\omega$. The well definiteness and convergence can be proven in the same manner as we did in the strongly interacting case in lemma 4.1.5. For our purposes this is not necessary as we only need the first orders of the expansion. This leads us to the following lemma.

**Lemma 6.1.1.** *We have*

$$\begin{aligned} &\widetilde{S}^{0,\beta_{i,j}}_{D_i,D_j}[\phi](\triangle \boldsymbol{x}) = 0, \qquad \widetilde{S}^{1,\beta_{i,j}}_{D_i,D_j}[\phi](\triangle \boldsymbol{x}) = -\frac{e^{\mathrm{i}\beta_{i,j}}}{4\pi\beta_{i,j}}\int_{\partial D_i}\phi(\boldsymbol{y})\,\mathrm{d}\sigma(\boldsymbol{y}), \\ &\widetilde{S}^{2,\beta_{i,j}}_{D_i,D_j}[\phi](\triangle \boldsymbol{x}) = \frac{e^{\mathrm{i}\beta_{i,j}}(1-\mathrm{i}\beta_{i,j})}{4\pi\beta_{i,j}^2}\int_{\partial D_i}\widehat{\boldsymbol{d}}_{i,j}\cdot(\triangle \boldsymbol{x} - \triangle \boldsymbol{y})\phi(\boldsymbol{y})\,\mathrm{d}\sigma(\boldsymbol{y}), \\ &\frac{\mathrm{d}}{\mathrm{d}\boldsymbol{n}_x}\widetilde{S}^{0,\beta_{i,j}}_{D_i,D_j}[\phi](\triangle \boldsymbol{x}) = \frac{\mathrm{d}}{\mathrm{d}\boldsymbol{n}_x}\widetilde{S}^{1,\beta_{i,j}}_{D_i,D_j}[\phi](\triangle \boldsymbol{x}) = 0 \\ &\frac{\mathrm{d}}{\mathrm{d}\boldsymbol{n}_x}\widetilde{S}^{2,\beta_{i,j}}_{D_i,D_j}[\phi](\triangle \boldsymbol{x}) = \frac{e^{\mathrm{i}\beta_{i,j}}(1-i\beta_{i,j})}{4\pi\beta_{i,j}^2}\int_{\partial D_i}\widehat{\boldsymbol{d}}_{i,j}\cdot\boldsymbol{n}_x\phi(\boldsymbol{y})\,\mathrm{d}\sigma(\boldsymbol{y}) \end{aligned} \tag{6.1.9}$$

*for $\boldsymbol{x} \in \partial D_j$ and $j \neq i$.*

*Proof.* Let us first examine $|\boldsymbol{x}-\boldsymbol{y}|$ for $\boldsymbol{x} \in D_j, \boldsymbol{y} \in D_i$. Using the Taylor expansion of $\sqrt{1+x}$ we get

$$\begin{aligned} |\boldsymbol{x}-\boldsymbol{y}| =& d\left|\widehat{\boldsymbol{d}}_{i,j} + (\triangle \boldsymbol{x} - \triangle \boldsymbol{y})\frac{1}{d}\right| \\ =& d + \widehat{\boldsymbol{d}}_{i,j}\cdot(\triangle \boldsymbol{x} - \triangle \boldsymbol{y}) + \mathcal{O}\left(\frac{1}{d^2}\right). \end{aligned} \tag{6.1.10}$$

This can be applied to the single layer potential to get

$$\begin{aligned} S^{k_l}_{D_1}[\psi](\boldsymbol{x}) =& \frac{-1}{4\pi}e^{\mathrm{i}k_l d}\int_{\partial D_1} e^{\mathrm{i}k_l\widehat{\boldsymbol{d}}_{i,j}\cdot(\triangle \boldsymbol{x}-\triangle \boldsymbol{y})}\left(\frac{1}{d} - \widehat{\boldsymbol{d}}_{i,j}\cdot(\triangle \boldsymbol{x} - \triangle \boldsymbol{y})\frac{1}{d^2}\right)\psi(\boldsymbol{y})\,\mathrm{d}\sigma(\boldsymbol{y}) + \mathcal{O}(\omega^3) \\ =& \frac{-1}{4\pi}\frac{e^{\mathrm{i}k_l d}}{d}\int_{\partial D_1}\left(1 - \widehat{\boldsymbol{d}}_{i,j}\cdot(\triangle \boldsymbol{x} - \triangle \boldsymbol{y})\frac{1}{d}(1-\mathrm{i}k_l d)\right)\psi(\boldsymbol{y})\,\mathrm{d}\sigma(\boldsymbol{y}) + \mathcal{O}(\omega^3). \end{aligned} \tag{6.1.11}$$

□

Die approbierte gedruckte Originalversion dieser Diplomarbeit ist an der TU Wien Bibliothek verfügbar
The approved original version of this thesis is available in print at TU Wien Bibliothek.
TU Bibliothek Your knowledge hub WIEN

In order to use this decomposition more easily we are going to apply it to a different single layer representation (see [10]) of the multi bubble system compared to the strongly interacting case. We have

$$\mathrm{p}(\boldsymbol{x}) = \begin{cases} \sum_i S_{D_i}^{k_l}[\psi_i](\boldsymbol{x}) + \mathrm{p_{in}}(\boldsymbol{x}) & \boldsymbol{x} \in \mathbb{R}^d/\overline{D}, \\ S_{D_i}^{k_b}[\phi_i](\boldsymbol{x}) & \boldsymbol{x} \in D_i, \end{cases} \tag{6.1.12}$$

with

$$\begin{cases} S_{D_i}^{k_b}[\phi_i](\boldsymbol{x}) - S_{D_i}^{k_l}[\psi_i](\boldsymbol{x}) = \mathrm{p_{in}}(\boldsymbol{x}) + \sum_{j\neq i} S_{D_j}^{k_l}[\psi_j](\boldsymbol{x}), \\ \left(-\frac{1}{2} + K_{D_i}^{k_b}\right)[\phi_i](\boldsymbol{x}) - \delta\left(\frac{1}{2} + K_{D_i}^{k_l}\right)[\psi_i](\boldsymbol{x}) = \delta\left(\frac{\mathrm{d}\mathrm{p_{in}}}{\mathrm{d}\boldsymbol{n}_i}(\boldsymbol{x}) + \sum_{j\neq i} \frac{\mathrm{d}}{\mathrm{d}\boldsymbol{n}_i} S_{D_j}^{k_l}[\psi_j](\boldsymbol{x})\right) \end{cases} \tag{6.1.13}$$

on $\partial D_i$. Next we will again rewrite the surface condition in terms of an operator equation. We define the operator

$$\mathcal{A}_D \begin{pmatrix} \phi \\ \psi \end{pmatrix}\Big|_{\partial D_i \times \partial D_i} := \begin{pmatrix} S_{D_i}^{k_b}[\phi_i] - \sum_j S_{D_j}^{k_l}[\psi_j] \\ \left(-\frac{1}{2} + K_{D_i}^{k_b}\right)[\phi_i] - \delta\left(\frac{1}{2} + K_{D_i}^{k_l}\right)[\psi_i] - \sum_{j\neq i} \frac{\mathrm{d}}{\mathrm{d}\boldsymbol{n}_i} S_{D_j}^{k_l}[\psi_j] \end{pmatrix} \tag{6.1.14}$$

and the vector valued function

$$\boldsymbol{F}_{D_i} := \boldsymbol{F}|_{\partial D_i \times \partial D_i} := \begin{pmatrix} \mathrm{p_{in}} \\ \delta \frac{\mathrm{d}}{\mathrm{d}\boldsymbol{n}_i} \mathrm{p_{in}} \end{pmatrix} = \begin{pmatrix} \tilde{\mathrm{p}}_{\mathrm{in}} e^{\mathrm{i}\boldsymbol{k}\cdot\boldsymbol{z}_i} e^{\mathrm{i}\boldsymbol{k}\cdot\triangle\boldsymbol{z}} \\ \delta \tilde{\mathrm{p}}_{\mathrm{in}} e^{\mathrm{i}\boldsymbol{k}\cdot\boldsymbol{z}_i} e^{\mathrm{i}\boldsymbol{k}\cdot\triangle\boldsymbol{z}} \mathrm{i}\boldsymbol{k}\cdot\boldsymbol{n}_{D_i} \end{pmatrix}. \tag{6.1.15}$$

We get

$$\mathcal{A}_D \begin{pmatrix} \phi \\ \psi \end{pmatrix} = \boldsymbol{F}. \tag{6.1.16}$$

### 6.1.2. Separated and interaction parts

In this section we will split up the operators into interaction and seperated parts. Then we will invert the system in equation 6.1.16 in a similar way as we did in the strongly interacting case. Like before the potentials will then be decomposed.

We will now start out by splitting up the contributions into a separated and an interaction part. The former corresponds to only internal interactions, namely only the terms that map between the inclusions $D_{i,j}$ and $D_{i,k}$ of the same inclusion cluster $D_i$. The interaction part on the other hand contains the terms that "feel" the other inclusion clusters. Further a singular subscript $D_i$ of an operator denotes the operator of a system that is made up of only $D_i$ and $|_{\partial D_i}$ next to a vector valued function denotes the vector, where all coordinates are limited to the domain $\partial D_i$. We will denote operators on all inclusion with a subscript $D$. In the next section we will expand $\mathcal{A}_{D_i,D_j}$ in $\omega$ and $\delta$, namely

$$\mathcal{A}_{D_i,D_j} = \sum_{m=0}^{\infty} \sum_{n=0}^{1} \omega^m \delta^n \mathcal{A}_{D_i,D_j}^{m,n}. \tag{6.1.17}$$

Die approbierte gedruckte Originalversion dieser Diplomarbeit ist an der TU Wien Bibliothek verfügbar
The approved original version of this thesis is available in print at TU Wien Bibliothek.
TU Bibliothek Your knowledge hub WIEN

But first we will be using the embedding $\iota_{D_i}$ of $\partial D_i$ into $\partial D$ to define other useful operators

$$\iota_{D_i}(\phi)(\boldsymbol{x}) \coloneqq \begin{cases} \phi(\boldsymbol{x}) & \boldsymbol{x} \in \partial D_i, \\ 0 & \boldsymbol{x} \in \partial D / \partial D_i \end{cases} \tag{6.1.18}$$

and $\boldsymbol{\iota}_{D_i} = \iota_{D_i} \times \iota_{D_i}$. Further we define the Projection onto a bubble cluster $\boldsymbol{P}_{D_i}(\boldsymbol{\phi}) \coloneqq \boldsymbol{\phi}|_{\partial D_i \times \partial D_i}$. We decompose the operator $\mathcal{B}_D = \mathcal{A}_D^{m,n}, \mathcal{A}_D$ into parts mapping from bubble cluster $i$ to cluster $j$, namely

$$\boxed{\mathcal{B}_{D_i,D_j} \coloneqq \boldsymbol{P}_{D_j} \circ \mathcal{B}_D \circ \boldsymbol{\iota}_{D_i}.} \tag{6.1.19}$$

Note that $\mathcal{B}_{D_i} \coloneqq \mathcal{B}_{D_i,D_i}$ can be viewed as the operator for a system with only the strongly interacting inclusion cluster $D_i$ and we are thus able to analyse it by using the theory of the last chapter. We further define the separated and interaction operators piecewise by

$$\boldsymbol{P}_{D_j} \circ \mathcal{B}_D^s \circ \boldsymbol{\iota}_{D_i} \coloneqq \delta_{i,j} \mathcal{B}_{D_i}, \qquad \mathcal{B}_D^i \coloneqq \mathcal{B}_D - \mathcal{B}_D^s, \tag{6.1.20}$$

which correspond to the part acting inside a bubble cluster and between them respectively. We now get the following expansion between different bubble clusters.

**Lemma 6.1.2.** *We get for $i \neq j$, $n > 0$ that*

$$\mathcal{A}_{D_i,D_j}^{0,0} = \mathcal{A}_{D_i,D_j}^{0,1} = \mathcal{A}_{D_i,D_j}^{1,1} = \begin{pmatrix} 0 & 0 \\ 0 & 0 \end{pmatrix}, \qquad \mathcal{A}_{D_i,D_j}^{n,0} \coloneqq \begin{pmatrix} 0 & -\frac{1}{c_l} \widetilde{S}_{D_i}^{n,\beta_{i,j}} \\ 0 & 0 \end{pmatrix}, \tag{6.1.21}$$

$$\mathcal{A}_{D_i,D_j}^{n+1,1} = \begin{pmatrix} 0 & 0 \\ 0 & -\frac{\mathrm{d}}{\mathrm{d}\boldsymbol{n}_x} \widetilde{S}_{D_i}^{n+1,\beta_{i,j}} \end{pmatrix} \tag{6.1.22}$$

*and $\mathcal{A}_{D_i}^{m,n} = \mathcal{A}_{D_i,D_i}^{m,n}$ corresponding to the operators of the strongly interaction case described in definition 5.1.7.*

*Proof.* Follows directly from lemma 6.1.1. □

With this lemma we can immediately see that

$$\mathcal{A}_D^{0,0} = \mathcal{A}_D^{0,0,s}. \tag{6.1.23}$$

We can thus define the invertible extension for the whole system by considering the extension of it for the clusters separately. We get again for all $i, j$ by piecewise definition

$$\boldsymbol{P}_{D_j} \circ \tilde{\mathcal{A}}_D \circ \boldsymbol{\iota}_{D_i} \coloneqq \delta_{i,j} \tilde{\mathcal{A}}_{D_i}. \tag{6.1.24}$$

We will now split up the potentials again.

**Definition 6.1.3.** *For $\boldsymbol{\varphi}_{D_i,j}$ being defined in lemma 5.1.1 and extended with 0 on $\partial D_j$ for $j \neq i$ we set*

$$\boldsymbol{\phi} = \boldsymbol{\varphi} + \tilde{\boldsymbol{\phi}}, \tag{6.1.25}$$

*with*

$$\boldsymbol{\varphi} \coloneqq \sum_{i,j} \boldsymbol{c}_{D_i,j} \boldsymbol{\varphi}_{D_i,j} \tag{6.1.26}$$

*and $\tilde{\boldsymbol{\phi}} \perp \boldsymbol{\varphi}_{D_i,j}$ for all $i, j$.*

Die approbierte gedruckte Originalversion dieser Diplomarbeit ist an der TU Wien Bibliothek verfügbar
The approved original version of this thesis is available in print at TU Wien Bibliothek.
TU Bibliothek Your knowledge hub WIEN

With this we are going to extend theorem 5.1.5 to weakly interacting systems. The main difference is going to be that we will split up all contributions into interacting and separated parts. Interaction operators are made up of at least one term that couples between bubble clusters, while for separated operators only contain operators acting on one cluster.

**Lemma 6.1.4.** *For inclusions clusters $D_i$ with connected parts $D_{i,j}$, $\mathcal{B}_D \coloneqq \mathcal{A}_D - \mathcal{A}_D^0$, $\left\|\tilde{\mathcal{A}}_D^{-1}\mathcal{B}_D\right\| < 1$ and $\boldsymbol{c}, \boldsymbol{\phi}, \boldsymbol{\varphi}$ defined in definition 6.1.3 we get*

$$\boldsymbol{\phi}|_{\partial D_k} = \overbrace{\left(\mathrm{I}_{D_k}[(\tilde{\mathcal{A}}_{D_k})^{-1}\boldsymbol{F}|_{\partial D_k} + \boldsymbol{\varphi}|_{\partial D_k}]\right)}^{\boldsymbol{\phi}^s|_{\partial D_k}} + \overbrace{\left(\mathrm{I}^i[(\tilde{\mathcal{A}}_D)^{-1}\boldsymbol{F} + \boldsymbol{\varphi}]\right)\Big|_{\partial D_k}}^{\boldsymbol{\phi}^i|_{\partial D_k}}. \tag{6.1.27}$$

*with*

$$\mathrm{I}^i[\xi] \coloneqq \left(\sum_{n=0}(-\tilde{\mathcal{A}}_D^{-1}\mathcal{B}_D)^n - (-\tilde{\mathcal{A}}_D^{-1}\mathcal{B}_D^s)^n\right)\xi. \tag{6.1.28}$$

*Furthermore we have a Matrix $\boldsymbol{A}_D$ and a vector $R_D[\boldsymbol{F}]$ with tuples $(k,l)$ as indices, where $k$ notifies the cluster and $l$ the bubble in said cluster with*

$$\begin{aligned}(\boldsymbol{A}_D\boldsymbol{c})_{(k,l)} &\coloneqq \overbrace{(\boldsymbol{A}_{D_k}\boldsymbol{c}_{D_k})_l}^{(\boldsymbol{A}_D^s\boldsymbol{c})_{(k,l)}} + \overbrace{\boldsymbol{T}^i_{(k,l)}[\boldsymbol{\varphi}]}^{(\boldsymbol{A}_D^i\boldsymbol{c})_{(k,l)}},\\ (\boldsymbol{R}_D[\boldsymbol{F}])_{(k,l)} &\coloneqq \overbrace{(\boldsymbol{R}_{D_k,l}[\boldsymbol{F}|_{\partial D_k}])}^{\boldsymbol{R}^s_{(k,l)}[\boldsymbol{F}]} \overbrace{-\boldsymbol{T}^i_{(k,l)}[\tilde{\mathcal{A}}_D^{-1}\boldsymbol{F}]}^{\boldsymbol{R}^i_{(k,l)}[\boldsymbol{F}]}.\end{aligned} \tag{6.1.29}$$

*for $\boldsymbol{A}_{D_k}, \boldsymbol{R}_{D_k,l}$ being the matrix and vector defined for the strongly interacting case in theorem 5.1.5 and*

$$\boldsymbol{T}^i_{(k,l)}[\boldsymbol{\xi}] \coloneqq \int_{\partial D_{k,l}} \left((\mathcal{B}_D^i\,\mathrm{I}_D + \mathcal{B}_D\,\mathrm{I}_D^i)\boldsymbol{\xi}\right)_2 \mathrm{d}\sigma. \tag{6.1.30}$$

*We then get*

$$\boldsymbol{A}_D\boldsymbol{c} = R_D[\boldsymbol{F}]. \tag{6.1.31}$$

*Proof.* Equivalent proof. We just separate the interaction and separated part. □

### 6.1.3. Resonance frequency and resonance coefficient

This section will generalize the statements of the strongly interacting system. It will show that in the lowest order we can calculate the potentials of the whole system by calculating the potentials for the isolated bubble clusters. In the next lemma we will calculate $\boldsymbol{A}_D$ up to order $\omega^4 + \omega^2\delta$. For this we will denote it as a matrix with row and column indices $(i,j)$, which correspond to the coefficients of the functions $\varphi_{D_i,j}$ and inclusion $D_{i,j}$.

**Lemma 6.1.5.** *The matrices $\boldsymbol{A}_D^s$ and $\boldsymbol{A}_D^i$ of lemma 6.1.4 can be, up to order $\mathcal{O}(\omega^4+\delta\omega^2)$ written as*

$$\begin{aligned}(A^s_{D,4})_{(i,l),(i,j)} \coloneqq &\left(-k_b^2\boldsymbol{D}_{D_i} + \delta\boldsymbol{C}_{D_i} + \frac{\mathrm{i}}{8\pi}\delta\,(k_b - k_l)\,\boldsymbol{C}_{D_i}\mathbf{1}_{M_i}\boldsymbol{C}_{D_i}\right)_{j,l}\\ &- \left(\frac{\mathrm{i}}{8\pi}k_b^2(k_b + k_l)\boldsymbol{D}_{D_i}\mathbf{1}_{M_i}\boldsymbol{C}_{D_i}\right)_{j,l},\end{aligned} \tag{6.1.32}$$

Die approbierte gedruckte Originalversion dieser Diplomarbeit ist an der TU Wien Bibliothek verfügbar
The approved original version of this thesis is available in print at TU Wien Bibliothek.
TU Bibliothek Your knowledge hub WIEN

$(A^s_{D,4})_{(k,l),(i,j)} = 0$ *for* $k \neq l$ *and*

$$(A^i_{D,4})_{(k,l),(i,j)} \coloneqq \frac{1}{8\pi}\boldsymbol{M}_{i,k}k_l\left(\delta\boldsymbol{C}_{D_i}\mathbf{1}_{M_i,M_k}\boldsymbol{C}_{D_k} + k_b^2\boldsymbol{D}_{D_i}\mathbf{1}_{M_i,M_k}\boldsymbol{C}_{D_k}\right)_{j,l}, \tag{6.1.33}$$

*where* $\boldsymbol{D}_{D_i} \coloneqq \mathrm{Diag}(|D_{D_i,1}|,\dots,|D_{D_i,M_i}|)$, $\boldsymbol{C}_{D_i}$ *is the capacity matrix of* $D_i$, $\boldsymbol{M}_{i,j} \coloneqq \frac{e^{\mathrm{i}\beta_{i,j}}}{\beta_{i,j}}$ *for* $i \neq j$, $\boldsymbol{M}_{i,i} = 0$ *and* $\mathbf{1}_{M_i,M_k}$ *a matrix filled with ones and dimensions* $M_i$ *by* $M_k$.

*Proof.* The separated part directly follows from the systems with only one bubble cluster, see lemma 5.1.8.
We note that due to lemma 6.1.2 we have for $m+2n<4$ that $(\mathcal{A}^{m,n}_{D_i,D_j}\boldsymbol{c})_2 = (\mathcal{A}^{1,0}_{D_i}\boldsymbol{c})_2 = (\mathcal{A}^{1,1}_{D_i}\boldsymbol{c})_2 = 0$ and thus not get a second component up to order $(\omega^2+\delta)^2$ through operators coupling between clusters. We now need for $i \neq k$ to only consider

$$\begin{aligned}A^i_{(k,l),(i,j)} = \int_{\partial D_{i,j}} \left(\left(-\omega^3\mathcal{A}^{2,0}_{D_i}(\tilde{\mathcal{A}}_{D_i})^{-1}\mathcal{A}^{1,0}_{D_k,D_i} - \omega\delta\mathcal{A}^{0,1}_{D_i}(\tilde{\mathcal{A}}_{D_i})^{-1}\mathcal{A}^{1,0}_{D_k,D_i}\right)[\boldsymbol{\varphi}_{D_k,l}]\right)_2 \mathrm{d}\sigma \\ + \mathcal{O}(\omega^4+\delta\omega^2).\end{aligned} \tag{6.1.34}$$

We get

$$\begin{aligned}\int_{\partial D_{i,j}} (\mathcal{A}^{0,1}_{D_i}(\tilde{\mathcal{A}}_{D_i})^{-1}\mathcal{A}^{1,0}_{D_k,D_i}[\boldsymbol{\varphi}_{D_k,l}])_2\,\mathrm{d}\sigma &= -\int_{\partial D_{i,j}} \frac{1}{2}\frac{1}{c_l}\widetilde{S}^{1,\beta_{k,i}}_{D_k}[\varphi_{D_k,l}]\sum_n \varphi_{D_i,n}\,\mathrm{d}\sigma \\ &= \frac{e^{\mathrm{i}\beta_{k,i}}}{8\pi\beta_{k,i}c_l}\sum_m(\boldsymbol{C}_{D_k})_{m,l}\sum_n(\boldsymbol{C}_{D_i})_{j,n} \\ &= \frac{1}{8\pi c_l}\boldsymbol{M}_{k,i}(\boldsymbol{C}_{D_i}\mathbf{1}_{M_i,M_k}\boldsymbol{C}_{D_k})_{j,l}\end{aligned} \tag{6.1.35}$$

and

$$\begin{aligned}\int_{\partial D_{i,j}} (\mathcal{A}^{2,0}_{D_i}(\tilde{\mathcal{A}}_{D_i})^{-1}\mathcal{A}^{1,0}_{D_k,D_i}[\boldsymbol{\varphi}_{D_k,l}])_2\,\mathrm{d}\sigma &= \frac{-1}{2c_b^2}\frac{1}{c_l}\int_{\partial D_{i,j}} \widetilde{S}^{1,\beta_{k,i}}_{D_k}[\varphi_{D_k,l}]\sum_n K^2_{D_i}[\varphi_{D_i,n}]\,\mathrm{d}\sigma \\ &= \frac{e^{\mathrm{i}\beta_{k,i}}}{8\pi\beta_{k,i}c_b^2}\frac{1}{c_l}\sum_n(\boldsymbol{D}_{D_i})_{j,n}\sum_m(\boldsymbol{C}_{D_k})_{m,l} \\ &= \frac{1}{8\pi c_b^2 c_l}\boldsymbol{M}_{k,i}(\boldsymbol{D}_{D_i}\mathbf{1}_{M_i,M_k}\boldsymbol{C}_{D_k})_{j,l}.\end{aligned} \tag{6.1.36}$$

We note for the case $i=j$ that we only get a component inside the integral if the last operator does not act between bubble clusters. Thus for the interaction part we would need to couple to another cluster, back and then use an operator to couple to the second component. This is however of higher order and we arrive thus at the statement. □

The next lemma shows that the resonance frequency of the system is in the lowest order equivalent to the frequency of the isolated inclusions.

Die approbierte gedruckte Originalversion dieser Diplomarbeit ist an der TU Wien Bibliothek verfügbar
The approved original version of this thesis is available in print at TU Wien Bibliothek.
TU Bibliothek Your knowledge hub WIEN

**Lemma 6.1.6.** *For each resonance frequency $\omega_{D_i,j}$ we have a normalized eigenvector $\boldsymbol{v}_{D_i,j}$ with eigenvalue $\lambda_{D_i,j}$ of $\boldsymbol{D}_{D_i}^{-1}\boldsymbol{C}_{D_i}$ for $\boldsymbol{D}_{D_i} \coloneqq \mathrm{Diag}(|D_{D_i,1}|,\dots,|D_{D_i,M_i}|)$ so that we get*

$$\omega_{D_i,j} = \omega_{M,D_i,j} + \mathcal{O}(\delta^{3/2}), \tag{6.1.37}$$

*for the frequencie $\omega_{M,D_i,j} \coloneqq \sqrt{\delta\lambda_{D_i,j}c_b^2}$. If the matrices $\boldsymbol{D}_{D_i}^{-1}\boldsymbol{C}_{D_i}$ for all $i$ do not share eigenvalues then we get*

$$\omega_{D_i,j} = \omega_{M,D_i,j} + \mathrm{i}\tau_{D_i,j} + \mathcal{O}(\delta^{3/2}), \tag{6.1.38}$$

*and*

$$\tau_{D_i,j} \coloneqq -\frac{1}{8\pi}\frac{c_b^2}{c_l}\delta\lambda_{D_i,j}^2\frac{\boldsymbol{v}_{D_i,j}^H\boldsymbol{D}_{D_i}\mathbf{1}_{M_i}\boldsymbol{D}_{D_i}\boldsymbol{v}_{D_i,j}}{\boldsymbol{v}_{D_i,j}^H\boldsymbol{D}_{D_i}\boldsymbol{v}_{D_i,j}}, \tag{6.1.39}$$

*with the matrix of ones $\mathbf{1}_{M_i}$ of dimension $M_i \times M_i$.*

*Proof.* The lowest order does not contain any interaction. Thus we can use the arguments for a single cluster. If $\lambda_{D_i,j}$ is only eigenvalue for a single cluster $D_i$ then for $i \neq j$ we get $\boldsymbol{v}_{D_j} = \mathcal{O}(\omega|\boldsymbol{v}|)$ and thus all interaction terms disappear up to order $\delta^2$. □

We will again introduce a scaling relation.

**Definition 6.1.7.** *We have the scaling relation*

$$\omega - \omega_{M,D_i,j} \sim \delta^{\mu_{D_i,j}} \tag{6.1.40}$$

*for all $i$ with $\frac{1}{2} \leq \mu_{D_i,j} \leq 1$, $\mu_- \coloneqq \min_{i,j}\mu_{D_i,j}$, $\mu_+ \coloneqq \max_{i,j}\mu_{D_i,j}$ and $\mu \coloneqq 2 + 2(\mu_- - 2\mu_+)$*

The interactions disappear in the lowest orders, therefore we find the following corollaries.

**Corollary 6.1.8.** *If the matrices $\boldsymbol{D}_{D_i}^{-1}\boldsymbol{C}_{D_i}$ do not share eigenvalues, the scaling relation 6.1.7 holds then we have for $\boldsymbol{c}$ defined in 6.1.3 that*

$$c_{D_i,j} + \frac{\tilde{p}_{in}}{2} = e^{\mathrm{i}\beta_i}(\boldsymbol{V}_{D_i}\boldsymbol{d}_{D_i}\boldsymbol{V}_{D_i}^{-1}\mathbf{1}_{M_i,1})_j + \mathcal{O}(\omega^\mu) \tag{6.1.41}$$

*and*

$$c_{D_i,j} - \frac{\tilde{p}_{in}}{2} = e^{\mathrm{i}\beta_i}\omega^2(\boldsymbol{V}_{D_i}\boldsymbol{\Omega}_{M,D_i}^{-2}\boldsymbol{d}_{D_i}\boldsymbol{V}_{D_i}^{-1}\mathbf{1}_{M_i,1})_j + \mathcal{O}(\omega^\mu) \tag{6.1.42}$$

*for $\boldsymbol{d}_{D_i}$ being the matrix $\boldsymbol{d}$ for $D_i$ defined in lemma 5.3.3.*

*Proof.* We will first note that by subtracting

$$\mathcal{A}_D(\omega_{D_i,j},\delta)\boldsymbol{v}_{D_i,j} = 0 \tag{6.1.43}$$

we get

$$A_4^s = \prod_i \frac{1}{c_b^2}\boldsymbol{D}_{D_i}\left(-\boldsymbol{V}_{D_i}(\boldsymbol{\omega}^2 - \boldsymbol{\Omega}_{D_i}^2)\right) + \mathcal{O}(\omega^{2+2\mu_-}), \tag{6.1.44}$$

Die approbierte gedruckte Originalversion dieser Diplomarbeit ist an der TU Wien Bibliothek verfügbar
The approved original version of this thesis is available in print at TU Wien Bibliothek.
TU Bibliothek Your knowledge hub WIEN

and the interaction part

$$A_4^i = \mathcal{O}(\omega^{2+2\mu_-}). \tag{6.1.45}$$

Next we have

$$(\mathcal{A}^{1,0}_{D_i,D_j}\xi)_2 = (\mathcal{A}^{2,0}_{D_i,D_j}\xi)_2 = (\mathcal{A}^{0,1}_{D_i,D_j}\xi)_2 = 0 \tag{6.1.46}$$

and thus no interaction part of $R$, namely

$$R_3^i = 0 \tag{6.1.47}$$

up to order $\omega^3$. Using

$$\boldsymbol{F}|_{\partial D_i} = \begin{pmatrix} \tilde{\mathrm{p}}_{\mathrm{in}} e^{\mathrm{i}\boldsymbol{k}\cdot\boldsymbol{z}_i} e^{\mathrm{i}\boldsymbol{k}\cdot\triangle\boldsymbol{z}} \\ \delta\tilde{\mathrm{p}}_{\mathrm{in}} e^{\mathrm{i}\boldsymbol{k}\cdot\boldsymbol{z}_i} e^{\mathrm{i}\boldsymbol{k}\cdot\triangle\boldsymbol{z}} \mathrm{i}\boldsymbol{k}\cdot\boldsymbol{n}_i \end{pmatrix} \tag{6.1.48}$$

and lemma 5.3.1 we get

$$R_3^s = \frac{\tilde{\mathrm{p}}_{\mathrm{in}}}{2} \prod_i e^{\mathrm{i}\boldsymbol{k}\cdot\boldsymbol{z}_i} \frac{\boldsymbol{D}_{D_i}}{c_b^2}(\boldsymbol{\omega}^2 + \boldsymbol{\Omega}^2_{D_i}). \tag{6.1.49}$$

We can use the same prove as in lemma 5.3.3. □

Finally we will state a corollary for the potentials. It shows that it suffices to calculate the potentials in the bubble clusters individually.

**Corollary 6.1.9.** *If the matrices $\boldsymbol{D}_{D_i}^{-1}\boldsymbol{C}_{D_i}$ do not share eigenvalues and the scaling relations hold 6.1.7 then we get*

$$\phi = \sum_{i,j} \zeta_{D_i,j} e^{\mathrm{i}\beta_i} d_{D_i,j} (\boldsymbol{V}_{D_i}^{-1}\mathbf{1}_{M_i,1})_j + \mathcal{O}(\omega^{\mu}) \tag{6.1.50}$$

*and*

$$\psi = \sum_{i,j} \zeta_{D_i,j} e^{\mathrm{i}\beta_i} d_{D_i,j} \frac{\omega^2}{\omega^2_{M,D_i,j}} (\boldsymbol{V}_{D_i}^{-1}\mathbf{1}_{M_i,1})_j + \mathcal{O}(\omega^{\mu}) \tag{6.1.51}$$

*the resonance potentials $\zeta_{D_i,j} \coloneqq \sum_l (\boldsymbol{V}_{D_i})_{l,j}\varphi_{D_i,l}$ and $d_{D_i,j}$ defined in lemma 5.3.3.*

*Proof.* We have

$$\Gamma^i[\xi] = \mathcal{O}(\omega) \tag{6.1.52}$$

and thus

$$\Gamma^i[\varphi] = \mathcal{O}(\omega^{2-2\mu_+}). \tag{6.1.53}$$

This results in

$$\tilde{\boldsymbol{\phi}}^s = \prod_i \frac{\tilde{\mathrm{p}}_{\mathrm{in}} e^{\mathrm{i}\boldsymbol{k}\boldsymbol{z}_i}}{2} \sum_{j=0}^{M_{D_i}} \varphi_{D_i,j} \begin{pmatrix} 1 \\ -1 \end{pmatrix} + \mathcal{O}(\omega^{2-2\mu_+}). \tag{6.1.54}$$

□

Die approbierte gedruckte Originalversion dieser Diplomarbeit ist an der TU Wien Bibliothek verfügbar
The approved original version of this thesis is available in print at TU Wien Bibliothek.
TU Bibliothek Your knowledge hub WIEN

## 6.2. Far field interaction between spheres

We will now look at the case of bubble clusters $D_i$ being made up of a single sphere each. This allows us to prove the following theorem for the pressure and its derivative on the surfaces. Note that we gain an additional term compared to a one bubble system. This will be the source of the secondary Bjerknes force as we will see later. Note that we will drop the second index that notifies which bubble we choose in a cluster, for example $d_{D_i,j}$ is now $d_{D_i}$.

**Theorem 6.2.1.** *For spherical inclusions and a flat incident wave 6.1.3 and the scaling relation 6.1.7 we get*

$$\begin{aligned}\nabla p\Big|_{D_j,-} =&\tilde{\boldsymbol{c}}\boldsymbol{n} - 3\tilde{p}_{in}\delta\sin(\beta_j)\boldsymbol{k} - \delta\tilde{p}_{in}\cos(\beta_j)\frac{5}{2}r_j(\boldsymbol{k}\cdot\boldsymbol{n})\boldsymbol{k}\\ &-\sum_{i\neq j}\delta k_l^2\cos(\beta_i)\frac{d_{D_i}\omega^2}{\omega_{M,D_i}^2}\frac{e^{\mathrm{i}\beta_{i,j}}}{4\pi\beta_{i,j}^2}(1-\mathrm{i}\beta_{i,j})C_{D_i}3\widehat{\boldsymbol{d}}_{i,j}+\mathcal{O}(\omega^{4+\mu})\end{aligned} \tag{6.2.1}$$

*on $\partial D_j$. We further have in a lower order that*

$$\nabla p\Big|_{D_j,-} = -\cos(\beta_j)d_{D_j}k_b^2\frac{r_j}{3}\boldsymbol{n}+\mathcal{O}(\omega^{2+\mu}). \tag{6.2.2}$$

The rest of this section will prove this theorem, readers not interested in the details may skip this part. We start out by categorizing the images of different different spaces under $\mathcal{A}_D^{m,n}$. We can immediately by the definition of the operators see the following corollary.

**Corollary 6.2.2.** *For all $s,t$ we have*

$$\mathcal{A}_{D_i,D_j}^{1,0}(H_{D_i}^{s,t})\subseteq H_{D_j}^{0,0},\qquad \mathcal{A}_{D_i,D_j}^{r,0}(H_{D_i}^{s,t})\subseteq L^2(\partial D_j)\times\mathbb{R} \tag{6.2.3}$$

*for $H_D^{s,t}$ defined in 5.4.5.*

We will next look at the interaction terms

**Lemma 6.2.3.** *We have for $i\neq j$ that*

$$(\mathrm{I}_{D_i,D_j}^i)_1\begin{pmatrix}0\\ \varphi_{D_i}\end{pmatrix} = \tilde{c}\varphi_{D_j}+\delta\omega^2\frac{e^{\mathrm{i}\beta_{i,j}}}{4\pi\beta_{i,j}^2}(1-\mathrm{i}\beta_{i,j})C_{D_i}9\widehat{\boldsymbol{d}}_{i,j}\cdot\boldsymbol{n}_j+\mathcal{O}(\omega^5) \tag{6.2.4}$$

*and*

$$(\mathrm{I}_{D_i,D_j}^i)_1\begin{pmatrix}\varphi_{D_i}\\ 0\end{pmatrix} = \tilde{c}\varphi_{D_i}+\mathcal{O}(\omega^5). \tag{6.2.5}$$

*Furthermore we get*

$$(\mathrm{I}_{D_i,D_i}^i)_1\begin{pmatrix}\tilde{c}_1\varphi_{D_i}\\ \tilde{c}_2\varphi_{D_i}\end{pmatrix} = \tilde{c}\varphi_{D_i}+\mathcal{O}(\omega^5). \tag{6.2.6}$$

*We also have the separated part*

$$\mathrm{I}_{D_i,D_i}^s = -\delta\tilde{p}_{in}e^{\mathrm{i}\boldsymbol{k}\cdot\boldsymbol{z}_i}9\mathrm{i}\boldsymbol{k}\cdot\boldsymbol{n}+\delta\tilde{p}_{in}e^{\mathrm{i}\boldsymbol{k}\cdot\boldsymbol{z}_i}\left(\frac{5}{2}\right)^2 r_i(\boldsymbol{k}\cdot\boldsymbol{n})^2+\tilde{c}\varphi_{D_i}+\mathcal{O}(\omega^5). \tag{6.2.7}$$

Die approbierte gedruckte Originalversion dieser Diplomarbeit ist an der TU Wien Bibliothek verfügbar
The approved original version of this thesis is available in print at TU Wien Bibliothek.
TU Bibliothek Your knowledge hub WIEN

*Proof.* We get due to the previous corollary that

$$\begin{aligned}(\mathrm{I}^i_{D_i,D_j})_1 \begin{pmatrix} 0 \\ \varphi_{D_i} \end{pmatrix} =& \tilde{c}\varphi_{D_j} + \mathcal{O}(\omega^5) \\ &+ \left( \left( \delta\omega^2 (\tilde{\mathcal{A}}_{D_j})^{-1} \mathcal{A}^{0,1}_{D_j} (\tilde{\mathcal{A}}_{D_j})^{-1} \mathcal{A}^{2,0}_{D_i,D_j} - \delta\omega^2 (\tilde{\mathcal{A}}_{D_j})^{-1} \mathcal{A}^{2,1}_{D_i,D_j} \right) \begin{pmatrix} 0 \\ \varphi_{D_i} \end{pmatrix} \right)_1 \\ =& \tilde{c}\varphi_{D_j} - \delta k_l^2 \frac{e^{\mathrm{i}\beta_{i,j}}}{4\pi\beta_{i,j}^2} (1 - \mathrm{i}\beta_{i,j}) C_{D_i} \left( (\tilde{\mathcal{A}}_{D_j})^{-1} \begin{pmatrix} 0 \\ 3\widehat{\boldsymbol{d}}_{i,j} \cdot \boldsymbol{n}_j \end{pmatrix} \right)_1 + \mathcal{O}(\omega^5) \\ =& \tilde{c}\varphi_{D_j} + \delta k_l^2 \frac{e^{\mathrm{i}\beta_{i,j}}}{4\pi\beta_{i,j}^2} (1 - \mathrm{i}\beta_{i,j}) C_{D_i} 9\widehat{\boldsymbol{d}}_{i,j} \cdot \boldsymbol{n}_j + \mathcal{O}(\omega^5). \end{aligned} \tag{6.2.8}$$

We note for the other statements that only $\mathcal{A}^{2,1}_{D_i,D_j}, \mathcal{A}^{2,0}_{D_i}, \mathcal{A}^{0,1}_{D_i}, \mathcal{A}^{3,0}_{D_i}, \mathcal{A}^{2,1}_{D_i}, \mathcal{A}^{4,0}_{D_i}$ results in a second coordinate up to order $\mathcal{O}(\omega^5)$ and thus need to be the last operator that gets applied before $\tilde{\mathcal{A}}_D^{-1}$. The coupling of two bubbles has at least order $\omega$. Thus for $i = j$ we only need to consider $\mathcal{A}^{2,0}_{D_i}, \mathcal{A}^{0,1}_{D_i}$. Due to the coupling being only of lowest order this results in both coordinates being constant and getting transformed to constants by the operators. For $i \neq j$ we note that

$$\left( \mathcal{A}^{m,n}_{D_i,D_j} \begin{pmatrix} \varphi_{D_i} \\ 0 \end{pmatrix} \right)_2 = 0 \tag{6.2.9}$$

and we thus apply the operators that we listed above only on constant functions, which results in a constant second coordinate. The seperated part directly follows from the statement for strongly interacting systems. □

Using the last lemma we arrive at the layer potential corresponding to the function on the inside of the sphere

**Lemma 6.2.4.** *We get*

$$\begin{aligned}\phi|_{\partial D_j} =& \sum_{i \neq j} \delta k_l^2 \cos(\beta_i) \frac{d_{D_i}\omega^2}{\omega^2_{M,D_i}} \frac{e^{\mathrm{i}\beta_{i,j}}}{4\pi\beta_{i,j}^2} (1 - \mathrm{i}\beta_{i,j}) C_{D_i} 9\widehat{\boldsymbol{d}}_{i,j} \cdot \boldsymbol{n} \\ &+ \sin(\beta_j)\delta\tilde{p}_{in} 9\boldsymbol{k} \cdot \boldsymbol{n} + \cos(\beta_j)\delta\tilde{p}_{in} \left(\frac{5}{2}\right)^2 r_j (\boldsymbol{k} \cdot \boldsymbol{n})^2 + \tilde{c}\varphi_{D_j} + \mathcal{O}(\omega^{4+\mu}) \end{aligned} \tag{6.2.10}$$

*and*

$$\phi|_{\partial D_j} = \cos(\beta_j) d_{D_j} \varphi_{D_j} + \mathcal{O}(\omega^\mu). \tag{6.2.11}$$

To finish the proof of the theorem we note that we have to only calculate $S_D^{k_b}[\phi]$ on a single bubble and can thus proceed exactly like in lemma 5.4.9 and 5.4.8.

Die approbierte gedruckte Originalversion dieser Diplomarbeit ist an der TU Wien Bibliothek verfügbar
The approved original version of this thesis is available in print at TU Wien Bibliothek.
TU Bibliothek Your knowledge hub WIEN

## 6.3. Secondary Bjerknes force

We will look at a special case of the scaling relation 6.1.7 with

$$\mu_+ - \mu_- \leq \frac{1}{6} - \epsilon \tag{6.3.1}$$

for $0 < \epsilon \leq \frac{1}{6}$ and thus

$$\mu - 2\mu_+ = 2 + 2(\mu_- - 3\mu_+) \geq 1 - 4\mu_- + 6\epsilon. \tag{6.3.2}$$

We have to take this assumption so that the force is not of higher order. The condition is especially true if

$$\omega - \omega_{M,D_i} \sim \delta^{\frac{1}{2}} \qquad \text{for all } i. \tag{6.3.3}$$

The next lemma gives an estimate for the second Bjerknes force in the far field.

**Lemma 6.3.1.** *In the case of a standing wave $p_{in} = \tilde{p}_{in}\cos(\boldsymbol{k}\cdot\boldsymbol{x})\cos(\omega t)$ with the scaling described in equation 6.3.1 the force estimate on the bubble turns in the far field to*

$$\begin{aligned}\boldsymbol{F}_2^b =& 2\delta\tilde{p}_{in}^2 \sum_{i\neq j} \frac{2\pi\omega^2 r_i r_j}{\rho_l d_{i,j}^2} \frac{\cos(\alpha_{D_i} + \beta_{i,j} + \tilde{\beta}_{i,j} - \alpha_{D_j})}{\sqrt{(\omega^2 - \omega_{M,D_i}^2)^2 + \left(r_j k_l \omega_{M,i}^2\right)^2}} \\ &\times \frac{\cos(\beta_j)\cos(\beta_i)\sqrt{1+\beta_{i,j}^2}}{\sqrt{(\omega^2 - \omega_{M,D_j}^2)^2 + \left(r_j k_l \omega_{M,i}^2\right)^2}} \widehat{\boldsymbol{d}}_{i,j} + \mathcal{O}(\rho_l^{-1}\omega^{4-4\mu_-+6\epsilon}).\end{aligned} \tag{6.3.4}$$

*$\tilde{\beta}_{i,j}$ is defined by the relation*

$$\sqrt{1+\beta_{i,j}^2}\, e^{\mathrm{i}\tilde{\beta}_{i,j}} = 1 - \mathrm{i}\beta_{i,j}. \tag{6.3.5}$$

Especially the following corollary holds true with $\beta_0$ small (Note that we need to choose $\beta_0$ first and for this fixed $\beta_0$ we look at the $\omega$ limit).

**Corollary 6.3.2.** *Under the same conditions as lemma 6.3.1 we get*

$$\begin{aligned}\boldsymbol{F}_2^b =& 2\delta\tilde{p}_{in}^2 \sum_{i\neq j} \frac{2\pi\omega^2 r_i r_j}{\rho_l d_{i,j}^2} \frac{\cos(\alpha_{D_j} - \alpha_{D_i})\cos(\beta_j)\cos(\beta_i)}{\sqrt{(\omega^2 - \omega_{M,j}^2)^2 + \left(r_j k_l \omega_{M,j}^2\right)^2}\sqrt{(\omega^2 - \omega_{M,i}^2)^2 + \left(r_j k_l \omega_{M,i}^2\right)^2}} \widehat{\boldsymbol{d}}_{i,j} \\ &+ \mathcal{O}\left(\rho_l^{-1}\omega^{4-4\mu_-+6\epsilon} + \sum_j \beta_{i,j}\right).\end{aligned} \tag{6.3.6}$$

**Remark 6.3.3.** *This result is consistent with the classical results 2.3.10 if we take two bubbles. Note that we again get a factor $2\delta$ due to us not working with the effective mass.*

We will now proceed with the proof of lemma 6.3.1.

Die approbierte gedruckte Originalversion dieser Diplomarbeit ist an der TU Wien Bibliothek verfügbar
The approved original version of this thesis is available in print at TU Wien Bibliothek.
TU Bibliothek Your knowledge hub WIEN

*Proof.* We remind ourselves that the secondary Bjerknes force on the bubble can be written as

$$\boldsymbol{F}_2^{\mathrm{b}} = \frac{1}{T}\int_0^T \frac{1}{\rho_b \omega^2}\int_{\partial D} (\nabla_T \mathrm{p}|_-)^2 \boldsymbol{n} - (\nabla \mathrm{p}|_- \cdot \boldsymbol{n})\,\nabla_T \mathrm{p}|_-\,\mathrm{d}\sigma\,\mathrm{d}t - \boldsymbol{F}_{1,i}^{\mathrm{b}}. \tag{6.3.7}$$

We have due to theorem 6.2.1 that

$$\nabla_T \mathrm{p} = \mathcal{O}(\omega^{2+\mu}). \tag{6.3.8}$$

We also get

$$\frac{\mathrm{dp}}{\mathrm{d}\boldsymbol{n}} = -\cos(\beta_j)\frac{\tilde{\mathrm{p}}_{\mathrm{in}}\omega^2_{M,D_j}\cos(\alpha_{D_j}+\omega t)}{\sqrt{(\omega^2-\omega^2_{M,D_j})^2+\left(4\tau^2_{D_j}\omega^2_{M,D_j}\right)}} k_b^2\frac{r_j}{3} + \mathcal{O}(\omega^{2+\mu}). \tag{6.3.9}$$

and

$$\begin{aligned}\nabla_T \mathrm{p}\Big|_{D_j,-} =& \tilde{\boldsymbol{c}}\boldsymbol{n} - 3\tilde{\mathrm{p}}_{\mathrm{in}}\delta\sin(\beta_j)\boldsymbol{k} - \delta\tilde{\mathrm{p}}_{\mathrm{in}}\cos(\beta_j)\frac{5}{2}r_j(\boldsymbol{k}\cdot\boldsymbol{n})\boldsymbol{k}\\ &- \sum_{i\neq j}\delta k_l^2\cos(\beta_i)\frac{d_{D_i}\omega^2}{\omega^2_{M,D_i}}\frac{e^{\mathrm{i}\beta_{i,j}}}{4\pi\beta^2_{i,j}}(1-\mathrm{i}\beta_{i,j})C_{D_i}3\widehat{\boldsymbol{d}}_{i,j} + \mathcal{O}(\omega^{4+\mu})\end{aligned} \tag{6.3.10}$$

The term $3\tilde{\mathrm{p}}_{\mathrm{in}}\delta\sin(\beta_j)\boldsymbol{k}$ corresponds to the primary Bjerknes force, we are thus going to ignore it for calculating the secondary Bjerknes force. Furthermore we note that

$$\int_{\partial D_j}(\boldsymbol{k}\cdot\boldsymbol{n})(\boldsymbol{k}-(\boldsymbol{k}\cdot\boldsymbol{n})\boldsymbol{n})\,\mathrm{d}\sigma = 0 \tag{6.3.11}$$

and

$$\int_{\partial D_j}(\widehat{\boldsymbol{d}}_{i,j}-(\widehat{\boldsymbol{d}}_{i,j}\cdot\boldsymbol{n})\boldsymbol{n})\,\mathrm{d}\sigma = \widehat{\boldsymbol{d}}_{i,j}\left(|\partial D_j| - \frac{1}{r_j}|D_j|\right) = \widehat{\boldsymbol{d}}_{i,j}\frac{8\pi r_j^2}{3}. \tag{6.3.12}$$

We thus arrive at

$$\begin{aligned}\boldsymbol{F}_2^{\mathrm{b}}(\mathrm{p}) =& \mathcal{O}(\rho_l^{-1}\omega^{3-2\mu_+ +\mu}) + \frac{4\pi k_l^2 k_b^2\omega^2_{M,D_j}}{3\rho_l}\\ &\sum_{i\neq j}\frac{\tilde{\mathrm{p}}^2_{\mathrm{in}} r_i r_j^3\cos(\alpha_{D_i}+\beta_{i,j}+\tilde{\beta}_{i,j}-\alpha_{D_j})\cos(\beta_j)\cos(\beta_i)\sqrt{1+\beta^2_{i,j}}}{\beta^2_{i,j}\sqrt{(\omega^2-\omega^2_{M,D_i})^2+\left(4\tau^2_{D_i}\omega^2_{M,D_i}\right)}\sqrt{(\omega^2-\omega^2_{M,D_j})^2+\left(4\tau^2_{D_j}\omega^2_{M,D_j}\right)}}\widehat{\boldsymbol{d}}_{i,j}\\ =&\frac{4\pi\omega^2\delta}{\rho_l}\sum_{i\neq j}\frac{\tilde{\mathrm{p}}^2_{\mathrm{in}} r_i r_j\cos(\alpha_{D_i}+\beta_{i,j}+\tilde{\beta}_{i,j}-\alpha_{D_j})}{d^2_{i,j}\sqrt{(\omega^2-\omega^2_{M,D_i})^2+\left(4\tau^2_{D_i}\omega^2_{M,D_i}\right)}}\\ &\times\frac{\cos(\beta_j)\cos(\beta_i)\sqrt{1+\beta^2_{i,j}}}{\sqrt{(\omega^2-\omega^2_{M,D_j})^2+\left(4\tau^2_{D_j}\omega^2_{M,D_j}\right)}}\widehat{\boldsymbol{d}}_{i,j} + \mathcal{O}(\rho_l^{-1}\omega^{3-2\mu_+ +\mu})\end{aligned} \tag{6.3.13}$$

Using $\mu - 2\mu_+ \geq 1 - 4\mu_- + 6\epsilon$ concludes the proof. □

Die approbierte gedruckte Originalversion dieser Diplomarbeit ist an der TU Wien Bibliothek verfügbar
The approved original version of this thesis is available in print at TU Wien Bibliothek.
TU Bibliothek Your knowledge hub WIEN

Die approbierte gedruckte Originalversion dieser Diplomarbeit ist an der TU Wien Bibliothek verfügbar
The approved original version of this thesis is available in print at TU Wien Bibliothek.

# 7. Multiple strongly interacting bubbles

In this chapter we will calculate the secondary Bjerknes force for strongly interacting bubble systems. We will first state the main results of the first three sections. Readers not interested in the details of the proof may skip to section 7.5. In section 7.1 we will find a formula for general systems. In the two sections afterwards we will derive representations of the operators and potentials in spherical harmonics for two sphere systems. After that we will derive a general form of the capacity matrix and see that it is consistent with past results. Section 7.4 covers a derivation of the capacity matrix and resonance frequencies. Then we will look at the asymptotic cases: bubbles that are close to touching or far apart. We will derive an approximation of the force for the later case and compare it to past results. Finally, in the last section some empirical studies will be performed in the basis of the spherical harmonics on the bubble surfaces and the sign reversal is discussed.
We will now state the two main results of this chapter. The following theorem describes the secondary Bjerknes force for general systems. Remarkably we can see in the asymptotic regime that the force depends only on the frequency and amplitude of the incident wave but not the orientation. Thus the secondary Bjerknes forces dominate for bubbles that are not too far apart.

**Theorem 7.0.1.** *We have for a system of bubbles $\boldsymbol{D}_i$ and $\omega - \omega_{M,i} \sim \delta^{1/2}$ the secondary Bjerknes force*

$$\boldsymbol{F}^b_{2,i} = \frac{k_b^4}{2\omega^2 \delta \rho_l} \sum_{j,k} e_j e_k \boldsymbol{F}_{D_i,j,k} + \mathcal{O}(\omega) \tag{7.0.1}$$

*for the force coefficients $e_i := d_i (V^{-1}\mathbf{1}_M)_i$ with $d_i$ defined in lemma 5.3.3, the force contributions $\boldsymbol{F}_{D_i,j,k}$ and*

- $\boldsymbol{F}_{D_i,j,k} := \boldsymbol{F}^{\boldsymbol{n}}_{D_i}(q^{\boldsymbol{n}}[\zeta_j,\lambda_j], q[\zeta_k,\lambda_k]) + \boldsymbol{F}^T_{D_i}(q[\zeta_j,\lambda_j], q[\zeta_k,\lambda_k])$,
- $\boldsymbol{F}^{\boldsymbol{n}}_{D_i}(q_1,q_1) := -\int_{\partial D_i} q_1 \nabla_T q_2 \,\mathrm{d}\sigma$,
- $\boldsymbol{F}^T_{D_i}(q_1,q_2) := \int_{\partial D_i} (\nabla_T q_1)(\nabla_T q_2)\boldsymbol{n} \,\mathrm{d}\sigma$,
- $q[\zeta_i,\lambda_i] := \left((-\mathcal{N}_D^{-1} P K_D^2 + P S_D^2) + \frac{1}{\lambda_i}\mathcal{N}_D^{-1} P\right)[\zeta_i]$,
- $q^{\boldsymbol{n}}[\zeta_i,\lambda_i] := \left((1-P)K_D^2 + \frac{1}{\lambda_i} P\right)[\zeta_i]$,

*where $\lambda_i$ are the eigenvalues of $\tilde{\boldsymbol{C}}$ and $\boldsymbol{V}$ is the corresponding matrix of normalized eigenvectors. Further $\zeta_i := \sum_j \boldsymbol{V}_{j,i}\varphi_j$ are the resonance functions, $1-P$ is the orthogonal*



Die approbierte gedruckte Originalversion dieser Diplomarbeit ist an der TU Wien Bibliothek verfügbar
The approved original version of this thesis is available in print at TU Wien Bibliothek.

*projection onto the functions $c\chi_{D_i}$ and $\mathcal{N}_D$ is the Dirichlet-to-Neumann operator, which is defined in 7.1.1. We further have*

$$\begin{aligned}\frac{\mathrm{d}p}{\mathrm{d}\boldsymbol{n}} =& k_b^2 \sum_i e_i q^{\boldsymbol{n}}[\zeta_i, \lambda_i] + \mathcal{O}(\omega^3),\\ p =& k_b^2 \sum_i e_i q[\zeta_i, \lambda_i] + \mathcal{O}(\omega^3).\end{aligned} \tag{7.0.2}$$

*Proof.* The theorem follows from lemma 3.3.3 and lemma 7.1.6. The factor $\frac{1}{2}$ is due to the time integral. □

**Remark 7.0.2.** *We can also see that we get force contributions $\boldsymbol{F}_{D_i,j,k}$ to the Bjerknes force for all combinations of $e_i e_j$. $e_i$ contains a singularity at the resonance frequency $\omega_i$. We thus can expect that the term $e_i^2$ dominates close to that frequency. We are going to see such a pattern at the end of this chapters in the simulations. Furthermore this shows us that the sign of $\boldsymbol{F}_{D_i,j,j}$ defines the sign of the total Bjerknes force close to the singularity and is one of the mechanisms for sign reversal of that force. This happens because changes in distance between the bubbles result in shifting resonance frequencies and can thus move one of them closer to the forcing frequency. If the term near corresponding to that singularity has the opposite sign then we can locally expect a sign reversal to take place. Another mechanism is the change due to the changing of relative magnitude of the force contributions $\boldsymbol{F}_{D_i,j,k}$ towards each other. We will see in the two spherical bubble case that for bubbles far apart one of the contributions declines asymptomatically slower than the rest, while for closer ranges another force contribution dominates.*

Next, we are going to describe the forces for systems made up of two spherical bubbles. Due to symmetry of the system the direction of the force is fixed by the vector between the centres of the bubbles. The next formula is going to find explicit formulas for the forces, by working in the basis made up of two sets of spherical harmonics centred at the first and second spherical bubble. We will further assume without loss of generality that the bubble centres lie on the z-axis. One has a positive and the other a negative $z$ component. The spherical harmonic parameters $\theta, \phi$ correspond to the common spherical coordinates with the centres of the bubbles being the origins. For simpler notation we will in this chapter use the indices $\pm$. They represent a variable with choice $+$ or $-$ and will be used as an index and as a sign in mathematical operations. Note that $\pm_1, \pm_2$ represent two different variables with the before mentioned properties. $+$ as an index will be used to represent the upper bubble except for $\zeta_+$, where it corresponds to the resonance function of the bigger frequency $\omega_+$. This does not create an inconsistency because we choose $r_- > r_+$ and note that the frequency $\omega_+$ corresponds to the upper bubble $D_+$ in the far field. We will also write $Y^0_{l_\pm}$ short for $Y^0_{l_\pm}(\theta_\pm, \phi_\pm)\chi_{\partial D_\pm}$ the spherical harmonic centred in $\partial D_\pm$ to reduce clutter. The next lemma summarizes the results of sections 7.2, 7.3 and 7.4. Although it is very complex it can be used to simulate the secondary Bjerknes force and most importantly the force contributions separately. Compared to the direct numerical inversion of the system we thus get additional information, which can help analyse the system.

Die approbierte gedruckte Originalversion dieser Diplomarbeit ist an der TU Wien Bibliothek verfügbar
The approved original version of this thesis is available in print at TU Wien Bibliothek.
TU Bibliothek Your knowledge hub WIEN

**Lemma 7.0.3.** *For two spherical bubbles with $\omega - \omega_{M,\pm} \sim \delta^{1/2}$ we can describe the force contributions described in theorem 7.0.1 in the spherical harmonic basis*

$$\boldsymbol{F}^{\boldsymbol{n}}_{D_\pm}(Y^0_l, Y^0_{l'}) = -r_\pm \widehat{\boldsymbol{e}}_z \begin{cases} \frac{(l+1)(l+2)}{\sqrt{(2l+1)(2l+3)}} & l' = l+1, \\ -\frac{(l-1)(l+1)}{\sqrt{(2l-1)(2l+1)}} & l' = l-1, \\ 0 & else, \end{cases} \tag{7.0.3}$$

*and*

$$\boldsymbol{F}^{T}_{D_\pm}(Y^0_l, Y^0_{l'}) = \widehat{\boldsymbol{e}}_z \begin{cases} \frac{l(l+1)(l+2)}{\sqrt{(2l+1)(2l+3)}} & l' = l+1, \\ \frac{l(l+1)(l-1)}{\sqrt{(2l+1)(2l-1)}} & l' = l-1, \\ 0 & else. \end{cases} \tag{7.0.4}$$

*We further have the relations*

$$q[Y^0_{l_{\pm_1}}, \lambda]|_{\partial D_{\pm_2}} = \sum_l G_{l,D_{\pm_2}}(Y^0_{l_{\pm_1}}, \lambda) Y^0_l. \tag{7.0.5}$$

*where for $l_{\pm_2} > 0$*

$$G_{l_{\pm_2},D_{\pm_2}}(Y^0_{l_{\pm_1}}, \lambda) := \begin{cases} -\frac{r_+^{l_+ +2} r_-^{l_- +2}}{d^{l_+ + l_- +1}} \frac{\binom{l_+ + l_-}{l_+}(-1)^{l_+}}{(2l_\mp+3) l_\mp \sqrt{(2l_+ +1)(2l_- +1)}} & \pm = \pm_1 = \mp_2, \\ -\frac{r_\pm^3}{(2l_\pm+1)(2l_\pm+3) l_\pm} + \frac{r_\pm}{\lambda l_\pm} & \pm = \pm_1 = \pm_2 \end{cases} \tag{7.0.6}$$

*and $G_{l,D_\pm}(Y^0_{l_\pm}, \lambda) := 0$ for $l \neq l_\pm$. Additionally we get*

$$q^{\boldsymbol{n}}[Y^0_{l_{\pm_1}}, \lambda]|_{\partial D_{\pm_2}} = \sum_l G^{\boldsymbol{n}}_{l,D_{\pm_2}}(Y^0_{l_{\pm_1}}, \lambda) Y^0_l. \tag{7.0.7}$$

*with*

$$G^{\boldsymbol{n}}_{l_{\pm_2},D_{\pm_2}}(Y^0_{l_{\pm_1}}, \lambda) = \begin{cases} \frac{r_\pm^{l_\pm+2} r_\mp}{d^{l_\pm+1}} \frac{(\mp 1)^{l_\pm}}{\sqrt{2l_\pm+13}} \delta_{0,l_\mp} & \pm = \pm_1 = \mp_2, \\ \delta_{l_\pm,0} \frac{r_\pm^2}{3} + (1 - \delta_{l_\pm,0}) \frac{1}{\lambda} & \pm = \pm_1 = \pm_2 \end{cases} \tag{7.0.8}$$

*and $G^{\boldsymbol{n}}_{l,D_\pm}(Y^0_{l_\pm}, \lambda) := 0$ for $l \neq l_\pm$. We further have for the matrix of eigenvectors $\boldsymbol{V}$ of $\tilde{\boldsymbol{C}}$ that*

- $\zeta_{\pm_1} := \sum_{\pm_2} \boldsymbol{V}_{\pm_2,\pm_1} \varphi_{\pm_2}$,
- $\varphi_{\pm_1}|_{\partial D_{\pm_2}} = \sum_l Y^0_l(\theta_{\pm_2}, \phi) E_{l,\pm_1,D_{\pm_2}}$,
- $E_{l,\pm_1,D_{\pm_2}} := \mp_2 (2a)^{-1} \sqrt{\frac{4\pi}{2l+1}} \sum_{\pm_3} \sum_{h=0}^{\infty} \tilde{A}_{h,\pm_1,\pm_3}|_{\eta_{\pm_2}} C_{h,l,\pm_3}|_{\eta_{\pm_2}}$,
- $\tilde{A}_{l,\pm_1,\pm_3}|_{\eta_{\pm_2}} := \pm_3 \, l e^{\mp_3 \eta_{\pm_2}} (A_{l,\pm_1,\pm_3} - A_{l-1,\pm_1,\pm_3})$
  $\pm_3 \, (l+1) e^{\pm_3 \eta_{\pm_2}} (A_{l,\pm_1,\pm_3} - A_{l+1,\pm_1,\pm_3})$,

Die approbierte gedruckte Originalversion dieser Diplomarbeit ist an der TU Wien Bibliothek verfügbar
The approved original version of this thesis is available in print at TU Wien Bibliothek.
TU Bibliothek Your knowledge hub WIEN

- $A_{l,\pm_1,\pm_2} \coloneqq (\pm_1 1)(\pm_2 1)\frac{e^{(l+\frac{1}{2})(-|\eta_{\pm_1}|\pm_2\eta_{\pm_1}-2|\eta_{\pm_2}|)}}{1-e^{-(2l+1)(|\eta_+|+|\eta_-|)}}$,
- $$C^m_{l,h,\pm}|_{\eta_\pm} \coloneqq \sum_{k=m}^{l\wedge h}\binom{l+m}{k+m}\binom{h-m}{k-m}(\pm 1)^{h+m} (-1)^{h+k}e^{(2k-h+1)|\eta_\pm|}\left(1-e^{-2|\eta_\pm|}\right)^{k+1},$$
- $$C^m_{l,h,\mp}|_{\eta_\pm} \coloneqq \sum_{k=m}^{l}\binom{l+m}{k+m}\binom{k+h}{k-m}(\pm 1)^{m+h} (-1)^{k+h}e^{-h|\eta_\pm|}\left(1-e^{-2|\eta_\pm|}\right)^{k+1}.$$

*Furthermore the bi-spherical parameters are defined as*

$$\begin{aligned} a &\coloneqq \frac{\sqrt{(d+r_++r_-)(d-r_++r_-)(d+r_+-r_-)(d-r_+-r_-)}}{2d}, \\ \eta_\pm &\coloneqq \pm\sinh^{-1}\left(\frac{a}{r_\pm}\right), \end{aligned} \tag{7.0.9}$$

*the capacity matrix is*

$$\boldsymbol{C}_{\pm_2,\pm_1} = 4\pi f\sum_l \frac{e^{-(2l+1)|\eta_{\pm_1}|}}{1-e^{-(2l+1)(|\eta_+|+|\eta_-|)}} \times \begin{cases} 1 & \pm_1 = \pm_2, \\ -e^{-(2l+1)|\eta_{\mp_1}|} & \pm_1 \neq \pm_2 \end{cases} \tag{7.0.10}$$

*and* $\tilde{\boldsymbol{C}}_{i,j} \coloneqq |D_i|^{-1}\boldsymbol{C}_{i,j}$.

*Proof.* The relation for the forces follow from lemma 7.2.5. We get $G$ by lemma 7.2.4 and lemma 7.2.3. Corollary 7.3.6 can be used to find the expansion of $\varphi_\pm$ in spherical harmonics. The capacity matrix representation can be found in lemma 7.4.4. □

## 7.1. Surface pressure and displacement

In this section we will prove theorem 7.0.1. We start out by defining the Dirichlet-to-Neumann operator $\mathcal{N}_D$.

**Definition 7.1.1.** *We have the Dirichlet-to-Neumann operator* $\mathcal{N}_D : H^1_0(\partial D) \to L^2_0(\partial D)$ *with* $L^2_0(\partial D) \coloneqq \{f \in L^2(\partial D) : \int_{\partial D_i} f\,\mathrm{d}\sigma = 0, \forall i\}$, $H^1_0(\partial D) \coloneqq H^1(\partial D) \cap L^2_0(\partial D)$ *and* $\mathcal{N}_D[u]|_{\partial D_i} \coloneqq \frac{\mathrm{d}v_i}{\mathrm{d}\boldsymbol{n}}|_{\partial D_i}$ *for* $v_i$ *solution to*

$$\begin{cases} \Delta v_i = 0 & \text{in } D_i, \\ v_i = u & \text{on } \partial D_i. \end{cases} \tag{7.1.1}$$

We will now prove useful relations for later use.

Die approbierte gedruckte Originalversion dieser Diplomarbeit ist an der TU Wien Bibliothek verfügbar
The approved original version of this thesis is available in print at TU Wien Bibliothek.
TU Bibliothek Your knowledge hub WIEN

**Lemma 7.1.2.** *We have*

$$\left(-\frac{1}{2}+K_D^0\right)[(\tilde{\mathcal{A}}_D^{-1}\boldsymbol{v})_1] = Pv_2 \tag{7.1.2}$$

*and for some* $\tilde{c}_i$ *that*

$$S_D^0[(\tilde{\mathcal{A}}_D^{-1}\boldsymbol{v})_1] = \mathcal{N}_D^{-1}Pv_2 + \sum_i \tilde{c}_i \chi_{\partial D_i}, \tag{7.1.3}$$

*with the Dirichlet to Neumann operator* $\mathcal{N}_D$ *and the orthogonal projection* $P$ *onto* $L_0^2(\partial D)$.

*Proof.* We assume

$$\boldsymbol{\phi} = \tilde{\mathcal{A}}_D^{-1}\boldsymbol{v} \tag{7.1.4}$$

and get

$$\left(-\frac{1}{2}+K_D^0\right)[\phi_1] + (P_0 P_{\ker}[\boldsymbol{\phi}])_2 = \boldsymbol{v}_2. \tag{7.1.5}$$

Applying $P$ to both sides provides the first result. The Neumann condition fixes the function on the boundary up to a constant on all bounded domains. Due to $\frac{\mathrm{d}}{\mathrm{d}\boldsymbol{n}} S_D^0|_- = \left(-\frac{1}{2}+K_D^0\right)$ this concludes the proof. □

The next lemma gives us a representation of the pressure and its normal derivative on the surface by calculating the potentials defined in theorem 5.1.5.

**Lemma 7.1.3.** *We have for an incident plane wave* $p_{in}$ *and resonance potentials* $\zeta_i$ *that*

$$\begin{aligned} S_D^{k_b}[\phi] &= \sum_j k_b^2 e_j \left((-\mathcal{N}_D^{-1}PK_D^2 + PS_D^2) + \frac{1}{\lambda_j}\mathcal{N}_D^{-1}P\right)[\zeta_j] \\ &\quad + \sum_i \tilde{c}_i \chi_{\partial D_i} + \mathcal{O}(\omega^3+\omega\delta+\delta^2), \\ \frac{\mathrm{d}S_D^{k_b}[\phi]}{\mathrm{d}\boldsymbol{n}} &= \sum_j k_b^2 e_j \left((1-P)K_D^2 + \frac{1}{\lambda_j}P\right)[\zeta_j] + \mathcal{O}(\omega^3+\omega\delta+\delta^2). \end{aligned} \tag{7.1.6}$$

*for* $e_j := d_j(V^{-1}\mathbf{1}_M)_j$.

*Proof.* We have with theorem 5.1.5 that

$$\boldsymbol{\phi} = (\mathbf{1} - \tilde{\mathcal{A}}_D^{-1}(\omega\mathcal{A}_D^{1,0} + \omega^2\mathcal{A}_D^{2,0} + \delta\mathcal{A}_D^{0,1}) + (\omega\tilde{\mathcal{A}}_D^{-1}\mathcal{A}_D^{1,0})^2)\left(\tilde{\mathcal{A}}_D^{-1}\begin{pmatrix}\mathrm{p_{in}}\\0\end{pmatrix} + \boldsymbol{\varphi}\right) + \mathcal{O}(\omega^3+\omega\delta+\delta^2). \tag{7.1.7}$$

$\mathcal{A}_D^{1,0}$ provides only constant functions, which in turn get transformed to $\varphi_i$ by $\tilde{\mathcal{A}}_D^{-1}$ and thus have for some $\tilde{\boldsymbol{c}}_i$ that

$$\begin{aligned} \phi &= \sum_i \tilde{c}_i\varphi_i - \left(\tilde{\mathcal{A}}_D^{-1}(\omega^2\mathcal{A}_D^{2,0} + \delta\mathcal{A}_D^{0,1})\left(\tilde{\mathcal{A}}_D^{-1}\begin{pmatrix}\tilde{\mathrm{p}}_{\mathrm{in}}\\0\end{pmatrix} + \boldsymbol{\varphi}\right)\right)_1 + \mathcal{O}(\omega^3+\omega\delta+\delta^2) \\ &= \sum_i \tilde{c}_i\varphi_i - \left(\tilde{\mathcal{A}}_D^{-1}(\omega^2\mathcal{A}_D^{2,0} + \delta\mathcal{A}_D^{0,1})\left(\sum_i \frac{\tilde{\mathrm{p}}_{\mathrm{in}}}{2}\tilde{\boldsymbol{\varphi}}_i + \boldsymbol{\varphi}\right)\right)_1 + \mathcal{O}(\omega^3+\omega\delta+\delta^2). \end{aligned} \tag{7.1.8}$$

Die approbierte gedruckte Originalversion dieser Diplomarbeit ist an der TU Wien Bibliothek verfügbar
The approved original version of this thesis is available in print at TU Wien Bibliothek.
TU Bibliothek Your knowledge hub WIEN

We now have for some $\tilde{\boldsymbol{c}}_i$ by using lemma 5.3.3 and 7.1.2 that

$$\begin{aligned} S_D^{k_b}[\phi] =& \sum_i -\mathcal{N}_D^{-1} P \left( k_b^2 \left( \frac{\tilde{\mathrm{p}}_{\mathrm{in}}}{2} + c_i \right) K_D^2[\varphi_i] - \delta \left( -\frac{\tilde{\mathrm{p}}_{\mathrm{in}}}{2} + c_i \right) \left( \frac{1}{2} + K_D^0 \right) [\varphi_i] \right) \\ &+ \sum_i \tilde{c}_i \chi_{\partial D_i} + k_b^2 \left( \frac{\tilde{\mathrm{p}}_{\mathrm{in}}}{2} + c_i \right) S_D^2[\varphi_i] + \mathcal{O}(\omega^3 + \omega\delta + \delta^2) \\ =& \sum_i \tilde{c}_i \chi_{\partial D_i} + \sum_j e_j \left( k_b^2 \left( -\mathcal{N}_D^{-1} P K_D^2 + P S_D^2 \right) + \delta \frac{\omega^2}{\omega_{M,j}^2} \mathcal{N}_D^{-1} P \right) [\zeta_j] \\ &+ \mathcal{O}(\omega^3 + \omega\delta + \delta^2), \end{aligned} \tag{7.1.9}$$

where $\mathcal{N}_D^{-1}$ goes from $L_0^2(\partial D)$ to $H_0^1(\partial D)$. Further we get

$$\begin{aligned} \frac{\mathrm{d}S_D^{k_b}[\phi]}{\mathrm{d}\boldsymbol{n}} =& \sum_i \left( \frac{\tilde{\mathrm{p}}_{\mathrm{in}}}{2} + c_i \right) \left( -k_b^2 P K_D^2[\zeta_i] + k_b^2 K_D^2[\zeta_i] \right) + \left( -\frac{\tilde{\mathrm{p}}_{\mathrm{in}}}{2} + c_i \right) \delta P \left( \frac{1}{2} + K_D^0 \right) [\varphi_i] \\ &+ \mathcal{O}(\omega^3 + \omega\delta + \delta^2) \\ =& \sum_j e_j \left( k_b^2 (1 - P) K_D^2 + \delta \frac{\omega^2}{\omega_{M,i}^2} P \right) [\zeta_j] + \mathcal{O}(\omega^3 + \omega\delta + \delta^2). \end{aligned} \tag{7.1.10}$$

□

## 7.2. Coupling spherical bubbles

In this section we will prove lemma 7.0.3 by looking at spherical bubbles and deriving formulas for $S_D^0, S_D^2$ in spherical harmonics. For simplicity we will assume that their centres lie on the $z$-axis and we will work with spherical coordinate systems, where the bubble centres are the origins. For the proof of the following statement see appendix B.

**Theorem 7.2.1.** *We have*

1. $S_{D_\pm}^0[Y_{l_\pm}^m]|_{\partial D_\mp} = -r_\pm^2 \sum_{l_\mp=0}^\infty \frac{r_+^{l_+} r_-^{l_-}}{d^{l_+ + l_- + 1}} a_{l_+,l_-,m} Y_{l_\mp}^m$,
2. $K_{D_\pm}^0[Y_{l_\pm}^m]|_{\partial D_\mp} = -\frac{r_\pm^2}{r_\mp} \sum_{l_\mp=0}^\infty \frac{r_+^{l_+} r_-^{l_-}}{d^{l_+ + l_- + 1}} a_{l_+,l_-,m} l_\mp Y_{l_\mp}^m$,
3. $S_{D_\pm}^2[Y_{l_\pm}^m]|_{\partial D_\mp} = \frac{1}{2} r_\pm^2 \sum_{l_\mp=0}^\infty \frac{r_+^{l_+} r_-^{l_-}}{d^{l_+ + l_- + 1}} Y_{l_\mp}^m a_{l_+,l_-,m} b_{l_+,l_-,m}(r_+, r_-, d)$,
4. $K_{D_\pm}^2[Y_{l_\pm}^m]|_{\partial D_\mp} = \frac{r_\pm^2}{2 r_\mp} \sum_{l_\mp=0}^\infty \frac{r_+^{l_+} r_-^{l_-}}{d^{l_+ + l_- + 1}} Y_{l_\mp}^m a_{l_+,l_-,m} c_{l_\pm,l_\mp,m}(r_\pm, r_\mp, d)$

Die approbierte gedruckte Originalversion dieser Diplomarbeit ist an der TU Wien Bibliothek verfügbar
The approved original version of this thesis is available in print at TU Wien Bibliothek.
TU Bibliothek Your knowledge hub WIEN

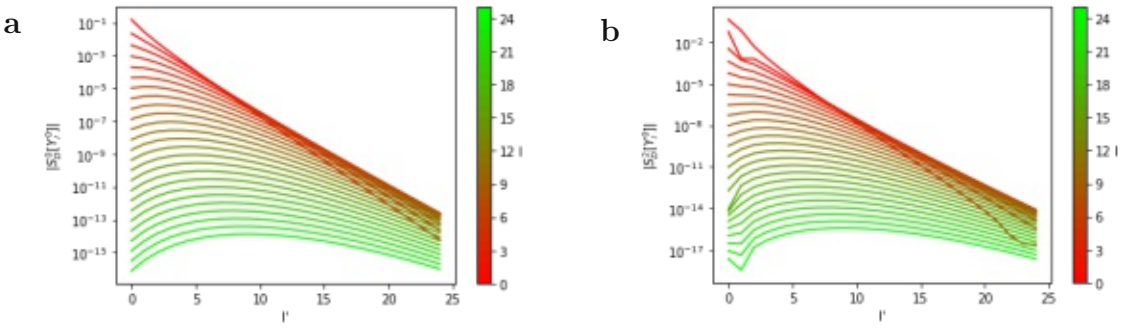


Figure 7.1.: (a) and (b) show plots of the absolute values of the coefficients for the spherical harmonic basis of $S_D^0$ and $S_D^2$. The system is made up of 2 spheres with radii 5/6 and a distance of 20. The color represents the spherical harmonic on which we apply the operators. The $x$ axis represents discrete coefficients but for easier readability we plotted continuous lines. Note that we validated the results by using Lebedev quadrature on the spheres, where we replaced the singularity by an analytical expression, which is exact for locally constant functions. We get a maximal absolute error of $\sim 2 \cdot 10^{-14}$ and $\sim 5 \cdot 10^{-14}$.

*with*

$$
\begin{aligned}
a_{l,l',m} &:= \frac{(l+l')!(-1)^{l+m}}{\sqrt{(2l+1)(2l'+1)(l+m)!(l-m)!(l'+m)!(l'-m)!}}, \\
b_{l,l',m}(r,r',d) &:= \begin{cases} \frac{r^2}{2l+3} + \frac{r'^2}{2l'+3} - d^2 \frac{2ll'-(l+l')+2m^2}{(2l-1)(2l'-1)(l+l')} & l+l' \neq 0, \\ \frac{r^2}{2l+3} + \frac{r'^2}{2l'+3} + d^2 & l+l' = 0, \end{cases} \\
c_{l,l',m}(r,r',d) &:= \frac{2r'^2}{2l'+3} + l' b_{l,l',m}
\end{aligned}
\tag{7.2.1}
$$

*for* $|m| \leq l_+ \wedge l_-$.

Note that the asymmetric $(-1)^{l_+}$ term in $a_{l,l',m}$ is due to the direction of the axis. If we reflect the coordinate system on the upper bubble through its center (so that the spherical harmonics point at each other) then this term disappears due to $Y_{l_+}^m(-\boldsymbol{n}_+) = (-1)^{l_+} Y_{l_+}^m(\boldsymbol{n}_+)$.
We also have the following formula for a self coupling term of a bubble.

**Corollary 7.2.2.** *We have on a sphere*

$$
S_{D_\pm}^2[Y_l^m]|_{\partial D_\pm} = -2r_\pm^3 \frac{1}{(2l-1)(2l+1)(2l+3)} Y_l^m. \tag{7.2.2}
$$

The proof can be found in appendix B.

**Lemma 7.2.3.** *We have*

$$
(\mathcal{N}_D[v])|_{\partial D_i} = \mathcal{N}_{D_i}[v|_{\partial D_i}] \tag{7.2.3}
$$

*and for spherical inclusions with* $l > 0$ *we have*

$$
\mathcal{N}_{D_i}^{-1}[Y_l^m] = \frac{r_i}{l} Y_l^m. \tag{7.2.4}
$$

Die approbierte gedruckte Originalversion dieser Diplomarbeit ist an der TU Wien Bibliothek verfügbar
The approved original version of this thesis is available in print at TU Wien Bibliothek.

*Proof.* Assume that $v$ is the solution of

$$\begin{cases} \Delta v = 0 & \text{in } D_i, \\ \frac{\mathrm{d}v}{\mathrm{d}n} = Y_l^m & \text{on } \partial D_i. \end{cases} \tag{7.2.5}$$

The Laplace equation without singularity is solved by

$$v = \sum_k a_k r^k Y_k^m. \tag{7.2.6}$$

We can see that

$$\delta_{k,l} = a_k k r_i^{k-1} \tag{7.2.7}$$

and thus

$$v = \frac{r^l}{l r_i^{l-1}} Y_l^m. \tag{7.2.8}$$

□

We will now look at the operators that appear in the force terms.

**Lemma 7.2.4.** *We have*

$$(-\mathcal{N}_D^{-1} P K_D^2 + P S_D^2)[Y_{l_\pm}^m \chi_{\partial D_\pm}]|_{\partial D_\mp} = -\sum_{l_\mp=1}^{\infty} \frac{r_+^{l_+ +2} r_-^{l_- +2}}{d^{l_+ + l_- +1}} \frac{1}{(2l_\mp + 3) l_\mp} Y_{l_\mp}^m a_{l_+,l_-,m}. \tag{7.2.9}$$

*and for $l_\pm > 0$ that*

$$(-\mathcal{N}_D^{-1} P K_D^2 + P S_D^2)[Y_{l_\pm}^m \chi_{\partial D_\pm}]|_{\partial D_\pm} = -\frac{r_\pm^3}{(2l_\pm + 1)(2l_\pm + 3) l_\pm} Y_{l_\pm}^m. \tag{7.2.10}$$

*Additionally we can see that we have*

$$(1-P) K_D^2 [Y_{l_\pm}^m \chi_{\partial D_\pm}]|_{\partial D_\mp} = \frac{r_\pm^{l_\pm +2} r_\mp}{d^{l_\pm +1}} \frac{(\mp 1)^{l_\pm}}{3\sqrt{2l_\pm + 1}} Y_0^0 \tag{7.2.11}$$

*and*

$$(1-P) K_D^2 [Y_{l_\pm}^m \chi_{\partial D_\pm}]|_{\partial D_\pm} = \delta_{l_\pm,0} \frac{r_\pm^2}{3} Y_0^0. \tag{7.2.12}$$

*Proof.* We have

$$\begin{aligned} \mathcal{N}_D^{-1} P K_D^2 [Y_{l_\pm}^m \chi_{\partial D_\pm}]|_{\partial D_\mp} =& \frac{r_\pm^2}{2r_\mp} \sum_{l_\mp=1}^{\infty} \frac{r_+^{l_+} r_-^{l_-}}{d^{l_+ + l_- +1}} (\mathcal{N}_{D_\mp})^{-1} Y_{l_\mp}^m a_{l_+,l_-,m} c_{l_\pm,l_\mp,m}(r_\pm, r_\mp, d) \\ =& \frac{r_\pm^2}{2} \sum_{l_\mp=1}^{\infty} \frac{r_+^{l_+} r_-^{l_-}}{l_\mp d^{l_+ + l_- +1}} Y_{l_\mp}^m a_{l_+,l_-,m} c_{l_\pm,l_\mp,m}(r_\pm, r_\mp, d). \end{aligned} \tag{7.2.13}$$

Die approbierte gedruckte Originalversion dieser Diplomarbeit ist an der TU Wien Bibliothek verfügbar
The approved original version of this thesis is available in print at TU Wien Bibliothek.
TU Bibliothek Your knowledge hub WIEN

We get

$$-\frac{c_{l_\pm,l_\mp,m}(r_\pm,r_\mp,d)}{l_\mp}+b_{l_+,l_-,m}(r_+,r_-,d)=-\frac{2r_\mp^2}{(2l_\mp+3)l_\mp}. \tag{7.2.14}$$

This proves the first statement. We have due to lemma 4.2.4

$$\begin{aligned}\mathcal{N}_D^{-1}K_D^2[Y_{l_\pm}^m\chi_{\partial D_\pm}]|_{\partial D_\pm} =&\frac{1}{2r_\pm}\mathcal{N}_D^{-1}S_D^2[Y_{l_\pm}^m\chi_{\partial D_\pm}]|_{\partial D_\pm}\\ =&-r_\pm^3\frac{1}{(2l_\pm-1)(2l_\pm+1)(2l_\pm+3)l_\pm}Y_{l_\pm}^m\end{aligned} \tag{7.2.15}$$

and we now see that

$$\frac{1}{(2l_\pm-1)(2l_\pm+1)(2l_\pm+3)l_\pm}-2\frac{1}{(2l_\pm-1)(2l_\pm+1)(2l_\pm+3)}=-\frac{1}{(2l_\pm+1)(2l_\pm+3)l_\pm}. \tag{7.2.16}$$

To arrive at the third statement we note that we get

$$a_{l,0,0}=\frac{(-1)^l}{\sqrt{2l+1}},\qquad a_{0,l,0}=\frac{1}{\sqrt{2l+1}} \tag{7.2.17}$$

and

$$c_{l,0,0}(r,r',d)=\frac{2r'^2}{3}. \tag{7.2.18}$$

□

The formula of the forces relies on the tangential derivative on the surface, which we will now calculate. We first transform the gradient in spherical coordinates and see that

$$\nabla=\boldsymbol{n}\partial_r+\frac{1}{r}\begin{pmatrix}\cos(\theta)\cos(\phi)\\ \cos(\theta)\sin(\phi)\\ -\sin(\theta)\end{pmatrix}\partial_\theta+\frac{1}{r\sin(\theta)}\begin{pmatrix}-\sin(\phi)\\ \cos(\phi)\\ 0\end{pmatrix}\partial_\phi. \tag{7.2.19}$$

Due to rotational symmetry in $\phi$ we are able to neglect the last term and get

$$\nabla_T S_D^{k_b}[\phi]=\frac{1}{r}\begin{pmatrix}\cos(\theta)\cos(\phi)\\ \cos(\theta)\sin(\phi)\\ -\sin(\theta)\end{pmatrix}\partial_\theta S_D^{k_b}[\phi]. \tag{7.2.20}$$

and

$$(\nabla_T S_D^{k_b}[\phi])^2=\frac{1}{r^2}(\partial_\theta S_D^{k_b}[\phi])^2. \tag{7.2.21}$$

**Lemma 7.2.5.** *We have on a sphere $B_r$ that*

$$\int_{\partial B_r}Y_l^0\nabla_T Y_{l'}^0\,\mathrm{d}\sigma=r\widehat{\boldsymbol{e}}_z\begin{cases}\frac{(l+1)(l+2)}{\sqrt{(2l+1)(2l+3)}} & l'=l+1,\\ -\frac{(l-1)l}{\sqrt{(2l-1)(2l+1)}} & l'=l-1,\\ 0 & \textit{else.}\end{cases} \tag{7.2.22}$$

Die approbierte gedruckte Originalversion dieser Diplomarbeit ist an der TU Wien Bibliothek verfügbar
The approved original version of this thesis is available in print at TU Wien Bibliothek.
TU Bibliothek Your knowledge hub WIEN

*and*

$$\int_{\partial B_r} \left(\nabla_T Y_l^0\right)\left(\nabla_T Y_{l'}^0\right) \boldsymbol{n}\,\mathrm{d}\sigma = \widehat{\boldsymbol{e}}_z \begin{cases} \frac{l(l+1)(l+2)}{\sqrt{(2l+1)(2l+3)}} & l' = l+1, \\ \frac{l(l+1)(l-1)}{\sqrt{(2l+1)(2l-1)}} & l' = l-1, \\ 0 & \textit{else.} \end{cases} \tag{7.2.23}$$

*Furthermore we can see that*

$$(\nabla_T Y_l^0)_3 = \frac{l(l+1)}{r\sqrt{2l+1}}\left(\frac{1}{\sqrt{2l-1}} Y_{l-1}^0 - \frac{1}{\sqrt{2l+1}} Y_{l+1}^0\right). \tag{7.2.24}$$

*Proof.* We are going to use the well known recurrence relation for Legendre polynomials

$$(P_l^0)'(x)(1-x^2) = \frac{l(l+1)}{2l+1}(P_{l-1}^0 - P_{l+1}^0). \tag{7.2.25}$$

Thus we have

$$\begin{aligned} -\sin(\theta)\partial_\theta(P_l^0(\cos(\theta))) =& (1-\cos^2(\theta))(P_l^0)'(\cos(\theta)) \\ =& \frac{l(l+1)}{2l+1}(P_{l-1}^0(\cos(\theta)) - P_{l+1}^0(\cos(\theta))) \end{aligned} \tag{7.2.26}$$

from this follows the first statement. We next see that

$$\begin{aligned} \left(\nabla_T P_l^0\right)\left(\nabla_T P_{l'}^0\right)\cos(\theta) =& \frac{1}{r^2}\partial_\theta(P_l^0(\cos(\theta))\partial_\theta(P_{l'}^0(\cos(\theta)))\cos(\theta) \\ =& \frac{1}{r^2}(P_l^0)'(\cos(\theta))(P_{l'}^0)'(\cos(\theta))\sin^2(\theta)\cos(\theta). \end{aligned} \tag{7.2.27}$$

We will also use another well known relation for Legendre polynomials, namely

$$xP_l^0 = \frac{1}{2l+1}((l+1)P_{l+1}^0 + lP_{l-1}^0). \tag{7.2.28}$$

Combining the two recurrence relations results in

$$(P_l^0)'(x)(x-x^3) = \left(\frac{(l-1)l(l+1)P_{l-2}^0}{(2l-1)(2l+1)} + \frac{l(l+1)P_l^0}{(2l-1)(2l+3)} - \frac{l(l+1)(l+2)P_{l+2}^0}{(2l+1)(2l+3)}\right). \tag{7.2.29}$$

On the other hand we also have the relation

$$(P_{l'}^0)' = (2l'-1)P_{l'-1}^0 + (P_{l'-2}^0)' \tag{7.2.30}$$

and thus

$$(P_{l'}^0)' = \sum_{k=0}^{\lceil l'/2-1\rceil} (2l'-1-4k)P_{l'-1-2k}^0. \tag{7.2.31}$$

Due to $\int_{-1}^{1} P_l^0(x)P_l'^0(x)\,\mathrm{d}x = \delta_{l,l'}\frac{2}{2l+1}$ we see that $l+l'$ has to be odd for the integral to be nonzero. Next we note that due to equation 7.2.29 and 7.2.31 we get for $l'-1 < l-2$ that

$$\int_{-1}^{1} (P_l^0)'(x)(P_{l'}^0)'(x)(x-x^3)\,\mathrm{d}x = 0. \tag{7.2.32}$$

Die approbierte gedruckte Originalversion dieser Diplomarbeit ist an der TU Wien Bibliothek verfügbar
The approved original version of this thesis is available in print at TU Wien Bibliothek.
TU Bibliothek Your knowledge hub WIEN

Due to symmetry the same is true for $l-1 < l'-2$. Thus only $l = l'+1, l'-1$ provide values. For $l = l'+1$ we get

$$\begin{aligned}\int_{\partial B_r} \left(\nabla_T Y_l^0\right)\left(\nabla_T Y_{l'}^0\right) \boldsymbol{n}_3 \,\mathrm{d}\sigma =& \frac{\sqrt{(2l+1)(2l'+1)}}{2}\int_{-1}^{1} (P_l^0)'(x)(P_{l'}^0)'(x)(x-x^3)\,\mathrm{d}x \\ =& \sqrt{(2l+1)(2l-1)}\frac{(l-1)l(l+1)}{(2l-1)(2l+1)} = \frac{(l-1)l(l+1)}{\sqrt{(2l-1)(2l+1)}}.\end{aligned} \tag{7.2.33}$$

Finally we exchanging $l$ and $l'$ provides the result for $l = l'-1$. □

## 7.3. Eigenfunction of two spheres

The Helmholtz equation is invariant under translation and rotation. We can therefore position both spheres along the z axis and consider them in bispherical coordinates. The bispherical coordinates have an associated focal length $f \coloneqq 2a$ and parameters $\eta \in \mathbb{R}$, $\xi \in [0,\pi)$, $\phi \in [0, 2\pi)$ so that

$$\begin{aligned}\boldsymbol{r}_x =& a\frac{\sin(\xi)\cos(\phi)}{\cosh(\eta)-\cos(\xi)}, \qquad \boldsymbol{r}_y = a\frac{\sin(\xi)\sin(\phi)}{\cosh(\eta)-\cos(\xi)}, \\ \boldsymbol{r}_z =& a\frac{\sinh(\eta)}{\cosh(\eta)-\cos(\xi)}.\end{aligned} \tag{7.3.1}$$

Figure 7.2 (a) shows the bispherical coordinates for constant $\eta$ or $\xi$. Note that for $\eta \to \pm\infty$ we focus in on the focal points with $\boldsymbol{r}_x = \boldsymbol{r}_y = 0$ and $\boldsymbol{r}_z = \pm a$ respectively. We can see that for constant $\eta \neq 0$ the coordinates describe spheres around the focal point on the same side of the $z$ axis. In order to describe the two bubbles we define, for $d$ being the distance between the centres of the spheres,

$$\begin{aligned}a \coloneqq& \frac{\sqrt{(d+r_+ + r_-)(d-r_+ + r_-)(d+r_+ - r_-)(d-r_+ - r_-)}}{2d}, \\ \eta_\pm \coloneqq& \pm \sinh^{-1}\left(\frac{a}{r_\pm}\right),\end{aligned} \tag{7.3.2}$$

where $r_\pm$ for consistency with the other sections $r_- \geq r_+$. If we now place the centres of the spheres along the z axis with coordinates

$$z_\pm \coloneqq a\coth(\eta_\pm) \tag{7.3.3}$$

then the surfaces of the spheres are described by bispherical coordinates with constant $\eta = \eta_\pm$. A sketch of this is shown in figure 7.2 (b).
It is further well known that

$$e^{\pm\eta} = \frac{r_{a\mp}}{r_{a\pm}} \tag{7.3.4}$$

where $r_{a\pm}$ is the distance from the upper and lower focal point respectively. We also note that $\xi$ is the angle between these connecting lines and $\phi$ takes on the same role as in spherical coordinates. We can see a sketch of this in figure 7.3 (a).

Die approbierte gedruckte Originalversion dieser Diplomarbeit ist an der TU Wien Bibliothek verfügbar
The approved original version of this thesis is available in print at TU Wien Bibliothek.
TU Bibliothek Your knowledge hub WIEN

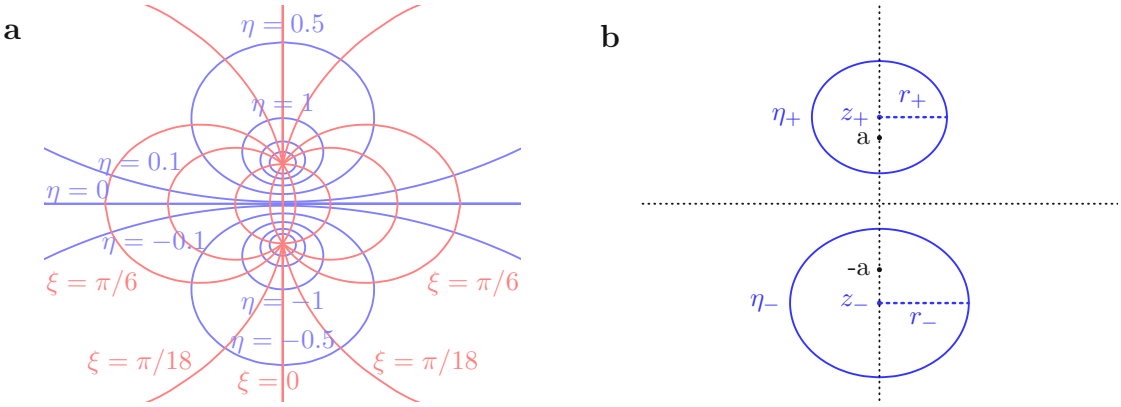


Figure 7.2.: In figure (a) we can see a sketch of the bispherical coordinate system for fixed $\eta$ and $\xi$ respectively. Note that $\phi$ corresponds to a rotation around the $z$ axis. Figure (b) shows a sketch of the bubbles $D_\pm$ and the focal points at $z = \pm a$. Each sphere can be represented by bispherical coordinates by an appropriate fixed $\eta_\pm$.

The Laplace equation separates in bispherical coordiantes and we are going to make use of the bispherical harmonics to solve for the resonance potential of two spheres.

**Definition 7.3.1.** *Using bispherical coordinates we define the bispherical harmonics*

$$B^m_{l,\pm}(\eta,\xi,\phi) \coloneqq \sqrt{2(\cosh(\eta)-\cos(\xi))}e^{\pm(l+\frac{1}{2})\eta}\tilde{Y}^m_l(\xi,\phi). \tag{7.3.5}$$

We note that going forward we are going to notify $B^0_{l,\pm}$ by $B_{l,\pm}$. Finally we will later on need that

$$\sqrt{2(\cosh(\eta)-\cos(\xi))e^{\pm\eta}} = \frac{1}{r_{a\pm}}\sqrt{r^2_{a\mp}+r^2_{a\pm}-2\cos(\xi)r_{a\mp}r_{a\pm}} = \frac{f}{r_{a\pm}} \tag{7.3.6}$$

and the following fact.

**Remark 7.3.2.** *We get*

$$z_{\pm_1} \pm_2 a = \frac{a}{\sinh(\eta_{\pm_1})}(\cosh(\eta_{\pm_1}) \pm_2 \sinh(\eta_{\pm_1})) = \pm_1 r_{\pm_1} e^{\pm_2\eta_{\pm_1}} \tag{7.3.7}$$

*and*

$$\frac{f}{r_\pm} = e^{|\eta_\pm|}(1-e^{-2|\eta_\pm|}). \tag{7.3.8}$$

### 7.3.1. Eigenfunction in bispherical coordinates

We will in this section derive the resonance potential in a similar way as in [11]. It is well known that the $\phi$ symmetric solution to the laplace equation can be written as

$$v(\eta,\xi) \coloneqq \sum_l A_{l+}B_{l,+} + A_{l-}B_{l,-}. \tag{7.3.9}$$

Die approbierte gedruckte Originalversion dieser Diplomarbeit ist an der TU Wien Bibliothek verfügbar
The approved original version of this thesis is available in print at TU Wien Bibliothek.
TU Bibliothek Your knowledge hub WIEN

Using the generating function of the legendre function we get

$$\frac{1}{\sqrt{\cosh(\eta)-\cos(\xi)}} = \frac{\sqrt{2}}{e^{|\eta/2|}\sqrt{1+e^{-2|\eta|}-2\cos(\xi)e^{-|\eta|}}} = \sqrt{2}\sum_l e^{-(l+\frac{1}{2})|\eta|}P_l(\cos(\xi)). \tag{7.3.10}$$

We will now derive the solutions $v_\pm$ with $v_\pm|_{\partial D} = \chi_{\partial D_\pm}$. We have $\pm\eta_\pm = |\eta_\pm|$ and looking at $v_\pm$ on $\partial D_\pm$ we get

$$\sum_l A_{l+}B_{l,+} + A_{l-}B_{l,-} = \sum_l B_{l,\mp} \tag{7.3.11}$$

and thus

$$A_{l+} = e^{(l+\frac{1}{2})(-|\eta_\pm|-\eta_\pm)} - A_{l-}e^{-(2l+1)\eta_\pm}. \tag{7.3.12}$$

On the other hand we see on $\partial D_\mp$ that

$$\sum_l A_{l+}B_{l,+} + A_{l-}B_{l,-} = 0, \tag{7.3.13}$$

which results in

$$A_{l-} = -A_{l+}e^{(2l+1)\eta_\mp}. \tag{7.3.14}$$

Finally we see that for $v_\pm$ we get

$$A_{l,\pm,+} \coloneqq \frac{e^{(l+\frac{1}{2})(-|\eta_\pm|+\eta_\pm)}}{e^{(2l+1)\eta_\pm} - e^{(2l+1)\eta_\mp}}, \qquad A_{l,\pm,-} \coloneqq \frac{e^{(l+\frac{1}{2})(-|\eta_\pm|-\eta_\pm)}}{e^{-(2l+1)\eta_\pm} - e^{-(2l+1)\eta_\mp}}. \tag{7.3.15}$$

This can be rewritten, using the choices of sign $\pm_1, \pm_2$,

$$A_{l,\pm_1,\pm_2} \coloneqq (\pm_1 1)(\pm_2 1)\frac{e^{(l+\frac{1}{2})(-|\eta_{\pm_1}|\pm_2\eta_{\pm_1}-2|\eta_{\pm_2}|)}}{1-e^{-(2l+1)(|\eta_+|+|\eta_-|)}}. \tag{7.3.16}$$

Next we note that

$$\left.\frac{\mathrm{d}\boldsymbol{r}}{\mathrm{d}\eta}\right|_{\eta_\pm} = \frac{\mp a}{\cosh\eta_\pm - \cos\xi}\boldsymbol{n}_\pm \tag{7.3.17}$$

and see that

$$\begin{aligned}
\left.\frac{\mathrm{d}B_{l,\pm_1}}{\mathrm{d}\boldsymbol{n}_{\pm_2}}\right|_{\eta_{\pm_2}} &= \mp_2 a^{-1}(\cosh\eta_{\pm_2} - \cos\xi)\left.\frac{\mathrm{d}B_{l,\pm_1}}{\mathrm{d}\eta}\right|_{\eta_{\pm_2}} \\
&= \mp_2 (2a)^{-1}\left(\sinh(\eta_{\pm_2}) \pm_1 (2l+1)(\cosh\eta_{\pm_2} - \cos\xi)\right) B_{l,\pm_1}|_{\partial D_{\pm_2}} \\
&= \mp_2 (2a)^{-1}(\sinh(\eta_{\pm_2}) \pm_1 (2l+1)\cosh\eta_{\pm_2})\, B_{l,\pm_1}|_{\eta_{\pm_2}} \\
&\quad \mp_2 (\mp_1 1)(2a)^{-1}\left((l+1)e^{\mp_1\eta_{\pm_2}}\, B_{l+1,\pm_1}|_{\eta_{\pm_2}} + l e^{\pm_1\eta_{\pm_2}}\, B_{l-1,\pm_1}|_{\eta_{\pm_2}}\right).
\end{aligned} \tag{7.3.18}$$

Finally we see that

$$\varphi_{\pm_1}|_{\partial D_{\pm_2}} = \left.\frac{\mathrm{d}v_{\pm_1}}{\mathrm{d}\boldsymbol{n}_{\pm_2}}\right|_{\partial D_{\pm_2}} = \sum_l A_{l,+}\left.\frac{\mathrm{d}B_{l,+}}{\mathrm{d}\boldsymbol{n}_{\pm_2}}\right|_{\partial D_{\pm_2}} + A_{l,-}\left.\frac{\mathrm{d}B_{l,-}}{\mathrm{d}\boldsymbol{n}_{\pm_2}}\right|_{\partial D_{\pm_2}}. \tag{7.3.19}$$

Combining these results gives us

Die approbierte gedruckte Originalversion dieser Diplomarbeit ist an der TU Wien Bibliothek verfügbar
The approved original version of this thesis is available in print at TU Wien Bibliothek.
TU Bibliothek Your knowledge hub WIEN

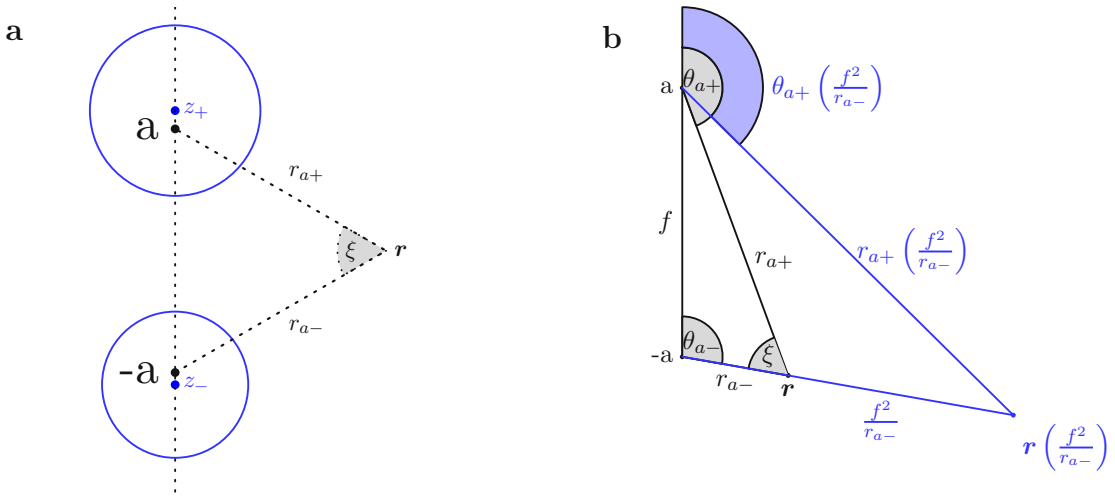


Figure 7.3.: Figure a shows $\xi$ and $r_{a\pm}$, which can be used to calculate the bispherical coordinates. We can see in b the change in the spherical coordinates centered at the upper focal point due to a transformation of $r_{a-}$.

**Lemma 7.3.3.** *We have for two spheres in bispherical coordinates*

$$\varphi_{\pm_1}|_{\partial D_{\pm_2}} = \mp_2 f^{-1} \sum_l \tilde{A}_{l,\pm_1,+}|_{\eta_{\pm_2}} \, B_{l,+}|_{\eta_{\pm_2}} + \tilde{A}_{l,\pm_1,-}|_{\eta_{\pm_2}} \, B_{l,-}|_{\eta_{\pm_2}} \tag{7.3.20}$$

*with*

$$\tilde{A}_{l,\pm_1,\pm_3}|_{\eta_{\pm_2}} := \pm_3 \, l e^{\mp_3 \eta_{\pm_2}} (A_{l,\pm_1,\pm_3} - A_{l-1,\pm_1,\pm_3}) \pm_3 (l+1) e^{\pm_3 \eta_{\pm_2}} (A_{l,\pm_1,\pm_3} - A_{l+1,\pm_1,\pm_3}). \tag{7.3.21}$$

### 7.3.2. Connecting bispherical to spherical coordinates

In this section we are following the proof of [18] to connect the bispherical harmonics to spherical harmonics with centers in the focal points. Then we will shift them to the centers of the two bubbles.

**Lemma 7.3.4.** *We have for two bubbles*

$$B^m_{l\pm}(\eta, \xi, \phi) = \sum_{k=m}^{l} \binom{l+m}{k+m} (\pm 1)^{k+m} \left(\frac{f}{r_{a\pm}}\right)^{k+1} \tilde{Y}^m_k(\theta_{a\pm}, \phi). \tag{7.3.22}$$

*Proof.* We will denote by $r_{a\pm} \to \frac{f^2}{r_{a\pm}}$ the transformation of $r_{a\pm}$ to $\frac{f^2}{r_{a\pm}}$, i.e. $r_{a\mp}(r_{a\pm} \to \frac{f^2}{r_{a\pm}})$ is the distance towards a focal point if we transform the distance to the other one. See figure 7.3(b) for a sketch.

Die approbierte gedruckte Originalversion dieser Diplomarbeit ist an der TU Wien Bibliothek verfügbar
The approved original version of this thesis is available in print at TU Wien Bibliothek.
TU Bibliothek Your knowledge hub WIEN

We first note by using the cosine law that

$$\frac{f^2+r_{a-}^2-r_{a+}^2}{2fr_{a-}}=\cos(\theta_-)=\frac{f^2+\left(\frac{f^2}{r_{a-}}\right)^2-r_{a+}^2\left(r_{a-}\to\frac{f^2}{r_{a-}}\right)}{2f\frac{f^2}{r_{a-}}}. \tag{7.3.23}$$

This provides us with $r_{a+}\left(r_{a-}\to\frac{f^2}{r_{a-}}\right)=\frac{r_{a+}f}{r_{a-}}$. In general we get

$$r_{a\pm}\left(r_{a\mp}\to\frac{f^2}{r_{a\mp}}\right)=\frac{r_{a\pm}f}{r_{a\mp}}. \tag{7.3.24}$$

Next we note that

$$\cos\theta_{a+}\left(r_{a-}\to\frac{f^2}{r_{a-}}\right)=-\frac{f^2+\left(\frac{r_{a+}f}{r_{a-}}\right)^2-\left(\frac{f^2}{r_{a-}}\right)^2}{2f\frac{r_{a+}f}{r_{a-}}}=-\frac{r_{a+}^2+r_{a-}^2-f^2}{2fr_{a+}r_{a-}}=-\cos(\xi), \tag{7.3.25}$$

where we again used the cosine rule and in general we get

$$\cos\theta_{a\pm}\left(r_{a\mp}\to\frac{f^2}{r_{a\mp}}\right)=\mp\cos(\xi). \tag{7.3.26}$$

We can now connect the spherical with the bispherical harmonic, namely

$$\begin{aligned}B_{l\pm}^m=&\sqrt{2(\cosh(\eta)-\cos(\xi))}e^{\pm(l+\frac{1}{2})\eta}\tilde{Y}_l^m(\xi,\phi)\\=&(\pm1)^{l+m}\frac{f}{r_{a\pm}}\left(\left(\frac{r_{a\mp}}{f}\right)^l\tilde{Y}_l^m(\theta_{a\mp},\phi)\right)\left(r_{a\pm}\to\frac{f^2}{r_{a\pm}}\right)\end{aligned} \tag{7.3.27}$$

where we used equation 7.3.26 and that $P_l^m(-x)=(-1)^{l+m}P_l^m(x)$. We are next using the shift lemma for spherical harmonics 4.2.3 to shift them to the other focal point

$$\begin{aligned}B_{l\pm}^m=&(\pm1)^{l+m}\frac{1}{r_{a\pm}f^{l-1}}\sum_{l'=0}^{l}\frac{(-1)^{l'}(l+m)!(\mp f)^{l'}}{l'!(l-l'+m)!}\left(r_{a\pm}^{l-l'}\tilde{Y}_{l-l'}^m(\theta_{a\pm},\phi)\right)\left(r_{a\pm}\to\frac{f^2}{r_{a\pm}}\right)\\=&(\pm1)^{l+m}\frac{1}{r_{a\pm}f^{l-1}}\sum_{l'=0}^{l}\binom{l+m}{l'}(\pm f)^{l'}\left(\frac{f^2}{r_{a\pm}}\right)^{l-l'}\tilde{Y}_{l-l'}^m(\theta_{a\pm},\phi)\\=&(\pm1)^{l+m}\sum_{l'=0}^{l}\binom{l+m}{l'}(\pm1)^{l'}\left(\frac{f}{r_{a\pm}}\right)^{l-l'+1}\tilde{Y}_{l-l'}^m(\theta_{a\pm},\phi)\\=&\sum_{k=m}^{l}\binom{l+m}{k+m}(\pm1)^{k+m}\left(\frac{f}{r_{a\pm}}\right)^{k+1}\tilde{Y}_k^m(\theta_{a\pm},\phi),\end{aligned} \tag{7.3.28}$$

where we used that $\tilde{Y}_{l'}^{m'}(\pm\hat{f})=\delta_{m',0}(\pm1)^{l'}$. □

Die approbierte gedruckte Originalversion dieser Diplomarbeit ist an der TU Wien Bibliothek verfügbar
The approved original version of this thesis is available in print at TU Wien Bibliothek.
TU Bibliothek Your knowledge hub WIEN

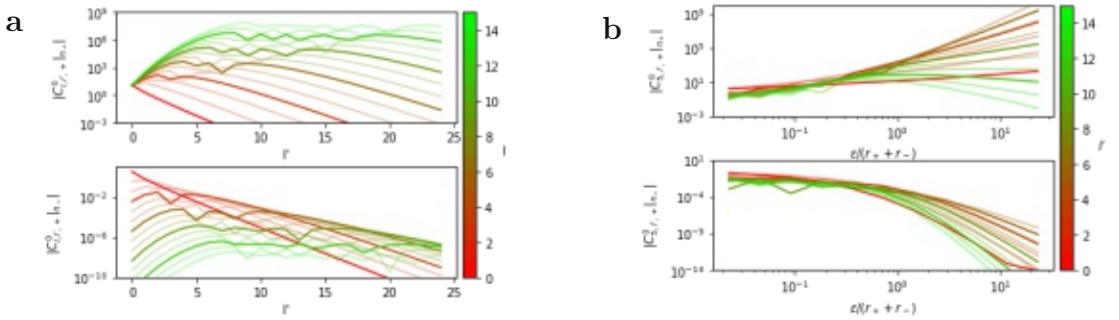


Figure 7.4.: (a) shows the coupling coefficients for different bispherical harmonics. The system is made up of two spheres with radius $r_\pm = 5,6$ and separation $d = 20$. The color represents the coefficient $l$ of $B_{l,+}$ (For better readability every third line is bold) and on the x axis we have the parameter $l'$ of the spherical harmonics. In the upper/lower plot we see the coefficient on the upper/lower sphere. The results were checked by Lebedev quadrature and produced a maximal $L^2$ error of $\sim 4.6 \cdot 10^{-2}$ for the upper and $\sim 2 \cdot 10^{-10}$ for the lower case. In (b) we instead look at $B_{5,+}$ for different distances. This time the color corresponds to the spherical harmonic. The maximal $L^2$ errors to the quadrature are $\sim 7.7 \cdot 10^{-3}$ and $\sim 1.8 \cdot 10^{-12}$ respectively.

Finally we will shift the spherical harmonics to the centers $\boldsymbol{z}_\pm := (0, 0, z_\pm)$ with $z_\pm := a \coth(\eta_\pm)$ of the two spheres with radius $r_\pm := \frac{a}{\sinh(|\eta_\pm|)}$. We will look at the points on the surfaces of the spheres and derive a series of spherical harmonics to represent the bispherical harmonics.

**Lemma 7.3.5.** *We have*

$$B^m_{l,\pm_1}|_{\eta_{\pm_2}} = \sum_{h=m}^{\infty} \tilde{Y}^m_h(\theta_{\pm_2}, \phi) C^m_{l,h,\pm_1}|_{\eta_{\pm_2}} \tag{7.3.29}$$

*for*

$$\begin{aligned} C^m_{l,h,\pm}|_{\eta_\pm} &:= \sum_{k=m}^{l\wedge h} \binom{l+m}{k+m}\binom{h-m}{k-m}(\pm 1)^{k+m} \frac{(-z_\pm \pm a)^{h-k} f^{k+1}}{r_\pm^{h+1}}, \\ C^m_{l,h,\mp}|_{\eta_\pm} &:= -\sum_{k=m}^{l} \binom{l+m}{k+m}\binom{k+h}{k-m} \frac{(\pm 1)^{k+m+1} r_\pm^h f^{k+1}}{(-z_\pm \mp a)^{k+h+1}}. \end{aligned} \tag{7.3.30}$$

*Proof.* First we will shift the spherical harmonics along the $z$-axis from $\pm a$ to $z_\pm$. We have $|\boldsymbol{z}_\pm \mp a| \leq r_\pm$ and can thus see that

$$\frac{1}{r_{a\pm}^{l+1}} \tilde{Y}^m_l(\theta_{a\pm}, \phi) = \sum_{h=l}^{\infty} \binom{h-m}{l-m} \frac{(-z_\pm \pm a)^{h-l}}{r_\pm^{h+1}} \tilde{Y}^m_h(\theta_\pm, \phi). \tag{7.3.31}$$

Die approbierte gedruckte Originalversion dieser Diplomarbeit ist an der TU Wien Bibliothek verfügbar
The approved original version of this thesis is available in print at TU Wien Bibliothek.
TU Bibliothek Your knowledge hub WIEN

Inserting this for the bispherical harmonics we get on the sphere $D_\pm$ that

$$\begin{aligned} B^m_{l\pm}|_{\eta_\pm} :=& \sqrt{2(\cosh(\eta_\pm)-\cos(\xi))}e^{(l+\frac{1}{2})|\eta_\pm|}\tilde{Y}^m_l(\xi,\phi) \\ =& \sum_{k=m}^{l}\binom{l+m}{k+m}(\pm 1)^{k+m}\sum_{h=k}^{\infty}\binom{h-m}{k-m}\frac{(-z_\pm \pm a)^{h-k}f^{k+1}}{r_\pm^{h+1}}\tilde{Y}^m_h(\theta_\pm,\phi) \\ =& \sum_{h=m}^{\infty}\tilde{Y}^m_h(\theta_\pm,\phi)\sum_{k=m}^{l\wedge h}\binom{l+m}{k+m}\binom{h-m}{k-m}(\pm 1)^{k+m}\frac{(-z_\pm \pm a)^{h-k}f^{k+1}}{r_\pm^{h+1}}. \end{aligned} \tag{7.3.32}$$

On the other hand shifting the spherical harmonics from $\mp a$ to $z_\pm$. We have $|z_\pm \mp a| > r_\pm$ and can thus see that

$$\frac{1}{r_{a\mp}^{l+1}}\tilde{Y}^m_l(\theta_{a\mp},\phi) = \mp\sum_{h=m}^{\infty}\binom{l+h}{l-m}\frac{(-1)^{l+m}r_\pm^h}{(-z_\pm \mp a)^{l+h+1}}\tilde{Y}^m_h(\theta_\pm,\phi) \tag{7.3.33}$$

where we used $\tilde{Y}^m_l(\widehat{\boldsymbol{x}-\boldsymbol{y}}) = (-1)^l\tilde{Y}^m_l(\widehat{\boldsymbol{y}-\boldsymbol{x}})$ and $(Y_l^{-m})^* = (-1)^m Y_l^m$. Inserting this in equation 7.3.28 results in

$$\begin{aligned} B^m_{l\mp}|_{\eta_\pm} :=& \sqrt{2(\cosh(\eta_\pm)-\cos(\xi))}e^{-(l+\frac{1}{2})|\eta_\pm|}\tilde{Y}^m_l(\xi,\phi) \\ =& \sum_{k=m}^{l}\binom{l+m}{k+m}(\pm 1)^{k+m+1}\sum_{h=m}^{\infty}(-1)^{l+m}\binom{k+h}{k-m}\frac{r_\pm^h f^{k+1}}{(-z_\pm \mp a)^{k+h+1}}\tilde{Y}^m_h(\theta_\pm,\phi) \\ =& -\sum_{h=m}^{\infty}\tilde{Y}^m_h(\theta_\pm,\phi)\sum_{k=m}^{l}\binom{l+m}{k+m}\binom{k+h}{k-m}\frac{(\pm 1)^{k+m+1}r_\pm^h f^{k+1}}{(-z_\pm \mp a)^{k+h+1}}. \end{aligned} \tag{7.3.34}$$

This concludes the proof. □

Finally combining the results of the last two sections provides us with

**Corollary 7.3.6.** *The basis functions of the kernel of* $\left(-\frac{1}{2}+K_D^0\right)$ *has the following spherical harmonic representation*

$$\varphi_{\pm_1}|_{\partial D_{\pm_2}} = \sum_l Y_l^0(\theta_{\pm_2},\phi)E_{l,\pm_1}|_{\eta_{\pm_2}} \tag{7.3.35}$$

*for*

$$E_{l,\pm_1,D_{\pm_2}} := \mp_2 f^{-1}\sqrt{\frac{4\pi}{2l+1}}\sum_{\pm_3}\sum_{h=0}^{\infty}\tilde{A}_{h,\pm_1,\pm_3}|_{\eta_{\pm_2}}C_{h,l,\pm_3}|_{\eta_{\pm_2}}. \tag{7.3.36}$$

## 7.4. Capacity matrix

We will first establish a general form for the eigenvalues and eigenvectors of the normalized capacity matrix for general inclusions. Then we establish the capacity matrix for a two sphere system and see that the result is consistent with literature.

Die approbierte gedruckte Originalversion dieser Diplomarbeit ist an der TU Wien Bibliothek verfügbar
The approved original version of this thesis is available in print at TU Wien Bibliothek.
TU Bibliothek Your knowledge hub WIEN

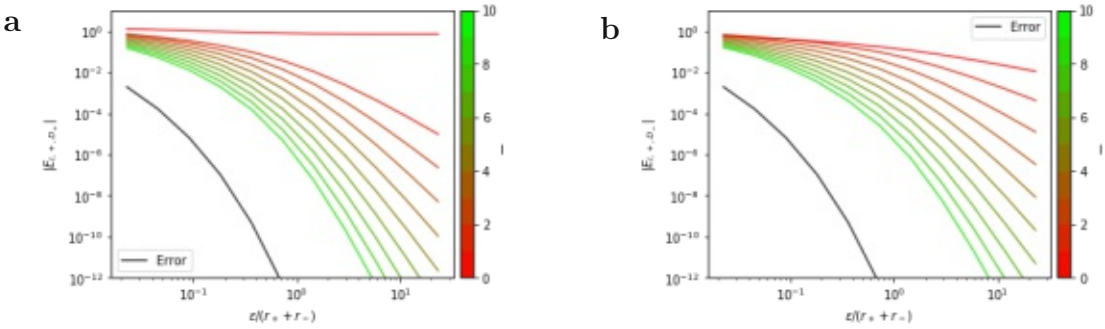


Figure 7.5.: In this figure we look at the coefficients of the resonance potential $\varphi_+$ in spherical harmonics for two bubbles with radii $r = 5, 6$. The color of the lines correspond to the parameter $l$ of the spherical harmonics $Y_l^0$. In (a)/(b) we look at the potential on the upper/lower sphere. The black curve represents the $L^2$ error to the function $\chi_{D_+}$ after applying the formula of $S_D^0$ to the potential.

**Lemma 7.4.1.** *For two inclusions, which do not need to be spheres, the resonance frequency $\omega_\pm$ is*

$$\omega_\pm = \sqrt{\delta c_b^2 \lambda_\pm} - i\delta \frac{1}{8\pi} \frac{c_b^2}{c_l} \lambda_\pm^2 \frac{|D_1|(\lambda_\pm + \tilde{\boldsymbol{C}}_{1,2} - \tilde{\boldsymbol{C}}_{2,2})^2}{(\tilde{\boldsymbol{C}}_{2,2} - \lambda_\pm)^2 + \tilde{\boldsymbol{C}}_{2,1}\tilde{\boldsymbol{C}}_{1,2}} + \mathcal{O}(\delta^{3/2}), \tag{7.4.1}$$

*for the eigenvalues $\lambda_\pm$ of the matrix $\tilde{\boldsymbol{C}}$,*

$$\lambda_\pm := \frac{1}{2}\left(\tilde{\boldsymbol{C}}_{1,1} + \tilde{\boldsymbol{C}}_{2,2} \pm \sqrt{(\tilde{\boldsymbol{C}}_{1,1} - \tilde{\boldsymbol{C}}_{2,2})^2 + 4\tilde{\boldsymbol{C}}_{1,2}\tilde{\boldsymbol{C}}_{2,1}}\right) \tag{7.4.2}$$

*with eigenvectors*

$$\boldsymbol{v}_+ := \left(\lambda_+ - \tilde{\boldsymbol{C}}_{2,2}, \tilde{\boldsymbol{C}}_{2,1}\right)^T \tag{7.4.3}$$

*and*

$$\boldsymbol{v}_- := \left(\tilde{\boldsymbol{C}}_{1,2}, \lambda_- - \tilde{\boldsymbol{C}}_{1,1}\right)^T. \tag{7.4.4}$$

*Proof.* The eigenvalues and eigenvectors can be directly checked. We can also see due to the symmetry of $\boldsymbol{C}$ that

$$\frac{\boldsymbol{v}_+^H \boldsymbol{D}\mathbf{1}_{M,M}\boldsymbol{D}\boldsymbol{v}_+}{\boldsymbol{v}_+^H \boldsymbol{D}\boldsymbol{v}_+} = \frac{(|D_1|(\lambda_+ - \tilde{\boldsymbol{C}}_{2,2}) + |D_2|\tilde{\boldsymbol{C}}_{2,1})^2}{|D_1|(\tilde{\boldsymbol{C}}_{2,2} - \lambda_+)^2 + |D_2|\tilde{\boldsymbol{C}}_{2,1}^2} = \frac{|D_1|^2(\lambda_+ + \tilde{\boldsymbol{C}}_{1,2} - \tilde{\boldsymbol{C}}_{2,2})^2}{|D_1|((\tilde{\boldsymbol{C}}_{2,2} - \lambda_+)^2 + \tilde{\boldsymbol{C}}_{2,1}\tilde{\boldsymbol{C}}_{1,2})}. \tag{7.4.5}$$

We can now use lemma 5.2.3 to conclude the proof. □

**Remark 7.4.2.** *For two identical inclusions, which do not need to be spheres, we get $\tilde{\boldsymbol{C}}_{1,1} = \tilde{\boldsymbol{C}}_{2,2}$ and thus*

$$\lambda_\pm = \tilde{\boldsymbol{C}}_{1,1} \pm \tilde{\boldsymbol{C}}_{1,2}. \tag{7.4.6}$$

Die approbierte gedruckte Originalversion dieser Diplomarbeit ist an der TU Wien Bibliothek verfügbar
The approved original version of this thesis is available in print at TU Wien Bibliothek.
TU Bibliothek Your knowledge hub WIEN

Together with lemma 7.4.1 this results in the following corollary.

**Corollary 7.4.3.** *For two identical inclusion we have*

$$\begin{aligned}\omega_+ &= \sqrt{\delta c_b^2(\tilde{\boldsymbol{C}}_{1,1}+\tilde{\boldsymbol{C}}_{1,2})} - i\delta\frac{1}{4\pi}\frac{c_b^2}{c_l}(\tilde{\boldsymbol{C}}_{1,1}+\tilde{\boldsymbol{C}}_{1,2})^2|D_1| + \mathcal{O}(\delta^{3/2}),\\ \omega_- &= \sqrt{\delta c_b^2(\tilde{\boldsymbol{C}}_{1,1}-\tilde{\boldsymbol{C}}_{1,2})} + \mathcal{O}(\delta^{3/2}).\end{aligned} \tag{7.4.7}$$

In the next lemma we will derive a formula for the capacity matrix, which is consistent with the known results, see for example [11].

**Lemma 7.4.4.** *The capacity matrix for two spheres, which do not need to be spheres, is*

$$\boldsymbol{C}_{\pm_2,\pm_1} = 4\pi f\sum_l \frac{e^{-(2l+1)|\eta_{\pm_1}|}}{1-e^{-(2l+1)(|\eta_+|+|\eta_-|)}} \times \begin{cases} 1 & \pm_1 = \pm_2,\\ -e^{-(2l+1)|\eta_{\mp_1}|} & \pm_1 \neq \pm_2.\end{cases} \tag{7.4.8}$$

*Proof.* We use formula corollary 7.3.6 and the orthogonality of spherical harmonics to get

$$\begin{aligned}\boldsymbol{C}_{\pm_2,\pm_1} &\coloneqq -\int_{\partial D_{\pm_2}} \varphi_{\pm_1}\,\mathrm{d}\sigma\\ &= \pm_2 f^{-1}\sum_l \int_{\partial D_{\pm_2}} \sqrt{\frac{4\pi}{2l+1}}Y_l^0(\theta_{\pm_2},\phi)\sum_{\pm_3}\sum_{h=0}^{\infty}\tilde{A}_{h,\pm_1,\pm_3}|_{\eta_{\pm_2}}C_{h,l,\pm_3}|_{\eta_{\pm_2}}\,\mathrm{d}\sigma\\ &= \pm_2 f^{-1}r_{\pm_2}^2 4\pi\sum_{\pm_3}\sum_{h=0}^{\infty}\tilde{A}_{h,\pm_1,\pm_3}|_{\eta_{\pm_2}}C_{h,0,\pm_3}|_{\eta_{\pm_2}}\\ &= \pm_2 4\pi f\sum_{\pm_3}\sum_{h=0}^{\infty}\frac{\tilde{A}_{h,\pm_1,\pm_3}|_{\eta_{\pm_2}}}{(e^{\pm\eta_\pm}-e^{\mp\eta_\pm})^2}\times\begin{cases} e^{\pm\eta_\pm}-e^{\mp\eta_\pm} & \pm=\pm_2=\pm_3,\\ e^{\pm 2(h+1)\eta_\mp}-e^{\pm 2\eta_\mp h} & \pm=\pm_2=-\pm_3\,.\end{cases}\end{aligned} \tag{7.4.9}$$

Where we use that

$$\begin{aligned}\sum_{k=0}^{h}\binom{h}{k}\frac{(\mp 1)^{k+1}f^{k+1}}{(-z_\mp\pm a)^{k+1}} &= \frac{\pm f}{(z_\mp\mp a)}\left(1\pm\frac{f}{z_\mp\mp a}\right)^h\\ &= (e^{\pm 2\eta_\mp}-1)e^{\pm 2\eta_\mp h} = e^{\pm 2(h+1)\eta_\mp}-e^{\pm 2\eta_\mp h}.\end{aligned} \tag{7.4.10}$$

We further have that

$$\begin{aligned}\sum_l \tilde{A}_{l,\pm_1,\pm_3}|_{\eta_{\pm_2}} &= \sum_l \pm_3 l e^{\mp_3\eta_{\pm_2}}(A_{l,\pm_1,\pm_3}-A_{l-1,\pm_1,\pm_3})\\ &\quad \pm_3 (l+1)e^{\pm_3\eta_{\pm_2}}(A_{l,\pm_1,\pm_3}-A_{l+1,\pm_1,\pm_3})\\ &= \pm_3\sum_l A_{l,\pm_1,\pm_3}(e^{\pm_3\eta_{\pm_2}}-e^{\mp_3\eta_{\pm_2}})\\ &= \pm_3 (e^{\pm_3\eta_{\pm_2}}-e^{\mp_3\eta_{\pm_2}})\sum_l \frac{e^{(l+\frac{1}{2})(-|\eta_{\pm_1}|\pm_3\eta_{\pm_1})}}{e^{\pm_3(2l+1)\eta_{\pm_1}}-e^{\pm_3(2l+1)\eta_{\mp_1}}}\end{aligned} \tag{7.4.11}$$

Die approbierte gedruckte Originalversion dieser Diplomarbeit ist an der TU Wien Bibliothek verfügbar
The approved original version of this thesis is available in print at TU Wien Bibliothek.
TU Bibliothek Your knowledge hub WIEN

and further for $\pm_2 = \pm_3 = \pm$ that

$$\begin{aligned}
&\sum_l \tilde{A}_{l,\pm_1,\pm}|_{\eta_\pm}(e^{\pm 2(l+1)\eta_\mp} - e^{\pm 2\eta_\mp l}) = \\
&= \pm_3 \sum_l A_{l,\pm_1,\pm} e^{\mp\eta_\pm}(l(e^{\pm 2(l+1)\eta_\mp} - e^{\pm 2\eta_\mp l}) - (l+1)(e^{\pm 2(l+2)\eta_\mp} - e^{\pm 2\eta_\mp (l+1)})) \\
&\quad \pm_3 \sum_l A_{l,\pm_1,\pm} e^{\pm\eta_\pm}((l+1)(e^{\pm 2(l+1)\eta_\mp} - e^{\pm 2\eta_\mp l}) - l(e^{\pm 2l\eta_\mp} - e^{\pm 2\eta_\mp (l-1)})) \\
&= 0.
\end{aligned} \tag{7.4.12}$$

Combining these equations provides the result. □

Using the last lemma we can derive a formula for the rescaled capacity matrix

$$\tilde{\boldsymbol{C}} \coloneqq \boldsymbol{D}^{-1}\boldsymbol{C} = 3f \begin{pmatrix} \sum_l \frac{r_+^{-3} e^{-(2l+1)|\eta_+|}}{1-e^{-(2l+1)(|\eta_+|+|\eta_-|)}} & \sum_l \frac{-r_+^{-3} e^{-(2l+1)(|\eta_+|+|\eta_-|)}}{1-e^{-(2l+1)(|\eta_+|+|\eta_-|)}} \\ \sum_l \frac{-r_-^{-3} e^{-(2l+1)(|\eta_+|+|\eta_-|)}}{1-e^{-(2l+1)(|\eta_+|+|\eta_-|)}} & \sum_l \frac{r_-^{-3} e^{-(2l+1)|\eta_-|}}{1-e^{-(2l+1)(|\eta_+|+|\eta_-|)}} \end{pmatrix}. \tag{7.4.13}$$

## 7.5. Asymptotic case

In this section we will look at the two extreme cases of bubble separation. For bubbles close to touching we are going to see that in the lowest order only the resonance coefficient of the in phase oscillation of the bubbles is going to have an impact on the scattered solution. Furthermore we will describe the asymptotic behaviour of the resonance frequencies for that case. For bubbles far apart we will see that in the lowest order the resonance frequencies correspond to systems of isolated bubbles. Then we will derive a formula for low order coupling and see that it is consistent with past results. Finally we will look at the Bjerknes forces in this regime and arrive at the historical approximation.

### 7.5.1. Close to touching

For this approximation we will assume that the separation $\epsilon \coloneqq d - r_+ - r_-$ scales with $\epsilon \sim e^{-\delta^{(\beta-1)}}$ for $0 < \beta < 1$. We will rely on [11] and cite the results. We have the eigenvectors

$$\boldsymbol{v}_+ = \begin{pmatrix} 1 \\ -\frac{r_+^3}{r_-^3} \end{pmatrix} + \mathcal{O}(\delta^{\beta/2}), \qquad \boldsymbol{v}_- = \begin{pmatrix} 1 \\ 1 \end{pmatrix} + \mathcal{O}(\delta^{\beta/2}). \tag{7.5.1}$$

We can see that the first eigenvector represents bubbles oscillating out of phase, while the second one are bubbles in phase. This results in

$$\boldsymbol{V}^{-1}\mathbf{1}_{2,1} = \begin{pmatrix} 0 \\ 1 \end{pmatrix} + \mathcal{O}(\delta^{\beta/2}) \tag{7.5.2}$$

for $\boldsymbol{V}$ being the matrix of these eigenvectors. This shows us that the contribution of the out of phase oscillation gets scaled down for the scattered field. This makes sense

Die approbierte gedruckte Originalversion dieser Diplomarbeit ist an der TU Wien Bibliothek verfügbar
The approved original version of this thesis is available in print at TU Wien Bibliothek.
TU Bibliothek Your knowledge hub WIEN

insofar as that the bubbles get driven by the same field and due to the large wavelength experience almost the same incident pressure field. We further have

**Theorem 7.5.1.** *We have in the close to touching case*

$$\begin{aligned}\omega_+ =&\sqrt{\delta c_b^2 \lambda_{+,0}(\epsilon)} + \mathcal{O}(\delta^{1/2}),\\ \omega_- =&\sqrt{\delta c_b^2 \lambda_{-,0}} + \mathcal{O}(\delta^{3/2-\beta})\end{aligned} \tag{7.5.3}$$

*for*

$$\begin{aligned}\lambda_{+,0}(\epsilon) :=&\frac{3}{2}\left(\frac{1}{r_+^3}+\frac{1}{r_-^3}\right)\frac{r_+ r_-}{r_+ + r_-}\log\left(\frac{2r_+r_-}{(r_++r_-)\epsilon}\right),\\ \lambda_{-,0} :=&\frac{r_+^3\sigma_+ + r_-^3\sigma_-}{r_+^3+r_-^3}\end{aligned} \tag{7.5.4}$$

*with*

$$\sigma_\pm := \frac{3r_\mp}{(r_++r_-)^2 r_\pm}\sum_{n=1}^{\infty}\frac{1}{n(n-\frac{r_\pm}{r_++r_-})}. \tag{7.5.5}$$

*Proof.* See Theorem 4.4 in [11] for the proof. We extend it with the statement for $\omega_-$ by inserting

$$\frac{a}{|\eta_+|+|\eta_-|} = \frac{r_1 r_2}{r_1+r_2} + \mathcal{O}(\epsilon) \tag{7.5.6}$$

into the definition of $\sigma_i$ in the reference. □

In the simulations we are going to see these relations empirically.

### 7.5.2. Far field

In the far field case we assume that the distance between the bubble centres $d$ is large. We can then expand the capacity matrix and the force in $d^{-1}$. We will next prove the representation of the resonance frequencies. Readers not interested in the calculations may skip to equation 7.5.14. We will start by stating the following expansions

$$a = \frac{d}{2}\sqrt{\left(1-\frac{(r_++r_-)^2}{d^2}\right)\left(1-\frac{(r_+-r_-)^2}{d^2}\right)} = \frac{d}{2}\left(1-\frac{r_+^2+r_-^2}{d^2}\right)+\mathcal{O}(d^{-3}) \tag{7.5.7}$$

and

$$\begin{aligned}e^{-|\eta_\pm|} =& \left(\frac{a}{r_\pm}+\sqrt{1+\left(\frac{a}{r_\pm}\right)^2}\right)^{-1} = \frac{r_\pm}{a}\left(1+\sqrt{1+\left(\frac{r_\pm}{a}\right)^2}\right)^{-1}\\ =&\frac{r_\pm}{a}\left(2+\frac{1}{2}\left(\frac{r_\pm}{a}\right)^2+\mathcal{O}(a^{-4})\right)^{-1} = \frac{r_\pm}{2a}\left(1-\left(\frac{r_\pm}{2a}\right)^2\right)+\mathcal{O}(a^{-4})\\ =&\frac{r_\pm}{d}\left(1+\frac{r_+^2+r_-^2}{d^2}\right)\left(1-\left(\frac{r_\pm}{d}\right)^2\right)+\mathcal{O}(d^{-5})\\ =&\frac{r_\pm}{d}\left(1+\frac{r_\pm^2}{d^2}\right)+\mathcal{O}(d^{-5}).\end{aligned} \tag{7.5.8}$$

Die approbierte gedruckte Originalversion dieser Diplomarbeit ist an der TU Wien Bibliothek verfügbar
The approved original version of this thesis is available in print at TU Wien Bibliothek.
TU Bibliothek Your knowledge hub WIEN

This results in

$$\frac{2a}{1-e^{-(|\eta_+|+|\eta_-|)}} = d\left(1+\frac{r_+r_- - (r_+^2+r_-^2)}{d^2}\right)+\mathcal{O}(d^{-3}). \tag{7.5.9}$$

The last two equations allow us to restate the capacity matrix

$$\boldsymbol{C} = 4\pi\begin{pmatrix} r_+ + r_+^2\frac{r_-}{d^2} & -\frac{r_+r_-}{d} \\ -\frac{r_+r_-}{d} & r_- + r_-^2\frac{r_+}{d^2}\end{pmatrix}+\mathcal{O}(d^{-3}) \tag{7.5.10}$$

In order to find the resonance frequencies we will state the normalized capacity matrix

$$\tilde{\boldsymbol{C}} = 3\begin{pmatrix} r_+^{-2} + \frac{r_-}{d^2r_+} & -\frac{r_+^{-2}r_-}{d} \\ -\frac{r_+r_-^{-2}}{d} & r_-^{-2} + \frac{r_+}{d^2r_-}\end{pmatrix}+\mathcal{O}(d^{-3}). \tag{7.5.11}$$

We note that

$$\left(r_+^{-2}-r_-^{-2}+\frac{r_-}{d^2r_+}-\frac{r_+}{d^2r_-}\right)^2 = (r_+^{-2}-r_-^{-2})^2+2\frac{(r_-^2-r_+^2)^2}{d^2r_+^3r_-^3}+\mathcal{O}(d^{-4}). \tag{7.5.12}$$

Using lemma 7.4.1 and equation 7.5.11 we see that

$$\begin{aligned}
\lambda_\pm =& \frac{3}{2}\left(r_+^{-2}+r_-^{-2}+\frac{r_-^2+r_+^2}{d^2r_+r_-} \pm \sqrt{(r_+^{-2}-r_-^{-2})^2+2\frac{(r_-^2-r_+^2)^2}{d^2r_+^3r_-^3}+4\frac{1}{d^2r_+r_-}+\mathcal{O}(d^{-4})}\right)\\
=& \frac{3}{2}\left(r_+^{-2}+r_-^{-2}+\frac{r_-^2+r_+^2}{d^2r_+r_-} \pm \sqrt{(r_+^{-2}-r_-^{-2})^2+2\frac{r_-^4+r_+^4}{d^2r_+^3r_-^3}}\right)+\mathcal{O}(d^{-4})\\
=& \frac{3}{2}\left(r_+^{-2}+r_-^{-2}+\frac{r_-^2+r_+^2}{d^2r_+r_-} \pm \left(|r_+^{-2}-r_-^{-2}|+\frac{r_-^4+r_+^4}{d^2r_+r_-|r_-^2-r_+^2|}\right)\right)+\mathcal{O}(d^{-4}).
\end{aligned} \tag{7.5.13}$$

Due to $r_- > r_+$ this results in

$$\boxed{\lambda_\pm = 3r_\pm^{-2} \pm \frac{3r_\mp^4}{d^2r_+r_-(r_-^2-r_+^2)}+\mathcal{O}(d^{-4}).} \tag{7.5.14}$$

Note that $\omega_\pm = \sqrt{\delta\lambda_\pm c_b^2}$ now solves

$$(\omega_{M,+}^2-\omega_\pm^2)(\omega_{M,-}^2-\omega_\pm^2)-\frac{r_+r_-}{d^2}\omega_\pm^4 = \mathcal{O}(d^{-4}) \tag{7.5.15}$$

for $\omega_{M,\pm}^2 := \delta c_b^2 3r_\pm^{-2}$ being the resonance frequency corresponding to the isolated bubble. This equation has been previously used to estimate the change in the resonance frequency due to the inclusion of the lowest order interactions between the bubbles [19, 20].

Die approbierte gedruckte Originalversion dieser Diplomarbeit ist an der TU Wien Bibliothek verfügbar
The approved original version of this thesis is available in print at TU Wien Bibliothek.
TU Bibliothek Your knowledge hub WIEN

Note that our general lemma for the capacity matrix (lemma 7.4.4) contains all linear interactions between the bubbles and holds therefore over all distances.
We now get using the Taylor expansion of $\sqrt{1+x}$ that

$$\boxed{\omega_\pm = \sqrt{3\delta c_b^2 r_\pm^{-2}}\left(1 \pm \frac{r_\mp^3 r_\pm}{2d^2(r_-^2 - r_+^2)}\right) + \mathcal{O}(\delta + \delta^{1/2}d^{-4}).} \tag{7.5.16}$$

Note that in the above equation the larger resonance frequency is increasing and the lower one decreasing for decreasing distances. Although this is only a low order approximation we will later on observe this over the whole simulation domain.
We now get for the matrix of eigenvectors of $\tilde{\boldsymbol{C}}$ by using lemma 7.4.1 and rescaling that

$$\boldsymbol{V} = \begin{pmatrix} 1 & 0 \\ 0 & 1 \end{pmatrix} + d^{-1}\begin{pmatrix} 0 & -\frac{r_-^3}{r_+^2 - r_-^2} \\ \frac{r_+^3}{r_+^2 - r_-^2} & 0 \end{pmatrix} + \mathcal{O}(d^{-2}) \tag{7.5.17}$$

and

$$\boldsymbol{V}^{-1}\mathbf{1}_{2,1} = \begin{pmatrix} 1 \\ 1 \end{pmatrix} - d^{-1}\begin{pmatrix} -\frac{r_-^3}{r_+^2 - r_-^2} \\ \frac{r_+^3}{r_+^2 - r_-^2} \end{pmatrix} + \mathcal{O}(d^{-2}). \tag{7.5.18}$$

The first equation tells us that in the lowest order the resonance functions correspond to oscillations of the individual bubbles. The latter equation thus tells us that the resonance potentials will both be present in the potential of the scattered field for bubbles far apart.

### Bjerknes force

In this subsection we will now calculate an approximation of the secondary Bjerknes force. For that we use lemma 7.0.3 and evaluate $G$.

**Lemma 7.5.2.** *We have in the far field*

$$\begin{aligned} G^{\boldsymbol{n}}_{0,D_\pm}(\varphi_\pm, \lambda) &= -\frac{\sqrt{4\pi}}{3} r_\pm + \mathcal{O}(d^{-3}), \\ G^{\boldsymbol{n}}_{1,D_\pm}(\varphi_\mp, \lambda) &= \mp\sqrt{12\pi}\frac{1}{\lambda}\frac{r_\mp}{d^2} + \mathcal{O}(d^{-3}) \end{aligned} \tag{7.5.19}$$

*and* $G^{\boldsymbol{n}}_{l,D_{\pm_2}}(\varphi_{\pm_1}, \lambda) = \mathcal{O}(d^{-3})$ *for the rest. We also have*

$$\begin{aligned} G_{1,D_\pm}(\varphi_\pm, \lambda) &= \mp\frac{\sqrt{12\pi}}{\lambda}\frac{r_\pm r_+ r_-}{d^3} + \mathcal{O}(d^{-3}), \\ G_{1,D_\pm}(\varphi_\mp, \lambda) &= \mp\frac{\sqrt{12\pi}}{\lambda}\frac{r_+ r_-}{d^2} + \mathcal{O}(d^{-3}) \end{aligned} \tag{7.5.20}$$

*and* $G_{l,D_{\pm_2}}(\varphi_{\pm_1}, \lambda) = \mathcal{O}(d^{-3})$ *for* $l \geq 2$.

*Proof.* For a proof see appendix C. □

Die approbierte gedruckte Originalversion dieser Diplomarbeit ist an der TU Wien Bibliothek verfügbar
The approved original version of this thesis is available in print at TU Wien Bibliothek.
TU Bibliothek Your knowledge hub WIEN

Note that this tells us that the bubbles oscillate uniformly up to order $\mathcal{O}(d^{-2})$. We can now calculate the pressure gradient.

**Lemma 7.5.3.** *We have*

$$\left.\frac{\mathrm{d}p}{\mathrm{d}\boldsymbol{n}}\right|_{D_\pm} = -k_b^2\frac{\sqrt{4\pi}r_\pm}{3}\frac{\tilde{p}_{in}\omega_\pm^2}{\omega_\pm^2-\omega^2}\left(1+\frac{r_\mp}{d}\frac{\omega^2}{\omega_\mp^2-\omega^2}\right)Y_0^0+\mathcal{O}(\omega^3+d^{-2}), \tag{7.5.21}$$

*Proof.* We use lemma 7.5.2 and lemma 7.0.3 to get

$$\begin{aligned}
\left.\frac{\mathrm{dp}}{\mathrm{d}\boldsymbol{n}}\right|_{D_\pm} &= -k_b^2\frac{\sqrt{4\pi}r_\pm}{3}\left(V_{\pm,\pm}\frac{\omega_\pm^2}{\omega_\pm^2-\omega^2}(\boldsymbol{V}^{-1}\mathbf{1}_{2,1})_\pm + V_{\pm,\mp}\frac{\omega_\mp^2}{\omega_\mp^2-\omega^2}(\boldsymbol{V}^{-1}\mathbf{1}_{2,1})_\mp\right)Y_0^0\\
&\quad+\mathcal{O}(\omega^3+d^{-2})\\
&= -k_b^2\frac{\sqrt{4\pi}r_\pm}{3}\left(\frac{\omega_\pm^2}{\omega_\pm^2-\omega^2}-\frac{\omega_\pm^2}{\omega_\pm^2-\omega^2}\frac{r_\mp^3}{d(r_\mp^2-r_\pm^2)}+\frac{\omega_\mp^2}{\omega_\mp^2-\omega^2}\frac{r_\mp^3}{d(r_\mp^2-r_\pm^2)}\right)Y_0^0\\
&\quad+\mathcal{O}(\omega^3+d^{-2})\\
&= -k_b^2\frac{\sqrt{4\pi}r_\pm}{3}\left(\frac{\omega_\pm^2}{\omega_\pm^2-\omega^2}+\frac{r_\mp\omega_\pm^2}{d}\frac{\omega^2}{(\omega_\mp^2-\omega^2)(\omega_\pm^2-\omega^2)}\right)Y_0^0+\mathcal{O}(\omega^3+d^{-2})\\
&= -k_b^2\frac{\sqrt{4\pi}r_\pm}{3}\frac{\omega_\pm^2}{\omega_\pm^2-\omega^2}\left(1+\frac{r_\mp}{d}\frac{\omega^2}{\omega_\mp^2-\omega^2}\right)Y_0^0+\mathcal{O}(\omega^3+d^{-2}),
\end{aligned} \tag{7.5.22}$$

where we used

$$\frac{\omega_\mp^2}{\omega_\mp^2-\omega^2}-\frac{\omega_\pm^2}{\omega_\pm^2-\omega^2}=\frac{\omega^2(\omega_\pm^2-\omega_\mp^2)}{(\omega_\mp^2-\omega^2)(\omega_\pm^2-\omega^2)} \tag{7.5.23}$$

to arrive at the result. □

We can see that this corresponds to the solution of the linearized Rayleigh-Plesset equation of two bubbles with linear coupling [21, p. 10]. It is now straightforward to calculate the secondary Bjerknes force.

**Lemma 7.5.4.** *In the far field the secondary Bjerknes force on Bubble $D_\pm$ turns to*

$$\boldsymbol{F}_{2,D_\pm} = \mp 2\delta\frac{2\pi\omega^2\tilde{p}_{in}^2}{\rho_l}\frac{1}{\omega_+^2-\omega^2}\frac{1}{\omega_-^2-\omega^2}\frac{r_+r_-}{d^2}\widehat{\boldsymbol{e}}_z+\mathcal{O}(\omega+d^{-3}). \tag{7.5.24}$$

*Proof.* Lemma 7.0.3 tells us that

$$\boldsymbol{F}^{\boldsymbol{n}}_{D_\pm}(Y_0^0,Y_1^0) = -r_\pm\widehat{\boldsymbol{e}}_z\frac{2}{\sqrt{3}}. \tag{7.5.25}$$

Further we remind ourselves that $\lambda_\pm = 3/r_\pm^2$, $\omega_\pm^2 = \lambda_\pm c_b^2\delta$ and $e_\pm = d_\pm + \mathcal{O}(d^{-1})$. We

Die approbierte gedruckte Originalversion dieser Diplomarbeit ist an der TU Wien Bibliothek verfügbar
The approved original version of this thesis is available in print at TU Wien Bibliothek.
TU Bibliothek Your knowledge hub WIEN

get

$$\begin{aligned}
\boldsymbol{F}_{2,D_\pm} =& \frac{k_b^4}{2\omega^2\delta\rho_l} e_+e_- \boldsymbol{F}^{\boldsymbol{n}}_{D_\pm}(\varphi_\pm,\varphi_\mp) + \mathcal{O}(\omega + d^{-3}) \\
=& -\frac{k_b^4}{2\omega^2\delta\rho_l} e_+e_- r_\pm \frac{2}{\sqrt{3}} G^{\boldsymbol{n}}_{0,D_\pm}(\varphi_\pm,\lambda_\pm) G_{1,D_\pm}(\varphi_\mp,\lambda_\mp)\widehat{\boldsymbol{e}}_z + \mathcal{O}(\omega + d^{-3}) \\
=& \mp \frac{k_b^4}{2\omega^2\delta\rho_l} e_+e_- r_\pm \frac{2}{\sqrt{3}} \frac{\sqrt{4\pi}}{3} r_\pm \frac{\sqrt{12\pi}}{\lambda_\mp} \frac{r_+r_-}{d^2}\widehat{\boldsymbol{e}}_z + \mathcal{O}(\omega + d^{-3}) \\
=& \mp \frac{4\pi k_b^4}{3\omega^2\delta\rho_l} d_+d_- \frac{1}{\lambda_\mp} \frac{r_\pm^3 r_\mp}{d^2}\widehat{\boldsymbol{e}}_z + \mathcal{O}(\omega + d^{-3}) \\
=& \mp \frac{4\pi k_b^2}{9c_b^2\delta\rho_l} \frac{\tilde{\mathrm{p}}_{\mathrm{in}}\omega_+^2}{\omega_+^2 - \omega^2} \frac{\tilde{\mathrm{p}}_{\mathrm{in}}\omega_-^2}{\omega_-^2 - \omega^2} \frac{r_\pm^3 r_\mp^3}{d^2}\widehat{\boldsymbol{e}}_z + \mathcal{O}(\omega + d^{-3}) \\
=& \mp 2\delta \frac{2\pi\omega^2\tilde{\mathrm{p}}_{\mathrm{in}}^2}{\rho_l} \frac{1}{\omega_+^2 - \omega^2} \frac{1}{\omega_-^2 - \omega^2} \frac{r_+r_-}{d^2}\widehat{\boldsymbol{e}}_z + \mathcal{O}(\omega + d^{-3}).
\end{aligned} \tag{7.5.26}$$

□

We can see that this matches up nicely with the historic considerations that we derived in lemma 2.3.10. For later reference in our simulations we will describe the asymptotic behaviour of the force contributions defined in theorem 7.0.1.

**Lemma 7.5.5.** *We have the asymptotic scaling*

$$\begin{aligned}
\boldsymbol{F}_{D_+,+,+} &\sim d^{-3}, \quad \boldsymbol{F}_{D_+,+,-} \sim d^{-2}, \\
\boldsymbol{F}_{D_+,-,+} &\sim d^{-4}, \quad \boldsymbol{F}_{D_+,-,-} \sim d^{-3}.
\end{aligned} \tag{7.5.27}$$

*Proof.* We have

$$\begin{aligned}
\boldsymbol{F}_{D_+,+,+} &\sim G^{\boldsymbol{n}}_{0,D_+}(\varphi_+) G_{1,D_+}(\varphi_+) \sim d^{-3}, \\
\boldsymbol{F}_{D_+,+,-} &\sim G^{\boldsymbol{n}}_{0,D_+}(\varphi_+) G_{1,D_+}(\varphi_-) \sim d^{-2}, \\
\boldsymbol{F}_{D_+,-,+} &\sim V_{+,-} G^{\boldsymbol{n}}_{0,D_+}(\varphi_+) G_{1,D_+}(\varphi_+) \sim d^{-4}, \\
\boldsymbol{F}_{D_+,-,-} &\sim V_{+,-} G^{\boldsymbol{n}}_{0,D_+}(\varphi_+) G_{1,D_+}(\varphi_-) \sim d^{-3}.
\end{aligned} \tag{7.5.28}$$

□

## 7.6. Numerical illustration

In this section we will empirically analyse the two bubble system by considering a specific example. We will look at a system of two bubbles for characteristic lengths $\epsilon/(r_+ + r_-)$ between $10^{-2}$ and $10^2$. Further we set

$$\delta = 10^{-13}, \quad c_b = 1, \quad c_l = 1. \tag{7.6.1}$$

The simulations were done in the basis of the spherical harmonics on the bubble surfaces and by using the formulas derived in this chapter.

Die approbierte gedruckte Originalversion dieser Diplomarbeit ist an der TU Wien Bibliothek verfügbar
The approved original version of this thesis is available in print at TU Wien Bibliothek.
TU Bibliothek Your knowledge hub WIEN

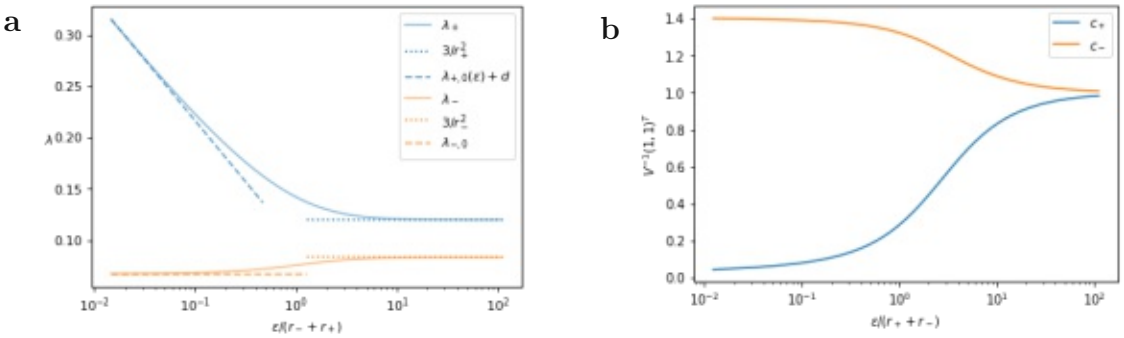


Figure 7.6.: In the figures we look at the case of two spheres with radii 5 and 6 for different separations. In $a$ we show the eigenvalues of the normalized capacity matrix $\tilde{\boldsymbol{C}}$. We have indicated the theoretical predictions of the asymptotic approximation with dotted and slashed lines. Note that the constant $d$ was fitted by least square error. In figure $b$ we look at the coordinates of the vector $(1,1)^T$ in the normalized eigenbasis of $\tilde{\boldsymbol{C}}$.

**Remark 7.6.1.** *For easier comparisons we will invert the sign of the Force on the upper bubble. Thus a positive force on a bubble represents an attractive force toward the other bubble.*

We are going to cover two cases. On the one hand we will look at a system with similar sized bubbles $r = 5, 6$ and on the other hand a system with bubbles of very different sizes $r = 1, 5$.
Before going into detail we will shortly summarize the patterns of the two systems, which can be seen in figures 7.8 and figure 7.10. The numerics show different patterns in our scope, some of which are already well known [21]. The first one describes the bubbles attracting each other over all distances, which will be seen for example in the first system for $\omega_1$. Further bubbles can repel each other if they are far apart, which turns to attraction at shorter distances, we will see this in the first system for $\omega_4$. The inverse is also the case, where bubbles attract each other at large separations but repel at shorter ones. This will be seen in the second system for $\omega_5$. This creates a stable distance for the bubbles.
Further we are going to see a few more complex patterns. In the first system for $\omega_5$ we will see that the bubbles attract each other at large distances, but when they move closer they will start to repel but finally at very short ranges this will change again to attraction. Another interesting example are $\omega_1$ and $\omega_2$ in the second system, where at close ranges the smaller bubble feels an attractive force, while the larger one gets accelerated away. This is noteworthy insofar that the two bubble system experiences a total acceleration and it does not depend on the direction of the incident waves. If the simulations accurately depict reality this could create a travelling bubble pair without the direct influence of the incident wave gradient.
We will first look at the case of the similar sized bubbles. Then we will look at the second system of differently sized bubbles. For some consideration of the accuracy of our formulas by comparing it to direct inversion of the system see appendix D.

Die approbierte gedruckte Originalversion dieser Diplomarbeit ist an der TU Wien Bibliothek verfügbar
The approved original version of this thesis is available in print at TU Wien Bibliothek.
TU Bibliothek Your knowledge hub WIEN

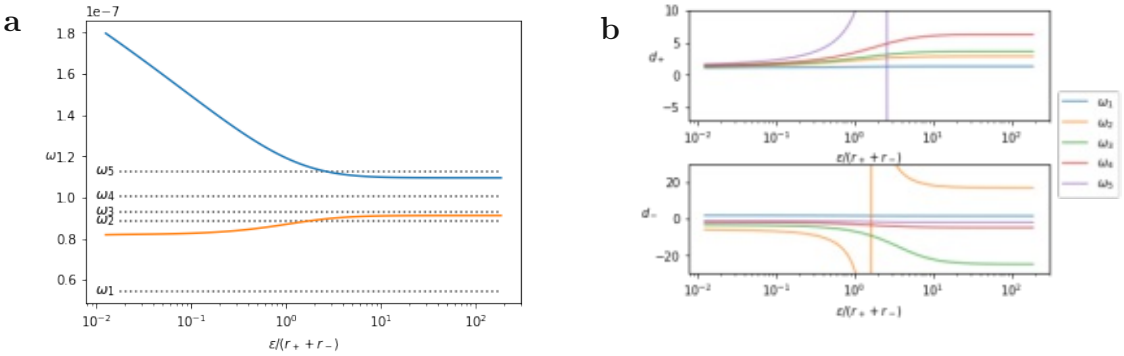


Figure 7.7.: In (a) the choice of driving frequencies in relation to the resonance frequencies is visualized. (b) shows the change of the coefficients $d_\pm$.

### 7.6.1. Similar sized bubbles

We set the radii of the bubbles to 5 and 6. We will first take a look at the eigenvalues and eigenvectors of $\tilde{\boldsymbol{C}}$, which correspond to the resonance frequencies. In figure 7.6 (a) the change of eigenvalues due to the interactions is presented. For large characteristic lengths we can see that they match up nicely with the asymptotic behaviour for the far field. This corresponds to the frequencies of two isolated spheres. For decreasing distances we can see that the upper resonance frequency, which in the far field is associated to the smaller sphere, starts increasing. On the other hand the eigenvalue corresponding to the other sphere decreases slightly and stays similarly sized. We see that the divergence rate of the bigger eigenvalue and the asymptotic value of the smaller eigenvalue matches up nicely for the prediction for the close to touching case.

In figure 7.6 (b) we look at the vector $\begin{pmatrix}1\\1\end{pmatrix}$ in the normalized eigenbasis of $\tilde{\boldsymbol{C}}$. This corresponds to an equal and constant stimulation of both bubbles. In the far field we have almost no interactions and each resonance function is associated to a bubble. On the other hand for the close to touching case the resonance functions correspond to the bubbles oscillating exactly in or exactly out of phase. We can see in the figure how the coefficients move between these extremes.

We will now take a look at the coefficients $d_\pm$. Figure 7.7 (a) shows different scenarios for incident frequencies and (b) the corresponding coefficients. We can see the singularities of $d_\pm$ at the crossing points of $\omega_2, \omega_5$ with the resonance frequencies.

We will now look at the forces on the smaller bubble $D_+$. We can see in figure 7.8 a plot of the scaled force contributions for the upper bubble defined by

$$F^s_{\pm_1,\pm_2} := F_{D_+,\pm_1,\pm_2}\left(\boldsymbol{V}^{-1}\begin{pmatrix}1\\1\end{pmatrix}\right)_{\pm_1}\left(\boldsymbol{V}^{-1}\begin{pmatrix}1\\1\end{pmatrix}\right)_{\pm_2}. \tag{7.6.2}$$

The relations that we derived in lemma 7.5.5 for the far field match up with the growth rate in (a). Thus in the far field $F^s_{+,-}$ dominates and declines slower than the rest. In our range $F^s_{-,-}$ is one order bigger than the other contributions for small distances. We

Die approbierte gedruckte Originalversion dieser Diplomarbeit ist an der TU Wien Bibliothek verfügbar
The approved original version of this thesis is available in print at TU Wien Bibliothek.
TU Bibliothek Your knowledge hub WIEN

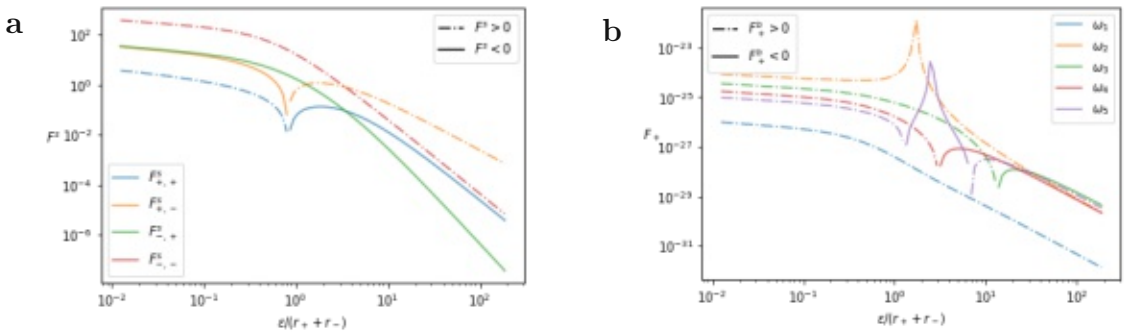


Figure 7.8.: A two bubble system with radii 5,6 is considered. (a) shows the scaled force contributions acting on the smaller bubble for a range of distances. Note that due to the scaling the contribution of $F^s_{-,-}$ dominates for small $\epsilon$. (b) shows the total forces on the smaller bubble for different driving frequencies. A stable distance can be seen in $\omega_5$.

can also see that both of these contributions are positive over the part where they are largest respectively.

As long as $d_+$ is not significantly bigger than $d_-$ this results in the force being attractive for small distances due to $F^s_{-,-}$ dominating. On the other hand for large distances we also get an attractive force if $d_+d_-$ is positive and repulsive otherwise. That are exactly the cases described in the historical formula for the secondary Bjerknes force. In Figure 7.8 (b) we can see the total force at different incident frequencies. For $\omega_1$ both $d_+, d_-$ are similarly sized, have the same sign and thus we get an attractive force over the whole domain. $\omega_2$ lies just below the lower resonance frequency for the far field and is just above it in the near field. The behaviour is similar to $\omega_1$, except that due to the lowering of the resonance frequency for closer distances $d_-$ has a singularity. This results in a stronger attraction of the bubble at that point. Although for closer distances $d_-$ is negative any positive contributions of $F^s_{+,-}$ get dominated by the contributions of $F^s_{-,-}$ because of $d_+d_- \ll d_-^2$. Next we look at $\omega_3$. It lies just above the lower resonance frequency. In the far field this produces a repulsive force, but for smaller distances due to the growth of $F^s_{-,-}$ the force gets attractive. $\omega_4$ lies in the middle between both resonance frequencies. The case is almost identical to $\omega_3$ except that now due to $|d_-|$ being smaller the attractive behavior sets on later. Finally $\omega_5$ lies a bit above the larger resonance frequency. For large distances the far field behavior produces an attractive force. If the bubbles move closer together then when the bigger resonance frequency hits the driving frequency the term $F^s_{+,+}$ becomes significant and creates a repulsive force. This creates a stable distance where the bubble does not move closer or further away. For even smaller $\epsilon$ we get an attractive force again. The forces on the larger bubble (r=6) are not completely symmetric to the ones on the smaller bubble (r=5) for smaller distances. We note that the liquid also has momentum and thus the momentum of the bubbles in general does not get conserved. For more details see appendix D.

Die approbierte gedruckte Originalversion dieser Diplomarbeit ist an der TU Wien Bibliothek verfügbar
The approved original version of this thesis is available in print at TU Wien Bibliothek.
TU Bibliothek Your knowledge hub WIEN

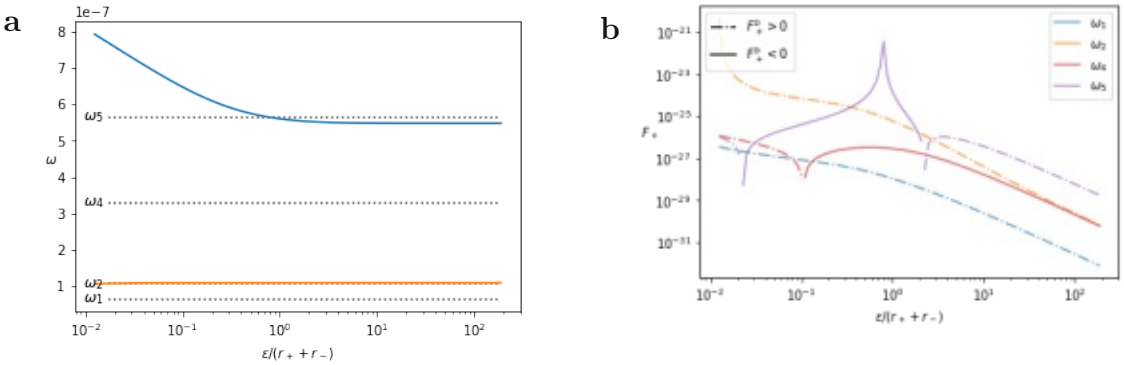


Figure 7.9.: (a) shows the change of resonance frequencies for changing distances and the choice of driving frequencies. In (b) the forces on the smaller bubble (r=1) due to a larger bubble (r=5) are presented.

### 7.6.2. Differently sized bubbles

Here we will work with two bubbles with radius 1 and 5. We will again first look at the forces on the smaller bubble. In 7.9 (a) we can see that the lower resonance frequency hardly changes, while the upper one increases for small distances. The driving frequencies that we will use are also shown in (a). In (b) we consider the force on the smaller bubble. The forces are similar to the case of two bubbles of similar size that we already covered. $\omega_1$ and $\omega_2$ have curves of an attractive force over the whole domain. Note that we now do not get a singularity for $\omega_2$ because the lower frequency is changing only slightly. $\omega_4$ is again a repulsive force and changes to an attractive one at close ranges. Finally we again get a stable distance for $\omega_5$, because of the singularity due to the increase in the upper resonance frequency. For a plot of the force contributions see appendix D.
Figure 7.10 (a) shows the force contributions for the larger bubble. We can see that four sign changes take place, two for $F^s_{+,-}$, and one for $F^s_{+,+}$ and $F^s_{-,+}$ each. This time the forces at $\omega_5$ stay attractive even at the singularity. This is the case because of $F_{+,+}$ being attractive near the singularity and $F_{-,-}$ for small separation distances. Interestingly this would suggest that both bubbles get accelerated in the direction from the bigger to the smaller bubble. Also noteworthy is that for small separations we again see an attraction for all frequencies due to dominating $F_{-,-}$.

Die approbierte gedruckte Originalversion dieser Diplomarbeit ist an der TU Wien Bibliothek verfügbar
The approved original version of this thesis is available in print at TU Wien Bibliothek.
TU Bibliothek Your knowledge hub WIEN

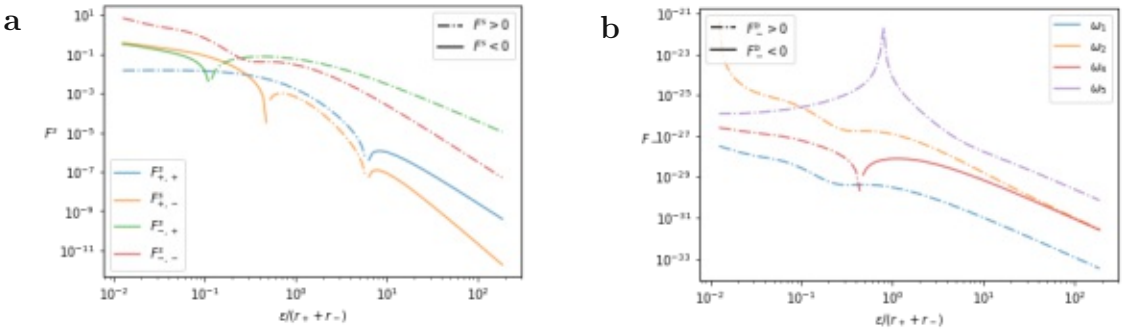


Figure 7.10.: (a) shows the force contributions of the larger bubble in the 2 bubble system (r=1,5). In (b) the total forces are presented for a range of frequencies.

Die approbierte gedruckte Originalversion dieser Diplomarbeit ist an der TU Wien Bibliothek verfügbar
The approved original version of this thesis is available in print at TU Wien Bibliothek.
TU Bibliothek Your knowledge hub WIEN

# 8. Summary, limitations and outlook

In this thesis we derived an approach of analyzing the Bjerknes forces and applied it to one or two strongly-interacting and multiple weakly-interacting spherical bubble systems. To the best knowledge of the author this is the first time that the system with complete interaction in the linear regime has been considered for analyzing the Bjerknes forces. The derived analytic formula proved to be consistent with past results for well separated bubbles, see lemma 7.5.4. Traditionally only uniform expansion of the bubbles has been looked at, which as we have seen in lemma 7.5.3, does only hold up to order $\mathcal{O}(d^{-2})$. Our new method allows us to observe complex effects at small separations caused in part by deformations of the bubble interface. Due to the scope of the thesis already being very large, we looked in section 7.6 empirically at two systems and considered different cases of interactions. We saw multiple occasions, where sign reversal of the Bjerknes force took place and even observed an example of both bubbles getting accelerated in the same direction. Multiple simulations for verification of partial results and asymptotic approximations of our formula, to show consistency with past results, were performed.
Due to the complexity of the topic some simplifications had to be made to allow a reasonable formulation of the problem. First, we neglected the viscosity and lamé terms in the Navier-Stokes equation. In past derivations they were often considered and resulted in phase shifts of the oscillations near the resonance frequencies, see 2.2.17. It may be possible to modify our approach to include these contributions to achieve higher accuracy. Furthermore, our approach is limited by the linear nature of the differential equation, which breaks for high amplitudes of the incident wave. Finally, we limited ourselves so far to frequencies not too close to resonance, but our approach allows for higher order calculations of the coefficients $d_i$, which would provide better approximations of the phase shifts near the singularity.
This thesis shows that our approach produces consistent results with literature and allows an analysis of bubbles, which are strongly interacting. We saw that layer potential techniques can be used to derive the Bjerknes forces and future investigations, especially for the close to touching regime, could provide insight into the sign reversal and further effects at closer ranges.



Die approbierte gedruckte Originalversion dieser Diplomarbeit ist an der TU Wien Bibliothek verfügbar
The approved original version of this thesis is available in print at TU Wien Bibliothek.
TU Bibliothek Your knowledge hub WIEN

Die approbierte gedruckte Originalversion dieser Diplomarbeit ist an der TU Wien Bibliothek verfügbar
The approved original version of this thesis is available in print at TU Wien Bibliothek.

# Bibliography


[1] V. Bjerknes and C. Bjerknes, *Vorlesung über hydrodynamische Fernkräfte nach C. A. Bjerknes' Theorie*, vol. 2. Johann Ambrosius Barth, 1900.

[2] L. Werner and K. Thomas, "Physics of bubble oscillations," *Reports on Progress in Physics*, vol. 73, p. 106501, 09 2010.

[3] L. A. Crum, "Bjerknes forces on bubbles in a stationary sound field," *The Journal of the Acoustical Society of America*, vol. 57, no. 6, pp. 1363–1370, 1975.

[4] A. Eller, "Force on a bubble in a standing acoustic wave," *The Journal of the Acoustical Society of America*, vol. 43, no. 1, pp. 170–171, 1968.

[5] M. Minnaert, "On musical air bubbles and the sounds of running water," *Philos. Mag*, vol. 16, pp. 235–248, 1933.

[6] A. Prosperetti, "Bubble phenomena in sound fields: part one," *Ultrasonics*, vol. 22, no. 2, pp. 69–77, 1984.

[7] C. Crowe, J. Schwarzkopf, M. Sommerfeld, and Y. Tsuji, *Multiphase Flows with Droplets and Particles*. Taylor & Francis, 1997.

[8] C. Vanhille and C. Campos-Pozuelo, "Numerical simulations of the primary bjerknes force experienced by bubbles in a standing ultrasonic field: Nonlinear vs. linear," *Wave Motion*, vol. 51, 11 2014.

[9] D. Martin, H. Thierry, B. Jean-Claude, and L. Valentin, "The minnaert bubble: An acoustic approach," *European Journal of Physics*, vol. 29, p. 1263, 09 2008.

[10] H. Ammari, B. Fitzpatrick, H. Kang, M. Ruiz, S. Yu, and H. Zhang, *Mathematical and Computational Methods in Photonics and Phononics*, vol. 235 of *Mathematical Surveys and Monographs*. Providence, RI: American Mathematical Society, 2018.

[11] H. Ammari, B. Davies, and S. Yu, "Close-to-touching acoustic subwavelength resonators: eigenfrequency separation and gradient blow-up," *arXiv e-prints*, p. arXiv:2001.04888, Jan. 2020.

[12] H. Ammari and H. Kang, *Polarization and Moment Tensors: With Applications to Inverse Problems and Effective Medium Theory*, vol. 162. 01 2007.

[13] H. Ammari, B. Fitzpatrick, H. Lee, S. Yu, and H. Zhang, "Double-negative acoustic metamaterials," 2017.




Die approbierte gedruckte Originalversion dieser Diplomarbeit ist an der TU Wien Bibliothek verfügbar
The approved original version of this thesis is available in print at TU Wien Bibliothek.
TU Bibliothek Your knowledge hub WIEN

[14] M. van Gelderen, "The shift operators and translations of spherical harmonics," 1998.

[15] H. Ammari, B. Fitzpatrick, D. Gontier, H. Lee, and H. Zhang, "Minnaert resonances for acoustic waves in bubbly media," 2016.

[16] H. Ammari, H. Kang, and H. Lee, *Layer potential techniques in spectral analysis*. No. 153, American Mathematical Soc., 2009.

[17] T. Barbat, N. Ashgriz, and C. Liu, "Dynamics of two interacting bubbles in an acoustic field," *Journal of Fluid Mechanics*, vol. 389, p. 137–168, 1999.

[18] M. Majic, "Relationships between spherical and bispherical harmonics, and an electrostatic t-matrix for dimers," 11 2019.

[19] I. Masato, "Alternative interpretation of the sign reversal of secondary bjerknes force acting between two pulsating gas bubbles," *Phys. Rev. E*, vol. 67, p. 056617, May 2003.

[20] E. A. Zabolotskaya, "Interaction of gas bubbles in a sound field.," *Soviet physics. Acoustics*, vol. 30, pp. 365–368, 1984.

[21] A. Harkin, T. J. Kaper, and A. Nadim, "Coupled pulsation and translation of two gas bubbles in a liquid," *Journal of Fluid Mechanics*, vol. 445, p. 377–411, 2001.

[22] M. Gurtin, *An Introduction to Continuum Mechanics*. ISSN, Elsevier Science, 1982.

[23] H. Ammari, B. Davies, E. O. Hiltunen, and S. Yu, "Topologically protected edge modes in one-dimensional chains of subwavelength resonators," *Journal de Mathématiques Pures et Appliquées*, Aug 2020.

Die approbierte gedruckte Originalversion dieser Diplomarbeit ist an der TU Wien Bibliothek verfügbar
The approved original version of this thesis is available in print at TU Wien Bibliothek.
TU Bibliothek Your knowledge hub WIEN

# Appendix

## A. Reynolds transport theorem

$C^n(\bar{D})$ stands for the n times continously differentiable functions in $D$ where the *function* and its derivatives can be continously extended to $\bar{D}$.

**Theorem A.1.** *(Reynolds transport theorem) For a coordinatisation $\hat{\boldsymbol{z}} \in C^2(\overline{D} \times (t_0, t_1))$ of the volume $D(t)$, where the inverse in space $\boldsymbol{x}(\cdot, t)$ is $C(D(t))$, with reference domain $D$ and a function $f \in C^1(M)$ with*

$$M \coloneqq \{(\boldsymbol{z}, t) | t \in (t_0, t_1), \boldsymbol{z} \in \overline{D(t)}\}. \tag{A.1}$$

*We get*

$$\frac{\mathrm{d}}{\mathrm{d}t} \int_{D(t)} f = \int_D \left( \frac{\mathrm{d}}{\mathrm{d}t} \hat{f} + \hat{f}((\boldsymbol{T}^{-1} \nabla) \cdot \partial_t \boldsymbol{u}) \right) \det(\boldsymbol{T}) \, \mathrm{d}\boldsymbol{x} = \int_{D(t)} \frac{\mathrm{d}f}{\mathrm{d}t} + \int_{\partial D(t)} f \, (\boldsymbol{v} \cdot \boldsymbol{n}) \, \mathrm{d}\sigma \tag{A.2}$$

*with the velocity $\boldsymbol{v}(\boldsymbol{z}, t) \coloneqq (\partial_t \boldsymbol{u})(\boldsymbol{x}(\boldsymbol{z}, t), t)$ with displacement $\boldsymbol{u}(\boldsymbol{x}, t) \coloneqq \hat{\boldsymbol{z}}(\boldsymbol{x}, t) - \boldsymbol{x}$.*

*Proof.* The proof of reynolds theorem is similar to the proof of [22]. We define

$$\hat{f}(\boldsymbol{x}, t) \coloneqq f(\hat{\boldsymbol{z}}(\boldsymbol{x}, t), t), \qquad \boldsymbol{T}_{i,j}(\boldsymbol{x}, t) \coloneqq \partial_i \hat{\boldsymbol{z}}_j(\boldsymbol{x}, t) = \delta_{i,j} + \partial_i \boldsymbol{u}_j(\boldsymbol{x}, t) \tag{A.3}$$

and note that $\hat{f} \in C^1(\overline{D} \times (t_0, t_1))$, $\boldsymbol{T} \in C^1(\overline{D} \times (t_0, t_1))$. Next we see that

$$\int_{D(t)} f(\boldsymbol{z}, t) \, \mathrm{d}z = \int_D f(\hat{\boldsymbol{z}}(\boldsymbol{x}, t), t) \det(\boldsymbol{T})(\boldsymbol{x}, t) \, \mathrm{d}\boldsymbol{x}. \tag{A.4}$$

For invertible $\boldsymbol{T}$

$$\partial_t \det(\boldsymbol{T}) = \det(\boldsymbol{T}) \operatorname{Tr}(\boldsymbol{T}^{-1} \partial_t \boldsymbol{T}), \tag{A.5}$$

which follows from the fact that $\partial_\epsilon \det(\mathbf{1} + \epsilon \boldsymbol{T})|_{\epsilon=0} = \operatorname{Tr}(\boldsymbol{T})$. Further we can see that

$$\begin{aligned} \partial_t \boldsymbol{T}_{i,j}(\boldsymbol{x}, t) &= \frac{\mathrm{d}}{\mathrm{d}x_i} (\partial_t \boldsymbol{u}_j)(\boldsymbol{x}, t) = \frac{\mathrm{d}}{\mathrm{d}x_i} (\partial_t \boldsymbol{u}_j)(\boldsymbol{x}(\hat{\boldsymbol{z}}(\boldsymbol{x}, t), t), t) \\ &= \left( \frac{\mathrm{d}^{(\partial_t \boldsymbol{u}_j)(\boldsymbol{x}(\cdot, t), t)}}{\mathrm{d}\boldsymbol{z}_k^{(\partial_t \boldsymbol{u}_j)(\boldsymbol{x}(\cdot, t), t)}} \right) (\hat{\boldsymbol{z}}(\boldsymbol{x}, t)) \frac{\mathrm{d}\hat{\boldsymbol{z}}_k}{\mathrm{d}x_i}(\boldsymbol{x}, t) \\ &= \sum_k \boldsymbol{T}_{i,k}(\boldsymbol{x}, t) \frac{\mathrm{d}}{\mathrm{d}\boldsymbol{z}_k} \boldsymbol{v}_j(\hat{\boldsymbol{z}}(\boldsymbol{x}, t), t). \end{aligned} \tag{A.6}$$

This results in

$$\partial_t \det(\boldsymbol{T})(\boldsymbol{x}, t) = \det(\boldsymbol{T})(\boldsymbol{x}, t)(\nabla \cdot \boldsymbol{v})(\hat{\boldsymbol{z}}(\boldsymbol{x}, t), t). \tag{A.7}$$



Die approbierte gedruckte Originalversion dieser Diplomarbeit ist an der TU Wien Bibliothek verfügbar
The approved original version of this thesis is available in print at TU Wien Bibliothek.
TU Bibliothek Your knowledge hub WIEN

We thus arrive at

$$\begin{aligned}\frac{\mathrm{d}}{\mathrm{d}t}\int_{D(t)} f\,\mathrm{d}\boldsymbol{z} &= \int_D \frac{\mathrm{d}}{\mathrm{d}t}\hat{f}\det(\boldsymbol{T}) + \hat{f}(\nabla\cdot\boldsymbol{v})\det(\boldsymbol{T})\,\mathrm{d}\boldsymbol{x}\\ &= \int_{D(t)} \frac{\mathrm{d}}{\mathrm{d}t}f + \boldsymbol{v}\cdot\nabla f + f\nabla\cdot\boldsymbol{v}\,\mathrm{d}\boldsymbol{z}.\end{aligned} \tag{A.8}$$

We additionally note that

$$\nabla_{\boldsymbol{z}}\cdot((\partial_t\boldsymbol{u})(\boldsymbol{x}(\boldsymbol{z},t),t)) = (\boldsymbol{T}^{-1}\nabla_{\boldsymbol{x}}\cdot(\partial_t\boldsymbol{u}))(\boldsymbol{x}(\boldsymbol{z},t),t). \tag{A.9}$$

□

## B. Coupling spherical bubbles

First we will decompose $|\boldsymbol{x}-\boldsymbol{y}|$ in spherical harmonics.

**Lemma B.1.** *We have for $|\boldsymbol{x}|\geq|\boldsymbol{y}|$ that*

$$|\boldsymbol{x}-\boldsymbol{y}| = 4\pi|\boldsymbol{x}|\sum_l\left(\frac{|\boldsymbol{y}|}{|\boldsymbol{x}|}\right)^l\frac{1}{2l+1}\left(-\frac{1}{2l-1}+\frac{1}{2l+3}\frac{\boldsymbol{y}^2}{\boldsymbol{x}^2}\right)\sum_{m=-l}^{l}Y_l^{m,*}(\widehat{\boldsymbol{y}})Y_l^m(\widehat{\boldsymbol{x}}). \tag{B.1}$$

*Proof.* By the generating function of the Legendre polynomials we get that

$$\frac{1}{|\boldsymbol{x}-\boldsymbol{y}|} = \frac{1}{|\boldsymbol{x}|}\sum_l\left(\frac{|\boldsymbol{y}|}{|\boldsymbol{x}|}\right)^l P_l(\widehat{\boldsymbol{x}}\cdot\widehat{\boldsymbol{y}}). \tag{B.2}$$

Using the recurrence relation (lemma 4.2.1) we get

$$\begin{aligned}|\boldsymbol{x}-\boldsymbol{y}| =& \frac{1}{|\boldsymbol{x}|}\sum_l\left(\frac{|\boldsymbol{y}|}{|\boldsymbol{x}|}\right)^l(\boldsymbol{x}^2+\boldsymbol{y}^2)P_l(\widehat{\boldsymbol{x}}\cdot\widehat{\boldsymbol{y}})\\ &-2\left(\frac{|\boldsymbol{y}|}{|\boldsymbol{x}|}\right)^l|\boldsymbol{x}||\boldsymbol{y}|\left(\frac{l+1}{2l+1}P_{l+1}(\widehat{\boldsymbol{x}}\cdot\widehat{\boldsymbol{y}})+\frac{l}{2l+1}P_{l-1}(\widehat{\boldsymbol{x}}\cdot\widehat{\boldsymbol{y}})\right)\\ =&|\boldsymbol{x}|\sum_l\left(\frac{|\boldsymbol{y}|}{|\boldsymbol{x}|}\right)^l\left(1+\frac{\boldsymbol{y}^2}{\boldsymbol{x}^2}-2\frac{|\boldsymbol{y}|}{|\boldsymbol{x}|}\left(\frac{|\boldsymbol{x}|}{|\boldsymbol{y}|}\frac{l}{2l-1}+\frac{|\boldsymbol{y}|}{|\boldsymbol{x}|}\frac{l+1}{2l+3}\right)\right)P_l(\widehat{\boldsymbol{x}}\cdot\widehat{\boldsymbol{y}})\\ =&|\boldsymbol{x}|\sum_l\left(\frac{|\boldsymbol{y}|}{|\boldsymbol{x}|}\right)^l\left(-\frac{1}{2l-1}+\frac{1}{2l+3}\frac{\boldsymbol{y}^2}{\boldsymbol{x}^2}\right)P_l(\widehat{\boldsymbol{x}}\cdot\widehat{\boldsymbol{y}}).\end{aligned} \tag{B.3}$$

Finally with the addition theorem 4.2.2 we conclude the proof. □

This immediately provides us with

**Corollary B.2.** *We have for $\boldsymbol{x},\boldsymbol{y}$ on a sphere with radius $r$ that*

$$|\boldsymbol{x}-\boldsymbol{y}| = -16\pi r\sum_l\frac{1}{(2l-1)(2l+1)(2l+3)}\sum_{m=-l}^{l}Y_l^{m,*}(\boldsymbol{n}_y)Y_l^m(\boldsymbol{n}_x). \tag{B.4}$$

Die approbierte gedruckte Originalversion dieser Diplomarbeit ist an der TU Wien Bibliothek verfügbar
The approved original version of this thesis is available in print at TU Wien Bibliothek.
TU Bibliothek Your knowledge hub WIEN

Next we will look at the case of separated spheres

**Lemma B.3.** *For two spheres $B_-, B_+$, where the vector from the center of $B_-$ to the center of $B_+$ is called $\boldsymbol{d}$. We have for spherical harmonics with $z$ coordinate in the direction of $\boldsymbol{d}$ that*

$$\begin{aligned}
|\boldsymbol{x}_+ - \boldsymbol{x}_-| =& 4\pi \sum_{l_+,l_-=0}^{\infty} \frac{r_+^{l_+} r_-^{l_-}}{d^{l_++l_-+1}} \sum_{m=-(l_+\wedge l_-)}^{l_+\wedge l_-} Y_{l_+}^{m,*}(\boldsymbol{n}_+) Y_{l_-}^{m}(\boldsymbol{n}_-) a_{l_+,l_-,m} b_{l_+,l_-,m}, \\
\frac{(\boldsymbol{x}_+ - \boldsymbol{x}_-)\cdot \boldsymbol{n}_-}{|\boldsymbol{x}_+ - \boldsymbol{x}_-|} =& 4\pi \sum_{l_+,l_-=0}^{\infty} \frac{r_+^{l_+} r_-^{l_--1}}{d^{l_++l_-+1}} \sum_{m=-(l_+\wedge l_-)}^{l_+\wedge l_-} Y_{l_+}^{m,*}(\boldsymbol{n}_+) Y_{l_-}^{m}(\boldsymbol{n}_-) a_{l_+,l_-,m} c_{l_+,l_-,m}.
\end{aligned} \tag{B.5}$$

*Proof.* We set $\boldsymbol{y} \coloneqq r_-\boldsymbol{n}_- - \boldsymbol{d}$ and have

$$|\boldsymbol{x}_+ - \boldsymbol{x}_-| = |r_+\boldsymbol{n}_+ - \boldsymbol{y}|. \tag{B.6}$$

We note that $|\boldsymbol{y}| \geq r_+$. Next we will use lemma B.1 and then lemma 4.2.3 to shift $Y_l^m(\widehat{\boldsymbol{y}})$ to the center of the lower bubble (we set $\boldsymbol{x} = d$ and $\boldsymbol{y} = r_-\boldsymbol{n}_-$ in said lemma). This provides us with

$$\begin{aligned}
|\boldsymbol{x}_+ - \boldsymbol{x}_-| =& \sqrt{4\pi} \sum_l \frac{(-1)^l}{\sqrt{2l+1}} \left( -\frac{\boldsymbol{y}^2}{2l-1} + \frac{r_+^2}{2l+3} \right) \times \\
& \sum_{m=-l}^{l} Y_l^{m,*}(\boldsymbol{n}_+) \sqrt{\frac{(l-m)!}{4\pi(l+m)!}} \sum_{l'=m}^{\infty} \frac{r_+^l r_-^{l'}}{d^{l+l'+1}} \frac{(l+l')!}{(l-m)!(l'-m)!} (\tilde{Y}_{l'}^{-m})^*(\boldsymbol{n}_-) \\
=& -\sqrt{4\pi} \sum_l \left( \frac{d^2 + r_-^2 - 2r_-\boldsymbol{n}_-\cdot\boldsymbol{d}}{2l-1} - \frac{r_+^2}{2l+3} \right) \sum_{m=-l}^{l} \sum_{l'=m}^{\infty} \frac{r_+^l r_-^{l'}}{d^{l+l'+1}} \times \\
& \frac{(-1)^l (l+l')!}{\sqrt{(2l+1)(l-m)!(l+m)!(l'-m)!^2}} Y_l^{m,*}(\boldsymbol{n}_+) (\tilde{Y}_{l'}^{-m})^*(\boldsymbol{n}_-)
\end{aligned} \tag{B.7}$$

Furthermore we will next note by using the recurrence relation that

$$(\boldsymbol{n}_-\cdot\boldsymbol{d})(\tilde{Y}_{l'}^{-m})^*(\boldsymbol{n}_-) = d\left( \frac{l'+m+1}{2l'+1} (\tilde{Y}_{l'+1}^{-m})^*(\boldsymbol{n}_-) + \frac{l'-m}{2l'+1} (\tilde{Y}_{l'-1}^{-m})^*(\boldsymbol{n}_-) \right). \tag{B.8}$$

Die approbierte gedruckte Originalversion dieser Diplomarbeit ist an der TU Wien Bibliothek verfügbar
The approved original version of this thesis is available in print at TU Wien Bibliothek.
TU Bibliothek Your knowledge hub WIEN

This gives us

$$
\begin{aligned}
|\boldsymbol{x}_+ - \boldsymbol{x}_-| =& -\sqrt{4\pi}\sum_l \sum_{m=-l}^{l}\sum_{l'=m}^{\infty} \frac{r_+^l r_-^{l'}}{d^{l+l'+1}} \frac{(-1)^l (l+l')! Y_l^{m,*}(\boldsymbol{n}_+)(\tilde{Y}_{l'}^{-m})^*(\boldsymbol{n}_-)}{\sqrt{(2l+1)(l-m)!(l+m)!(l'-m)!^2}} \times \\
& \left(\frac{d^2}{2l-1}\left(1 - 2\frac{(l'+m)(l'-m)}{(2l'-1)(l+l')}\right) + \frac{r_-^2}{2l-1}\left(1 - 2\frac{l'+l+1}{2l'+3}\right) - \frac{r_+^2}{2l+3}\right) \\
=& -4\pi \sum_l \sum_{m=-l}^{l}\sum_{l'=m}^{\infty} \frac{(-1)^l (l+l')! Y_l^{m,*}(\boldsymbol{n}_+)(Y_{l'}^{-m})^*(\boldsymbol{n}_-)}{\sqrt{(2l+1)(2l'+1)(l-m)!(l+m)!(l'-m)!(l'+m)!}} \\
& \times \frac{r_+^l r_-^{l'}}{d^{l+l'+1}}\left(d^2 \frac{2l'l - (l+l') + 2m^2}{(2l'-1)(2l-1)(l+l')} - \frac{r_-^2}{2l'+3} - \frac{r_+^2}{2l+3}\right).
\end{aligned}
\tag{B.9}
$$

Noting that $(Y_l^{-m})^* = (-1)^m Y_l^m$ provides the first result. Taking the derivative in $r_+$ gives us the second one. □

In the same way as the last lemma we can arrive at the following statement.

**Lemma B.4.** *For two spheres $B_-, B_+$, where the vector from the center of $B_-$ to the center of $B_+$ is called $\boldsymbol{d}$. We have for spherical harmonics with $z$ coordinate in the direction of $\boldsymbol{d}$ that*

$$
\frac{1}{|\boldsymbol{x}_+ - \boldsymbol{x}_-|} = 4\pi \sum_{l_+,l_-=0}^{\infty} \frac{r_+^{l_+} r_-^{l_-}}{d^{l_++l_-+1}} \sum_{m=-(l_+\wedge l_-)}^{l_+\wedge l_-} (Y_{l_+}^m)^*(\boldsymbol{n}_+) Y_{l_-}^m(\boldsymbol{n}_-) a_{l_+,l_-,m}, \tag{B.10}
$$

*where $a_{l_+,l_-,m}$ is defined in lemma B.3.*

## C. Far field

In this section we will prove lemma 7.5.3. We have

$$
C^0_{h,l,\pm}|_{\eta_\pm} = \mathcal{O}(d^{2(l\wedge h)+1-l}), \quad C^0_{h,l,\mp}|_{\eta_\pm} = \mathcal{O}(d^{-l}) \tag{C.1}
$$

and more specifically

$$
\begin{aligned}
C^0_{0,0,\pm}|_{\eta_\pm} &= \tfrac{d}{r_\pm}\left(1 - \tfrac{r_+^2+r_-^2}{d^2}\right) + \mathcal{O}(d^{-3}), & C^0_{1,0,\pm}|_{\eta_\pm} &= \tfrac{d}{r_\pm}\left(1 - \tfrac{r_+^2+r_-^2}{d^2}\right) + \mathcal{O}(d^{-3}), \\
C^0_{0,1,\pm}|_{\eta_\pm} &= \mp\left(1 - \tfrac{r_+^2+r_-^2}{d^2}\right) + \mathcal{O}(d^{-4}), & C^0_{1,1,\pm}|_{\eta_\pm} &= \pm\left(\left(\tfrac{d}{r_\pm}\right)^2 - 1\right) + \mathcal{O}(d^{-2}), \\
C^0_{0,0,\mp}|_{\eta_\pm} &= \left(1 - \tfrac{r_\pm^2}{d^2}\right) + \mathcal{O}(d^{-4}), & C^0_{1,0,\mp}|_{\eta_\pm} &= \tfrac{r_\pm^2}{d^2}\left(1 - \tfrac{r_\pm^2}{d^2}\right) + \mathcal{O}(d^{-6}), \\
C^0_{0,1,\mp}|_{\eta_\pm} &= \pm\tfrac{r_\pm}{d} + \mathcal{O}(d^{-3}), & C^0_{1,1,\mp}|_{\eta_\pm} &= \pm\tfrac{r_\pm}{d} + \mathcal{O}(d^{-5}), \\
C^0_{0,2,\pm}|_{\eta_\pm} &= \tfrac{r_\pm}{d} + \mathcal{O}(d^{-3}), & C^0_{1,2,\pm}|_{\eta_\pm} &= \tfrac{d}{r_\pm} + \mathcal{O}(d^{-1}) \\
C^0_{2,2,\pm}|_{\eta_\pm} &= \left(\tfrac{d}{r_\pm}\right)^3 + \mathcal{O}(d^1)
\end{aligned}
\tag{C.2}
$$

Die approbierte gedruckte Originalversion dieser Diplomarbeit ist an der TU Wien Bibliothek verfügbar
The approved original version of this thesis is available in print at TU Wien Bibliothek.
TU Bibliothek Your knowledge hub WIEN

Furthermore for $l > 0$ we have

$$\begin{aligned} \tilde{A}_{l,\pm,\pm}|_{\eta_\pm} &= \mathcal{O}(d^{-2l}), \quad \tilde{A}_{l,\pm,\mp}|_{\eta_\pm} = \mathcal{O}(d^{3-4l}), \\ \tilde{A}_{l,\mp,\pm}|_{\eta_\pm} &= \mathcal{O}(d^{1-4l}), \quad \tilde{A}_{l,\mp,\mp}|_{\eta_\pm} = \mathcal{O}(d^{2-2l}) \end{aligned} \tag{C.3}$$

and

$$\begin{aligned} \tilde{A}_{0,\pm,\pm}|_{\eta_\pm} &= \pm\left(1 + \tfrac{r_+r_- - r_\pm^2}{d^2}\right) + \mathcal{O}(d^{-4}), & \tilde{A}_{0,\pm,\mp}|_{\eta_\pm} &= \mathcal{O}(d^{-3}), \\ \tilde{A}_{1,\pm,\pm}|_{\eta_\pm} &= \pm\left(\tfrac{r_\pm}{d}\right)^2\left(1 - \tfrac{r_+r_- + r_\pm + r_\pm^2}{d^2}\right) + \mathcal{O}(d^{-6}), & \tilde{A}_{1,\pm,\mp}|_{\eta_\pm} &= \mp\tfrac{r_\mp}{d} + \mathcal{O}(d^{-3}), \\ \tilde{A}_{0,\mp,\pm}|_{\eta_\pm} &= \mp\tfrac{r_\mp}{d} + \mathcal{O}(d^{-3}), & \tilde{A}_{0,\mp,\mp}|_{\eta_\pm} &= \mp\tfrac{r_+r_-}{d^2} + \mathcal{O}(d^{-4}), \\ \tilde{A}_{1,\mp,\pm}|_{\eta_\pm} &= \pm\tfrac{r_\pm^2 r_\mp}{d^3} + \mathcal{O}(d^{-5}), & \tilde{A}_{1,\mp,\mp}|_{\eta_\pm} &= \pm\tfrac{r_\mp}{r_\pm} + \mathcal{O}(d^{-4}), \\ \tilde{A}_{2,\pm,\pm}|_{\eta_\pm} &= \mp 2\left(\tfrac{r_\pm}{d}\right)^4 + \mathcal{O}(d^{-6}). \end{aligned} \tag{C.4}$$

For

$$E_{l,\pm_1,D_{\pm_2}} := \mp_2 f^{-1}\sqrt{\frac{4\pi}{2l+1}}\sum_{\pm_3}\sum_{h=0}^{\infty}\tilde{A}_{h,\pm_1,\pm_3}|_{\eta_{\pm_2}}C_{h,l,\pm_3}|_{\eta_{\pm_2}} \tag{C.5}$$

we can now immediately see that

**Lemma C.1.** *We have*

$$\begin{aligned} E_{0,\pm,D_\pm} &= -\frac{\sqrt{4\pi}}{r_\pm}\left(1 + \frac{r_+r_-}{d^2}\right) + \mathcal{O}(d^{-4}), \\ E_{0,\mp,D_\pm} &= \sqrt{4\pi}\frac{r_\mp}{dr_\pm} + \mathcal{O}(d^{-3}), \\ E_{1,\pm,D_\pm} &= \pm\sqrt{\frac{4\pi}{3}}3\frac{r_\pm r_\mp}{d^3} + \mathcal{O}(d^{-5}), \\ E_{1,\mp,D_\pm} &= \mp\sqrt{\frac{4\pi}{3}}3\frac{r_\mp}{d^2} + \mathcal{O}(d^{-4}). \end{aligned} \tag{C.6}$$

*Further for $l > 1$ we get*

$$E_{l,\pm,D_\pm} = \mathcal{O}(d^{-3}). \tag{C.7}$$

*Proof.*

$$\begin{aligned} E_{l,\pm,D_\pm} &= \mathcal{O}\left(d^{-1}\left(d^{1-l} + d^{-l}d^{-3} + \sum_{h=1}^{\infty} d^{2(l\wedge h)+1-l}d^{-2h} + d^{-l}d^{3-4h}\right)\right) = \mathcal{O}(d^{-l}), \\ E_{l,\mp,D_\pm} &= \mathcal{O}\left(d^{-1}\left(d^{1-l}d^{-1} + d^{-l} + \sum_{h=1}^{\infty} d^{2(l\wedge h)+1-l}d^{1-4h} + d^{-l}d^{2-2h}\right)\right) = \mathcal{O}(d^{-l-1}). \end{aligned} \tag{C.8}$$

Further we get

$$\begin{aligned} E_{0,\pm,D_\pm} &= \mp\sqrt{4\pi}d^{-1}\left(1 + \frac{r_+^2 + r_-^2}{d^2}\right)\left[\pm\left(1 + \frac{r_+r_- - r_\pm^2}{d^2}\right)\frac{d}{r_\pm}\left(1 - \frac{r_+^2 + r_-^2}{d^2}\right)\right. \\ &\quad \left. \pm\left(\frac{r_\pm}{d}\right)^2\frac{d}{r_\pm}\right] + \mathcal{O}(d^{-3}) \\ &= -\frac{\sqrt{4\pi}}{r_\pm}\left(1 + \frac{r_+r_-}{d^2}\right) + \mathcal{O}(d^{-4}) \end{aligned} \tag{C.9}$$

Die approbierte gedruckte Originalversion dieser Diplomarbeit ist an der TU Wien Bibliothek verfügbar
The approved original version of this thesis is available in print at TU Wien Bibliothek.
TU Bibliothek Your knowledge hub WIEN

and

$$\begin{aligned} E_{0,\mp,D_\pm} =& \mp \sqrt{4\pi} d^{-1} \left[ \mp \frac{r_\mp}{d} \frac{d}{r_\pm} \right] + \mathcal{O}(d^{-3}) \\ =& \sqrt{4\pi} \frac{r_\mp}{d r_\pm} + \mathcal{O}(d^{-3}). \end{aligned} \tag{C.10}$$

Further we see that

$$\begin{aligned} E_{1,\pm,D_\pm} =& \pm \sqrt{\frac{4\pi}{3}} d^{-1} \left[ \left( 1 + \frac{r_+ r_- - r_\pm^2}{d^2} \right) \left( 1 - \frac{r_+^2 + r_-^2}{d^2} \right) \right. \\ & \left. - \left( \frac{r_\pm}{d} \right)^2 \left( 1 - \frac{r_+ r_- + r_\pm^2 + r_\mp^2}{d^2} \right) \left( \left( \frac{d}{r_\pm} \right)^2 - 1 \right) + \frac{r_\pm r_\mp}{d^2} \right] + \mathcal{O}(d^{-4}) \\ =& \pm \sqrt{\frac{4\pi}{3}} 3 \frac{r_\pm r_\mp}{d^3} + \mathcal{O}(d^{-5}) \end{aligned} \tag{C.11}$$

and

$$\begin{aligned} E_{1,\mp,D_\pm} =& \mp \sqrt{\frac{4\pi}{3}} d^{-1} \left[ \frac{r_\mp}{d} + \frac{r_\pm^2 r_\mp}{d^3} \left( \frac{d}{r_\pm} \right)^2 + \frac{r_\mp}{r_\pm} \frac{r_\pm}{d} \right] + \mathcal{O}(d^{-4}) \\ =& \mp \sqrt{\frac{4\pi}{3}} 3 \frac{r_\mp}{d^2} + \mathcal{O}(d^{-4}). \end{aligned} \tag{C.12}$$

Finally we note that

$$\begin{aligned} E_{2,\pm,D_\pm} =& - \sqrt{\frac{4\pi}{5}} d^{-1} \left[ \frac{r_\pm}{d} + \left( \frac{r_\pm}{d} \right)^2 \frac{d}{r_\pm} - 2 \left( \frac{r_\pm}{d} \right)^4 \left( \frac{d}{r_\pm} \right)^3 \right] + \mathcal{O}(d^{-4}) \\ =& \mathcal{O}(d^{-4}). \end{aligned} \tag{C.13}$$

□

**Lemma C.2.** *Using this we can see that*

$$\begin{aligned} G^{\boldsymbol{n}}_{0,D_\pm}(\varphi_\pm, \lambda) =& - \frac{\sqrt{4\pi}}{3} r_\pm + \mathcal{O}(d^{-3}), \\ G^{\boldsymbol{n}}_{1,D_\pm}(\varphi_\mp, \lambda) =& \mp \sqrt{12\pi} \frac{1}{\lambda} \frac{r_\mp}{d^2} + \mathcal{O}(d^{-3}) \end{aligned} \tag{C.14}$$

*and* $G^{\boldsymbol{n}}_{l,D_{\pm_2}}(\varphi_{\pm_1}, \lambda) = \mathcal{O}(d^{-3})$ *for the rest. We also have*

$$\begin{aligned} G_{1,D_\pm}(\varphi_\pm, \lambda) =& \mp \frac{\sqrt{12\pi}}{\lambda} \frac{r_\pm r_+ r_-}{d^3} + \mathcal{O}(d^{-3}), \\ G_{1,D_\pm}(\varphi_\mp, \lambda) =& \mp \frac{\sqrt{12\pi}}{\lambda} \frac{r_+ r_-}{d^2} + \mathcal{O}(d^{-3}) \end{aligned} \tag{C.15}$$

*and* $G_{l,D_{\pm_2}}(\varphi_{\pm_1}, \lambda) = \mathcal{O}(d^{-3})$ *for* $l \geq 2$.

Die approbierte gedruckte Originalversion dieser Diplomarbeit ist an der TU Wien Bibliothek verfügbar
The approved original version of this thesis is available in print at TU Wien Bibliothek.
TU Bibliothek Your knowledge hub WIEN

*Proof.* We use lemma 7.0.3 to get

$$\begin{aligned} G^{\boldsymbol{n}}_{l_{\pm_2},D_{\pm_2}}(\varphi_{\pm_1},\lambda) =& \sum_{l_{\mp_2}} E_{l_{\mp_2},\pm_1,D_{\mp_2}} \frac{r_{\mp_2}^{l_{\mp_2}+2} r_{\pm_2}}{d^{l_{\mp_2}+1}} \frac{(\pm_2 1)^{l_{\pm_2}}}{\sqrt{2l_{\mp_2}+13}} \delta_{0,l_{\pm_2}} \\ &+ \delta_{l_{\pm_2},0} E_{0,\pm_1,D_{\pm_2}} \frac{r_{\pm_2}^2}{3} + (1-\delta_{l_{\pm_2},0}) \frac{1}{\lambda} E_{l_{\pm_2},\pm_1,D_{\pm_2}}. \end{aligned} \tag{C.16}$$

We have

$$G^{\boldsymbol{n}}_{0,D_\pm}(\varphi_\mp,\lambda) = \frac{r_\mp^2 r_\pm}{d} \frac{1}{3} E_{0,\mp,D_\mp} + E_{0,\mp,D_\pm} \frac{r_\pm^2}{3} + \mathcal{O}(d^{-3}) = \mathcal{O}(d^{-3}) \tag{C.17}$$

and

$$\begin{aligned} G^{\boldsymbol{n}}_{0,D_\pm}(\varphi_\pm,\lambda) =& \frac{r_\mp^2 r_\pm}{d} \frac{1}{3} E_{0,\pm,D_\mp} + E_{0,\pm,D_\pm} \frac{r_\pm^2}{3} + \mathcal{O}(\mathrm{d}^{-3}) \\ =& \frac{\sqrt{4\pi}}{3} \left( \frac{r_\mp r_\pm^2}{d^2} - \left(1 + \frac{r_+ r_-}{d^2}\right) r_\pm \right) + \mathcal{O}(\mathrm{d}^{-3}) \\ =& -\frac{\sqrt{4\pi}}{3} r_\pm + \mathcal{O}(d^{-3}). \end{aligned} \tag{C.18}$$

For $l > 1$ or $l > 0$ and $\pm_1 = \pm_2$ we have

$$G^{\boldsymbol{n}}_{l,D_{\pm_2}}(\varphi_{\pm_1},\lambda) = \frac{1}{\lambda} E_{l,\pm_1,D_{\pm_2}} + \mathcal{O}(d^{-3}) = \mathcal{O}(d^{-3}). \tag{C.19}$$

Finally we see that

$$G^{\boldsymbol{n}}_{1,D_\pm}(\varphi_{\mp_1},\lambda) = \mp\sqrt{12\pi} \frac{1}{\lambda} \frac{r_\mp}{d^2} + \mathcal{O}(d^{-3}). \tag{C.20}$$

We again use lemma 7.0.3 to get for $l_{\pm_2} > 0$ that

$$\begin{aligned} G_{l_{\pm_2},D_{\pm_2}}(\varphi_{\pm_1},\lambda) =& -\sum_{l_{\mp_2}} E_{l_{\mp_2},\pm_1,D_{\mp_2}} \frac{r_+^{l_+ +2} r_-^{l_- +2}}{d^{l_+ + l_- +1}} \frac{\binom{l_+ + l_-}{l_+} (\mp_2 1)^{l_{\pm_2}} (\pm_2 1)^{l_{\mp_2}}}{(2l_{\pm_2}+3) l_{\pm_2} \sqrt{(2l_+ +1)(2l_- +1)}} \\ &+ E_{l_{\pm_2},\pm_1,D_{\pm_2}} \left( -\frac{r_\pm^3}{(2l_\pm +1)(2l_\pm +3) l_\pm} + \frac{r_{\pm_2}}{\lambda l_{\pm_2}} \right). \end{aligned} \tag{C.21}$$

Next we have

$$\begin{aligned} G_{1,D_\pm}(\varphi_\pm,\lambda) =& \pm E_{0,\pm,D_\mp} \frac{r_\mp^2 r_\pm^3}{d^2} \frac{1}{5\sqrt{3}} + \frac{r_\pm}{\lambda} E_{1,\pm,D_\pm} - r_\pm^3 \frac{E_{1,\pm,D_\pm}}{15} + \mathcal{O}(d^{-3}) \\ =& \mp \frac{\sqrt{12\pi}}{\lambda} \frac{r_\pm r_+ r_-}{d^3} + \mathcal{O}(d^{-3}) \end{aligned} \tag{C.22}$$

and

$$\begin{aligned} G_{1,D_\pm}(\varphi_\mp,\lambda) =& \pm E_{0,\mp,D_\mp} \frac{r_\mp^2 r_\pm^3}{d^2} \frac{1}{5\sqrt{3}} + \frac{r_\pm}{\lambda} E_{1,\mp,D_\pm} - \frac{r_\pm^3 E_{1,\mp,D_\pm}}{15} + \mathcal{O}(d^{-3}) \\ =& \sqrt{4\pi} \left( \mp \frac{r_\mp r_\pm^3}{d^2} \frac{1}{5\sqrt{3}} \mp \frac{\sqrt{3}}{\lambda} 2 \frac{r_+ r_-}{d^2} \pm \frac{r_\pm^3 r_\mp}{d^2} \frac{1}{5\sqrt{3}} \right) + \mathcal{O}(d^{-3}) \\ =& \mp \frac{\sqrt{12\pi}}{\lambda} \frac{r_+ r_-}{d^2} + \mathcal{O}(d^{-3}). \end{aligned} \tag{C.23}$$

Die approbierte gedruckte Originalversion dieser Diplomarbeit ist an der TU Wien Bibliothek verfügbar
The approved original version of this thesis is available in print at TU Wien Bibliothek.
TU Bibliothek Your knowledge hub WIEN

Further we see for $l_{\pm_2} \geq 2$ that

$$G_{l_{\pm_2},D_{\pm_2}}(\varphi_{\pm_1},\lambda) = \mathcal{O}(d^{-3} + E_{l_{\pm_2},\pm_1,D_{\pm_2}}) = \mathcal{O}(d^{-3}). \tag{C.24}$$

□

# D. Empirical study

## D.1. Additional simulations

First we will revisit a system of two similar sized bubbles with radius 5 and 6. Figure D.1 shows the scaled force contributions and the total force on the bigger bubble. In (a) we can see that the main differences are the signs of $F^s_{+,-}$ and $F^s_{-,+}$ and that the sign changes occur at larger distances. Furthermore (b) looks similar to the case of the smaller bubble except that for $\omega_5$ due to the sign reversal of $F^s_{-,-}$ we get an area where the bubble gets attracted again. For smaller values we get a second repulsive area due to $F^s_{+,-}, F^s_{-,+}$ both being positive and dominating.

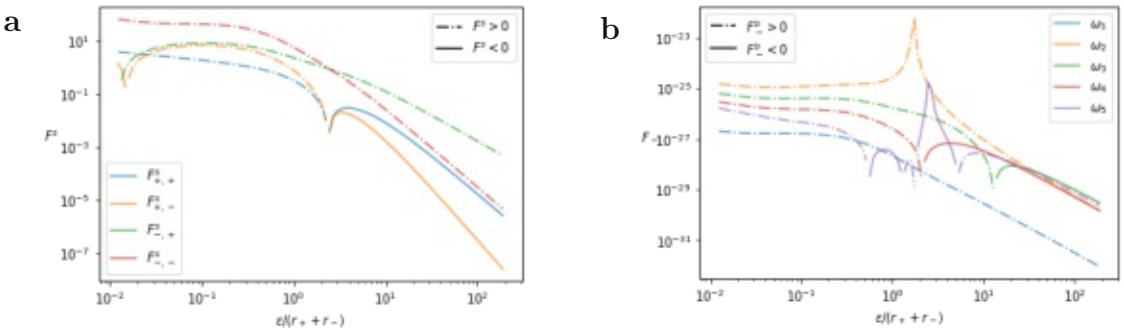


Figure D.1.: (a) shows the scaled force contributions for a bubble of radius 6 interacting with one of radius 5. In (b) the total Bjerknes force is shown for the frequencies defined in figure 7.7.

In figure D.2 we look at the case of two bubbles with radii 1 and 5. We already looked at the scaled force contributions for the bigger bubble and will now consider the smaller bubble. In our scope no sign transition takes place and the total force can be easily explained by $F_{+,+}$ near the singularity and by $F_{+,-}$ and $F_{-,-}$ dominating. We can again see that the force for $\omega_4$ is repellent up to a closer distance compared to the similarly sized bubble case.

## D.2. Error

To check the numeric simulations we will be using an exact formula for $\mathcal{A}_D$. For this we will be using the formulas found in [23, Appendix A].

Die approbierte gedruckte Originalversion dieser Diplomarbeit ist an der TU Wien Bibliothek verfügbar
The approved original version of this thesis is available in print at TU Wien Bibliothek.
TU Bibliothek Your knowledge hub WIEN

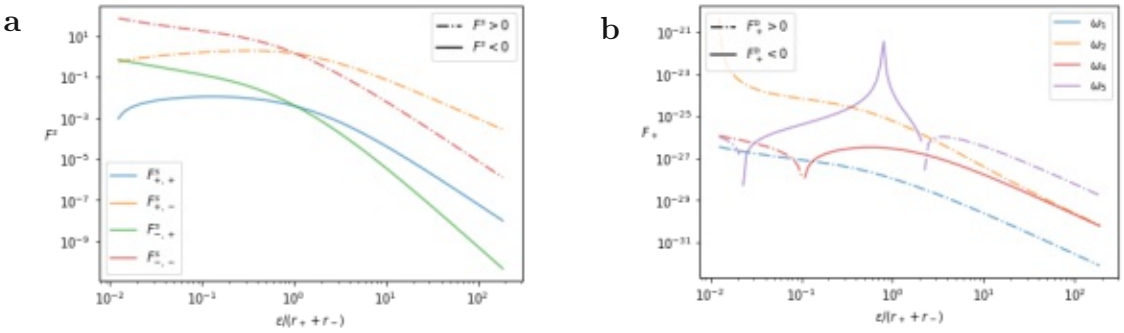


Figure D.2.: (a) shows the scaled force contributions for a bubble of radius 1 interacting with one of radius 5. In (b) the total Bjerknes force is shown for the frequencies defined in figure 7.9.

**Lemma D.1.** *For spherical inclusions we have for* $c := -\mathrm{i}kr_i^2$ *that*

$$S^k_{D_i}[Y^m_l]|_{D_i} = \begin{cases} cj_l(kr_i)h^{(1)}_l(kr)Y^m_l, & |r| > r_i, \\ cj_l(kr)h^{(1)}_l(kr_i)Y^m_l, & |r| \leq r_i \end{cases} \tag{D.1}$$

*and for* $j \neq i$ *that*

$$S^k_{D_i}[Y^m_l]|_{D_j} = ch^{(1)}_l(kr_i)\sum_{l'=0}^{\infty}\sum_{|m'|\leq l'} A^{lm}_{l'm'}j_{l'}(kr)Y^m_{l'} \tag{D.2}$$

*for*

$$A^{lm}_{l'm'} := \sum_{\lambda=0}^{\infty}\sqrt{\frac{2\lambda+1}{4\pi}}h^{(1)}_\lambda(kd)C(l,m,l',m',\lambda,0), \tag{D.3}$$

*d being the distance between the centers of the inclusions,*

$$\begin{aligned} C(l,m,l',m',\lambda,\nu) :=& \mathrm{i}^{l'-l+\lambda}(-1)^m\sqrt{4\pi(2l+1)(2l'+1)(2\lambda+1)}\times \\ & \begin{pmatrix} l & l' & \lambda \\ 0 & 0 & 0 \end{pmatrix}\begin{pmatrix} l & l' & \lambda \\ -m & m' & \nu \end{pmatrix} \end{aligned} \tag{D.4}$$

*and* $j_l, h^{(1)}_l$ *denotes the spherical bessel and hankel function of the first kind.*

Using these formulas we can build a matrix by truncating the spherical harmonic contributions and inverting the system to arrive at the potential functions. Applying $S^0_D$ and $K^0_D$ on them provides us with the derivatives on the surface. This provides us with a way to check the results of the simulations.
Looking at figure D.3 we can see that the curves match up for most of the bigger values. The plots show the forces calculated by inversion of $\mathcal{A}_D$ like we described above compared to the analytic formula. In the first line we cover the case of similarly sized bubbles ($r = 5, 6$) and in the second one the differently sized spheres($r = 1, 5$).The relative error gets large if the driving frequency gets close to a resonance frequency, near points where

Die approbierte gedruckte Originalversion dieser Diplomarbeit ist an der TU Wien Bibliothek verfügbar
The approved original version of this thesis is available in print at TU Wien Bibliothek.
TU Bibliothek Your knowledge hub WIEN

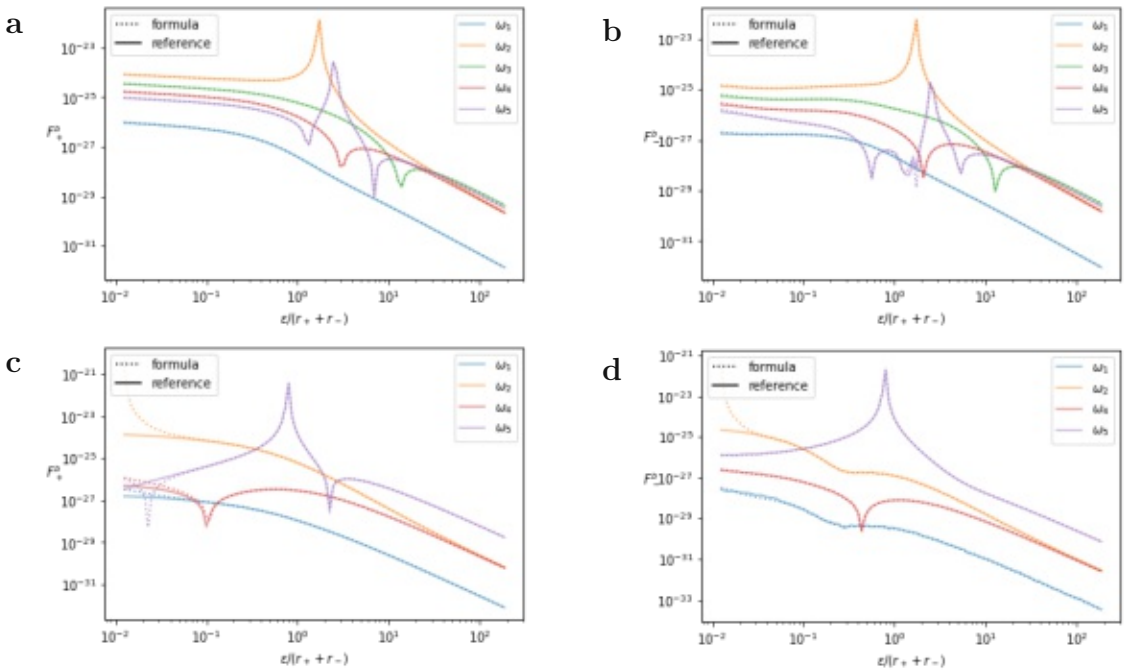


Figure D.3.: The figures show the forces calculated by direct inversion of $\mathcal{A}_D$ (reference) compared to the derived formula in this thesis. (a) and (b) cover the case of similar sized bubbles, where in the former we have the forces on the smaller bubble (r=5) and in the later (r=6). (c) (with r=1) and (d) (with r=5) in the same way describe the differently sized system.

the force changes sign and for very small bubble separations.
We can see the relative error in figure D.4. We removed all values with a characteristic distance of less than $2 \cdot 10^{-1}$, that are within 10% of a sign transition or where the driving frequency is within one percent of a resonance frequency. We can see that the relative error for (a), (b) and (c) around or below 1% except for the $\omega_5$. Finally, we can see that the relative error for (d) is very large, which is mainly present for small separations. There are multiple reasons that could explain these errors. For one, we work with non-zero $\delta$ therefore the formula that we derived cannot be exact as it describes an asymptotic behavior. Secondly the operator $\mathcal{A}_D$ for small $\delta$ and $\omega$ is almost singular and thus the inversion is ill conditioned. This is especially the case near the resonance frequencies, which are defined by the singularity of $\mathcal{A}_D$. Finally, near the sign reversal of the forces we can expect high relative errors due to the small values we get there.

Die approbierte gedruckte Originalversion dieser Diplomarbeit ist an der TU Wien Bibliothek verfügbar
The approved original version of this thesis is available in print at TU Wien Bibliothek.
TU Bibliothek Your knowledge hub WIEN

| Maximal relative error | | | | |
|---|---|---|---|---|
| Frequency | Similar size | | Different size | |
| | (**a**) $F^b_{D_+}$ | (**b**) $F^b_{D_-}$ | (**c**) $F^b_{D_+}$ | (**d**) $F^b_{D_-}$ |
| $\omega_1$ | 1.0% | 1.5% | 0.93% | 27 % |
| $\omega_2$ | 0.42% | 0.43% | 0.28% | 13 % |
| $\omega_3$ | 0.34% | 0.85% | - | - |
| $\omega_4$ | 0.27% | 1.5% | 0.37% | 6.8% |
| $\omega_5$ | 0.66% | 15% | 0.62% | 1.5% |

Figure D.4.: This table shows the relative error of our method and the reference. Note that we removed all values with $\epsilon/(r_+ + r_-) < 0.2$ and if the driving frequency is within 1% of a singularity or $\epsilon$ within 10% of a sign reversal.

Die approbierte gedruckte Originalversion dieser Diplomarbeit ist an der TU Wien Bibliothek verfügbar
The approved original version of this thesis is available in print at TU Wien Bibliothek.
TU Bibliothek Your knowledge hub WIEN